ISSN 2408-2384 (ONLINE)

Environment and Natural Resources Journal

Volume 23 Number 6 November - December 2025

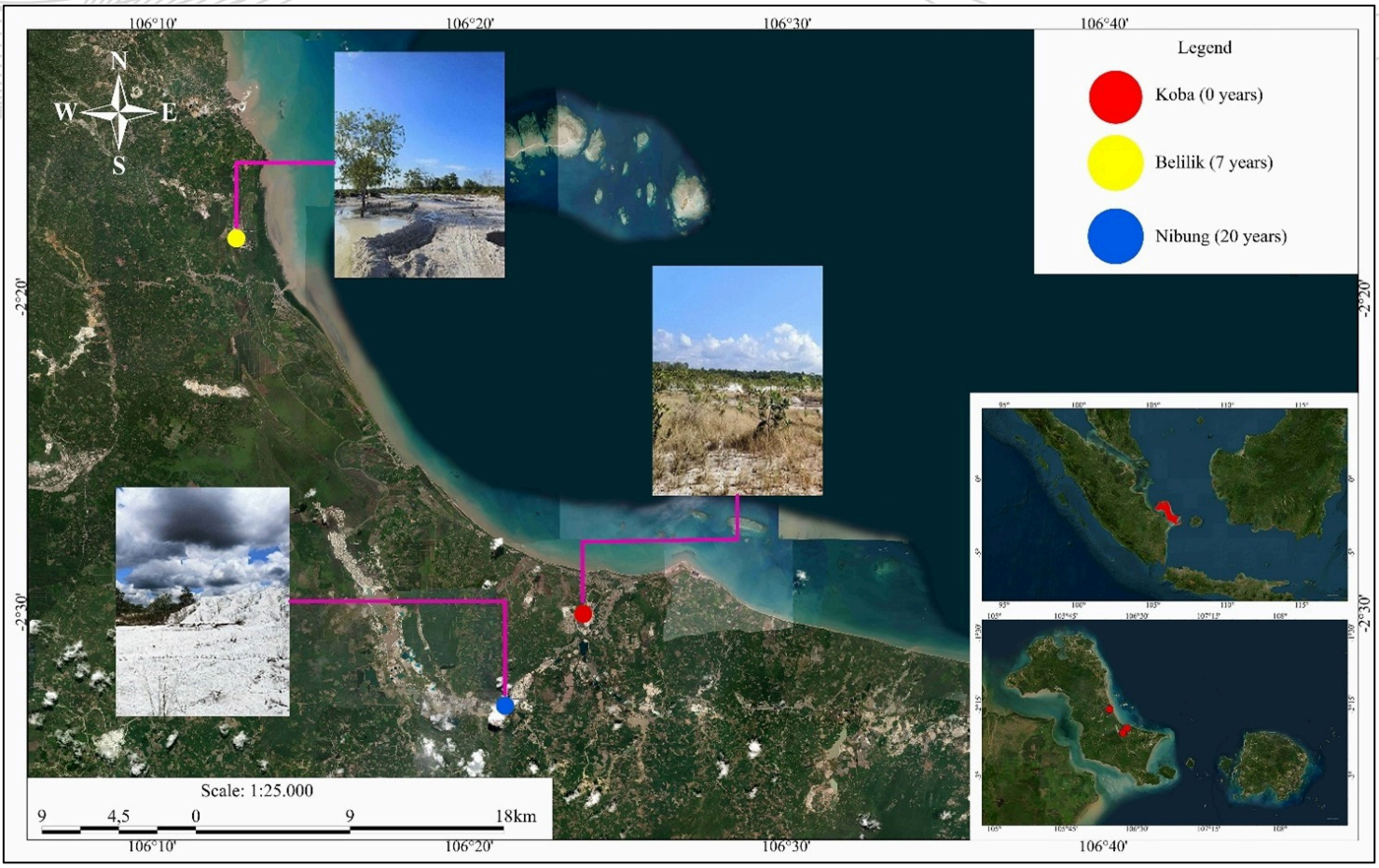

Sampling points in three post-tin mining lands on Bangka Island, Indonesia. The island is one of the largest tin producers in Indonesia and the world. Soil was collected from these points for evaluation.

Source: Erdaswin F, Rahayu, Rosariastuti R, Dewi WS, Herawati A, Fatimah, Ichsan N. The influence of age and management on soil physicochemical properties and heavy metal accumulation in post-tin mining lands on Bangka Island. Environ. Nat. Resour. J. 2025;23(6):537-551.

Environment and Natural Resources Journal (EnNRJ)
Volume 23, Number 6, November - December 2025 ISSN: 2408-2384 (Online)

FOCUS AND SCOPE

Environment and Natural Resources Journal (EnNRJ) is a peer-reviewed journal which provides a platform for exchanging and distributing knowledge and cutting-edge research in environmental science and natural resource management to academicians, scientists, and researchers.

The scope of the journal covers the integration of multidisciplinary sciences for prevention, control, treatment, environmental clean-up, and restoration. The study of existing or emerging problems related to the environment and natural resources in Southeast Asia and the development of innovative knowledge and/or creative recommendations for mitigation measures and sustainable development are emphasized. The subject areas are diverse, but specific topics of interest include:

- Biodiversity
- Climate change
- Detection and monitoring of pollutants and their sources (e.g., agriculture, industry, mining, urban activities, accidents)
- Disaster (e.g., forest fires, flooding, earthquakes, tsunamis or tidal waves)
- Ecological/Environmental modelling
- Emerging contaminants/hazardous wastes investigations and remediation
- Environmental dynamics (e.g., coastal erosion, rising sea levels)
- Environmental assessment tools, policy, and management [e.g., GIS, remote sensing, and Environmental Management Systems (EMS)]
- Pollution control and innovative solutions for pollution reduction
- Remediation technology in contaminated environments
- Transboundary pollution
- Waste and wastewater treatments and disposal technology

Schedule
Environment and Natural Resources Journal (EnNRJ) is published 6 issues per year in January-February, March-April, May-June, July-August, September-October, and November-December.

Publication Fees
An article publication fee in the Environment and Natural Resources Journal is set at a rate of 250 USD per article, payable after the final acceptance of the manuscript.

Ethics in publishing
EnNRJ follows closely a set of guidelines and recommendations published by Committee on Publication Ethics (COPE).

Environment and Natural Resources Journal (EnNRJ)
Volume 23, Number 6, November - December 2025 ISSN: 2408-2384 (Online)

Editorial Office Address
Research and Academic Service, Research Management Unit,
Faculty of Environment and Resource Studies, Mahidol University
999, Phutthamonthon Sai 4 Road, Salaya, Phutthamonthon, Nakhon Pathom, Thailand, 73170
Phone +662 441 5000 ext. 2108
Website: https://ph02.tci-thaijo.org/index.php/ennrj/index
E-mail: ennrjournal@gmail.com

Environment and Natural Resources Journal (EnNRJ)

Volume 23, Number 6, November - December 2025 ISSN: 2408-2384 (Online)

CONTENT

Environment and Natural Resources Journal

Volume 23
Issue 6
2025

Dynamic Integrated Model for Sustainable Solid Waste Management in Bengkulu City

Defi Ermayendri[1*], Marulak Simarmata[2], Wahyudi Arianto[3], Reflis[4], Riwandi[5], and Ketut Sukiyono[4]

[1]*Department of Environmental Health, Health Polytechnic, Ministry of Health, Bengkulu, Indonesia*
[2]*Agroecotechnology Study Program, Faculty of Agriculture, Bengkulu University, Indonesia*
[3]*Forestry Study Program, Faculty of Agriculture, Bengkulu University, Indonesia*
[4]*Agribusiness study program, Faculty of Agriculture, Bengkulu University, Indonesia*
[5]*Soil Science Study Program, Faculty of Agriculture, Bengkulu University, Indonesia*

ARTICLE INFO

Received: 25 Feb 2025
Received in revised: 12 Jul 2025
Accepted: 16 Jul 2025
Published online: 18 Aug 2025
DOI: 10.32526/ennrj/23/20250048

Keywords:
Municipal waste management/ Waste reduction/ Management costs/ Landfill space/ Dynamic systems

*** Corresponding author:**
E-mail:
defi@poltekkesbengkulu.ac.id

ABSTRACT

Rapid urbanization and increased consumption patterns have intensified municipal solid waste (MSW) challenges in developing cities. This study applies a system dynamics model to project waste generation, management costs, and landfill requirements in Bengkulu City, Indonesia, over a 20-year period. Four scenarios were simulated: business-as-usual, minimum (25%), moderate (50%), and optimistic (65%) waste reduction. The model integrates critical parameters including population growth, waste generation rates, recycling capacity, and community participation. Results indicate that without intervention, cumulative waste volume will overwhelm landfill capacity and escalate operational costs. Conversely, implementing waste reduction strategies—such as strengthening source separation, expanding composting and waste banks, adopting advanced technologies, and enforcing supportive policies—substantially reduces landfill dependency and operational expenses. The optimistic scenario demonstrates the highest efficiency, reducing required landfill land by over 85% and significantly lowering management costs. This study highlights the importance of multi-stakeholder collaboration, digital monitoring integration, and circular economy principles in urban waste governance. The model offers a practical decision-support framework for policymakers aiming to develop resilient, inclusive, and sustainable waste management systems in similar urban contexts.

HIGHLIGHTS

This study highlights a dynamic system model in solid waste management (SWM) that integrates waste reduction, landfill needs, management costs, and emphasizes the contribution of costs as environmental services to reduce dependence on regional budgets through the "Waste Independence-Waste Independence" strategy, which focuses on community awareness, infrastructure, and cross-sector collaboration.

1. INTRODUCTION

Solid waste management (SWM) has become an increasingly critical global issue due to the rapid urbanization and rising consumption patterns that contribute to escalating waste volumes. By 2050, global municipal solid waste is projected to reach 3.4 billion tons annually, with the steepest growth observed in developing countries. Currently, approximately 40% of waste is landfilled, 33% is openly dumped, 19% is recycled, and 11% is incinerated, with the remainder managed through other conventional methods (Govani et al., 2021). In many developing countries, SWM still relies on the basic "collect-transport-dispose" model. Improperly managed waste especially when uncollected or untreated leads to environmental degradation,

Citation: Ermayendri D, Simarmata M, Arianto W, Reflis, Riwandi, Sukiyono K. Dynamic integrated model for sustainable solid waste management in Bengkulu City. Environ. Nat. Resour. J. 2025;23(6):494-515. (https://doi.org/10.32526/ennrj/23/20250048)

including clogged waterways, contaminated water bodies, and increased disease vectors such as mosquitoes and rodents (Guerrero et al., 2013). This solid waste consists not only of organic and inorganic materials but also includes agricultural residues, hazardous substances, and microplastics, which have detrimental effects on aquatic life and, ultimately, pose broader risks to human health and the environment (Ferronato and Torretta, 2019; Rahman et al., 2023). In addition, the uncontrolled decomposition of organic waste in landfills produces methane, a potent greenhouse gas that significantly contributes to climate change (Lee et al., 2017).

Recent research has emphasized the importance of integrated, sustainable approaches to waste management that go beyond conventional practices. Biotechnological innovations, for instance, are being employed to detect and mitigate microplastic pollution through the use of biosensors, enzymatic degradation, and specialized microorganisms, while the development of biodegradable alternatives to single-use plastics offers promising long-term solutions (Mai et al., 2018; Rahman et al., 2023). Parallelly, the paradigm of urban wastewater management is shifting toward decentralized systems, resource recovery, and water reuse, which align closely with solid waste reduction and environmental protection goals. Additionally, the valorization of agricultural waste biomass for bioenergy production—such as biogas, bioethanol, and biochar—can simultaneously reduce landfill loads and support renewable energy transitions (Pfister et al., 2005). These strategies are essential for mitigating methane emissions from landfills, a major contributor to climate change (do Carmo Precci Lopes et al., 2022; Sołowski et al., 2020).

Furthermore, the transition toward a sustainable environment must be underpinned by the integration of green energy technologies (Hla and Roberts, 2015). While renewable energy sources such as solar, wind, and bioenergy present both advantages and limitations, their incorporation into waste and water management systems fosters resilience and lowers carbon footprints (Bruno et al., 2021; Zhang et al., 2024). Innovations in agricultural production, such as speed breeding, indirectly influence waste generation by increasing crop outputs, and consequently, agricultural residues (Meena et al., 2023). When properly harnessed, these residues serve as valuable feedstocks for energy production. In this context, sustainable solid waste management is no longer solely a matter of disposal but must be viewed as a complex, interdisciplinary challenge—requiring biotechnological, agricultural, and infrastructural innovations to ensure long-term ecological and human well-being (Moya et al., 2017).

Effective waste management is a multidimensional process that encompasses various interrelated aspects, each critical to ensuring environmental sustainability and public health. Effective management begins with understanding waste composition and implementing proper collection and source separation to enhance recycling and resource recovery. Treatment technologies such as composting, anaerobic digestion, and incineration help reduce landfill dependence and recover energy. Equally important are robust policy frameworks and active community participation, which are essential for sustainable and inclusive waste system (Kumar and Samadder, 2017; Wilson et al., 2006).

As a potential solution, the system dynamics approach provides a comprehensive framework for integrated waste management by capturing the complex interrelationships among waste reduction efforts, cost efficiency, landfill performance, and active community involvement. This methodology facilitates the simulation and assessment of diverse policy scenarios, such as economic incentives and public awareness campaigns, supporting the development of sustainable and adaptive waste management strategies. By incorporating dynamic feedback mechanisms and temporal variations, system dynamics provides policymakers with tools to identify critical leverage points for effective intervention. Ultimately, it enables the alignment of environmental objectives with the social and economic conditions of rapidly evolving urban environments (Bornstein, 2018; Radosavljevic et al., 2023; Sondh et al., 2024; Thatcher et al., 2024).

Dynamic systems modeling has been used by numerous researchers to analyze complex (Li et al., 2024), and the circular economy of waste (Ibarra Vega and Bautista-Rodriguez, 2024). This method has been applied in various fields such as the social sciences (Blakeslee et al., 2017; Smith and Thelen, 2003), fisheries (Free et al., 2023), mining (Friederich et al., 2022), wastewater management (Fragkoulis et al., 2011), agriculture (Pfister et al., 2005), food wast (Lam et al., 2018), and many other areas. The dynamic modeling approach allows policymakers and urban planners to simulate and evaluate the long-term impacts of various waste management strategies, integrating

socioeconomic and environmental dimensions (Dyson and Chang, 2005; Forrester, 1961).

This study introduces a waste management model designed to guide the development of effective waste reduction strategies. The model outlines four main scenarios: the first assumes no waste reduction efforts; the second, the Minimal Reduction scenario, targets a 25% reduction through basic recycling and composting; the third, the Moderate Reduction scenario, aims for a 50% reduction by expanding community-based programs and implementing green technologies; and the fourth, the Optimistic Reduction scenario, seeks a 65% reduction through a combination of stringent policy enforcement, technological innovation, and widespread public participation. The simulation of these four scenarios dynamically influences waste generation sent to landfills, waste management costs, fees, and the required landfill area over the next 20 years. Population projections, which reflect waste generation patterns, are based on historical demographic data and economic growth, measured by the Gross Regional Domestic Product (GRDP), in Kota Bengkulu from 2013 to 2022.

The novelty of this study lies in the application of a dynamic systems modeling approach specifically tailored to municipal solid waste management in Bengkulu City, integrating waste generation dynamics, financial management, landfill land requirements, and community participation into a single, interrelated framework. Unlike previous studies that typically focus on isolated aspects of waste management, this research offers a comprehensive, scenario-based simulation over a 20-year projection period, evaluating the long-term impacts of varying levels of waste reduction interventions. The study also provides a decision-support tool that enables policymakers to assess the trade-offs between operational costs, landfill capacity, and environmental impacts under different policy scenarios, thus bridging the gap between theoretical modeling and practical, locally adaptable waste management planning.

2. METHODOLOGY

2.1 Study site

Bengkulu City is the capital of Bengkulu Province, located on the western coast of Sumatra Island, directly facing the Indian Ocean. Geographically, it lies between 3°45′-3°59′ South Latitude and 102°14′-102°22′ East Longitude. The city covers a total area of 539.3 km^2, consisting of 151.7 km^2 of land and 387.6 km^2 of sea. Due to its coastal location, Bengkulu City is exposed to strong ocean waves, making the area vulnerable to natural coastal erosion or abrasion. Topographically, Bengkulu City is relatively flat. The majority of the land—approximately 142.24 km^2, or 98.42% of the total area—has a slope of 0-15%. Only a small portion, about 2.28 km^2 or 1.58%, has steeper slopes ranging from 15-40%. The flattest areas are located along the coastline, with elevations ranging from 0 to 10 meters above sea level. In contrast, the eastern part of the city rises slightly higher, with altitudes ranging from 25 to 50 meters above sea level.

2.2 Solid waste management in Bengkulu

Waste management in Bengkulu City is carried out by the local government through the Environmental Agency (Dinas Lingkungan Hidup, DLH). The institutional framework for waste management is outlined in the Bengkulu City Mayor Regulation No. 08 of 2018 concerning the establishment of a Technical Implementation Unit for Waste Management within the Environmental Agency of Bengkulu City. The institutional aspects of waste management in Bengkulu City are also detailed in the Strategic Plan of the Environmental Agency for the years 2019-2023, which designates the Environmental Agency as the authority responsible for waste management in the city. Within the agency, one of the departments with a primary responsibility for waste management is the Cleanliness Division. Additionally, the Environmental Services include the Waste and Hazardous Waste Management Division, which oversees the Waste Reduction Section, Waste Handling Section, and Hazardous Waste Section.

The actual waste management service in Bengkulu City begins with waste collection at the source and continues with transportation to the final processing site, following the “collect-transport-dispose” approach. Waste generation comes from household waste as well as similar waste from residential areas, commercial establishments, restaurants, hotels, offices, educational institutions, public facilities, and street sweeping activities, with organic waste dominating the composition. The majority of waste is transported directly to the landfill without any sorting efforts, except by scavengers who separate and collect waste at the landfill (Environmental Services of Bengkulu City, 2022).

2.3 Dynamic system

System dynamics, introduced by Jay Forrester in the 1960s at MIT, is a quantitative method for analyzing complex systems and long-term decision-making (Sterman, 2001). The analysis begins with identifying key problems, critical variables, and system boundaries using causal loop diagrams. This initial understanding forms the foundation for developing formal models that are applied across various fields, such as business, environment, and politics (Dyson and Chang, 2005; Zulkipli et al., 2018). The next stage involves developing hypotheses and stock-flow models to illustrate variable interactions. Model validation is conducted through structural and behavioral testing to ensure alignment with real-world patterns. Various policy scenarios are then tested to assess their effectiveness, providing a data-driven foundation for more accurate decision-making.

This study used PowerSim Studio 10 as a simulation tool to model the dynamic and interrelated nature of the waste management system. The software integrates key subsystems, such as waste production, reduction, landfill land requirements, management costs, and service charges. This enables scenario-based analysis to support long-term planning. PowerSim's causality and stock flow modeling features provide valuable insights into system behavior, helping stakeholders evaluate the impact of different strategies and make informed decisions for more sustainable and adaptive waste management. The stages of dynamic system analysis in this study are presented in Figure 1.

The dynamic system method is a structured framework commonly employed in the analysis of complex systems and policy design. It combines both qualitative and quantitative approaches to model dynamic behaviors over time. This methodology begins with system analysis, where researchers identify the key problems, variables, system boundaries, and time horizon relevant to the study. Establishing these fundamental components ensures that the scope and focus of the analysis are clear and aligned with the objectives of the research.

Following system analysis, the next stage is hypothesis development, where assumptions about causal relationships between variables are formulated. These hypotheses provide the theoretical basis for constructing the system dynamics model. In the subsequent stage, model development, the identified variables and hypothesized relationships are visualized through causal loop diagrams and stock-and-flow diagrams. This visual modeling enables a deeper understanding of the interactions within the system and allows researchers to simulate the system's behavior under various conditions.

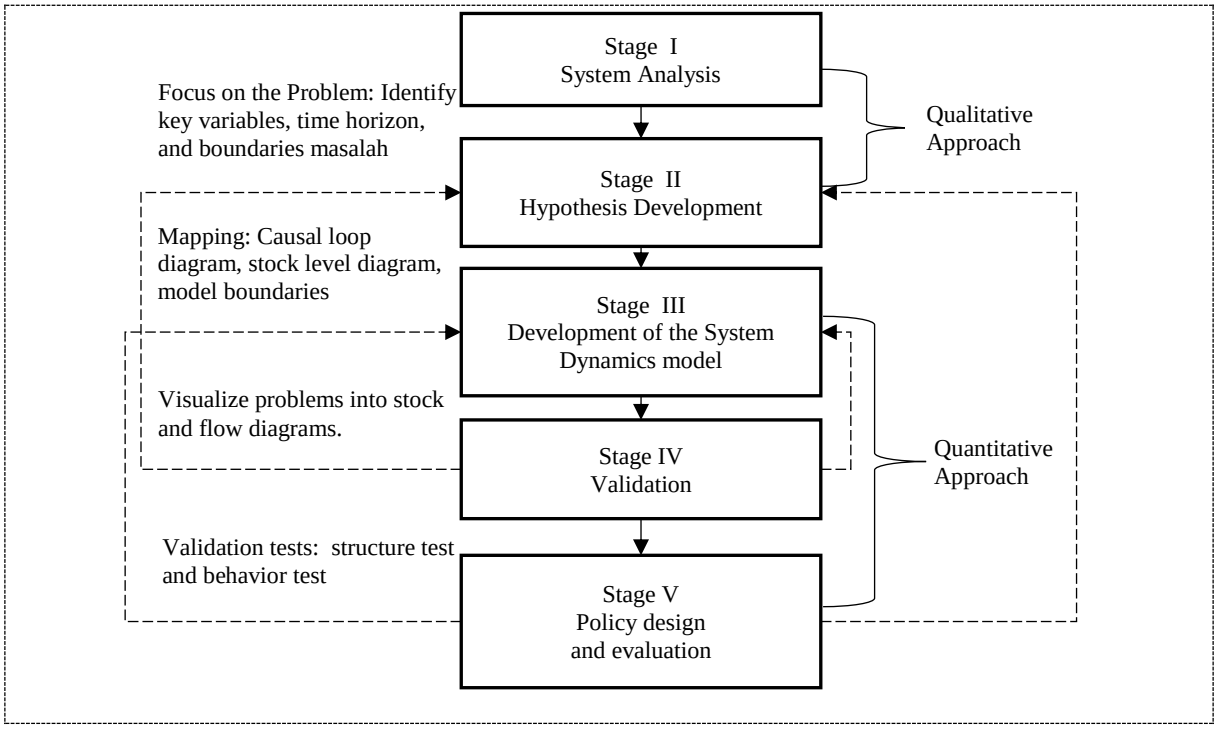

Figure 1. Stages of dynamic system methods

The fourth stage is validation, where the model undergoes structure and behavior tests to ensure its accuracy and reliability. Structure tests verify the internal consistency of the model, while behavior tests compare the simulated outputs against historical data. Once validated, the final stage, policy design and evaluation, involves using the model to simulate alternative scenarios and assess their potential impacts. This enables decision-makers to select the most effective policy options based on evidence derived from model simulations. Through this systematic process, dynamic system methods offer a robust tool for analyzing complex problems and supporting strategic policy formulation.

2.3.1 System identification: Key parameters for effective waste reduction

This study proposes a dynamic system model for sustainable municipal solid waste management in Bengkulu City, focusing on the issues of increasing waste generation, limited landfill capacity, and financial challenges faced by the local government. The system integrates key subsystems, including waste generation, waste reduction at source, waste collection and transportation, landfill land requirements, and financial management through government budgets and household waste fees. Critical variables modeled include the waste generation rate, percentage of waste reduction, volume of waste transported to the landfill, required landfill area, operational costs, and revenues from waste fees. These variables interact dynamically over time, influenced by population growth, economic activities, and community participation. The system boundaries are set within Bengkulu City's administrative area, covering household and similar domestic waste types over a 20-year planning period (2025-2045).

Four simulation scenarios are developed to assess policy effectiveness: Business as usual (0% reduction), minimum (25%), moderate (50%), and optimistic (65%) waste reduction by 2045. Each scenario will be analyzed for its impact on total waste generation, landfill land demand, operational costs, and financial sustainability, including government budget allocations and public waste collection fees. The dynamic model aims to produce evidence-based projections to guide strategic decisions, offering insights into how varying levels of waste reduction influence infrastructure needs, environmental outcomes, and municipal financial performance. This approach is expected to support the formulation of integrated, realistic, and sustainable waste management policies for Bengkulu City over the long term. Effective waste reduction is underpinned by several critical parameters that must be addressed systematically. Foremost among these is the strengthening of waste segregation at the source, which serves as the foundational step in minimizing overall waste volume. In parallel, implementing composting initiatives at both community and city scales can substantially decrease the amount of organic waste destined for landfills. The expansion of waste bank networks is equally essential, as it broadens public access to recycling opportunities and encourages community participation.

The reduction scenarios simulated in this dynamic model aim to generate evidence-based projections to guide strategic decisions, offering insights into how different levels of waste reduction affect the infrastructure needs, environmental outcomes and financial performance of the city. This approach is expected to support the formulation of integrated, realistic, and sustainable waste management policies for Bengkulu City in the long term. Furthermore, the adoption of advanced waste management technologies enhances operational efficiency, while the consistent enforcement of related policies ensures regulatory compliance and accountability. Collaboration with the private sector also plays a pivotal role by fostering innovation and resource mobilization. Lastly, the establishment of regular monitoring mechanisms is crucial for evaluating progress and informing policy adjustments. Collectively, these integrated measures contribute to the development of a more sustainable and responsible waste management system. The system identification in this study is shown in Figure 2.

2.3.2 Causal loop diagram

The black box description of the system performance variables is explained through the Causal Loop Diagram presented in Figure 3, illustrating the relationships between variables within the system. Causal Loop Diagram illustrates the dynamic interactions within the urban waste management system, emphasizing the relationship between population growth, waste generation, and municipal handling capacity. As the population increases, driven by the population growth rate, the number of households rises, leading to higher waste generation levels. This increase in waste generation directly affects the volume of both organic and inorganic

waste, placing greater demands on the city's waste management infrastructure. The escalation in waste volume subsequently leads to higher handling costs for waste management services, creating a feedback loop that influences municipal financial planning and operational efficiency.

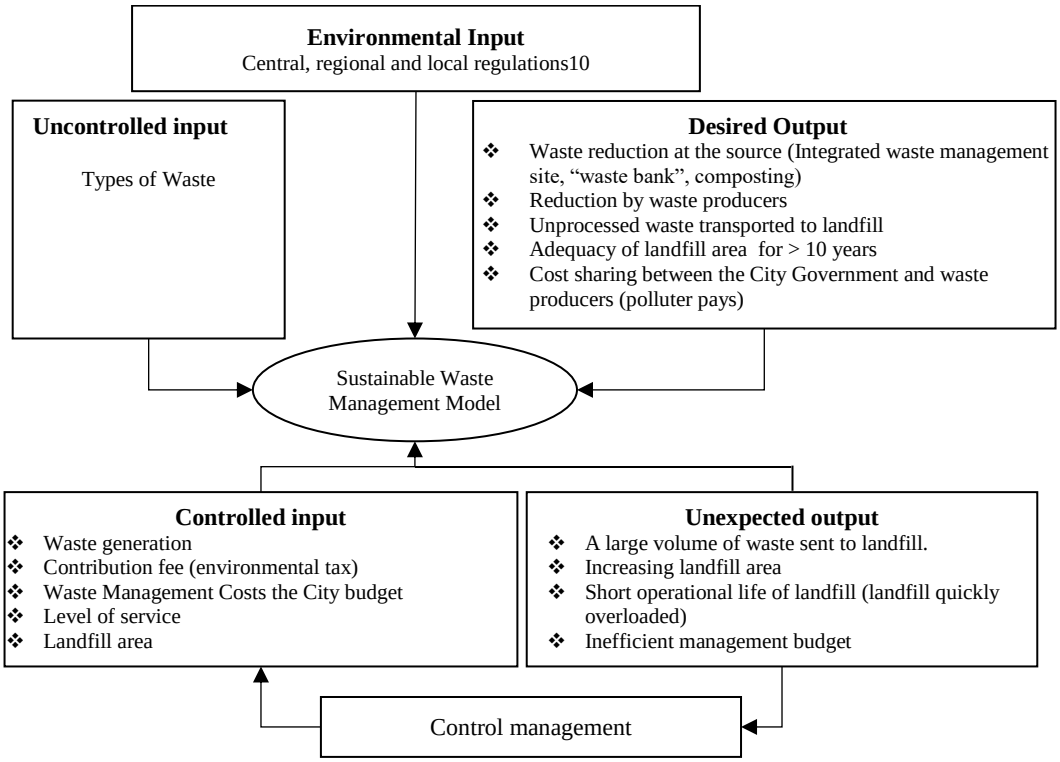

Figure 2. Variables affecting system performance (black box)

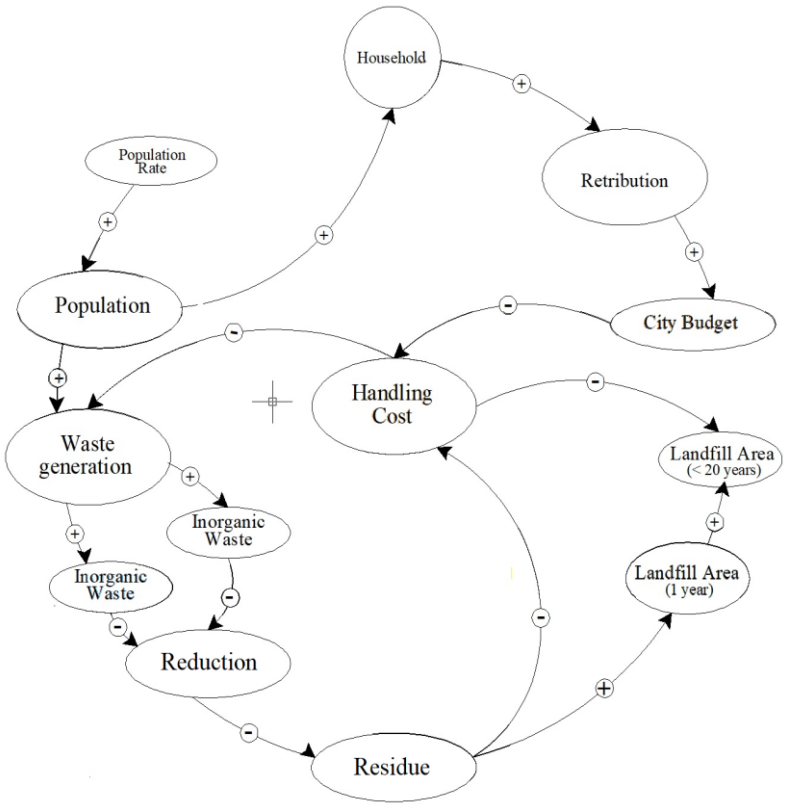

Figure 3. Causal loop diagram (CLD)

An essential component of the system is the waste reduction process, primarily through waste sorting activities. The reduction process helps decrease the volume of inorganic waste that becomes residual waste requiring landfill disposal. This reduction lowers the overall burden on the landfill, thereby moderating the rate of landfill area utilization. The feedback loop indicates that effective waste reduction strategies can reduce residual waste, leading to decreased handling costs and extended landfill lifespan. However, if reduction efforts are inadequate, residual waste will continue to accumulate, intensifying the pressure on landfill space and operational costs.

Additionally, the diagram captures the financial feedback loop between waste handling costs and the city budget, which is influenced by household waste service retributions. Increased retributions from a growing number of households contribute positively to the city budget, supporting waste management services. Conversely, higher handling costs, resulting from increased waste generation and residual accumulation, can strain the city budget if not matched by adequate financial inflows. The interplay between these factors highlights the importance of integrated waste management strategies and policy interventions, particularly in promoting waste sorting and reduction programs to achieve sustainable urban waste management outcomes.

In addition, the diagram captures the feedback cycle of five main components, namely: waste generation, waste reduction, landfill land requirement, management cost, and retribution. These five elements do not stand alone, but interact with each other to form an overall waste management system. The impact of the inter-subsystem linkages is very significant in achieving sustainable waste management. The volume of waste generation determines the initial burden of the management system, while the effectiveness of reduction efforts affects the amount of volume that must be treated or disposed of. The increase in waste volume drives the need for more landfill space, posing spatial and ecological challenges, especially in dense urban areas. On the other hand, an increase in management burden results in an increase in operational costs, which demands sustainability in terms of financing. In this case, retribution becomes an important instrument to cover the cost, but its effectiveness is highly dependent on an efficient collection mechanism and the level of community participation. The five subsystems thus form a dynamic system structure, which requires an integrated approach, intersectoral coordination and long-term planning to ensure a balance between environmental sustainability, economic viability and social acceptability.

2.3.3 Stock flow diagram (SFD)

Based on the CLD above, the SFD was made and is presented in Figure 4 along with the details of Variable Definitions in Table 1. In the SFD model, it can be explained that the number of residents affected by the population growth rate per year can be seen from the waste produced by each person per year, which is 915.5 liters/person/year. The assumption made for waste management planning in this study is the amount of waste produced in 2025, so that the graphs start in 2025, assuming that in 2025 waste management activities have been carried out in an integrated manner, and efforts to reduce the total waste are mentioned.

The Stock Flow Diagram (SFD) presented illustrates a dynamic systems model for sustainable waste management in Bengkulu City, incorporating the interconnected relationships between population growth, waste generation, financial resources, and landfill land use requirements. The model begins with the population stock, which increases over time based on a predetermined growth rate. This increase in population directly influences the number of households, subsequently determining the total waste generation volume. Cumulative waste generation is calculated by multiplying the waste generation rate per capita by the total population, establishing the primary inflow to the waste management system.

Waste generated in the city is handled through a waste management process at a specific handling rate, which determines the cumulative waste managed over time. The model recognizes that not all waste can be processed or diverted, and the residual waste—the portion that remains after handling and reduction efforts—flows into the landfill system. The reduction rate, which is influenced by implemented waste reduction scenarios (ranging from 0%, minimum 25%, moderate 50%, to optimistic 65%), determines the effectiveness of waste sorting, recycling, or other diversion programs. Higher reduction rates result in a lower volume of residual waste, reducing the cumulative waste sent to landfills and consequently limiting the need for landfill land expansion.

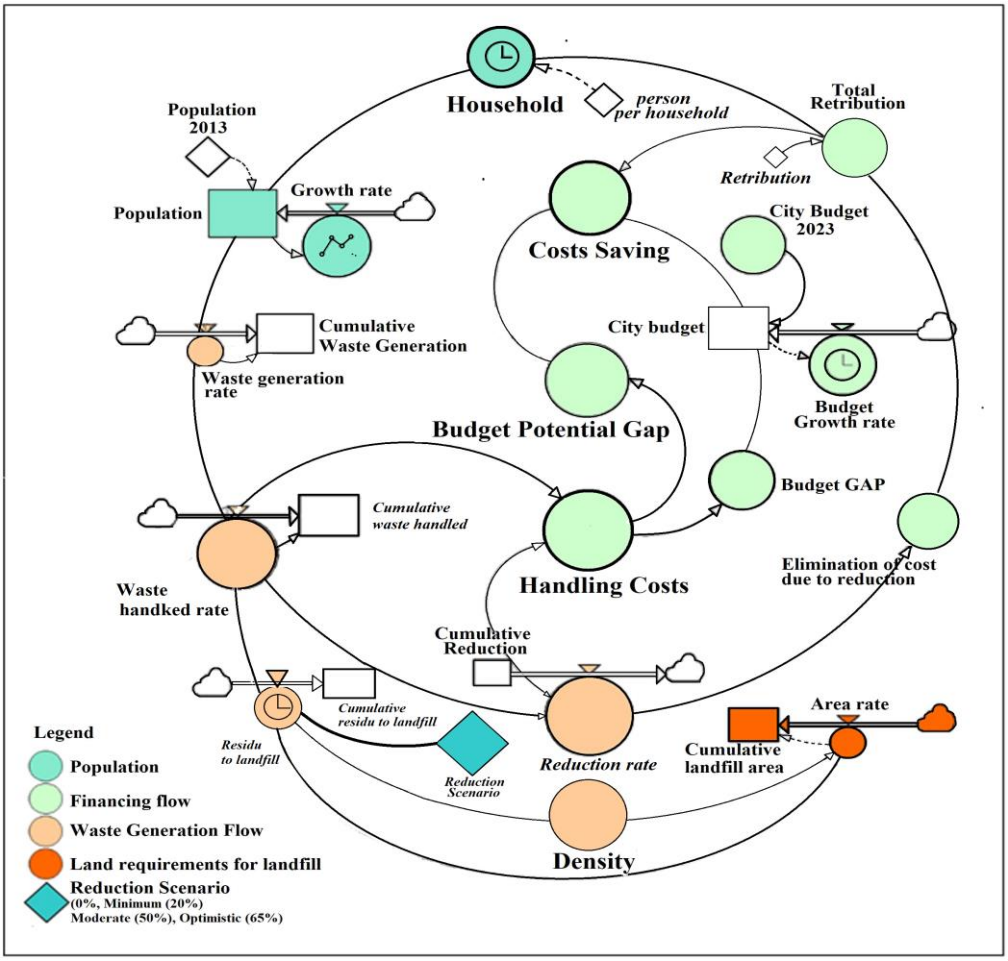

Figure 4. Stock flow diagram the proposed integrated waste management in Bengkulu City

An essential element of the model is the financing mechanism for waste management operations. Households contribute to municipal waste services through a retribution fee, which collectively forms the city's budget for waste management. This budget grows annually based on a predetermined growth rate. However, the model highlights a potential budget gap when handling costs increase at a rate faster than budget growth, particularly when waste generation surpasses the city's management capacity. To address this, cost savings from waste reduction programs are factored into the model as a feedback mechanism, reducing the overall handling cost burden and helping to stabilize the budget.

The diagram also integrates a spatial component by linking residual waste volumes to land requirements for landfill areas. Cumulative residual waste is translated into required landfill land based on landfill density and area rate factors. As residual waste accumulates, the model tracks the cumulative landfill area used over time. This aspect underscores the long-term land use implications of waste management decisions and highlights the importance of reducing residual waste volumes to prevent excessive land conversion for landfill purposes, particularly in urban areas with limited land availability such as Bengkulu City.

Overall, the Stock Flow Diagram serves as a strategic decision-support tool for evaluating the long-term impacts of various waste management scenarios. By simulating changes in population, waste generation rates, reduction strategies, and financial capacities, stakeholders can forecast potential budget gaps, identify operational bottlenecks, and estimate future landfill land needs. This system dynamics approach enables policymakers to design adaptive, data-driven waste management interventions that align with sustainability goals, resource constraints, and urban development priorities in Bengkulu City through 2045.

To offset these costs, the model factors in revenue streams from household and commercial waste retribution fees, simulating various compliance and collection efficiency rates. Furthermore, the residual waste volume—after reduction efforts—is

used to estimate the required landfill area, based on waste compaction rates and landfill design life. By linking population dynamics, technological interventions, financial viability, and spatial planning, this system dynamics model offers a comprehensive framework for evaluating long-term waste management strategies in Bengkulu City.

Table 1. Details of variable definitions in SFD

Description	Definition	
Population 2013-2022	2013: 334.500	2018: 368.784
	2014: 342.900	2019: 370.135
	2015: 351.300	2020: 373.600
	2016: 359.500	2021: 378.600
	2017: 366.435	2022: 384.800
		2023: 391.045
Growth rate	Population*(GRAPH (TIME,2013,1,{0.025112, 0.024497,0.023342,0.019291,0.00641,0.003663, 0.009361,0.013383,0.016376//Min:0,003663, Max:0,025//})//Min:0, Max:1//)	
Household constants	3,41	
Household	IF(TIME>2025, Population/'Constant household',0)	
Waste generation	0.9125 tons/person/year	
Waste generation rate	Population*2.5*365	
Waste handled rate	100%	
Reduction rate	'Waste handled rate '-'Residue to Landfill'	
Sampah ke TPA	IF(TIME>2024,'Waste handled rate'-('Waste handled rate'*'Reduction Scenario'))	
Density	'Residue to Landfill '* 0.6	
landfill area rate (hectare)	(('Residue to Landfill'-Density)/30)/10000	
Handling cost/cubic meter	$ 0.88,-	
Elimination of costs due to reduction	('Reduction rate'/Cubic)*Dollar	
Retribution	$ 23.35 per year/household	
Total Retribution	(Household*Retribution)-'Elimination of costs due to reduction'	
Handling Cost	(('Waste handled rate'-'Reduction rate')/Cubic)*Dollar	
Budget Growth Rate	IF(TIME>2025,'City Budget'*'Budget Constant')	
Reduction Scenario	Current (0%), 25% (minimal), 50% (moderate), 65% (optimistic)	

The system dynamics model developed in this study incorporates several interrelated variables to project the long-term implications of municipal solid waste management in Bengkulu City. Population data from 2013 to 2023 indicate steady growth from 334,500 to 391,045 inhabitants, with an average annual increase ranging from 0.37% to 2.51%. Waste generation is estimated at 0.9125 tons per person per year, equivalent to 2.5 liters per capita daily. Waste management simulations assume 100% collection efficiency, with varying reduction rates based on four scenarios: 0%, 25%, 50%, and 65%. The model calculates landfill area requirements using a waste density of 0.6 tons/m³ and a maximum landfill depth of 30 meters. Financial variables include a waste handling cost of $0.88 per cubic meter and a household retribution fee of $23.35 per year. The model also integrates budget growth projections and cost savings associated with waste reduction, enabling comprehensive scenario-based analysis of waste generation, operational expenses, and revenue from retributions over a 20-year period.

2.3.4 Validation

The value of "0" is between the range of μ_1 and μ_(2) or between (-18.724) – (+12.378); (P[(x¯_1-x¯_2)-hw ≤ μ_1-μ_(2)≤ (x¯_1-x¯_2)+hw]), so h0 is accepted or the simulation is valid (Table 2). There is no significant difference between real data and simulation results using Powersim software. This model is parameterized using historical data and relevant variables, allowing for the simulation of waste reduction across different scenarios. The waste reduction scenarios include a minimal scenario, which represents the lowest level of waste reduction; a moderate scenario, reflecting an intermediate level of

reduction; and an optimistic scenario, which achieves the highest level of waste reduction.

Model validation was conducted using a t-test comparison between real population data and simulation results for the period 2013-2022. The results show a very close alignment between observed and simulated values, with the average real population recorded at 363,055 and the simulated value at 366,228. The standard deviations were also nearly identical, at 15,959.99 and 15,959.85, respectively. Statistical testing using a two-tailed t-test with 18 degrees of freedom produced a t-count of 2.1788, which falls within the acceptance range of the T-table value of 2.179 at a 95% confidence level. This indicates no significant difference between real and simulated data. The absolute error remained within acceptable limits, with the mean error ranging from -3,172 to 12,378.56. These results confirm the validity and reliability of the dynamic system model in accurately representing demographic trends in Bengkulu City, providing a strong foundation for subsequent waste generation and management scenario simulations.

Table 2. T-test model validation

Year	Real data	Simulation data		
2013	334,500.00	334,500.00		
2014	342,900.00	342,899.96	25.472.127	25.471.673
2015	351,300.00	351,299.98	2.595.270.735.524.450	
2016	359,500.00	359,500.03	72.092.138.341.532	72.089.569.199.048
2017	366,435.00	366,435.14	144.181.707.540.581	
2018	368,784.00	368,783.99	Df 18	
2019	370,135.00	370,134.85	T Table 2.179	
2020	373,600.00	373,599.68	Hw 2.1788	25.472.127
2021	378,600.00	378,599.57	2.1788	7.137
2022	384,800.00	384,799.51	15.551	
Average	363,055.40	366,228.08	-3,172.68	(18.724)
Standard Deviation	15,959.99	15,959.85	-3,172.68	12,378.56

3. RESULTS AND DISCUSSION

3.1 Current waste management process flow in Bengkulu City

The process begins with the source of waste, which primarily originates from residential areas and public places such as markets, streets, and commercial zones. Following waste generation, the next step is waste collection, which is carried out by both the private sector and the city authority, ensuring that waste is gathered efficiently from different locations. After collection, waste is transported through the transportation system, which is also managed by both private operators and the city authority, delivering the waste to designated disposal sites. The final stage of the process is the landfill, where waste is disposed of through open dumping. This traditional method poses environmental concerns, emphasizing the need for improved waste management practices, such as sustainable disposal techniques and waste reduction strategies. The flow of the solid waste management process in Bengkulu City is presented in Figure 5.

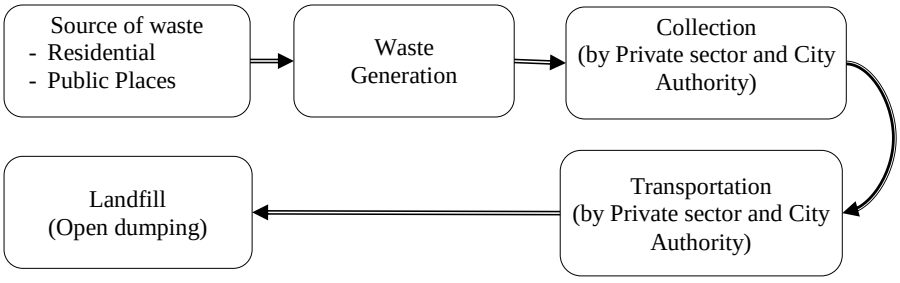

Figure 5. Process flow of solid waste management in Bengkulu City

3.2 Population projections

The population growth of Bengkulu City has demonstrated a consistent upward trend over the past decade. Based on historical data, the population increased from 334,500 persons in 2013 to 384,800 persons in 2022. In the period between 2013 and 2017, the city experienced a relatively steady annual growth rate, with the population rising from 334,500 to 366,435 persons, driven by natural population growth and rural-to-urban migration (Figure 6).

However, starting in 2018, the growth rate began to decelerate slightly. This slowing trend became more apparent during the onset of the COVID-19 pandemic in 2020. The pandemic, which caused significant social and economic disruption globally, also impacted population dynamics in Bengkulu City. Although the city's population continued to grow during 2020-2022, the rate of increase was moderated due to several factors, including restrictions on population movement, increased mortality rates, and delays in internal migration. In 2020, the population reached 373,600 persons, increasing modestly to 378,600 in 2021 and 384,800 in 2022.

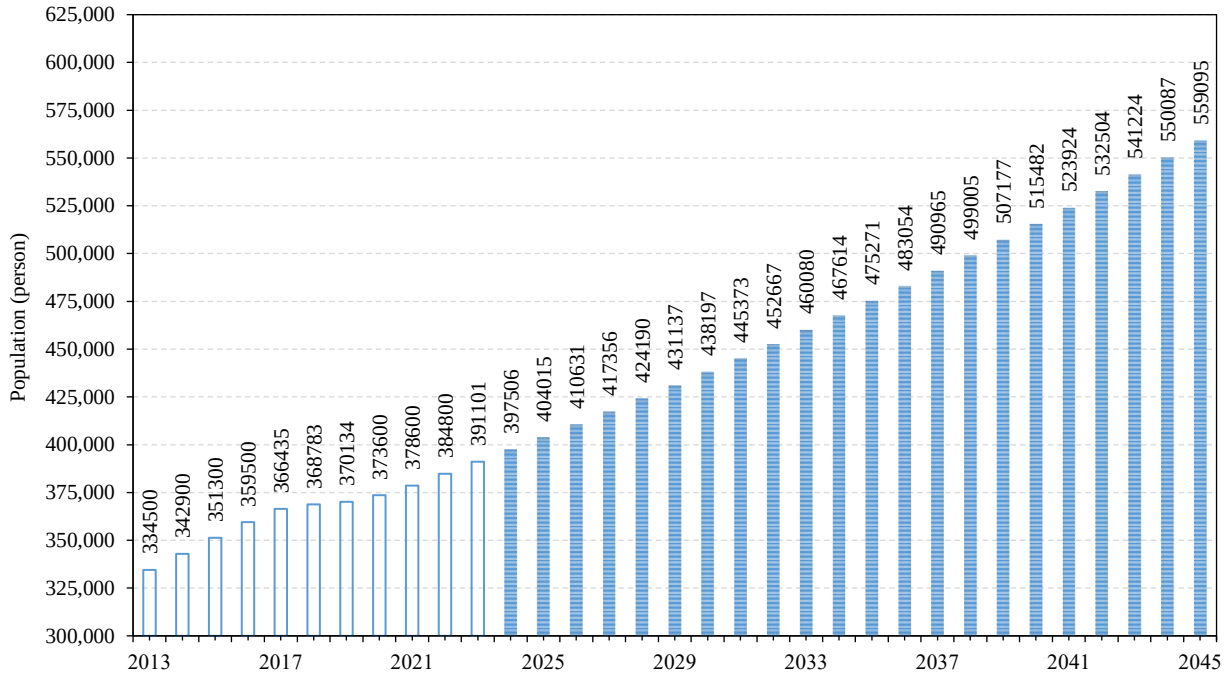

Figure 6. Population projections until 2045

Post-pandemic recovery, beginning in 2023, is projected to restore the city's population growth trajectory. With improvements in public health conditions, economic activities, and mobility, Bengkulu City's population is expected to continue increasing, reaching 559,095 persons by 2045. The projection suggests that, while the pandemic temporarily affected the growth rate, its long-term impact on the overall population trend remains limited, as growth is anticipated to steadily resume in the years following the pandemic. This population forecast provides critical input for urban planning, infrastructure development, and public service provision in Bengkulu City, ensuring that future growth is accommodated in a sustainable and well-managed manner.

3.3 Waste generation

Based on Figure 7, the volume of waste generation in Bengkulu City is projected to increase steadily from 368,664 cubic meters in 2025 to 510,174 cubic meters by 2045. This growth is closely linked to the city's rising population, driven by natural growth and ongoing internal migration from rural areas to the urban center. The movement of people seeking better economic opportunities, education, and services contributes to a higher concentration of waste production, particularly in residential, commercial, and public areas.

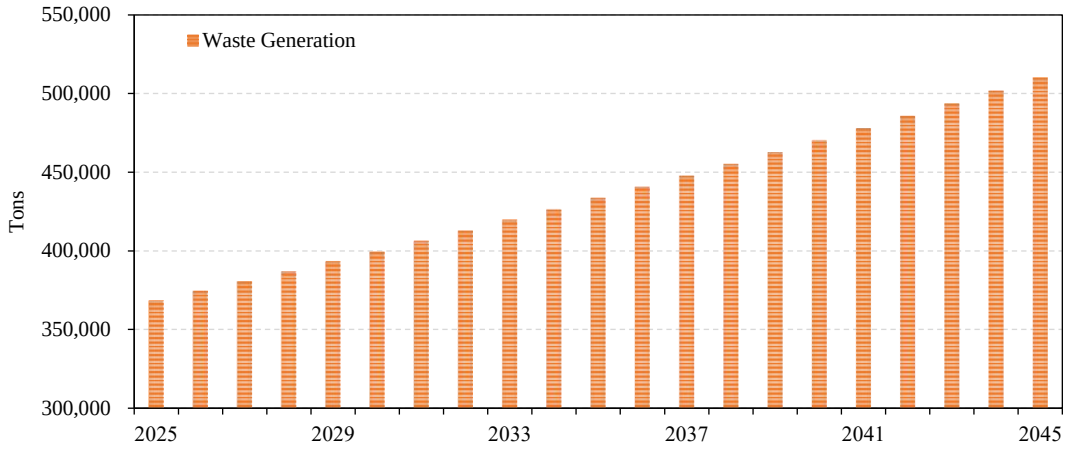

Figure 7. Graph of total waste increase in Bengkulu City from 2025 to 2045

In addition, Bengkulu's improving economic conditions following the COVID-19 pandemic are expected to influence waste generation patterns. As household incomes rise and consumption habits shift towards packaged and processed goods, the volume of waste produced per capita will gradually increase. This projection underscores the urgent need for the city to strengthen its waste management infrastructure, expand waste reduction programs, and promote sustainable lifestyle practices to ensure environmental sustainability in line with future urban and economic development.

Without intervention, the surge in waste could overburden landfills, increase pollution, and escalate management costs. Sustainable strategies such as source reduction, recycling, composting, and advanced waste processing technologies are crucial. The Integrated Solid Waste Management (ISWM) approach, based on the 3R (Reduce, Reuse, Recycle) concept, offers a systematic solution tailored to local conditions (Behera and Samal, 2022; Devi et al., 2023; Pinha and Sagawa, 2020).

3.4 The challenges involved in solid waste reduction

In the years ahead, Bengkulu City is expected to encounter serious challenges in managing and reducing its solid waste. The combination of rapid population growth, internal migration, and increasing economic activities will contribute to a steady rise in waste generation. A significant portion of this waste consists of organic materials such as food waste, leaves, and market waste, while the rest is dominated by plastics and other non-organic materials. Limited public awareness, weak waste segregation practices, and overdependence on the already overloaded Air Sebakul landfill are major obstacles in reducing the volume of waste disposed of at final disposal sites.

To address these issues, Bengkulu City must prioritize integrated waste reduction strategies by promoting recycling and composting at the source. Community-based waste banks (bank sampah) and local recycling initiatives should be expanded to encourage residents to sort recyclable materials like plastics, paper, and metals. Meanwhile, composting programs targeting organic waste from households, traditional markets, and public spaces can significantly reduce the amount of biodegradable waste sent to landfills. The introduction of decentralized composting sites and household composting campaigns would help manage organic waste efficiently while producing valuable compost for urban agriculture. These combined efforts, supported by strong policy enforcement, public education, and private sector participation, will be crucial in creating a sustainable and effective solid waste management system for Bengkulu City in the future.

In this study, four levels of waste reduction scenario simulation were conducted. Reduction scenarios were developed to project varying levels of intervention within the waste management system, ranging from a business-as-usual approach to the most ambitious reduction targets. These scenarios reflect not only the expected reduction rates but also the complexity and intensity of the efforts required at each level. The no reduction scenario (0%) represents the existing condition, where the waste management system operates without significant improvements. At this stage, most waste is collected and disposed of in landfills, with minimal sorting, processing, or recycling. The system remains focused on end-of-pipe

solutions such as collection and disposal, with limited upstream intervention or waste minimization strategies. The minimum reduction scenario (25%) reflects early-stage efforts to reduce waste generation. This includes the introduction of basic waste separation at the household level, as well as the promotion of community-scale composting and waste bank initiatives. Public participation begins to emerge, but institutional transformation remains limited. Waste reduction reaches approximately one-fourth of the total waste generated.

The moderate reduction scenario (50%) represents a transitional phase toward a more integrated system. Institutional roles become stronger, with increased involvement from local governments, the private sector, and civil society. Waste processing technologies are introduced more systematically, regulations are enforced more consistently, and cross-sector partnerships are established. At this stage, up to 50% of the waste is successfully diverted through composting, recycling, and source reduction efforts. The optimistic reduction scenario (60-65%) reflects an ideal condition in which nearly all organic waste is converted into compost, while inorganic materials such as plastic, paper, and metal are recycled to the fullest extent possible. The waste management system becomes holistic and fully integrated, supported by appropriate technologies, strong policy enforcement, financing mechanisms, and stakeholder collaboration. Waste reduction reaches its highest level, demonstrating the realization of circular economy principles at the city scale.

3.5 Waste generation with reduction

Based on Figure 8, Bengkulu City is projected to generate a cumulative waste volume of 12,979,047 m^3 over the next 20 years, reflecting a significant challenge in waste management amid population growth and lifestyle changes. This increasing waste volume demands more effective management strategies, particularly in reducing waste generation at its source. The Air Sebakul landfill, which has been in operation for 32 years, is now in a critical condition with its capacity exceeded, making it unable to accommodate more waste. This challenge is further complicated by the Regional Spatial Planning Regulation of Bengkulu City 2021-2041, which does not allocate land for a new landfill, accelerating the urgency of waste reduction strategies such as composting, recycling, and reducing plastic use. Programs like Waste Banks, public education, and the development of recycling infrastructure are priority steps to ensure sustainable waste management. Without proper intervention, Bengkulu City risks facing an environmental crisis that could impact public health and overall quality of life. Therefore, collaboration between the government, the community, and the private sector is essential to establish a more sustainable waste management system and ensure Bengkulu City's livability in the future.

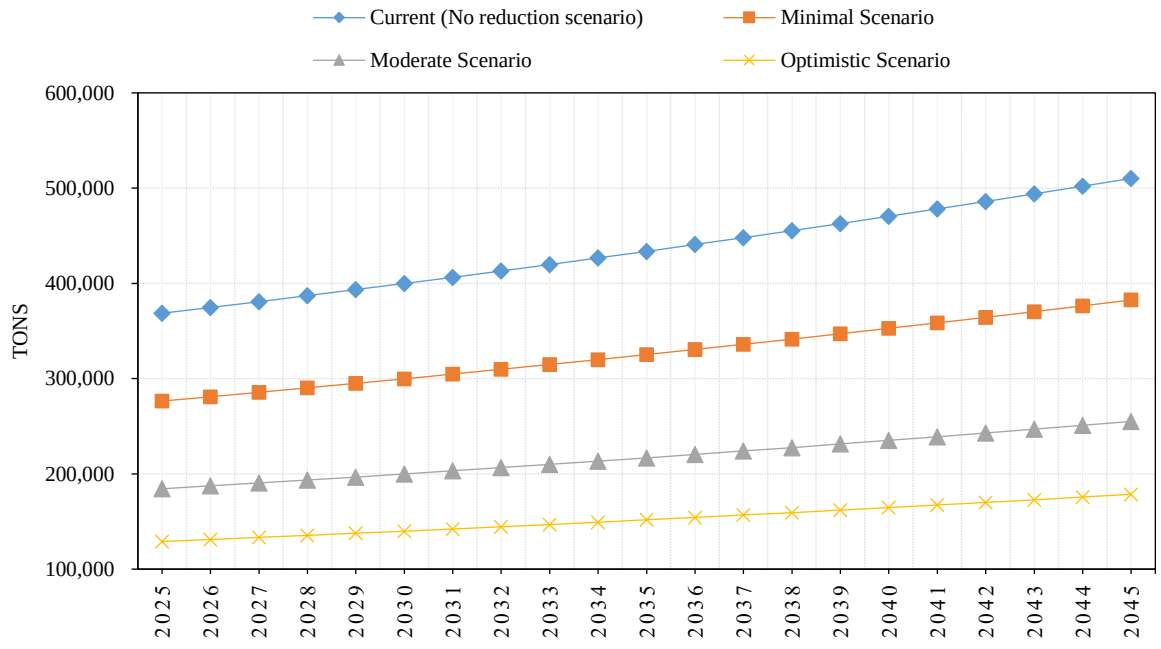

Figure 8. Simulation and projection of residue to landfill with not reduction and reduction scenarios

The simulation and projection results in Figure 8 illustrate the trends of waste residue directed to the landfill under four reduction scenarios in Bengkulu City from 2025 to 2045. In the Existing Reduction scenario, where no substantial waste minimization improvements are applied, the amount of residue increases steadily each year, driven by continuous population growth and rising waste generation rates. The Minimum Reduction scenario, assuming a 20% reduction effort, results in a slightly lower but still increasing trend of landfill residue, indicating that minimal intervention is insufficient to control waste accumulation in the long term. These two scenarios demonstrate how inadequate reduction efforts will sustain high dependency on landfill disposal and threaten the availability of landfill space in the city.

Conversely, the Moderate Reduction scenario, targeting a 50% reduction rate, effectively slows the growth of waste residue sent to the landfill. This projection highlights the positive impact of applying intermediate reduction measures such as waste sorting, recycling programs, and community-based composting initiatives. The Optimistic Reduction scenario, assuming a 65% reduction rate, shows the most promising outcome, maintaining a relatively stable and low volume of landfill residue throughout the projection period. This scenario underscores the importance of comprehensive and consistent waste reduction efforts to sustainably manage urban waste and minimize environmental and spatial burdens from landfill dependency. The comparison between these scenarios confirms that achieving higher reduction rates is essential for ensuring sustainable waste management in Bengkulu City over the next two decades.

3.6 Projection of landfill land requirements until 2045

To estimate the land area required for landfilling purposes, the volume of waste must be calculated from the mass using a density-based conversion. According to SNI 19-2454-2002, the maximum waste thickness (before final closure) is typically 20-30 meters, depending on site-specific design and geological conditions. For the purpose of this estimation, the final depth is assumed to be 30 meters. The density of household waste varies significantly depending on the level of compaction: uncompacted waste averages 150-250 kg/m³, medium compacted 300-400 kg/m³, and densely compacted (e.g., sanitary landfills) about 500 kg/m³ (Table 3).

$$\text{Volume } (m^3) = \frac{\text{Density } (\frac{kg}{m^3})}{\text{Weight (kg)}} e; \quad (m^3)$$

Table 3. Landfill area by waste weight

Waste compaction level	Density (kg/m³)	Volume (m³) per ton	Land area required for landfill (layer depth 30 m)
Uncompacted	200	5,000	167 m^2
Moderately compacted	300	3,300	111 m^2
Densely compacted	500	2,000	67 m^2

The implementation of waste reduction strategies across four distinct reduction scenarios demonstrates substantial potential for land use efficiency. The current scenario requires 29.28 hectares, whereas the Minimum, Moderate, and Optimistic scenarios require only 8.78, 5.86, and 4.10 hectares, respectively. The Optimistic scenario represents the smallest land increase, approximately 0.17-0.24 hectares per year. By implementing waste reduction strategies, the city can save more than 23 hectares, reduce environmental impact, and enhance waste management sustainability (Figure 9). Without intervention, waste accumulation over 20 years is projected to reach 8,782,842.61 m³, requiring 29.28 hectares of land. Waste reduction by 25%, 50%, and 65% would decrease land requirements to 8.78, 5.86, and 4.10 hectares, respectively. Compaction of waste up to 70% can save land and costs by up to 73% (Banerjee et al., 2023) . Moreover, landfills contribute 15% of global methane emissions, exacerbating climate change (Guo et al., 2024).

The simulation and projection results in Figure 9 reveal the long-term implications of four waste reduction scenarios on cumulative landfill land requirements in Bengkulu City over a 20-year planning horizon (2025-2045). Under the Existing Reduction scenario, where current waste management practices continue without significant improvement, the projected landfill area requirement reaches 29.28 hectares by 2045. This substantial land demand

highlights the unsustainable nature of the existing system, where the continuous increase in waste generation and minimal reduction efforts result in accelerated land consumption for landfill purposes.

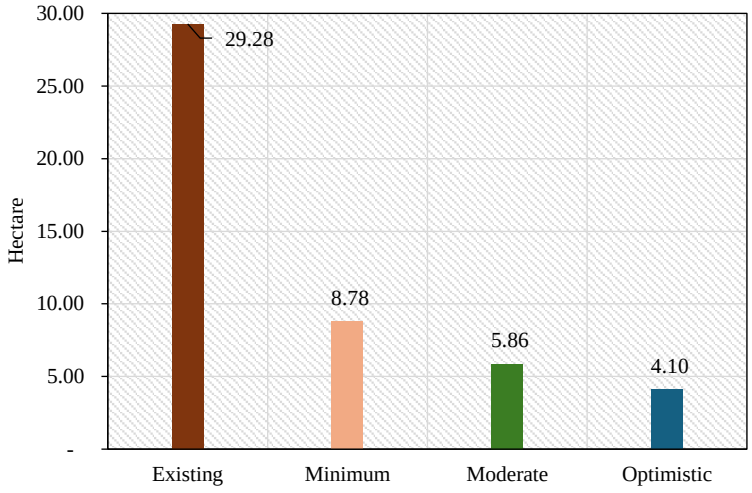

Figure 9. Simulation and projection of cumulative landfill area until 2045 with a reduction scenario

In contrast, implementing higher waste reduction rates considerably reduces the projected landfill area requirements. The Minimum Reduction scenario (21% reduction) lowers the need to 8.78 hectares, while the Moderate Reduction scenario (50% reduction) further decreases land requirements to 5.86 hectares. The most effective outcome is observed in the Optimistic Reduction scenario (65% reduction), which limits the cumulative landfill land requirement to only 4.10 hectares by 2045. These projections emphasize the critical importance of integrating progressive waste reduction strategies into urban waste management policies to ensure sustainable land use, protect environmental quality, and extend the operational lifespan of landfill facilities in Bengkulu City.

3.7 Handling cost, total retribution and saving cost

The simulation results demonstrate distinct financial patterns for waste management in Bengkulu City under four waste reduction scenarios over a 20-year projection. In the Existing Scenario, both handling costs and total retribution steadily increase from 2025 to 2045, with handling costs consistently surpassing revenue from retributions. Although cost savings show gradual growth, they remain insufficient to offset the rising operational expenses. This trend highlights the financial vulnerability of maintaining the current waste management system without adopting additional reduction measures.

Under the Minimum Reduction Scenario (20% reduction), financial performance improves modestly. Handling costs grow at a slower rate compared to the existing condition, while cost savings increase progressively due to reduced waste volumes requiring treatment and disposal. However, despite this improvement, a noticeable financial gap between handling costs and total retribution persists by 2045, suggesting that limited reduction efforts provide some relief but are inadequate for achieving sustainable financial equilibrium in waste management operations (Figure 10).

The Moderate Reduction Scenario (50%) and Optimistic Reduction Scenario (65%) show considerably better financial outcomes. In the Moderate Scenario, handling costs grow more gradually, while cost savings significantly increase, gradually narrowing the financial gap with retribution revenue. The most favorable outcome appears in the Optimistic Scenario, where waste reduction efforts substantially limit cost increases, and cumulative cost savings almost match the total handling expenses by 2045. This indicates that aggressive and well-integrated waste reduction strategies not only alleviate environmental pressure but also strengthen the city's fiscal capacity to manage waste sustainably in the long term.

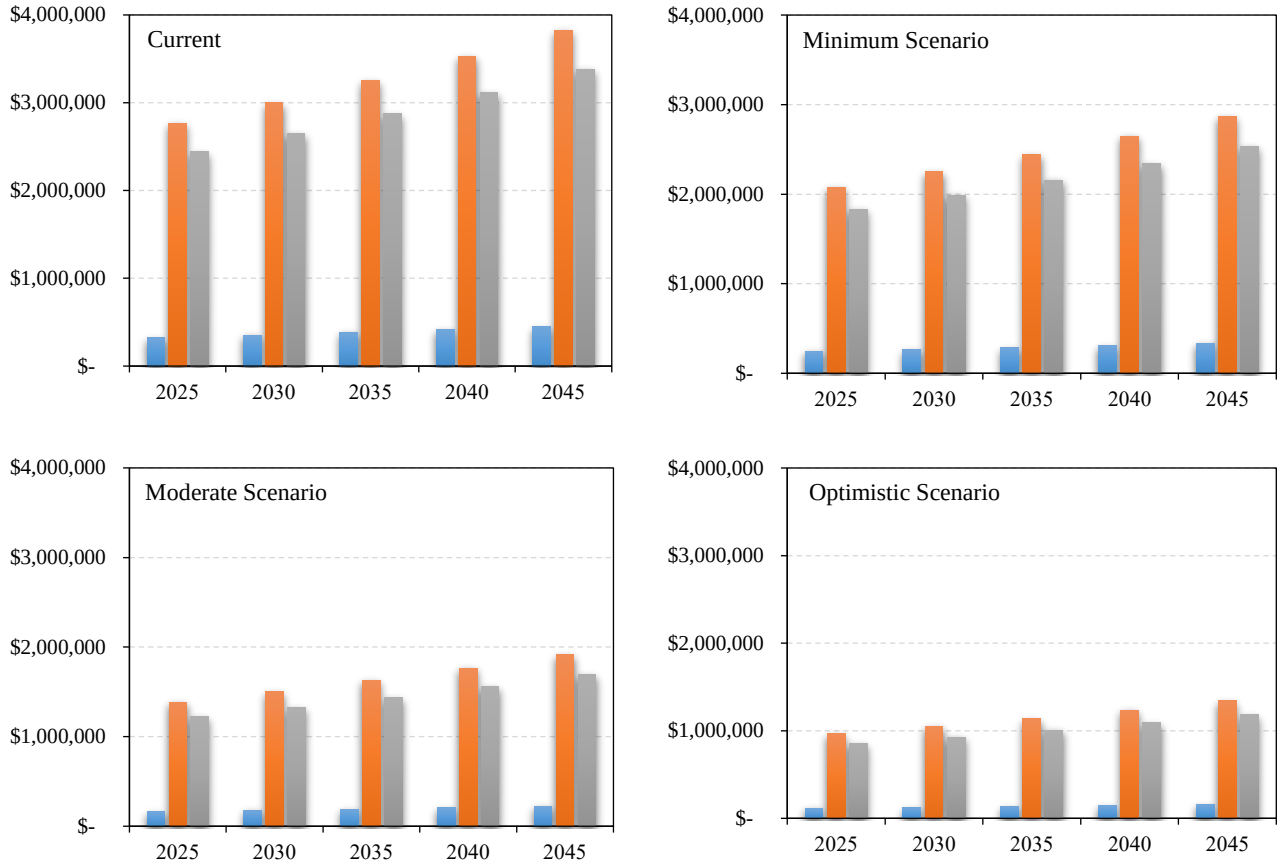

Figure 10. Simulation and projection of handling costs, total retribution and cost savings until 2045 with four reduction scenario

3.8 Scenario model

3.8.1 Without reduction (Existing)

In the absence of a waste reduction scenario, household waste volume will continue to increase, further burdening landfills. As these landfills fill quickly, they lead to soil, water, and air pollution. Methane emissions from decomposing organic waste contribute significantly to global warming, while landfill costs and space limitations will become increasingly problematic.

Therefore, reduction strategies such as reducing, reusing, and recycling are essential for sustainable waste management and budget optimization (Boateng et al., 2023; Del Carmen-Niño et al., 2023; Nepal et al., 2023; Ugwu et al., 2021).

3.8.2 Minimum scenario

The growth of Waste Banks in Bengkulu City since 2022 has shown positive development as part of the government's and community's efforts to enhance the effectiveness and sustainability of waste management. Currently, five active Waste Bank units operate with a primary focus on managing recyclable waste, such as plastic and paper. However, the absence of composting programs within Waste Bank operations has restricted the overall waste reduction impact. Therefore, there is significant potential to expand waste management initiatives, particularly by integrating composting into the Waste Bank system and Integrated Waste Management Facilities (IWMF). With optimal support from the community, government, and private sector, Bengkulu City has the potential to achieve a waste reduction target of up to 25% (Abubakar et al., 2022). Strategic measures such as developing waste processing infrastructure, educating the public on waste separation, and optimizing recycling and composting systems can enhance the effectiveness of sustainable waste management (Behera and Samal, 2022; Knickmeyer, 2020; Lim et al., 2016).

3.8.3 Moderate scenario

Achieving a 50% waste reduction through programs like "Merdeka Sampah" in Bengkulu City is certainly a significant challenge. However, with the right approach, the chances of success are considerable. The following factors need to be considered: 1) public awareness and participation; 2) development of infrastructure and technology; 3) multi-sector collaboration; 4) regulations and policies;

and 5) community independence and innovation. Achieving a 50% waste reduction through the "Merdeka Sampah" program in Bengkulu City is remains possible, but it requires intensive collaboration between the government, community, and private sector. Public awareness, infrastructure support, enabling policies, and local innovation are key factors that will determine the success of this program remains possible. With the right strategies and effective implementation, the chances of reaching this target are high, but it will require long-term commitment and continuous adaptation to emerging challenges. Recycling capacity can be increased from 39% to 100% by strengthening informal recycling facilities (Kala et al., 2022).

3.8.4 Optimistic scenario

To achieve the 65% waste reduction target in Bengkulu City, an integrated strategy is required, which includes: 1) strengthening waste separation at the source by providing adequate facilities and incentives for residents, 2) developing composting programs at both community and city levels, 3) expanding Waste Banks across all neighborhoods with a specific focus on different waste types and collaboration with the recycling industry, 4) implementing innovative technologies, such as digital applications and waste-to-energy conversion, and 5) enforcing waste separation policies through clear regulations and sanctions.

Waste reduction can be achieved by limiting the use of hard-to-recycle materials, promoting composting, and engaging the private sector. Thus, it is essential to include corporate social responsibility CSR initiatives and strategic partnerships. The government should play a key role by facilitating education and training programs, as well as providing incentives and recognition for successful waste management efforts. Additionally, regular monitoring and evaluation are necessary to assess impact and make policy adjustments. With an integrated strategy that includes source separation, appropriate management technology, supportive policies, and multi-stakeholder collaboration, the target waste reduction target of up to 65% can be achieved. Through strong community involvement, Bengkulu City has the potential to become a model for effective and sustainable waste management.

3.9 Impact of parameters on achieving waste reduction

Effective waste reduction strategies must address critical parameters that enhance the efficiency and sustainability of urban solid waste management systems. First, strengthening the waste sorting system at the source is essential because it improves the effectiveness of downstream processes, such as recycling and composting.

Second, developing community- and municipal-level composting methods can divert large volumes of organic waste from landfills while producing valuable compost. Third, expanding the capacity and outreach of waste banks can incentivize recycling behavior and improve material recovery rates. Fourth, adopting advanced waste management technologies, such as mechanized sorting, anaerobic digestion, and incineration with energy recovery, can increase system-wide efficiency. Additionally, effectively enforcing policies and regulations ensures compliance and promotes accountability among stakeholders. Collaborating with the private sector is also vital for mobilizing investments, innovation, and operational expertise. Lastly, establishing mechanisms for periodic monitoring and evaluation enables data-driven decision-making, continuous improvement, and policy refinement. Together, these parameters form the foundation for a comprehensive, resilient waste reduction framework.

The structured evaluation presented in Table 3 demonstrates a clear progression in the perceived importance of seven key waste management parameters across four waste reduction scenarios: Existing (0%), Minimum (25%), Moderate (50%), and Optimistic (65%). Using a five-point ordinal scale (☆ to ☆☆☆☆☆), each parameter exhibits a steady increase in importance as the reduction targets become more ambitious. Descriptive statistical analysis reveals a strong linear trend, with the average importance score rising from 1.43☆ in the baseline scenario to 5.00☆ in the most ambitious scenario—representing an overall increase of more than 249%. These findings suggest a systemic transition from conventional waste handling practices to more integrated and transformative management approaches.

Table 3. Matrix of the importance level of parameter in each reduction scenario

No	Parameter	Scenario			
		Existing (0%)	Minimum (25%)	Moderate (50%)	Optimist (65%)
1	Strengthen the waste sorting system at the source	☆	☆☆	☆☆☆☆	☆☆☆☆☆
2	Develop composting methods at both community and city scales	☆	☆☆☆	☆☆☆☆☆	☆☆☆☆☆
3	Expand the capacity and reach of the waste bank	☆	☆☆☆	☆☆☆☆	☆☆☆☆☆
4	Implement advanced waste management technologies	☆	☆☆	☆☆☆☆	☆☆☆☆☆
5	Enforce policies and regulations effectively	☆☆	☆☆☆	☆☆☆☆	☆☆☆☆☆
6	Foster collaboration and partnership with the private sector	☆☆	☆☆☆	☆☆☆☆	☆☆☆☆☆
7	Conduct periodic monitoring and evaluation	☆☆	☆☆☆	☆☆☆☆	☆☆☆☆☆
	Amount	**1.43☆**	**2.71☆**	**4.14☆**	**5.00☆**

Description:

☆	Less important	☆☆☆☆	Very important
☆☆	Quite Important	☆☆☆☆☆	Very - very important
☆☆☆	Important		

In the baseline scenario (0%), the waste management system remains predominantly traditional, with most parameters rated as "less important" or "quite important." Strategies such as composting, waste bank expansion, and the implementation of advanced technologies are not yet considered priorities. However, in the Minimum (25%) scenario, the average score increases significantly to 2.71☆—an 89.5% improvement—indicating an emerging recognition of community-based and decentralized interventions. This upward trajectory continues in the Moderate (50%) scenario, where the average importance score reaches 4.14☆. At this stage, nearly all parameters are rated as "very important," reflecting a growing institutional commitment to strategies that integrate technological innovation, policy enforcement, and multi-sectoral collaboration.

In the Optimistic (65%) scenario, all parameters achieve the maximum rating of 5.00☆, indicating a consensus on the critical role each component plays in achieving substantial waste reduction. This uniformity underscores the necessity of a comprehensive and synergistic approach, encompassing source-level waste sorting, large-scale composting, expanded waste bank systems, advanced technological adoption, effective regulatory frameworks, private sector engagement, and continuous monitoring and evaluation. The high degree of linear correlation ($R^2 \approx 0.99$) between the level of reduction target and the average importance score further confirms that the prioritization of these parameters intensifies in direct proportion to the system's performance goals. Accordingly, the realization of ambitious waste reduction targets necessitates multi-dimensional interventions that extend beyond physical infrastructure and formal regulation, and instead emphasize behavioral change, institutional integration, and stakeholder-driven solutions.

Applying a dynamic system model to waste management in Bengkulu City provides a holistic, strategic approach to responding to the complexity of the waste management system while improving the effectiveness of policies and the efficiency of operations in accordance with the city's capacity and characteristics. Simulations of four waste reduction policy scenarios namely, no intervention, minimum reduction, moderate reduction, and optimistic reduction were conducted by considering important parameters such as population growth rate, waste generation volume, recycling capacity, and community participation.

The simulation results for each scenario provide projections for waste generation, management budget requirements, and estimated landfill area in the short and long term. This information is crucial for decision-makers to select the most rational and sustainable scenario, reducing operational costs and optimizing the use of available resources. Thus, this approach makes the planning process more data-driven and adaptable to environmental and social dynamics. Furthermore, integrating dynamic system models with digital technologies, such as real-time waste volume monitoring, citizen reporting applications, and information management systems, improves accountability and public engagement. Collaboration between stakeholders, including the community, the private sector, and educational institutions, can be

strengthened to create an inclusive, integrated waste management ecosystem. Therefore, Bengkulu City has strong potential to become a pilot medium-sized city for the implementation of smart, participatory, and sustainable environmental governance.

Bengkulu City and the Brazilian case study share similar challenges in waste management, particularly low recycling rates, limited public participation, and inadequate infrastructure. The Brazilian model, which aims to raise dry waste collection from 8.5% to 15% in ten years, highlights the importance of improving sorting efficiency—an equally relevant goal for Bengkulu. However, the financial unsustainability of recycling programs, as shown in Brazil's reliance on subsidies, also reflects conditions in Bengkulu. While Brazil has begun using system dynamics (SD) modeling to influence recycling behavior, Bengkulu is still in the early stages of exploring such tools (Pinha and Sagawa, 2020). Similar issues are evident in Yogyakarta and Depok (Artika and Chaerul, 2020; Habibah et al., 2020), where waste management policies face barriers such as low public awareness, weak institutional coordination, and poor infrastructure. In Yogyakarta, system modeling indicates ineffective implementation due to cultural and structural gaps, while in Depok, future waste projections call for expanded treatment capacity to reduce landfill use. However, this requires significant investment, posing financial challenges for local governments. These cases highlight the urgent need for integrated, participatory, and financially sustainable waste strategies across Indonesian cities, including Bengkulu.

Applying a dynamic systems model to waste management in Bengkulu City offers a comprehensive and strategic framework for addressing the complexity of urban waste systems. This approach aligns policies with the city's unique capacity and characteristics, while also enhancing the effectiveness of interventions and operational efficiency. By simulating four policy scenarios—no intervention, minimum reduction, moderate reduction, and optimistic reduction—the model provides insights into the implications of each strategy, incorporating critical parameters such as population growth, waste generation volume, recycling capacity, and levels of community participation. The results of these simulations yield valuable projections related to future waste generation, budgetary requirements, and the expansion of landfill areas. These outputs are essential for policymakers seeking to identify the most rational and sustainable options, particularly in balancing operational costs and resource availability. The data-driven nature of the model supports more informed and adaptive planning processes, allowing the city to anticipate environmental and social changes while maintaining effective waste services.

Further value is added when the dynamic model is integrated with emerging digital technologies. Tools such as real-time waste monitoring systems, citizen reporting apps, and centralized information platforms enhance both accountability and public involvement. These technologies facilitate transparent governance and efficient service delivery, while also encouraging citizens to actively participate in managing their waste. In turn, the model enables better responsiveness to public feedback and real-time data, fostering a more agile and effective system. Finally, the adoption of this model serves as a catalyst for multi-stakeholder collaboration involving local communities, the private sector, and academic institutions. Such engagement promotes the development of an inclusive and integrated waste management ecosystem. With these capabilities, Bengkulu City is well-positioned to serve as a model for other medium-sized cities aiming to implement smart, participatory, and sustainable environmental governance. The dynamic systems model not only offers technical improvements but also reinforces the long-term vision of a resilient and future-ready urban management framework.

4. CONCLUSION

This study demonstrates the effectiveness of a system dynamics approach in addressing the complex challenges of municipal solid waste management in Bengkulu City. By simulating four waste reduction scenarios over a 20-year period, the model provides valuable insights into the environmental and financial implications of various intervention levels. The findings reveal that without proactive measures, rapid population growth and increased consumption will severely strain existing landfill capacity and escalate management costs. Conversely, integrated waste reduction strategies—encompassing source separation, composting, waste bank expansion, technological innovation, and policy enforcement—substantially mitigate environmental pressures while optimizing land and financial resources.

The moderate and optimistic reduction scenarios, achieving 50% and 65% waste reduction respectively, offer the most sustainable outcomes by lowering landfill dependency, reducing operational

expenses, and enhancing resource recovery. Furthermore, the incorporation of digital monitoring tools and multi-stakeholder collaboration strengthens waste governance, promotes public participation, and improves service accountability. This study underscores the importance of systemic, data-driven planning to transition towards a circular economy framework. The proposed dynamic model serves as an adaptable decision-support tool for urban policymakers, providing a strategic pathway for medium-sized cities seeking to implement inclusive and sustainable waste management systems.

ACKNOWLEDGEMENTS

The author would like to thank the Department of Environmental Health, Health Polytechnic, Ministry of Health, Bengkulu, Indonesia, for facilitating this research and providing the necessary study permits.

AUTHOR CONTRIBUTIONS

Conceptualization, Formal Analysis, Investigation, Software, Resources and writing, Defi Ermayendri; Methodology, Wahyudi Arianto; Validation, Marulak Simarmata; Writing-Original Draft Preparation; Writing-Review and Editing, Riwandi and Ketut Sukiyono.

DECLARATION OF CONFLICT OF INTEREST

We hereby declare that the manuscript entitled "Dynamic Integrated Model of Sustainable Solid Waste Management in Bengkulu City" is an original scientific work that has never been published before in any form and is not in the process of being reviewed or published in other journals. We ensure that all data, analysis, and interpretation presented in this manuscript are the results of research conducted using valid methods and in accordance with scientific standards. All forms of quotations, references, and contributions from other parties have been given proper credit through appropriate citations. We also declare that there is no form of plagiarism in this manuscript, either directly or indirectly. If in the future there is a violation of publication ethics, I/we are willing to accept the consequences set by the journal. All authors involved in the preparation of this manuscript have made significant contributions, both in research design, data analysis, and preparation of scientific articles. No names are listed as authors without substantial scientific contributions.

We hereby submit the publication rights to the Environment and Natural Resources Journal, in accordance with the provisions applicable in the journal's publishing policy.

REFERENCES

Abubakar IR, Maniruzzaman KM, Dano UL, AlShihri FS, AlShammari MS, Ahmed SMS, et al. Environmental sustainability impacts of solid waste management practices in the global south. International Journal of Environmental Research and Public Health 2022;19(19):Article No. 12717.

Artika I, Chaerul M. Dynamic system model for waste management scenario evaluation in Depok City. Jurnal Wilayah dan Lingkungan 2020;8(3):261-79 (in Indonesian).

Banerjee S, Chakraborty S, Banerjee S, Dutta A. Decision making and economical optimization of a city scale solid waste management system: An integrated model simulation on Kolkata, India. Materials Today: Proceedings 2023. DOI: 10.1016/j.matpr.2023.07.238.

Behera S, Samal K. Sustainable approach to manage solid waste through biochar assisted composting. Energy Nexus 2022;7:Article No. 100121.

Blakeslee J, Kothari BH, McBeath B, Sorenson P, Bank L. Network indicators of the social ecology of adolescents in relative and non-relative Foster households. Children and Youth Services Review 2017;73:173-81.

Boateng S, Boakye-Ansah D, Baah A, Aboagye B, Kyeremeh PAG. Solid waste management practices and challenges in rural and urban senior high schools in Ashanti Region, Ghana. Journal of Environmental and Public Health 2023; 2023:Article No. 9694467.

Bornstein MH. Dynamic Systems Theory. In: The SAGE Encyclopedia of Lifespan Human Development. SAGE Publications, Inc.; 2018.

Bruno M, Abis M, Kuchta K, Simon FG, Grönholm R, Hoppe M, et al. Material flow, economic and environmental assessment of municipal solid waste incineration bottom ash recycling potential in Europe. Journal of Cleaner Production 2021;317:Article No. 128511.

Del Carmen-Niño V, Herrera-Navarrete R, Juárez-López AL, Sampedro-Rosas ML, Reyes-Umaña M. Municipal solid waste collection: Challenges, strategies and perspectives in the optimization of a municipal route in a Southern Mexican Town. Sustainability 2023;15(2):Article No. 1083.

Devi RU, Gangaraju G, Kumar KS, Balakrishna K. A sustainable approach for an integrated municipal solid waste management. In: Recent Trends in Solid Waste Management. Elsevier; 2023. p. 55-74.

do Carmo Precci Lopes A, Ebner C, Gerke F, Wehner M, Robra S, Hupfauf S, et al. Residual municipal solid waste as co-substrate at wastewater treatment plants: An assessment of methane yield, dewatering potential and microbial diversity. Science of the Total Environment 2022;804:Article No. 149936.

Dyson B, Chang N Bin. Forecasting municipal solid waste generation in a fast-growing urban region with system dynamics modeling. Waste Management 2005;25(7):669-79.

Environmental Services of Bengkulu City. Basic Information on the Air Sebakul Landfill, Bengkulu City. Bengkulu City Government; 2022.

Ferronato N, Torretta V. Waste mismanagement in developing countries: A review of global issues. International Journal of Environmental Research and Public Health 2019;16(6):Article No. 1060.

Forrester JW. Industrial Dynamics. MIT Press; 1961.

Fragkoulis D, Roux G, Dahhou B. Detection, isolation and identification of multiple actuator and sensor faults in nonlinear dynamic systems: Application to a waste water treatment process. Applied Mathematical Modelling 2011;35(1):522-43.

Free CM, Bellquist LF, Forney KA, Humberstone J, Kauer K, Lee Q, et al. Static management presents a simple solution to a dynamic fishery and conservation challenge. Biological Conservation 2023;285:Article No. 110249.

Friederich J, Lugaresi G, Lazarova-Molnar S, Matta A. Process mining for dynamic modeling of smart manufacturing systems: Data requirements. Procedia CIRP 2022;107:546-51.

Govani J, Singh E, Kumar A, Zacharia M, Rena, Kumar S. New generation technologies for solid waste management. In: Current Developments in Biotechnology and Bioengineering. Elsevier; 2021. p. 77-106.

Guerrero LA, Maas G, Hogland W. Solid waste management challenges for cities in developing countries. Waste Management 2013;33(1):220-32.

Guo D, Zhang S, Hou H, Zhang Y, Xu H. Synergistic evaluation methodology for pollution and carbon reduction in the field of solid waste resource utilization. Environmental Impact Assessment Review 2024;108:Article No. 107604.

Habibah E, Novianti F, Saputra H. Analysis of Factors Influencing the Implementation of Waste Management Policies in Yogyakarta Using Dynamic System Modeling. Jurnal Analisa Sociology 2020;9:124-36 (in Indinesia).

Hla SS, Roberts D. Characterisation of chemical composition and energy content of green waste and municipal solid waste from Greater Brisbane, Australia. Waste Management 2015;41:12-9.

Ibarra Vega D, Bautista-Rodriguez S. The impact of circular economy strategies on municipal waste management: A system dynamics approach. Cleaner Engineering and Technology 2024;21:Article No. 100761.

Kala K, Bolia NB, Sushil. Analysis of informal waste management using system dynamic modelling. Heliyon 2022;8(8):e09993.

Knickmeyer D. Social factors influencing household waste separation: A literature review on good practices to improve the recycling performance of urban areas. Journal of Cleaner Production 2020;245:Article No. 118605.

Kumar A, Samadder SR. A review on technological options of waste to energy for effective management of municipal solid waste. Waste Management 2017;69:407-22.

Lam CM, Yu IKM, Medel F, Tsang DCW, Hsu SC, Poon CS. Life-cycle cost-benefit analysis on sustainable food waste management: The case of Hong Kong International Airport. Journal of Cleaner Production 2018;187:751-62.

Lee U, Han J, Wang M. Evaluation of landfill gas emissions from municipal solid waste landfills for the life-cycle analysis of waste-to-energy pathways. Journal of Cleaner Production 2017;166:335-42.

Li G, Wang W-Jing, You X-Yi. Social-economic assessment of integrated waste pickers in municipal solid waste management system: A case of Tianjin in China. Journal of Cleaner Production 2024;434:Article No. 140302.

Lim SL, Lee LH, Wu TY. Sustainability of using composting and vermicomposting technologies for organic solid waste biotransformation: Recent overview, greenhouse gases emissions and economic analysis. Journal of Cleaner Production 2016;111:262-78.

Mai L, Bao LJ, Wong CS, Zeng EY. Microplastics in the terrestrial environment. In: Microplastic Contamination in Aquatic Environments. Elsevier; 2018. p. 365-78

Meena MD, Dotaniya ML, Meena BL, Rai PK, Antil RS, Meena HS, et al. Municipal solid waste: Opportunities, challenges and management policies in India: A review. Waste Management Bulletin 2023;1(1):4-18.

Moya D, Aldás C, López G, Kaparaju P. Municipal solid waste as a valuable renewable energy resource: A worldwide opportunity of energy recovery by using waste-to-energy technologies. Energy Procedia 2017;134:286-95.

Nepal M, Karki Nepal A, Khadayat MS, Rai RK, Shyamsundar P, Somanathan E. Low-cost strategies to improve municipal solid waste management in developing countries: Experimental evidence from Nepal. Environmental and Resource Economics 2023;84(3):729-52.

Pfister F, Bader HP, Scheidegger R, Baccini P. Dynamic modelling of resource management for farming systems. Agricultural Systems 2005;86(1):1-28.

Pinha ACH, Sagawa JK. A system dynamics modelling approach for municipal solid waste management and financial analysis. Journal of Cleaner Production 2020;269:Article No. 122350.

Radosavljevic S, Banitz T, Grimm V, Johansson LG, Lindkvist E, Schlüter M, et al. Dynamical systems modeling for structural understanding of social-ecological systems: A primer. Ecological Complexity 2023;56:Article No. 101052.

Rahman MN, Shozib SH, Akter MY, Islam ARMT, Islam MS, Sohel MS, et al. Microplastic as an invisible threat to the coral reefs: Sources, toxicity mechanisms, policy intervention, and the way forward. Journal of Hazardous Materials 2023;454:Article No. 131522.

Smith LB, Thelen E. Development as a dynamic system. Trends in Cognitive Sciences 2003;7(8):343-8.

Sołowski G, Konkol I, Cenian A. Production of hydrogen and methane from lignocellulose waste by fermentation: A review of chemical pretreatment for enhancing the efficiency of the digestion process Journal of Cleaner Production 2020;267:Article No. 121721

Sondh S, Upadhyay DS, Patel S, Patel RN. Strategic approach towards sustainability by promoting circular economy-based municipal solid waste management system: A review. Sustainable Chemistry and Pharmacy 2024;37:Article No. 101337.

Sterman JD. Systems dynamics modeling: Tools for learning in a complex world. IEEE Engineering Management Review 2002;30(1):8-25.

Thatcher A, Biyela P, Field TL, Hildebrandt D, Kidd M, Nadan S, et al. Contextualising urban sanitation solutions through complex systems thinking: A case study of the South African sanitation system. Journal of Cleaner Production 2024;451:Article No. 142084.

Ugwu CO, Ozoegwu CG, Ozor PA, Agwu N, Mbohwa C. Waste reduction and utilization strategies to improve municipal solid waste management on Nigerian Campuses. Fuel Communications 2021;9:Article No. 100025.

Wilson DC, Velis C, Cheeseman C. Role of informal sector recycling in waste management in developing countries. Habitat International 2006;30(4):797-808.

Zhang X, Feng D, Wang J, Sui A. Integrating renewable energy systems: Assessing financial innovation, renewable energy generation intensity, energy transition and environmental regulation with renewable energy sources. Energy Strategy Reviews 2024;56:Article No. 101567.

Zulkipli F, Nopiah ZM, Basri NEA, Kie CJ, Zulkepli J, Khalid KI. Integrated dynamical model for Malaysian solid waste management using system dynamics. International Journal of Engineering and Technology 2018;7(3):131-5.

Environment and Natural Resources Journal

Volume 23
Issue 6
2025

The Effect of Chemical Composition and Boiling Time in Kraft Method on Paper Making Based on Palm Oil Trunk (*Elaeis guineensis* Jacq.)

Muhammad Syukri[1*], Rina Maharany[2], M. Thoriq Al Fath[5], Ika Ucha Pradifta Rangkuti[3], Dina Arfianti Saragih[4], Dini Aprilia[3], Vikram Alexander[5], and Sarah Hafitz Syaurah[1]

[1]*Department of Chemical Engineering, Faculty of Science and Technology, Institut Teknologi Sawit Indonesia, Medan, Indonesia*
[2]*Department of Plantation Cultivation, Faculty of Vocation, Institut Teknologi Sawit Indonesia, Medan, Indonesia*
[3]*Department of Technology of Processing Plantation Products, Faculty of Vocation, Institut Teknologi Sawit Indonesia, Medan, Indonesia*
[4]*Department of Agribusiness, Faculty of Science and Technology, Institut Teknologi Sawit Indonesia, Medan, Indonesia*
[5]*Department of Chemical Engineering, Faculty of Engineering, Universitas Sumatera Utara, Jl. Almamater Kampus USU, Medan, Indonesia*

ARTICLE INFO

Received: 18 Nov 2024
Received in revised: 15 Jul 2025
Accepted: 16 Jul 2025
Published online: 20 Aug 2025
DOI: 10.32526/ennrj/23/20250004

Keywords:
Palm oil plantations / Waste / Cellulose / Tensile strength / Water absorption

*** Corresponding author:**
E-mail: msrk@itsi.ac.id

ABSTRACT

The rapid expansion of palm oil plantations in Indonesia generates significant waste, including an estimated 77.692 tons/ha of palm oil trunks. It is essential to recycling these trunks into valuable raw materials. Given their high cellulose content, palm oil trunks are promising for paper production. This study investigates the production of paper from palm oil trunks (*Elaeis guineensis* Jacq.) using the kraft process with variations in chemical composition and boiling time. Three chemical compositions are tested, involving sodium hydroxide (NaOH), sodium sulfate (Na_2SO_4), and sodium carbonate (Na_2CO_3), along with boiling times of 90, 120, and 150 min. Paper quality are analyzed through water absorption, tensile strength, grammage, and visual appearance. The optimal kraft method for water absorption and tensile strength involves a 120-minute boiling time and a chemical composition of 20% NaOH, 9% Na_2S, and 4% Na_2CO_3, resulting in a water absorption of 59.33 mm, tensile strength of 11.26 kN/m, and a grammage of 65 g/m². Additionally, the clean, hole-free surface of the best-performing paper further validates the method's effectiveness. This study demonstrates that high-quality paper can be produce from palm oil trunks using optimal kraft process parameters, supporting sustainable waste utilization.

HIGHLIGHTS

- Palm oil trunks were recycled into paper using the kraft process.
- The study varied chemicals and boiling times to optimize paper quality.
- The best results had 20% NaOH, 9% Na_2S, and 4% Na_2CO_3, boiled for 120 mins.
- Optimal paper showed 59.33 mm water absorption and 11.26 kN/m tensile strength.
- Findings support sustainable waste utilization by converting trunks to paper.

1. INTRODUCTION

The area of palm oil plantations continues to increase every year. The total area of palm oil plantations in Indonesia in 2022 is 14.99 million ha, an increase of 2.49% compared to the previous year, which was only 14.62% (Putra et al., 2024). Along with the increasing development of palm oil plantations, waste production will also increase, one of which is palm oil trunks. In 1 ha of palm oil plantations will produce palm oil trunk waste of 77.692 tons/ha (Veronika et al., 2019). If these palm oil trunks are left to rot on plantation land, during the rotting process,

Citation: Syukri M, Maharany R, Fath MTA, Rangkuti IUP, Saragih DA, Aprilia D, Alexander V, Syaurah SH. The effect of chemical composition and boiling time in kraft method on paper making based on palm oil trunk (*Elaeis guineensis* Jacq.). Environ. Nat. Resour. J. 2025;23(6):516-525. (https://doi.org/10.32526/ennrj/23/20250004)

they will release carbon into the atmosphere, thereby increasing the greenhouse effect (Ayundra et al., 2022). So far, palm oil trunks have been used as a substitute for wood, such as sandwich laminated lumber (SLL) or plywood (Kaima et al., 2023) and fiber cement (Zakaria and Soh, 2023). Apart from that, palm oil trunks can also be used as compost (Lau et al., 2024), fuel in the form of biopellets (Wistara et al., 2017), bioethanol (Siti et al., 2024), and brown sugar (Gozan et al., 2024).

Palm oil trunks have a high cellulose content, namely at the base of 51.58%, the middle of 50.86%, and the tip of 47.37%, palm oil trunk hemicellulose of 46.50%, and palm oil trunk lignin of 22.20% (Joseph et al., 2024). The high cellulose content in palm oil trunks can be used as raw materials in making paper. Some of the raw materials that have been used to make paper include *Acacia crassicarpa* (Sahan et al., 2024), a combination of sugarcane waste and rice husks (Abdelatif et al., 2024; Yennam et al., 2024), banana pseudo stem, banana leaf, and banana peduncle (Ferdous et al., 2021). Chemical papermaking can be done by three methods, namely the soda method, the sulfite method, and the kraft method (Michael et al., 2024). The soda method is done by cooking wood with a sodium hydroxide solution (Low et al., 2024). The sulfite method uses softwood as the raw material and an acidic cooking solution, namely a bisulfite solution of calcium (Ca) or magnesium (Mg) (Vachlepi, 2019).

The kraft method is a paper-making process with active chemicals consisting of sodium hydroxide (NaOH), sodium sulfate (Na_2SO_4), and sodium carbonate (Na_2CO_3) (Nova, 2011). In the kraft process, sodium sulfate (Na_2SO_4) is used to maximize the delignification process or removal of lignin from palm oil trunks. The lignin content in palm oil trunks will affect the boiling process (delignification). The delignification process aims to perfect the breaking of the lignin chain to produce a higher yield (Liu et al., 2024). The chemical composition of the kraft method in paper making is essential to study to enhance pulp production efficiency and ensure quality paper products.

Several researchers who have made paper using natural materials, such as Pulungan (2017), compared the composition of recycled paper made from organic and inorganic waste. The results obtained were 65% paper waste, 5% plastic waste, and 30% mustard greens with a grammage value of 110 g/m^2, a tensile strength of 3.37 kN/m, water absorption of 56.40 g/m^2, and a tensile strength value of >1,600 mN (Pulungan, 2017). Fenny and Farma (2016) utilized banana peels with newspaper and corn stalks with newspaper against recycled paper's tensile index and tear index. The results obtained using corn stalks and newspaper obtained a tensile index value of 7.31 Nm/g at a grammage of 50.90 g/m^2 (Fenny and Farma, 2016). Based on the results of previous studies, the results of parameter acquisition can be improved to achieve maximum results in accordance with the Indonesian National Standard (SNI). Previous studies focused on the composition of raw materials. This study uses the kraft method with the influence of chemical composition and boiling time, a novelty that fills in information that has been done by previous studies. This study uses palm oil trunks as raw materials in paper making.

This study aims to determine the effect of variations in the chemical composition and boiling time of the kraft method on paper making based on palm oil trunks. This research has the potential to encourage industry to develop efficient technology to process palm oil trunks into paper and switch to more sustainable and environmentally friendly raw materials, such as palm oil trunks. This research can also provide added value to palm oil trunks.

2. METHODOLOGY

2.1 Research materials and equipment

This research was conducted at the Chemistry and Physics Laboratory of the Institut Teknologi Sawit Indonesia, Medan, Indonesia, and the Forest Products Technology Laboratory, Universitas Sumatera Utara, Medan, Indonesia. The time of this research was carried out from February-March, 2023. The materials needed are palm oil trunks taken from the Institut Teknologi Sawit Indonesia garden area, Medan, Indonesia. Chemical used were purchased in local shop in Medan, Indonesia, such as aquadest, sodium hydroxide (NaOH, Merck, purity of 99%), sodium sulfate (Na_2SO_4, Merck, purity of 99%), sodium carbonate (Na_2CO_3, Merck, purity of 99%), hydrogen peroxide (H_2O_2, Merck, 10%) solution, and tapioca flour.

The tools used include A5 molds (14.8×21.0 cm), Memmert ovens, 30 mesh sieves, 5-liter capacity pans, machetes, Rinai brand stoves, thermo hotplates, 500 mL pyrex glass beakers, 30 cm rulers, turbo brand blenders, buckets with a capacity of 10 liters and kern analytical scales with an accuracy of 0.1 mg.

2.2 Research design

This research was conducted using a Factorial Completely Randomized Design (CRD), consisting of 2 factors:

2.2.1 Factor 1: Kraft method consists of 3 levels, namely:

- L1 = NaOH 10%+Na_2SO_4 5%+Na_2CO_3 2%
- L2 = NaOH 15%+Na_2SO_4 7%+Na_2CO_3 3%
- L3 = NaOH 20%+Na_2SO_4 9%+Na_2CO_3 4%

2.2.2 Factor 2: Boiling time consists of 3 levels, namely:

- T1 = 90 min
- T2 = 120 min
- T3 = 150 min

The number of treatment combinations is 3×3 totaling 9 treatments and there are 3 replications. If the data obtained is significantly different, it is continued with Duncan's Multiple Range Test at the 5% level.

2.3 Research procedure

The procedure described by (Hailemariam and Woldeyes, 2024) was followed with slight modification. The complete research scheme depicted in Figure 1. The palm oil trunks were chopped to a size of ±1 cm to reduce the size of the palm oil trunks, washed to remove dirt that stuck to them, and then dried in the sun until the water content reached 10%. The dried palm oil trunks were blended until smooth and then sieved using a 30 mesh sieve, resulting in 150 g of palm oil trunk powder.

The first boiling was carried out, the finely ground palm oil trunk powder was put into a pan, and then NaOH, Na_2SO_4, and Na_2CO_3 solutions were added sequentially according to the composition contained in the research design. The temperature was maintained at room temperature during the chemical addition step. Boiling at 100°C was carried out to soften the pulp and remove the lignin content contained in the pulp. After the boiling process was complete, the pulp was slowly filtered and rinsed with water at a temperature of 100°C, as much as 1 L; then, the pulp was squeezed and rinsed again with clean water until the resulting juice was clear.

The second boiling was carried out using a 7% H_2O_2 bleach solution for 1 hour at 90°C using a hotplate. After that, it was washed using clean water until the smell of the bleach solution was gone and then drained.

The pulp that has gone through the boiling process is mashed again using a blender until it becomes porridge, and 15 g of tapioca flour is added as an adhesive dissolved in hot water.

Before printing, the pulp is put into a bucket filled with ±10 liters of water. The pulp is filtered using a screen printing screen with a print size according to A5 paper (14.8×21.0 cm). After the printing process is complete, the paper is dried using an oven at 80°C for 45 min. After drying, the paper is removed from the mold using a knife.

2.4 Water adsorption analysis

The water adsorption test is carried out using the clamp method. A 1.5×20.0 cm paper is inserted, and the paper is hung perpendicular to the water surface, with one end dipped into the water to a depth of ±1 cm. After 10 min, a reading of the height of the increase in water absorbed on the surface of the paper is carried out using a ruler.

2.5 Grammage analysis

Paper grammage is a term used to determine the thickness of the same type of paper. The calculation is shown in equation 1.

$$G = \frac{A}{a} \quad (1)$$

Description: G=Paper sheet grammage (g/m^2); A=Tested sheet mass (g); a=Tested sheet area (m^2).

2.6 Tensile resistance analysis

Paper tensile resistance is measured using a Tensile Tester followed SNI 14-4737-1998 (National Standardization Agency (BSN), 1998). The tensile index can express the tensile strength and the tensile strength ratio to its grammage.

2.7 Appearance analysis

Analysis of the appearance of paper when it is clean and without holes. The appearance test can be done visually by carefully observing the entire surface of the paper. The paper appearance test involved ten respondents as representative respondents who filled out a questionnaire regarding the appearance of clean and without holes.

Figure 1. The complete research schemes applied in this study

3. RESULTS AND DISCUSSION

3.1 Results of water adsorption analysis

The results of observations and analysis of paper water adsorption test parameters can be seen in Figure 2. The best combination of treatment between boiling time and kraft method for the water adsorption test in Figure 2 is shown in the T2L3 treatment (boiling time 120 min and kraft method (NaOH 20%, Na_2S 9%, Na_2CO_3 4%) with a water adsorption value of 59.33 mm. This shows that the length of boiling time and the kraft method significantly affect the water adsorption value. The longer the boiling, the more the concentration of the solution must also be increased at least once from the boiling time because the dominant factor in the water adsorption test is the concentration of the solution. This is in line with the opinion of Ramadhani (2019), which states that the higher the concentration of the solution in the pulping process, the lower the lignin content produced will tend to be (Ramadhani, 2019).

The combination of boiling time and kraft method treatment with the lowest water adsorption test was in the T3L1 treatment (boiling time 150 min and NaOH concentration 10%, Na_2S 5%, Na_2CO_3 2%) with a water adsorption value of 19.00 mm. This shows that the longer the boiling, the lower the water adsorption if sufficient solution concentration is not given because boiling time that is too long will cause the fibers to become smoother and will affect the roughness of the paper surface. This is in line with the opinion of Syamsu et al. (2012), which states that smooth paper surfaces tend to have fewer pores compared to rough paper surfaces, so their water adsorption capacity also tends to be low (Syamsu et al., 2012). Statistical analysis using ANOVA on water adsorption was presented in Table 1. Based on the results of the analysis, the p value was obtained, which indicated that the data was normally distributed and therefore insignificant. The results of the statistical analysis showed that the treatments were not significantly different according to the Duncan test at the 5% test level.

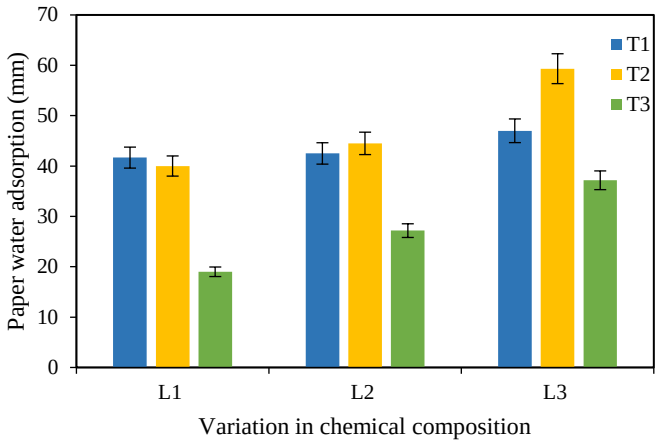

Figure 2. Effect of chemical composition and boiling time in kraft method on paper water adsorption

Table 1. Analysis of Variance (ANOVA) for the water adsorption analysis

Source	Degrees of freedom	Sum of squares	Mean squares	F-calculated	F-table	
					$F_{5\%}$	$F_{1\%}$
Variation	8	3196.41	399.55	26.47	2.51	3.71
T	2	2036.24	1018.12	67.46	3.55	6.01
L	2	959.13	479.56	31.77	3.55	6.01
T×L	4	201.04	50.26	3.33	2.93	4.58

3.2 Results of paper grammage analysis

The results of the observations and analysis of paper grammage test parameters were presented in Figure 3. Based on these results, the L1 and T1 treatment variations produced the highest paper grammage values of 76.11 g/cm^2 and 89.44 g/cm^2, respectively. Statistical analysis using ANOVA on grammage analysis was presented in Table 2. Based on the results of the analysis, the p value was obtained, which indicated that the data was normally distributed and therefore insignificant. Statistical analysis using Duncan's test at a 5% significance level showed that the treatments were not significantly different. Although some decreases in paper grammage were observed, it remained within an acceptable range and did not significantly impact the overall results. The lack of interaction between the two treatment factors such as boiling time and solution concentration, indicates that these factors did not support each other in enhancing paper grammage. Kraft pulping primarily targets lignin removal rather than drastic fiber structural changes (Silva et al., 2012). This suggests that boiling time and chemical variations in kraft methods may not sufficiently alter fiber morphology to affect grammage. This suggests that the observed variations were influenced by external factors such as equipment changes during the experimental process. One of the main external factors contributing to this was the change of tools during the paper printing process, which led to significant differences in paper thickness (Qiao et al., 2023). Additionally, the use of manual printing introduced surface unevenness, further contributing to variations in paper grammage (Itamiya and Sugita, 2015). Hence, grammage is primarily determined during the forming stage.

3.3 Results of paper tensile strength analysis

The results of observations and analysis of paper tensile strength test parameters can be seen in Figure 4. The best combination of treatment and kraft method for the tensile strength test based on Figure 4 is in the T2L3 treatment (120 min with 20% NaOH, 9% Na_2SO_4, 4% Na_2CO_3) with a tensile strength value of 11.26 kN/m. The boiling time and kraft method affect the tensile strength test value. The higher the solution concentration, the better the tensile strength test will be with sufficient boiling time (Kaima et al., 2023). The higher the solution concentration, the tensile strength will tend to increase. This is because the high concentration of the solution causes the cellulose to expand, the fiber cross-section becomes rounder, and the fiber crystallinity increases, which makes the tensile strength between fibers higher (Lu et al., 2023).

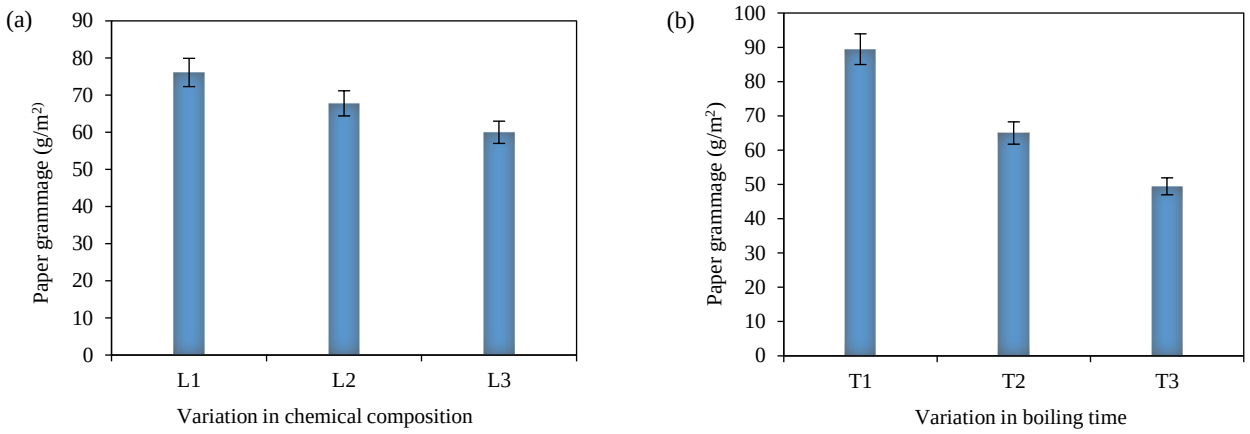

Figure 3. Average results of treatment on grammage parameters in variations of a) chemicals in the kraft method and b) boiling time.

Table 2. Analysis of Variance (ANOVA) for the paper grammage analysis

Source	Degrees of freedom	Sum of squares	Mean squares	F-calculated	F-table	
					$F_{5\%}$	$F_{1\%}$
Variation	8	8562.96	1070.37	20.28	2.51	3.71
T	2	7318.52	3659.26	69.33	3.55	6.01
L	2	1168.52	584.26	11.07	3.55	6.01
TxL	4	75.93	18.98	0.36	2.93	4.58

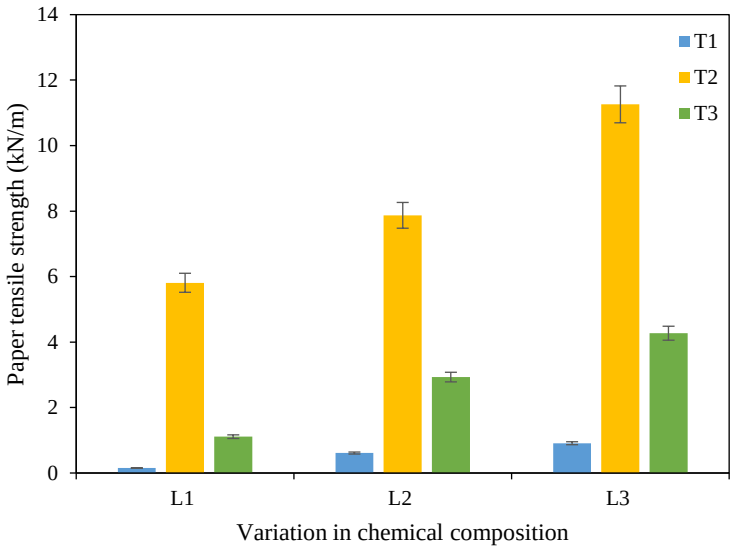

Figure 4. Effect of chemical composition and boiling time on paper tensile strength test parameters

The lowest combination of boiling time and kraft method treatment for tensile strength test was in T1L1 treatment (90 min with 10% NaOH, 5% Na_2SO_4, 2% Na_2CO_3) with a tensile strength value of 0.15 kN/m. This shows that boiling time is too fast, insufficient concentration causes lignin not to degrade properly, and cellulose is not perfectly soft, so there is no bond between fibers. Longer boiling times increase lignin removal by allowing more time for chemical or thermal breakdown of lignin bonds. However, low chemical concentrations require prolonged thermal exposure to compensate, which accelerates fiber degradation (Senthilkumar et al., 2025). Low chemical concentrations (e.g., in mild kraft pulping) necessitate longer boiling times, exacerbating thermal degradation (Sharma et al., 2019). This is in line with the opinion of Ek et al. (2009), which states that tensile strength is influenced by fiber strength, fiber length,

the number of bonds between fibers, and the surface structure of the paper (Ek et al., 2009).Statistical analysis using ANOVA on tensile strength was presented in Table 3. Based on the results of the analysis, the p value was obtained, which indicated that the data was normally distributed and therefore insignificant. The results of the statistical analysis showed that the treatments were not significantly different according to the Duncan test at the 5% test level.

Table 3. Analysis of Variance (ANOVA) for the tensile strength analysis

Source	Degrees of freedom	Sum of squares	Mean squares	F-calculated	F-table	
					$F_{5\%}$	$F_{1\%}$
Variation	8	348.37	43.55	140.10	2.51	3.71
T	2	287.01	143.50	461.69	3.55	6.01
L	2	43.91	21.96	70.64	3.55	6.01
T×L	4	17.44	4.36	14.03	2.93	4.58

3.4 Results of visual appearance of paper production

The results of paper produced from palm oil trunks using the kraft method can be seen in Figure 5. Paper made from palm oil trunks shows a variety of appearances. Paper close to SNI is found in the T2L3 treatment combination (120 min with a concentration of 20% NaOH, 9% Na_2SO_4, and 4% Na_2CO_3), which is clean and has no holes. The treatment with the highest concentration has a good appearance; this happens because when boiling palm oil trunks, there is lignin that can be degraded perfectly, so the higher the concentration of the solution used, the more lignin will be degraded with sufficient time. This is supported by Faris et al. (2017) about the observation that kraft lignin contains substantial guaiacyl units, which are more effectively degraded at higher concentrations (Faris et al., 2017). Study from Coura et al. (2023) about the FTIR analysis typically reveals specific peaks associated with functional groups present in lignin. For instance, peaks around 1,600 cm^{-1} indicate aromatic skeletal vibrations, while peaks near 1,500 cm^{-1} correspond to C=C stretching. A reduction in the intensity of these peaks after treatment suggests effective lignin degradation (Coura et al., 2023). The FTIR spectra may also show new peaks corresponding to functional groups formed as a result of lignin degradation. For example, the formation of ether bonds or other linkages can be detected, indicating that not only is lignin being degraded but also that new compounds are being synthesized from its breakdown products (Ghahri and Park, 2023). The combination of treatment between boiling time and the kraft method in the appearance test that does not comply with SNI is found in the T1L1 treatment (90 min with a concentration of 10% NaOH, 5% Na_2SO_4, 2% Na_2CO_3). Due to the low concentration of the solution, so it is not degraded properly. Boiling time also affects the appearance of the paper. Boiling time short enough will produce fibers that are not soft, and lignin is not thoroughly degraded.

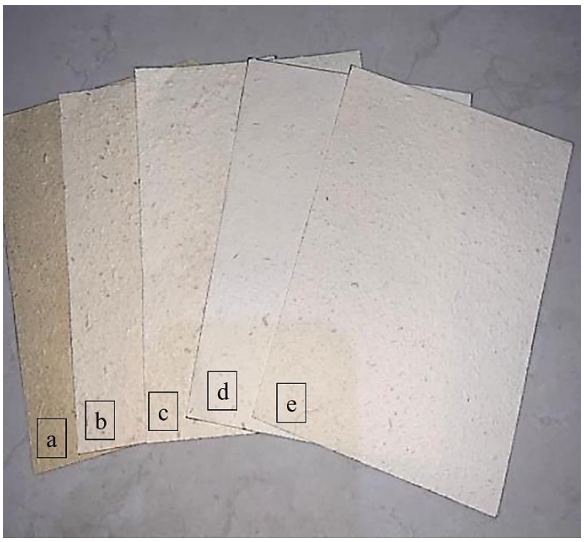

Figure 5. Appearance of the paper produced in this study (a) T1L1, (b) T1L2, (c) T2L2, (d) T3L2, and (e) T2L3

3.5 Comparative analysis

A summary of the results of this study compared with other studies and Indonesian national standards is shown in Table 4.

Table 4 summarized of the results of this study compared with other studies such as empty palm oil bunches, organic waste, banana peel and Indonesian national standards. However, there are other sources such as Moringa pods (Castelló et al., 2024) and Taro (*Colocasia esculenta* cv *fouê*) corm (Amon et al., 2014) are also noteworthy. The findings of this research demonstrate that palm oil trunk has

significant potential as a raw material for paper production. The grammage of paper produced in this study is 67.78 g/m², which is well within the SNI and ISO standard range. This value is lighter than paper derived from empty palm oil bunches (78.10 g/m²) (Tarigan, 2017) and organic waste (110.00 g/m²) (Pulungan, 2017), but closely comparable to banana peel-based paper (50.90 g/m²) (Fenny and Farma, 2016). The lightweight property of palm oil trunk paper makes it particularly suitable for applications requiring low grammage materials.

Table 4. Summary of the results of this study compared with other studies and Indonesian national standards

Raw material	Parameter analysis of paper			References
	Grammage (g/m^2)	Tensile strength (kN/m)	Water adsorption (mm)	
Empty palm oil bunches	78.10	4.30	-	Tarigan (2017)
Organic waste	110.00	3.35	56.40	Pulungan (2017)
Banana peel	50.90	7.31	-	Fenny and Farma (2016)
Palm oil trunk	67.78	11.26	59.33	This research
SNI	50-100	Min. 2.0	-	BSN (2008)
ISO	80-100	-	-	ISO (2019)
	-	10-20	-	ISO (2008)
	-	-	25-45	ISO (2014)

In terms of tensile strength, this research records a value of 11.26 kN/m, significantly exceeding the SNI minimum and ISO standard. This tensile strength is superior to papers made from empty palm oil bunches (4.3 kN/m) (Tarigan, 2017), organic waste (3.35 kN/m) (Pulungan, 2017), and banana peel (7.31 kN/m) (Fenny and Farma, 2016). The exceptionally high tensile strength highlights the structural advantages of palm oil trunk fibers, making it a strong candidate for high-strength applications, such as industrial packaging.

The water adsorption value of palm oil trunk paper is 59.33 mm, which is exceeds the ISO range but comparable to the water adsorption of organic waste-based paper (56.4 mm) (Pulungan, 2017). Although water adsorption data for papers made from empty palm oil bunches and banana peels were not available, the results suggest that palm oil trunk paper offers moderate water resistance. This property could be further enhanced through surface modifications or chemical treatments, enabling its use in environments with higher moisture exposure. This research highlights the balanced properties of palm oil trunk paper, combining lightweight characteristics with exceptional tensile strength and moderate water resistance. Compared to other raw materials, palm oil trunk demonstrates a unique potential for producing durable and sustainable paper products. Its performance exceeds many commonly cited lignocellulosic alternatives, highlighting the value of further investment in its processing optimization and supply chain development. Given the massive availability of palm-producing countries like Indonesia, its integration into the circular bio economy could support both environmental and economic sustainability targets.

4. CONCLUSION

This study demonstrates that both boiling time and the kraft method significantly influence key physical properties of paper produced from oil palm stem fibers in reducing greenhouse gas emissions from decomposing palm oil trunk. The optimal treatment, T2L3 (boiling for 120 min with 20% NaOH, 9% Na_2SO_4, and 4% Na_2CO_3), yielded water adsorption of 59.33 mm, paper grammage of 67.78 g/cm^2, and tensile strength of 11.26 kN/m, with physical characteristics that meet the requirements set by SNI 2008 standards. The results highlight the potential of utilizing agricultural residues like oil palm stems in sustainable paper production, offering a viable alternative to conventional wood-based sources. This approach not only adds value to biomass waste but also supports circular economy principles. To further assess its feasibility and impact, future research should use automated methods to standardize thickness, focus on pilot-scale implementation, cost-benefit analysis, and particularly on conducting life-cycle assessments to quantify the environmental advantages of the process compared to traditional paper manufacturing.

AUTHOR CONTRIBUTIONS

Conceptualization, Muhammad Syukri, Rina Maharany, M. Thoriq Al Fath, Ika Ucha Pradifta Rangkuti, and Dina Arfianti Saragih; Validation, Muhammad Syukri, Rina Maharany, M. Thoriq Al Fath, Ika Ucha Pradifta Rangkuti, Dini Aprilia, and Dina Arfianti Saragih; Formal Analysis, Dini Aprilia, Sarah Hafitz Syaurah, and Vikram Alexander; Investigation, Dini Aprilia, Sarah Hafitz Syaurah, and Vikram Alexander; Data Curation, Dini Aprilia, Sarah Hafitz Syaurah, and Vikram Alexander; Supervision, Muhammad Syukri, Rina Maharany, M. Thoriq Al Fath, Ika Ucha Pradifta Rangkuti, and Dina Arfianti Saragih.

DECLARATION OF CONFLICT OF INTEREST

The authors declare no conflict of interest.

REFERENCES

Abdelatif Y, Gaber A-AM, Fouda AE-AS, Elsokkary T. Sustainable utilization of calcined sugarcane mud waste as nanofiller for fine paper production. Biomass Conversion and Biorefinery 2024;14(7):8947-56.

Amon AS, Soro RY, Assemand EF, Dué EA, Kouamé LP. Effect of boiling time on chemical composition and physico-functional properties of flours from taro (*Colocasia esculenta* cv *fouê*) corm grown in Côte d'Ivoire. Journal of Food Science and Technology 2014;51(5):855-64.

Ayundra SD, Suwandi S, Herlinda S, Hamidson H, Wandri R, Asmono D. Soil physicochemical properties in respect to plant health in Ganodermainfested oil palm plantation. Journal of Scientific Agriculture 2022;6(1):9-13.

Castelló ML, Sesé T, García-Mares FJ, Juan-Borrás M del S, Ortolá MD. Influence of boiling time on chemical composition and properties of tender and mature Moringa pods. Foods 2024;13(12):Article No. 1823.

Coura MR, Demuner AJ, Demuner IF, Blank DE, Firmino MJM, Gomes FJB, et al. Technical kraft lignin from coffee parchment. Nordic Pulp and Paper Research Journal 2023;38(2):229-41.

Ek M, Gellerstedt G, Henriksson G. Paper Chemistry and Technology. Berlin, Germany: Walter de Gruyter; 2009.

Faris AH, Rahim A, Ibrahim MM, Hussin M, Alkurdi AM, Salehabadi A. Investigation of oil palm based Kraft and auto-catalyzed organosolv lignin susceptibility as a green wood adhesives. International Journal of Adhesion and Adhesives 2017;74(1):115-22.

Fenny FO, Farma W. The effect of the weight ratio of banana peel to newspaper and corn stalk to newspaper on the tensile index and tear index of recycled paper. Prosiding Semnastek 2016;2016(TK-011):1-7.

Ferdous T, Quaiyyum MA, Jin Y, Bashar MS, Yasin Arafat KM, Jahan MS. Pulping and bleaching potential of banana pseudo stem, banana leaf and banana peduncle. Biomass Conversion and Biorefinery 2021;13(1):893-904.

Ghahri S, Park B-D. Ether bond formation in waste biomass-derived, value-added technical hardwood kraft lignin using glycolic acid. Journal of Research Updates in Polymer Science 2023;12(1):171-9.

Gozan M, Abd-Aziz S, Jenol MA. Utilization of palm oil waste as a sustainable food resource. In: Bisaria V, editor. Handbook of Biorefinery Research and Technology: Production of Biofuels and Biochemicals. Singapre: Springer Nature; 2024. p. 573-92.

Hailemariam TT, Woldeyes B. Production and characterization of pulp and paper from flax straw. Scientific Reports 2024;14(1): Article No. 24300.

International Organization for Standardization (ISO). ISO 1924-2:2008 Paper and Board-Determination of Tensile Properties-Part 2: Constant Rate of Elongation Method (20 mm/min). Geneva, Switzerland: International Organization for Standardization; 2008.

International Organization for Standardization (ISO). ISO 535:2014(E) Paper and Board-Determination of Water Absorptiveness-Cobb Method. Geneva, Switzerland: International Organization for Standardization; 2014.

International Organization for Standardization (ISO). ISO 536:2019(E) Paper and Board-Determination of Grammage. Geneva, Switzerland: International Organization for Standardization; 2019.

Itamiya H, Sugita R. Effects of printing and ninhydrin treatment on forensic analysis of paper. Forensic Science International 2015;255(1):38-42.

Joseph N, Kassim MHM, Ibrahim M, Rawi NFM, Sudesh K, Arai T, et al. The effects of autohydrolysis pretreatment on the properties of opt pulps for the production of dissolving pulp. Pertanika Journal of Science and Technology 2024;32(S3):27-39.

Kaima J, Preechawuttipong I, Peyroux R, Jongchansitto P, Kaima T. Experimental investigation of alkaline treatment processes (NaOH, KOH and ash) on tensile strength of the bamboo fiber bundle. Results in Engineering 2023;18:Article No. 101186.

Lau GW, King PJH, Chubo JK, King IC, Ong KH, Ismail Z, et al. The potential benefits of palm oil waste-derived compost in embracing the circular economy. Agronomy 2024; 14(11):Article No. 2517.

Liu Y, Ding Y, Li Y, Wang X, Sun Y, Chen C. A comprehensive review of recent advances in delignification technology. The Journal of The Textile Institute 2024;115(12):2489-504.

Low LQ, Ilyas RA, Jalil R, Hawanis HSN, Ibrahim R, Azriena HAA, et al. Physical and mechanical properties enhancement of beaten oil palm trunk pulp and paper by optimizing starch addition: Towards sustainable packaging solutions. Industrial Crops and Products 2024;221(1):Article No. 119232.

Lu Z, Zhang H, Liu L, Cao H, Cheng Z, Liu H, et al. Study on cellulose nanofibers (CNF) distribution behaviors and their roles in improving paper property. Industrial Crops and Products 2023;201(1):Article No. 116897.

Michael, Fath MT Al, Alexander V, Hasibuan GCR, Syukri M, Ginting MHS, et al. MATLAB-empowered brightness defect prediction system in pulp processing bleaching stage: An empirical modelling approach. Case Studies in Chemical and Environmental Engineering 2024;10:Article No. 100934.

National Standardization Agency (BSN). SNI 14-4737-1998: Test Method: Tensile Strength of Paper and Cardboard. Jakarta, Indonesia: National Standardization Agency; 1998.

National Standardization Agency (BSN). 7274 Standar Nasional Indonesia Printing Paper Grade A. Jakarta, Indonesia: Standar Nasional Indonesia (SNI); 2008.

Nova S. Pre-Design of Pulp Making Plant from Agar-Agar Waste with Production Capacity of 28,900 Ton/Year (Pra Rancangan Pabrik Pembuatan Pulp dari Limbah Agar-Agar dengan

Kapasitas Produksi 28.900 Ton/Tahun) [dissertation]. Medan, Universitas Sumatera Utara; 2011 (in Indonesian).

Pulungan IT. Comparison Test of Recycled Paper Composition Based on Organic and Inorganic Waste [dissertation]. Medan, Universitas Sumatera Utara; 2017.

Putra SE, Dewata I, Barlian E, Syah N, Iswandi U, Gusman M, et al. Analysis of palm oil mill effluent quality. E3S Web of Conferences 2024;481:Article No. 03001.

Qiao C, Gong Y, Gong D. Distribution of in-plane physical properties of handmade Xuan paper: Revealing the effects of the sheet forming process and the folded state on handmade Xuan paper. Studies in Conservation 2023;69(1):35-49.

Ramadhani RP. Effect of Cooking Time and Sodium Hydroxide Concentration on Reducing Lignin Content of Corn Husk Pulp Using the Kraft Process [dissertation]. Surakarta, Universitas Muhammadiyah Surakarta; 2019.

Sahan Y, Rahmi SW, Herman S, Ohi H, Amri A. Enhancing dissolving pulp quality of mixed raw materials through pre-hydrolysis kraft-cooking: A study on Acacia crassicarpa and Terminalia catappa. Communications in Science and Technology 2024;9(2):372-8.

Senthilkumar ER, Sjöström J, Henriksson G, Vikström T, Sevastyanova O. Effect of storage conditions on the brownstock washing and oxygen delignification of kraft pulps. Cellulose 2025;32(1):2567-79.

Sharma A, Takanohashi T, Aizawa S, Kitao M, Anraku D. Effect of carbonization heating rate on the tensile strength of cokes prepared from chemically upgraded low rank coals. Iron and Steel Institute of Japan International 2019;59(8):1482-7.

Silva TCF, Gomide JL, Santos RB. Evaluation of chemical composition and lignin. BioResources 2012;7(3):3910-20.

Siti FMN, Dilaeleyana ABS, Aida M. Screening physical factors to enhance bioethanol production in oil palm trunk sap fermentation. Malaysian Journal of Analytical Sciences 2024;28(4):828-42.

Syamsu K, Puspitasari R, Roliadi H. Use of microbial cellulose from nata de cassava and coconut fiber as a substitute for wood cellulose in paper making. Jurnal Agroindustri indonesia 2012;1(2):118-24 (in Indonesian).

Tarigan FG. Determination of cellulose and lignin content of oil palm empty fruit bunch fiber through pulp making using soda process based on heating time. Jurnal Pembangunan Wilayah and Kota 2017;1(3):82-91 (in Indonesian).

Vachlepi A. Prospects for utilizing rubber wood as raw material for pulp making. Warta Perkaretan 2019;1(1):47-60 (in Indonesian).

Veronika N, Dhora A, Wahyuni S. Processing of palm oil waste into compost fertilizer using local microorganism decomposers (Mol) banana stems. Jurnal Teknologi Industri Pertanian 2019;29(2):154-61 (in Indonesian).

Wistara NJ, Rohmatullah MA, Febrianto F, Pari G, Lee S-H, Kim N-H. Effect of bark content and densification temperature on the properties of oil palm trunk-based pellets. Journal of the Korean Wood Science and Technology 2017;45(6):671-81.

Yennam R, Shivde P, Daware G, Mane V, Mawal V, Derle S. Synthesis of handmade craft-paper from agricultural waste. Indian Journal of Chemical Technology 2024;31(4):546-52.

Zakaria MA, Soh NMZN. The physical and mechanical properties of oil palm empty fruit bunch fibre (OPEFB) based on various fibre-cement ratios. Recent Trends in Civil Engineering and Built Environment 2023;4(3):428-38.

Environment and Natural Resources Journal

Volume 23
Issue 6
2025

Modelling Air Pollution in Thailand: Insights from Community Mobility Data

Padcharee Phasuk[1], Nattapon Siwareepan[2], and Ronnakron Kitipacharadechatron[1,2*]

[1]School of Economics, Sukhothai Thammathirat Open University, Thailand
[2]Faculty of Economics, Thammasat University, Thailand

ARTICLE INFO

Received: 19 Dec 2024
Received in revised: 18 Jul 2025
Accepted: 22 Jul 2025
Published online: 29 Aug 2025
DOI: 10.32526/ennrj/23/20240334

Keywords:
Air pollution/ Community mobility/ Machine learning/ Generalized method of moments

*** Corresponding author:**
E-mail: ronnakron.kit@stou.ac.th

ABSTRACT

This research investigates the relationship between community mobility and air pollution in Thailand, utilizing econometric and machine learning approaches to provide useful insights for policymakers to counter this issue. Data was sourced from the pollution database provided by the Ministry of Natural Resources and Environment and the community mobility database from a Google Trend search. The methodology of the research includes data extracting and pre-processing. The data analysis used an econometric model utilized Generalized Method of Moments, and a Machine Learning employed Support Vector Machines Results of the econometric analysis reveal that residential mobility, workplace mobility, and park mobility have a significant positive relationship with changes in air pollution. The support vector machine results show that community mobility explains 58.50% of air pollution variation and has a prediction accuracy of 94.47% on the training set. The results also suggest that pollution problems should be monitored closely when air pollution changes by 20%. These findings enhance the understanding of the complex factors influencing air pollution and offer valuable insights for developing effective mitigation strategies.

HIGHLIGHTS

- This paper employs alternative data sources, particularly the community mobility index, to investigate the association between its patterns and air pollution levels in Thailand.
- The findings suggest that changes in residential, workplace, and park-related mobility significantly influence air pollution levels.
- The research deepens our understanding of how the multifaceted drivers behind air pollution can craft sustainable and effective mitigation policies.

1. INTRODUCTION

Air pollution continues to pose a significant environmental and public health challenge, exerting wide-ranging effects on individual well-being, economic performance, and overall quality of life (Li et al., 2022). Exposure to clean air is consistently associated with better health outcomes, while elevated levels of pollution have been linked to respiratory illnesses, reduced outdoor activity, increased healthcare expenditures, and constraints on economic productivity (Freitas et al., 2020). To support mitigation and policy responses, many countries rely on the Air Quality Index (AQI) (Rajakumari and Priyanka, 2020), which synthesizes concentrations of key pollutants—namely sulfur dioxide (SO_2), nitrogen dioxide (NO_2), particulate matter (PM_{10} and $PM_{2.5}$), ozone (O_3), and carbon monoxide (CO)—to provide a standardized measure of air quality severity (Plaia and Ruggieri, 2011).

Nevertheless, the ability to estimate and forecast air quality in real time remains limited, particularly in rapidly urbanizing and economically diverse contexts such as Thailand. Traditional monitoring approaches, which primarily utilize ground-based sensors, periodic sampling, or satellite-derived observations, are often constrained by limited spatial and temporal resolution. These methods do not fully account for the dynamic nature of pollution, which is strongly influenced by human activity and mobility patterns. In this regard, emerging mobility data—tracking population

Citation: Phasuk P, Siwareepan N, Kitipacharadechatron R. Modelling air pollution in Thailand: Insights from community mobility data. Environ. Nat. Resour. J. 2025;23(6):526-536. (https://doi.org/10.32526/ennrj/23/20240334)

movement across categories such as retail, recreation, transit, and residential areas—offers a potentially valuable input for enhancing the responsiveness and accuracy of air quality assessments (Kondo et al., 2014; Li et al., 2022).

The existing literature indicates a strong correlation between mobility and pollution, particularly in urban and industrialized settings (Lo et al., 2022; Zhu et al., 2020). However, in many developing countries, the integration of mobility data into real-time AQI forecasting remains underutilized. Contributing factors include inadequate digital infrastructure, limited methodological familiarity, and institutional inertia in adopting new technologies. Consequently, environmental governance in such settings often continues to rely on conventional monitoring tools that may not reflect real-time conditions, potentially resulting in delayed or suboptimal policy interventions (Das et al., 2021; Harnkijroong and Panich, 2013).

Thailand's complex economic structure—encompassing agriculture, tourism, and industrial manufacturing—produces a varied pollution landscape (Suriyawong et al., 2023). In the northern and northeastern regions, seasonal crop burning and forest fires contribute substantially to $PM_{2.5}$ concentrations, while in the Eastern Economic Corridor (EEC), industrial emissions are the predominant concern. In metropolitan areas such as Bangkok, traffic-related emissions are particularly severe. Despite these differences, a unified national strategy for pollution monitoring remains constrained by the absence of a granular and timely monitoring system.

This study aims to address this methodological and policy gap by evaluating the extent to which community mobility data can serve as a real-time estimator of air quality in Thailand. Rather than emphasizing cross-national comparisons between developed and developing countries, the research adopts an empirical approach focused on the relationship between population movement and pollution levels within Thailand (Srikamdee and Onpans, 2019). This approach directly aligns with the study's central objective: to assess the viability of using digital mobility indicators as predictive tools for environmental outcomes.

The study further contributes to policy-relevant knowledge by proposing an applied framework for integrating mobility data into air quality management. Potential applications include urban planning, traffic regulation, and the issuance of public health alerts. By leveraging near real-time behavioral data, policymakers may be able to implement more timely and targeted responses to pollution events, thereby supporting sustainable development goals that reconcile environmental and economic considerations (Inthisorn and Puttanapong, 2022; Nyhan et al., 2019).

In summary, this research revisits a central question by examining whether community mobility data can function as a reliable, real-time predictor of air quality. Using Thailand as a representative case of a developing country, the study aims to generate empirical evidence that is both methodologically robust and practically applicable in advancing environmental governance.

Through the bodies of issues in air pollution monitoring, and modelling were widely discussed by Bahadur et al. (2024), Bahadur et al. (2025), and Beigh et al. (2025). Accurate estimation of air quality plays a critical role in informing environmental regulation, public health policy, and emissions control. Conventional estimation techniques typically rely on fixed-site air quality monitors or satellite-based remote sensing data. While these methods provide valuable pollutant, concentration estimates and broad spatial coverage, they are often characterized by delayed reporting and low temporal resolution. In rapidly changing urban environments, this temporal limitation presents challenges for the effective implementation of policy. The growing availability of high-frequency, device-generated data provides new opportunities for timely and behaviorally informed pollution modeling. Community mobility data have emerged as a promising proxy for real-time human activity, which may exert a measurable influence on pollution dynamics.

In countries where networks of air quality monitoring systems reach maturity, such as European countries or the US, a growing body of research has demonstrated the utility of mobility data in environmental analysis. Archer et al. (2020) and Badr et al. (2020), for example, documented significant reductions in NO_2 levels—exceeding 65% in some U.S. cities—during COVID-19 mobility restrictions, while $PM_{2.5}$ levels exhibited declines, albeit on a more modest scale. Similarly, Nyhan et al. (2019) employed anonymized mobile phone data to examine individual exposure to pollutants across spatial and temporal dimensions, highlighting its relevance for both environmental and epidemiological studies. In the UK, Reis et al. (2018) utilized census-linked spatial models to demonstrate that daily shifts in population density

elevated exposure risks to NO_2 and $PM_{2.5}$. Bahadur et al. (2023) employed machine learning in monitoring and modeling air quality. In the Singaporean context, Li and Tartarini (2020) found that pandemic-induced restrictions significantly improved air quality, reinforcing the link between mobility and emissions. Collectively, these studies illustrate the methodological maturity and policy relevance of integrating behavioral data into environmental monitoring systems.

By contrast, studies conducted in developing countries where mobility data may not be readily available frequently rely on broader satellite-based assessments or have utilized mobility-related events (e.g., lockdowns) as indirect proxies without measuring actual movement patterns. For instance, Liu et al. (2020) used a difference-in-differences approach to quantify the impact of lockdown policies on pollution in China, reporting an average reduction of 12%. In India, Srivastava et al. (2020) found that declines in vehicle use, and industrial activity led to short-term improvements in air quality during the pandemic. Othman and Latif (2021) observed significant reductions in NO_2 in Malaysia but did not incorporate mobility data directly into their models. Although these studies acknowledge the influence of human activity, their reliance on indirect measures underscores a persistent methodological gap.

This divergence highlights a significant research opportunity. While real-time behavioral data are increasingly applied in developed country contexts, their integration into environmental analysis in the developing world remains limited. With the growing availability of platforms such as Google Community Mobility Reports and anonymized mobile tracking data, it is now feasible to implement such models even in countries with limited monitoring infrastructure.

Thailand is emblematic of this opportunity. To the best of our knowledge, the study of community mobility related air quality issue in Thailand remains limited despite the country's diverse pollution sources ranging from biomass burning in the north to industrial activity in the east and traffic emissions in urban centers (Othman et al., 2022). At present, most assessments rely on satellite observations or data from a relatively small number of fixed monitoring stations. Although anecdotal and seasonal patterns clearly link mobility to pollution, for example, during public holidays or COVID-19 lockdowns there remains a paucity of research that systematically models these dynamics using contemporary analytical techniques.

The present study seeks to address this gap by testing whether mobility data from six distinct categories (e.g., retail, recreation, residential, transit) can serve as valid predictors of AQI in Thailand. By applying a combination of econometric and machine learning models, this research evaluates the predictive performance of mobility indicators in estimating air quality across different regional contexts. The findings are expected to yield methodological contributions as well as practical policy insights, particularly for enhancing adaptive environmental management in urban and semi-urban settings within developing economies. The independent variable uses in this investigation involving many categories of community movement such as retails and recreation, grocery and pharmacy, parks, transition station, workplace, and residential (Nowak and Heisler, 2010; Oudin et al., 2012; Tee Lewis et al., 2019) to explain how air pollution, which is represented by Air Quality Index, change as presented in Figure 1.

2. METHODOLOGY

To examine the association between community mobility and air pollution, this paper organizes the methodology into two parts: 1) Data Sources, which elaborates on the dataset used in this paper and the data preparation performed before proceeding to the next step, and 2) Analysis procedure, which provides information about the econometric and machine learning approaches used in this paper, as detailed below.

2.1 Data sources

This paper employed retrospective data from 2020 to 2022 from publicly accessible sources, including the pollution database, which provided average air pollution data from the Ministry of Natural Resources and Environment, and the community mobility database, which provided human movement data from random sampling by Google Co. Ltd. All retrieved data were aggregated into weekly data using the moving average approach and normalized on a scale from zero to one to reduce variation among datasets (Borkin et al., 2019). Descriptive statistics were performed using the mean and standard deviation if the data were normally distributed; otherwise, medians and interquartile ranges were used to summarize the overall characteristics of the data.

Details of the variables used in this investigation and were also present in Table 1 below.

Based on the empirical data, it was demonstrated that all the retrieved data were abnormally distributed, considering the statistical significance of the Shapiro-Wilk test, which evaluated the distribution by order statistics (sorted values) of the dataset (Royston, 1992). Therefore, medians and interquartile ranges were appropriate to present the overall characteristics of the data. The results showed that during the study period, air pollution levels in Thailand were still low, indicating that overall air quality was still good. In contrast, the community mobility index was high for all subcategories, especially workplace mobility as well as retail and recreation mobility. This outcome implied a moderate level of air pollution when considering air quality as a nationwide indicator over time. The results are shown in Table 2.

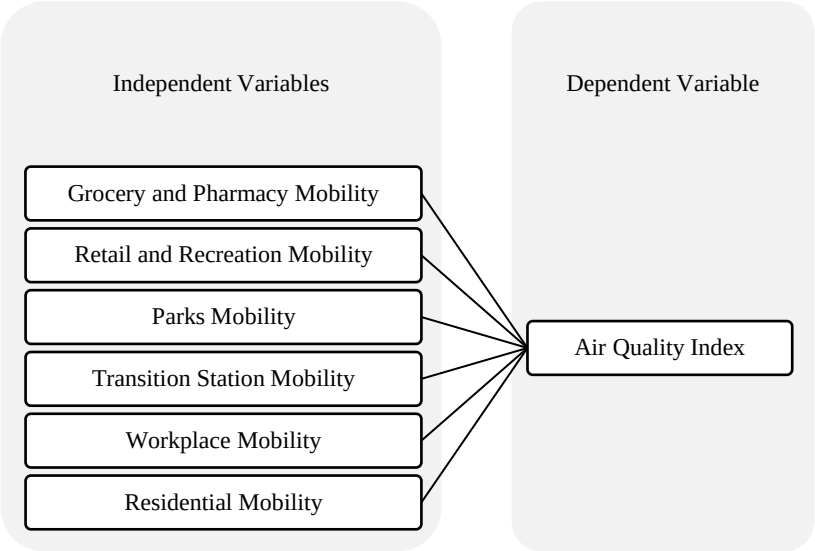

Figure 1. Conceptual framework

Table 1. Variable description

Variables	Unit
Air quality index (AQI)	Integer ranges from 0 to 500
Retail and recreation mobility (CM1)	Percent change from baseline
Grocery and pharmacy mobility (CM2)	Percent change from baseline
Parks mobility (CM3)	Percent change from baseline
Transition station mobility (CM4)	Percent change from baseline
Workplace mobility (CM5)	Percent change from baseline
Residential mobility (CM6)	Percent change from baseline

Remark: Baseline was the median value from the 5-week period Jan 3-Feb 6, 2020

Table 2. Descriptive statistics of the data

	Normality	Mean	Std. Dev.	Median	IQR
Air quality index (AQI)	6.925***	0.186	0.192	0.118	0.189
Retail and recreation mobility (CM1)	4.233***	0.588	0.204	0.642	0.219
Grocery and pharmacy mobility (CM2)	2.398***	0.510	0.206	0.473	0.318
Parks mobility (CM3)	2.876***	0.353	0.190	0.382	0.304
Transition station mobility (CM4)	4.090***	0.463	0.224	0.535	0.363
Workplace mobility (CM5)	2.059***	0.658	0.195	0.686	0.265
Residential mobility (CM6)	2.231***	0.391	0.224	0.366	0.340

***denote the statistically significant at 0.01

Remark: The data analyzed through STATA version 18 license from Thammasat University

2.2 The model

This section aims to elaborate on the details of the investigation model used in this paper, which consists of two parts: the econometric model–a conventional tool for estimation and prediction-and the machine learning model–an advanced tool for prediction. These two models have distinct advantages. For example, the econometric model can estimate the marginal rate of change through its parameters, which is beneficial for a deeper understanding of the impact of factors. However, its parameterization must be strictly aligned with the data distribution, leading to poor predictions when the data is not normally distributed (Inthisorn and Puttanapong, 2022). On the other hand, the machine learning model provides better predictions since it relies on finding the best solution based on data distribution, though it lacks detailed insights (Hua et al., 2024).

2.2.1 Econometric model

To investigate the relationship between community mobility (CM) and air pollution index (AQI), a generalized method of moments (GMM) is employed for parameter estimation. This method allows for obtaining unbiased coefficients even when the data exhibits a non-linear relationship and a non-normal distribution (Gujarati and Porter, 2008), as evidenced in Table 2. Additionally, this paper incorporates a time variable to capture the unobserved effects of time growth to the estimated model, which can be algebraically displayed as shown in Equation 1.

$$AQI_t = \alpha_o + \pi_i \sum_{i=1}^{N} CM_{it} + time + \upsilon_t \quad (1)$$

Where: AQI_t = the normalized index of air quality reported at time t; CM_{it} = the normalized volume vector of sub-categories for mobility types at time t (where: i = 1 is retails and recreation mobility, i = 2 is grocery and pharmacy mobility, i = 3 is parks mobility, i = 4 is transition station mobility, i = 5 is workplace mobility, i = 6 is residential mobility); time is time variable; α_o is constant terms; υ_t is disturbance terms; π_i is the vector of estimated parameters.

To identify the best-fitting model, parameter estimation is carried out in three steps: 1) estimation of the restricted model by expressing the dependent variable in terms of a time trend, 2) estimation of the unrestricted model by including all independent variables in the specification, and 3) determination of the final fitted model by removing variables that are not significant based on the Wald test criteria.

The robustness of the model is tested using the bootstrapping method after parameter estimation. To verify the validity and reliability of the estimated model, bootstrapping involves randomly selecting new values and re-estimating the model 1,000 times, assuming that the disturbance term is independent and identically distributed. If the results consistently show the same sign, magnitude, and statistical significance, this indicates that the model is robust (Escanciano and Lobato, 2009; Gujarati and Porter, 2008).

2.2.2 Machine learning model

Given the limitations of the specified methodology which only indicated the relationship between community mobility (CM) and air pollution index (AQI), therefore, a machine learning technique will be used to identify the prediction accuracy of the independent variable set on the air quality index utilizing support vector machines. This approach aims to find a function that best approximates the relationship between input features and continuous target variables. It is capable of handling complex and nonlinear problems, including noise, outliers, and high-dimensional feature spaces (Emsia and Coskuner, 2016). Kernel functions are employed to estimate these nonlinear relationships, as given in Equation 2.

$$AQI = f[\sum_{i=1}^{n} CM_i] \quad (2)$$

Then, non-linear relationships will be transformed into high-dimensional feature spaces to enable linear separation using kernel functions, as shown in Equation 3.

$$AQI = \sum_{i=1}^{n} (\theta_i - \theta_i^*) \cdot K(CM_i, CM^*) + \eta \quad (3)$$

Each dimension is a symmetric matrix with non-negative eigenvalues, according to the underlying probability density function as presented in Equation 4.

$$k(CM_i, CM_j) = (CM_i, CM_j)^d \quad (4)$$

Since this paper considers all subcategories of community mobility simultaneously, the hyperplane that maximizes the margin for each dimension can be expressed as shown in Equation 5.

$$AQI = \sum_{i=1}^{n} (\theta_i - \theta_i^*) (CM_i, CM_j)^d + \eta \quad (5)$$

The 70/30 data ratio was used for model training and model validation respectively. During the parameterization process. The goodness-of-fit for both technique are measured using R-squared and RMSE, by comparing the training and testing sets (Molinaro et al., 2005). The entire process is illustrated as shown in Figure 2 below.

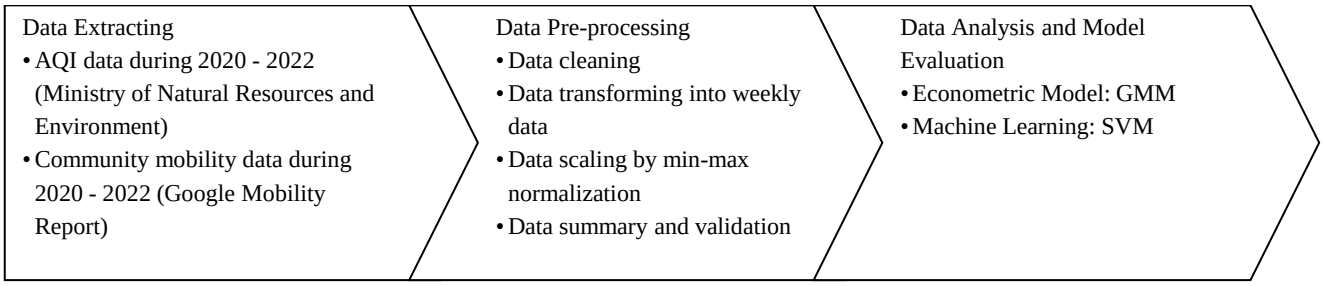

Figure 2. The research flowchart

3. RESULTS AND DISCUSSION

According to the previously discussed methodology, the results from the generalized method of moments estimation will be presented first, followed by the results from the support vector machine analysis. The details are as follows.

3.1 The econometric results

When employing an econometric model for parameterization, the primary concerns are model specification and its potential consequences, such as specification error, multicollinearity, and heteroskedasticity. Fortunately, the generalized method of moments (GMM) can address heteroskedasticity issues more effectively than the ordinary least squares (OLS) approach. However, including all variables simultaneously may lead to multicollinearity, which can increase the standard error of the estimates. To diagnose this issue, correlation analysis will be conducted as a preliminary step. The results indicated that retail and recreation mobility (CM1), grocery and pharmacy mobility (CM2), and park mobility (CM3) exhibited relatively high correlations among the variables, which could result in multicollinearity problems (Chen, 2012), excepted for transition station mobility (CM4), workplace mobility (CM5), residential mobility (CM6), as shown in Table 3.

To avoid these issues, the estimation process will be approached from three perspectives: First, the restricted model, which serves as the baseline for comparing the explanatory power of the model when additional variables are included. Second, the unrestricted model, which incorporates all variables. Lastly, the fitted model, which excludes retail and recreation mobility (CM1), grocery and pharmacy mobility (CM2), and transition station mobility (CM4) variables based on the Chow's test as a criterion for model selection. The fitted model demonstrated a higher adjusted R-squared while maintaining the same level of prediction error. This result suggests that the model is more robust after the removal of irrelevant variables.

Table 3. Correlation testing for multicollinearity diagnosis

	CM 1		CM 2		CM 3		CM 4		CM 5		CM 6	
CM 1	1.000											
CM 2	0.783	***	1.000									
CM 3	0.741	***	0.445	***	1.000							
CM 4	0.700	***	0.252	***	0.832	***	1.000					
CM 5	0.615	***	0.380	***	0.386	***	0.667	***	1.000			
CM 6	-0.790	***	-0.436	***	-0.401	***	-0.574	***	-0.575	***	1.000	***

***denote the statistically significant at 0.01

The investigation (Table 4) reveals that residential, workplace, and park mobility all have positive effects on air pollution, consistent with previous findings by Nowak and Heisler (2010), Oudin et al. (2012), and Tee Lewis et al. (2019). Specifically, a 1-percentage-point increase in

residential and workplace mobility is associated with increases in air pollution levels by approximately 24.2% and 36.2%, respectively. These results suggest that traffic congestion remains a primary contributor to air pollution in Thailand. In addition, park mobility is associated with a 24.3% increase in pollution; however, this may be linked to leisure-related travel patterns, which differ from commuting behavior and warrant separate policy consideration.

Table 4. Econometric estimation by using GMM method for investigating relationship between community mobility index and air pollution

	Restricted model			Unrestricted model			Fitted model		
	Coeff.		Std. Err.	Coeff.		Std. Err.	Coef.		Std. Err.
Retails and recreation mobility				-0.404		0.449			
Grocery and pharmacy mobility				0.087		0.235			
Transition station mobility				0.050		0.268			
Parks mobility				0.368		0.283	0.243	**	0.109
Workplace mobility				0.240	**	0.171	0.242	**	0.118
Residential mobility				0.182		0.210	0.362	***	0.095
Time	-0.001	**	0.000	-0.001		0.001	-0.002	**	0.001
Constant	0.254	***	0.034	0.066		0.200	-0.103		0.073
Observations	125			125			125		
Wald's Chi-squared	2.850	*		21.250	***		19.740	***	
R-squared	0.041			0.181			0.175		
Adjusted R-squared	0.033			0.132			0.147		
RMSE	0.187			0.173			0.173		
Robustness check	Yes			Yes			Yes		

***, **, * denoted the statistically significant at 0.01, 0.05, 0.10 respectively, Chow test was performed to fit the variables and standard error of estimate was robust. The fitted model was cleaned from endogeneity effect once compared to the IV-GMM approach, indicating that the estimated coefficient was unbiased.

These results align with existing literature that identifies workplace and residential mobility as key contributors to urban air pollution, primarily through traffic congestion and industrial emissions. Barua and Nath (2021) found that a 1% increase in transit-related mobility in the East Asia region can raise emissions by 1.6%. Similarly, Cui et al. (2019) highlights the long-term consequences of persistent pollution, including talent outmigration from cities with poor air quality. These findings underscore the importance of mobility control policies. As noted by Dang et al. (2020) and Das et al. (2021), implementing stricter regulations on traffic and commuting activities could significantly improve urban air quality.

Besides, the positive relationship between parks mobility and air pollution is likely driven by the transportation required to reach park areas. This is supported by findings from Shafeeque et al. (2021), who observed that reductions in overall mobility—including visits to parks—were significantly associated with decreased emission levels across South Asia.

Upon considering the prediction accuracy of the GMM by mapping the actual AQI values against the predicted AQI values, it is evident that the GMM yields relatively low prediction accuracy. This is reflected by the shaded area, which indicates that the 95% confidence interval is becoming wider. Furthermore, the result also confirms the model's low predictive power, as shown by the red dashed line, which does not intersect with the dots, indicating a weak trend prediction, as seen in Figure 3.

3.2 The support vector machine results

This section presents the results of the Support Vector Machine (SVM) analysis, based on a 70/30 split of the dataset—70% for training and 30% for testing. Besides, the SVM smooth curve is performed to evaluate the model's predictive performance, ensuring that the resulting curve reflects generalizable patterns rather than overfitting.

The model produced two key findings: 1) community mobility variables explained approximately 58.5% of the variance in air pollution levels, with a prediction accuracy of 94.47% on the training data. Although the accuracy on the testing set was slightly lower, it remained within an acceptable range (Hua et al., 2024), 2) The SVM model yielded relatively higher prediction accuracy, as reflected in

the shaded area of the 95% confidence interval, which becomes narrower, in addition, the model identified that a change of around 20% -as observed in the turning point of graph at 0.2 in the air quality index signal the onset of severe pollution events, as indicated by the red dashed line representing the smoothed SVM as illustrated in Figure 4.

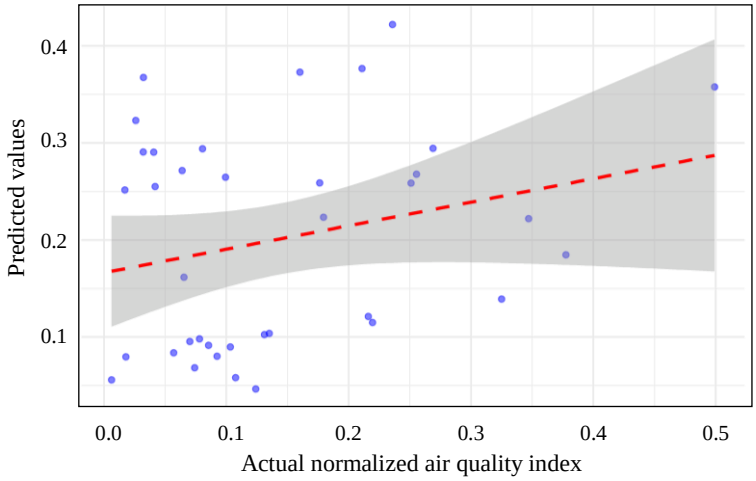

Figure 3. Assessment of GMM prediction accuracy for air quality index (Note: Author's calculation

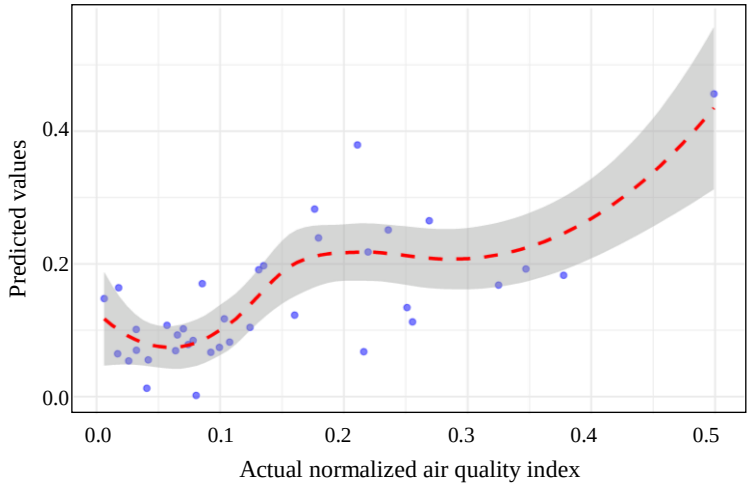

Figure 4. Assessment of SVM prediction accuracy for air quality index (Note: Author's calculation)

These instances fall outside the model's optimal margin of classification, suggesting high uncertainty and aligning with the 95% confidence threshold. Overall, these results demonstrate that community mobility can be a reliable predictor of air pollution using machine learning methods. Moreover, SVMs can be used for threshold-based classification, enabling early warnings for high pollution levels as present in Table 5.

Table 5. Support vector machine estimation

	Accuracy	R-squared	RMSE
Training set	94.47%	58.50%	0.0553
Testing set	91.48%	46.51%	0.0852

According to the empirical result consistent with these findings, Hua et al. (2024) report that mobility-based models, when implemented under appropriate methodological conditions, can predict air pollution levels with an accuracy ranging from 78% to 98%. However, prediction accuracy may vary

depending on local characteristics such as urban development, transportation infrastructure, and economic activity (Davis and Weinstein, 1999; Yasumoto et al., 2019; Wu et al., 2019). These unobservable factors introduce potential model discrepancies.

Taken together, the findings highlight the importance of integrating machine learning insights into environmental policymaking. Policymakers should consider collaborative efforts with relevant agencies to implement targeted interventions. For example, promote smart urban planning and support green commuting for integrating air pollution (Murad et al., 2025; Paoin et al., 2021).

4. CONCLUSION

This study examined the relationship between community mobility and model air pollution in Thailand by applying both econometric and machine learning approaches. The findings from econometric model suggest that changes in residential, workplace, and park-related mobility significantly influence air pollution levels, with residential movement emerging as the most impactful factor. Additionally, the machine learning model identified a critical threshold: A change of more than twenty percent in the air quality index may serve as an early warning signal for severe pollution events.

These results offer important policy implications. Strategies to manage community mobility—such as promoting green commuting, supporting remote or hybrid work arrangements, and implementing smart urban planning with expanded green spaces—could contribute to pollution reduction. However, as noted by Murad et al. (2025) and Sharma et al. (2003), the success of such interventions depends on contextual factors, including the level of public awareness regarding pollution, which may differ across regions and countries.

Despite its contributions, the study has several limitations. First, the national-level data may not capture local variations in mobility and pollution; future research should consider spatially disaggregated data and additional factors like seasonality and industrial activity. Second, the community mobility index may not fully reflect actual movement patterns. Developing a more comprehensive composite index, as suggested by Inthisorn and Puttanapong (2022), could improve measurement accuracy. Third, the use of a static model may obscure complex relationships; techniques such as quantile regression, ridge, or lasso regression could enhance robustness and prediction. Integrating satellite data may also improve the analysis, especially at a finer geographic scale.

In conclusion, the insights from this study can inform the design of urban environmental and public health policies in developing countries, helping to optimize resource allocation while addressing critical pollution challenges.

ACKNOWLEDGEMENTS

The authors would like to say thank you to the Faculty of Economics, Thammasat University, and the School of Economics, Sukhothai Thammatirat Open University, for sharing the accessibility of statistical programs as well as enabling academic collaboration. Additionally, we would love to express our deep gratitude to Christopher John Ireland, Ed.D, for his assisting in English proofreading.

REFERENCES

Archer CL, Cervone G, Golbazi M, Al Fahel N, Hultquist C. Changes in air quality and human mobility in the USA during the COVID-19 pandemic. Bulletin of Atmospheric Science and Technology 2020;1(3):491-514.

Badr HS, Du H, Marshall M, Dong E, Squire MM, Gardner LM. Association between mobility patterns and COVID-19 transmission in the USA: A mathematical modelling study. The Lancet Infectious Diseases 2020;20(11):1247-54.

Bahadur FT, Shah SR, Nidamanuri RR. Air-pollution monitoring and modelling: An overview. Environmental Forensics 2024;25(5):309-36.

Bahadur FT, Shah SR, Nidamanuri RR. A brief outline of indoor air quality: Monitoring, modelling, and impacts. Journal of Environmental Engineering 2025;151(5):Article No. 03125001.

Bahadur FT, Shah SR, Nidamanuri RR. Applications of remote sensing vis-à-vis machine learning in air-quality monitoring and modelling: A review. Environmental Monitoring and Assessment 2023;195(12):Article No. 1502.

Barua S, Nath SD. The impact of COVID-19 on air pollution: Evidence from global data. Journal of Cleaner Production 2021;298:Article No. 126755.

Beigh FA, Shah SR, Ahmad K. A perspective on indoor air-quality monitoring, guidelines, and the use of various sensors. Environmental Forensics 2025;26(3):350-67.

Borkin D, Némethová A, Michaľčonok G, Maiorov K. Impact of data normalisation on classification-model accuracy. Research Papers Faculty of Materials Science and Technology Slovak University of Technology 2019;27(45):79-84.

Chen GJ. A simple way to deal with multicollinearity. Journal of Applied Statistics 2012;39(9):1893-909.

Cui C, Wang Z, He P, Yuan S, Niu B, Kang P, et al. Escaping from pollution: The effect of air quality on inter-city population mobility in China. Environmental Research Letters 2019;14:Article No. 124025.

Dang HH, Dang HH, Trinh T. Does the COVID-19 lockdown improve global air quality? New cross-national evidence on its

unintended consequences. Journal of Environmental Economics and Management 2020;105:Article No. 102401.

Das M, Das A, Sarkar R, Mandal P, Saha S, Ghosh S. Exploring short-term spatio-temporal pattern of $PM_{2.5}$ and PM_{10} and their relationship with meteorological parameters during COVID-19 in Delhi. Urban Clim 2021;39:Article No. 100944.

Davis DR, Weinstein DE. Economic geography and regional production structure: An empirical investigation. European Economic Review 1999;43(2):379-407.

Emsia E, Coskuner C. Economic-growth prediction using optimised support-vector machines. Computer Economics 2016;48(3):453-62.

Escanciano JC, Lobato IN. An automatic portmanteau test for serial correlation. Journal of Economics 2009;151(2):140-9.

Freitas ED, Ibarra-Espinosa SA, Gavidia-Calderón ME, Rehbein A, Rafee SA, Martins JA, et al. Mobility restrictions and air quality under COVID-19 pandemic in São Paulo, Brazil. Preprints 2020. DOI: 10.20944/preprints202004.0515.v1

Gujarati DN, Porter DC. Basic Econometrics. 5th ed. New York, USA: McGraw-Hill/Irwin; 2008.

Harnkijroong T, Panich N. Influence of meteorological factors on PM10 at roadside of Bangkok. Proceedings of the 10th National Kasetsart University Kamphaeng Saen Conference; 2013 Dec 6-7. Nakhon Pathom, Thailand; 2013.

Hua V, Nguyen T, Dao M, Nguyen HD, Nguyen BT. The impact of data imputation on the air-quality-prediction problem. PLoS One 2024;19(9):e0306303

Inthisorn P, Puttanapong N. Associations between mobility indices and the COVID-19 pandemic in Thailand. Nakhara: Journal of Environmental Design and Planning 2022;21(2):Article No. 215.

Kondo MC, Mizes C, Lee J, McGady-Saier J, O'Malley L, Diliberto A, et al. Towards participatory air-pollution exposure assessment in a goods-movement community. Progress in Community Health Partnerships: Research, Education, and Action 2014;8(3):291-304.

Li J, Ding T, He W. Socio-economic driving forces of $PM_{2.5}$ emissions in China: A global meta-frontier-production-theoretical decomposition analysis. Environmental Science and Pollution Research 2022;29(51):77565-79.

Li J, Tartarini F. Changes in air quality during the COVID-19 lockdown in Singapore and associations with human-mobility trends. Aerosol and Air Quality Research 2020;20(8):1748-58.

Liu S, Kong G, Kong D. Effects of COVID-19 on air quality: Human mobility, spillover effects, and city connections. Environmental and Resource Economics 2020;76(4):635-53.

Lo K, Tung NT, Wu C-D, Thao HN X, Dung HB, Thuy TPC, et al. Air pollution mediates the association between human mobility and COVID-19 infection. Aerosol and Air Quality Research 2022;22(1):Article No. 210249.

Molinaro AM, Simon R, Pfeiffer RM. Prediction-error estimation: A comparison of resampling methods. Bioinformatics 2005;21(15):3301-7.

Murad SMW, Rahman A, Mohsin AKM. From policy to progress: Environmental taxation to mitigate air pollution in OECD countries. Journal of Environmental Management 2025;374: Article No. 124143.

Nowak D, Heisler G. Air-quality effects of urban trees and parks. National Recreation and Park Association; 2010. p. 44

Nyhan MM, Kloog I, Britter R, Ratti C, Koutrakis P. Quantifying population exposure to air pollution using individual mobility patterns inferred from mobile-phone data. Journal of Exposure Science and Environmental Epidemiology 2019;29(2):238-47.

Othman M, Latif MT. Air-pollution impacts from COVID-19 pandemic-control strategies in Malaysia. Journal of Cleaner Production 2021;291:Article No. 125992.

Othman M, Latif MT, Hamid HHA, Uning R, Khumsaeng T, Phairuang W, et al. Spatial-temporal variability and health impact of particulate matter during a 2019-2020 biomass-burning event in Southeast Asia. Scientific Reports 2022;12:Article No. 7630.

Oudin A, Forsberg B, Strömgren M, Beelen R, Modig L. Impact of residential mobility on exposure assessment in longitudinal air-pollution studies: A sensitivity analysis within the ESCAPE project. The Scientific World Journal 2012;2012(1): Article No. 125818.

Paoin K, Ueda K, Vathesatogkit P, Ingviya T, Buya S, Phosri A, et al. Effects of long-term air-pollution exposure on ankle-brachial index and cardio-ankle vascular index: A longitudinal cohort study using data from the electricity generating authority of Thailand study. International Journal of Hygiene and Environmental Health 2021;236:Article No. 113790.

Plaia A, Ruggieri M. Air-quality indices: A review. Reviews in Environmental Science and Bio/Technology 2011;10(2):165-79.

Rajakumari K, Priyanka V. Air-pollution prediction in smart cities by using machine-learning techniques. International Journal of Innovative Technology and Exploring 2020;9(5):1272-9.

Reis S, Liška T, Vieno M, Carnell EJ, Beck R, Clemens T, et al. The influence of residential and work-day population mobility on exposure to air pollution in the UK. Environment International 2018;121:803-13.

Royston P. Approximating the Shapiro-Wilk W-test for non-normality. Statistics and Computing 1992;2(3):117-9.

Shafeeque M, Arshad A, Elbeltagi A, Sarwar A, Pham QB, Khan S, et al. Understanding temporary reduction in atmospheric pollution and its impacts on coastal aquatic systems during the COVID-19 lockdown: A case study of South Asia. Geomatics, Natural Hazards and Risk 2021;12:560-80.

Sharma M, Pandey R, Maheshwari M, Sengupta B, Shukla BP, Gupta NK, et al. Interpretation of air-quality data using an air-quality index for the city of Kanpur, India. Journal of Environmental Engineering and Science 2003;2(6):453-62.

Srikamdee S, Onpans J. Forecasting daily air quality in Northern Thailand using machine-learning techniques. Proceedings of the 4th International Conference on Information Technology (InCIT); 2019 Oct 24-25. Bangkok, Thailand; 2019.

Srivastava S, Kumar A, Bauddh K, Gautam AS, Kumar S. 21-day lockdown in India dramatically reduced air-pollution indices in Lucknow and New Delhi, India. Bulletin of Environmental Contamination and Toxicology 2020;105(1):9-17.

Suriyawong P, Chuetor S, Samae H, Piriyakarnsakul S, Amin M, Furuuchi M, et al. Airborne particulate matter from biomass burning in Thailand: Recent issues, challenges, and options. Heliyon 2023;9(3):e14261.

Tee Lewis PG, Chen T-Y, Chan W, Symanski E. Predictors of residential mobility and its impact on air-pollution exposure among children diagnosed with early-childhood leukaemia. Journal of Exposure Science and Environmental Epidemiology 2019;29(4):510-9.

Wu Y, Song G. The impact of activity-based mobility pattern on assessing fine-grained traffic-induced air-pollution exposure.

International Journal of Environmental Research and Public Health 2019;16:Article No. 3291.

Yasumoto S, Jones AP, Oyoshi K, Kanasugi H, Sekimoto Y, Shibasaki R, et al. Heat-exposure assessment based on individual daily-mobility patterns in Dhaka, Bangladesh. Computers, Environment and Urban Systems 2019;77:Article No. 101367.

Zhu Y, Xie J, Huang F, Cao L. The mediating effect of air quality on the association between human mobility and COVID-19 infection in China. Environmental Research 2020;189:Article No. 109911.

Environment and Natural Resources Journal

Volume 23
Issue 6
2025

The Influence of Age and Management on Soil Physicochemical Properties and Heavy Metal Accumulation in Post-Tin Mining Lands on Bangka Island

Farhan Erdaswin[1], Rahayu[2*], Retno Rosariastuti[2], Widyatmani Sih Dewi[2], Aktavia Herawati[2], Fatimah[3], and Nurul Ichsan[4]

[1]Sebelas Maret University, Faculty of Agriculture, Master's Programme of Soil Science, Jebres, 57126, Surakarta, Indonesia
[2]Sebelas Maret University, Faculty of Agriculture, Department of Soil Science, Jebres, 57126, Surakarta, Indonesia
[3]Research Center for Applied Botany, National Research and Innovation Agency (BRIN), Cibinong Bogor, Indonesia
[4]Regional Development Planning and Research Agency of Kepulauan Bangka Belitung Province, Pangkalpinang, Indonesia

ARTICLE INFO

Received: 14 Mar 2025
Received in revised: 22 Jul 2025
Accepted: 29 Jul 2025
Published online: 9 Sep 2025
DOI: 10.32526/ennrj/23/20250066

Keywords:
Post-tin mining land age/ Post-tin mining management/ Soil physicochemical properties/ Heavy metal accumulation/ Partial least squares structural equation modeling

*** Corresponding author:**
E-mail:
rahayu_pn@staff.uns.ac.id

ABSTRACT

Bangka Island is one of the largest tin producers in Indonesia and the world, covering an area of 156,531.3 hectares. Tin mining activities have significantly degraded post-mining land, altering soil properties and increasing heavy metal retention. This study aimed to evaluate the impact of post-tin mining land age and management on soil physical and chemical properties and total heavy metal concentration. Soil samples were collected using a stratified sampling method from three representative sites with similar climatic conditions: newly mined land (0 years), reclaimed land (7 years), and minimally managed land (20 years). Physical parameters were measured directly in the field, except for bulk density, air-dried soil moisture, and texture fraction, which were analysed in the laboratory alongside chemical parameters. The findings indicate that as post-tin mining land ages, soil physical properties such as bulk density, soil hardness, air-dried soil moisture, and texture fractions change, while infiltration decreases, indicating compaction. Meanwhile, post-tin mining management in the form of reclamation significantly improves soil chemical quality, including pH, organic carbon, organic matter, and phosphorus availability. Heavy metal accumulation is more strongly influenced by land age than management practices; however, appropriate management can reduce heavy metal availability and enhance overall soil quality. Partial least squares structural equation modeling (PLS-SEM) analysis confirms that soil physicochemical properties mediate the relationship between land age, management, and heavy metal accumulation in post-tin mining sites.

HIGHLIGHTS

- Post-tin mining land age and post-tin mining management affect soil properties
- Post-tin mining land age increases soil compaction
- Post-tin mining management improves soil chemistry
- Heavy metal accumulation is more influenced by the land age of the post-tin mining land
- Soil physicochemical properties mediate the relationship between land age, management, and heavy metals.

1. INTRODUCTION

Bangka Belitung Islands Province is the largest tin producer in Indonesia and globally, with the mining area increasing from 144,783.81 ha (2018) to 156,531.3 ha (2021), covering 27.56% of Bangka Island (Harahap, 2016; Provincial Government of the Bangka Belitung Islands, 2022; Maftukhah et al., 2023). Massive mining activities, especially in Central Bangka Regency, which has 18,069 ha of post-tin mining land (Sukarman and Gani, 2017), have caused soil degradation and heavy metal accumulation, limiting land recovery and creating serious environmental problems.

Citation: Erdaswin F, Rahayu, Rosariastuti R, Dewi WS, Herawati A, Fatimah, Ichsan N. The influence of age and management on soil physicochemical properties and heavy metal accumulation in post-tin mining lands on Bangka Island. Environ. Nat. Resour. J. 2025;23(6):537-551. (https://doi.org/10.32526/ennrj/23/20250066)

Post-tin mining soils on Bangka Island are generally characterized by low fertility, high acidity, and degraded physical properties, including high bulk density, low porosity, and poor soil structure (Irzon et al., 2018; Sukarman et al., 2020). In addition, heavy metal contamination, particularly Pb (Sari et al., 2023), Cd (Yang et al., 2021), Cr (Anda et al., 2022), and Cu (Liu et al., 2021), negatively affects microbial activity, reduces plant productivity, and pollutes water sources, further complicating land rehabilitation efforts. Although soil can recover naturally through weathering, organic matter accumulation, and microbial succession (Li et al., 2021; Nyenda et al., 2021), the age of the land alone is insufficient to restore soil quality. A study on post-gold mining soil in the Amazon revealed the progressive accumulation of heavy metals over time. For instance, the concentration of lead (b) increased from 4.05-5.03 mg/kg in land affected for 1.5-5 years to 7.04-7.94 mg/kg in land aged 6-8 years (Velásquez et al., 2020). Similar patterns of increase were observed for other heavy metals, such as As, Cd, and Cu. This phenomenon underscores the importance of active intervention in post-mining land management, such as in post-tin mining areas, to mitigate soil degradation and accelerate ecological rehabilitation (Li et al., 2020).

Post-tin mining land management in Bangka varies from abandoned land without reclamation to revegetation and organic matter application, yielding mixed results (Setyawan et al., 2019). However, many reclamation efforts remain ineffective due to poor planning (Haryadi et al., 2023), and some areas are even repurposed for tourism without adequate rehabilitation (Kivinen et al., 2018). These shortcomings leave the land unproductive and a persistent source of environmental problems (Duncan et al., 2020).

Various reclamation initiatives have been implemented; however, the interaction between land age, management practices, and heavy metal accumulation in tropical environments such as Bangka Belitung remains poorly understood. Furthermore, no studies have specifically examined these interactions in post-tin mining lands, either locally or globally. Therefore, this study aims to evaluate the influence of post-tin mining land age and management practices on soil physicochemical properties and heavy metal retention in post-tin mining sites on Bangka Island. The findings are expected to provide insights for more sustainable post-tin mining land management.

2. METHODOLOGY

2.1 Study sites and research duration

This study was conducted in Central Bangka Regency, Bangka Island, Indonesia, a region heavily impacted by tin mining (Figure 1). Field surveys and soil sampling were carried out in August 2024 to evaluate how post-tin mining land age and management influence soil properties and heavy metal accumulation. Three sites with contrasting reclamation histories were selected: Koba (0 years, unreclaimed), Belilik (7 years, reclaimed), and Nibung (20 years, partially reclaimed). At Koba, informal mining persists, and earlier reclamation efforts, such as planting *Acacia auriculiformis*, were abandoned. Vegetation is very sparse, dominated by remnant *A. auriculiformis*, *Lepironia articulata*, and a few scattered grasses. Belilik underwent structured reclamation using compost blocks (60% cow manure, 40% plant litter with EM4 and tapioca), supporting the growth of *A. auriculiformis*, *Casuarina equisetifolia*, and *Anacardium occidentale* as pioneer reclamation species, and mostly covered with grass. In contrast, Nibung received minimal intervention; although A. auriculiformis was planted, efforts were not sustained, and the site was later converted for tourism. Vegetation developed through natural succession, including *Dicranopteris linearis*, *Nepenthes* spp., and *Dillenia suffruticosa*. These sites were selected to represent a gradient of post-tin mining land age and management intensity, providing a basis for assessing their effects on soil physicochemical properties and heavy metal retention (Table 1).

2.2 Methods and characteristics of research sites

Field measurements included soil hardness (SH), assessed using a digital soil hardness tester, model TYD-2, and soil infiltration rate (IR), measured with a double-ring infiltrometer (Gregory et al., 2005). Laboratory analyses encompassed soil bulk density (BD) and air-dry soil moisture (ADSM) determined by gravimetric methods (Blake and Hartge, 1986; Jabro et al., 2020); soil texture was analyzed by the pipette method (Palihakkara and Vitharana, 2019); soil pH was measured via potentiometry using a Eutech pH 5+; electrical conductivity (EC) was determined via conductometry using a Eutech Cond 6+; total nitrogen (TN) was measured using the Kjeldahl method (Rhee, 2001); available phosphorus (AP) was analysed by the Olsen method (Olsen et al., 1954); available potassium (AK) and cation exchange capacity (CEC) were determined via ammonium acetate extraction (Madaras

and Koubová, 2015; Jain and Taylor, 2023); soil organic carbon (SOC) was measured using the Walkley-Black method (Nelson and Sommers, 1983); and soil organic matter (SOM) was calculated by multiplying SOC by 0.58, a conversion factor proposed by van Bemmelen (Minasny et al., 2020). Finally, heavy metals (Pb, Cd, Cr, Cu) were determined using wet oxidation with HNO_3 and $HClO_4$ (BPSI, 2023). The concentrations were measured with a Thermo Scientific™ iCE™ 3000 Series Atomic Absorption Spectrophotometer (AAS) from Thermo Fisher Scientific Inc., with a detection limit of 0.01 mg/kg for all metals.

Table 2 presents the climate conditions and soil properties at the three study sites: Belilik, Koba, and Nibung. All locations share a similar climate, with an average annual temperature of 27.9°C, annual rainfall of 2,223 mm, and relative humidity of 85%, indicating a humid zone with high precipitation and no significant climatic differences. Drainage is classified as very good in Belilik and Koba, while in Nibung, it is considered moderately good.

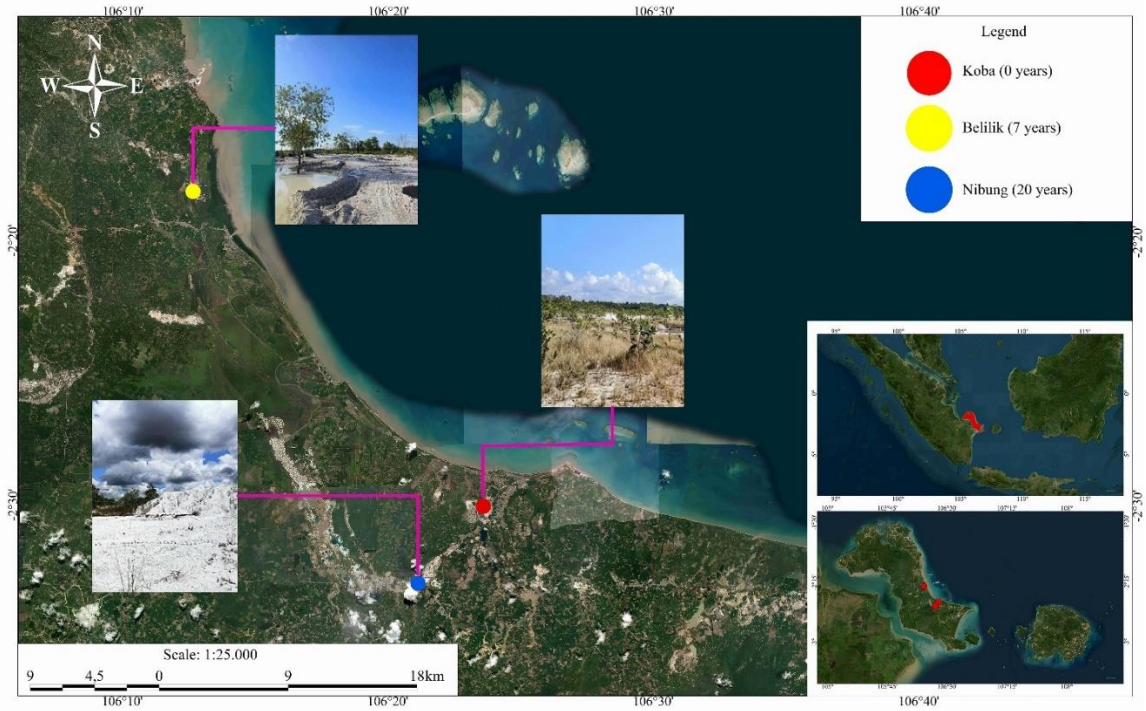

Figure 1. Map of sampling points in three post-tin mining lands on Bangka Island

Table 1. General information about each research and sampling sites

Sites	Altitude (MASL)	Coordinate		Area (ha)	Age of post-tin mining	Post-tin mining management
		X	Y			
Koba	4	-2°29'52.6"	106°23'36"	154.17	0	Previously mined but mined again by the community
Belilik	7	-2°18'05.4"	106°12'32.9"	100.1	7	Has been reclaimed
Nibung	43	-2°32'57.7"	106°21'09.6"	14.22	20	Focused on being a tourist attraction without optimal reclamation

Source: Data and Field Analysis

Table 2. Climate and study sites conditions

Sites	Mean annual temperature	Rainfall/Year (mm)	Relative humidity (%)	Drainage
Koba	27.9	2,223	85	Very good
Belilik	27.9	2,223	85	Very good
Nibung	27.9	2,223	85	Moderately good

Source: Data and Field Analysis

2.3 Data analysis

Field and laboratory data were processed using IBM SPSS version 27 and R Studio. ANOVA was performed, followed by Tukey's HSD post-hoc test (α=0.05) to identify significant differences between post-mining sites. Multivariate analyses, including hierarchical clustering analysis (HCA) and principal component analysis (PCA), were conducted to explore classification patterns and relationships between parameters. Additionally, partial least squares structural equation modeling (PLS-SEM) was applied to evaluate the relationships between post-mining land age, management practices, soil physicochemical properties, and heavy metal accumulation. Parameter estimation was performed using bootstrap resampling (1,000 iterations) to assess the significance of relationships between variables, while model evaluation was based on path coefficients and R^2 values to determine the proportion of explained variance.

3. RESULTS AND DISCUSSION

3.1 Soil physicochemical properties and heavy metal accumulation in the study area

3.1.1 Soil physical properties in the study area

The study results indicate significant differences in soil physical properties across post-tin mining sites on Bangka Island, influenced by land age and management practices (Table 3). Bulk density varied significantly between locations ($p<0.001$), with the highest value recorded in Nibung (20 years) (1.60±0.05 g/cm³) and the lowest in Koba (0 years) (1.39±0.05 g/cm³). The increase in BD with land age suggests soil compaction, which may hinder root growth and water infiltration. Meanwhile, Belilik (7 years), which underwent reclamation, exhibited an intermediate BD (1.50±0.01 g/cm³), highlighting the potential of reclamation efforts in reducing soil compaction.

Other parameters, including infiltration rate (IR), soil hardness (SH), air-dry soil moisture (ADSM), and soil texture fractions, also showed significant differences ($p<0.05$). Koba had the highest IR (135.75±9.13 cm/h), dominated by sand fraction (96.08±0.56%), whereas Nibung had the lowest IR (25.26±4.79 cm/h) due to increased clay content (14.08±8.31%). This trend was also reflected in SH values, with Nibung exhibiting the hardest soil (45.38±4.28 kg/cm²) and Koba the softest (25.88±1.22 kg/cm²). The highest ADSM was observed in Nibung (0.40±0.28%) and the lowest in Koba (0.14±0.02%) ($p=0.03$). These findings demonstrate that post-mining land age and management significantly influence soil physical properties. Soil compaction in Nibung may hinder ecosystem recovery (Zhang et al., 2019), while reclamation efforts in Belilik, incorporating organic matter, have improved soil quality compared to newly mined areas (Song, 2020).

Table 3. Comparison of soil physical properties on various post-tin mining lands in the study area

Sites And Ages	Parameters						
	BD (g/cm^3)	IR (cm/h)	SH (kg/cm^2)	ADSM (%)	Sand (%)	Silt (%)	Clay (%)
Koba (0 Years)	1.39±0.05^a	135.75±9.13^a	25.88±1.22^a	0.14±0.02^b	96.08±0.56^b	1.75±0.38^{ab}	2.16±0.93^b
Belilik (7 years)	1.50±0.01^b	74.16±5.49^b	29.09±3.84^a	0.18±0.05^{ab}	96.97±0.65^b	0.23±0.03^b	2.80±0.67^b
Nibung (20 Years)	1.60±0.05^c	25.26±4.79^c	45.38±4.28^b	0.40±0.28^a	80.08±13.62^a	5.84±5.31^a	14.08±8.31^a
p-value	**<0.001**	**<0.001**	**<0.001**	**0.03**	**0.003**	**0.018**	**<0.001**

BD=Bulk density, IR=Infiltration rate, SH=Soil hardness, ADSM=Air-dried soil moisture, ±; Standard deviation, Letter symbol=Numbers in the same column followed by different letters indicate significantly different according to Tukey's HSD test at the 5% level, while numbers in the same column followed by the same letter indicate not significantly different according to Tukey's test at the 5% level.

3.1.2 Soil chemical properties in the study area

The analysis of soil chemical properties revealed significant variations among the post-tin mining sites, particularly in pH, soil organic carbon (SOC), soil organic matter (SOM), and available phosphorus (AP). The highest pH was recorded in Belilik (6.34±0.94), whereas Koba (5.93±0.15) and Nibung (5.71±0.36) were more acidic ($p<0.001$). Belilik also exhibited the highest SOC (0.45±0.09%) and SOM (0.78±0.16%) compared to Koba (SOC: 0.24±0.06%; SOM: 0.42±0.10%) and Nibung (SOC: 0.33±0.11%; SOM: 0.56±0.19%) ($p=0.004$), indicating that reclamation efforts in Belilik have enhanced organic matter content, improved soil structure, and increased nutrient retention (Table 4).

Available phosphorus (AP) also varied significantly ($p=0.037$), with the highest concentration in Belilik (0.64±0.59 ppm) and the lowest in Koba

(0.10±0.06 ppm), while Nibung (0.19±0.14 ppm) was intermediate. The low AP in Koba suggests nutrient loss due to leaching and erosion. Other parameters, including electrical conductivity (EC), total nitrogen (TN), available kalium (AK), and cation exchange capacity (CEC), did not show significant differences among the sites ($p>0.05$). This can be attributed to the similar environmental conditions and post-mining land management practices, where short-term reclamation efforts primarily influence organic matter-related parameters (Li et al., 2021). These findings highlight that pH, SOC, SOM, and AP, which exhibited significant changes, are directly linked to organic matter dynamics.

Table 4. Comparison of soil chemical properties on various post-tin mining land in the study area

Sites and ages	Parameters							
	pH	EC (dS/m)	SOC (%)	SOM (%)	TN (%)	AP (ppm)	AK (meq/100g)	CEC (meq/100g)
Koba (0 Years)	5.93±0.15^{b}	0.07±0.02^{a}	0.24±0.06^{b}	0.42±0.10^{b}	0.12±0.01^{a}	0.10±0.06^{b}	0.29±0.11^{a}	2.62±0.22^{a}
Belilik (7 Years)	6.34±0.94^{a}	0.06±0.01^{a}	0.45±0.09^{a}	0.78±0.16^{a}	0.13±0.01^{a}	0.64±0.59^{a}	0.30±0.06^{a}	2.50±0.33^{a}
Nibung (20 Years)	5.71±0.36^{b}	0.07±0.02^{a}	0.33±0.11^{b}	0.56±0.19^{b}	0.13±0.01^{a}	0.19±0.14^{ab}	0.20±0.06^{a}	2.79±0.32^{a}
p-value	**<0.001**	0.828	**0.004**	**0.004**	0.699	**0.037**	0.086	0.246

Ec=Electrical conductivity, SOC=Soil organic carbon, SOM=Soil organic matter. TN=Total nitrogen, AP=Phosphorus availability, AK=Potassium availability, CEC=Cation exchange capacity, ±; Standard deviation, Letter symbol=Numbers in the same column followed by different letters indicate significantly different according to Tukey's HSD test at the 5% level, while numbers in the same column followed by the same letter indicate not significantly different according to Tukey's test at the 5% level.

3.1.3 Heavy metal accumulation of Cd, Cr, Cu, Pb in the study area

The analysis of total heavy metal concentrations in post-tin mining sites revealed variations across locations, although the differences were not statistically significant (Figure 2). Pb and Cd were not detected at any site, indicating either low concentrations or levels below detection limit. Despite being undetected, Pb and Cd remain a concern due to their persistent and toxic nature, posing risks to ecosystems (Angon et al., 2024). In contrast, Cr (45.64-49.58 mg/kg) and Cu (1.76-4.55 mg/kg) were detected at all locations, with the highest concentrations found in Nibung (20 years), though the differences were not statistically significant. Briffa et al., (2020) emphasized that while heavy metals play essential roles in biological functions, excessive concentrations can be toxic if not properly managed.

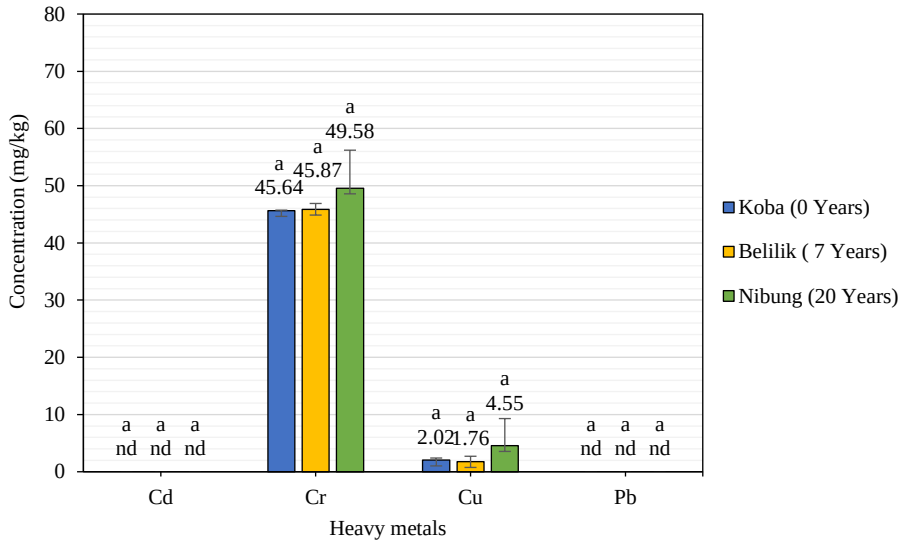

Figure 2. Comparison of total soil heavy metal on various post-tin mining lands in the study area with letter symbol which is mean numbers in the same bar followed by different letters indicate significantly different according to Tukey's HSD test at the 5% level, while numbers in the same bar followed by the same letter indicate not significantly different according to Tukey's test at the 5% level

3.2 Multivariate analysis of post-tin mining soils using hierarchical clustering and PCA

3.2.1 Soil classification based on Hierarchical Clustering Analysis (HCA)

The Hierarchical Clustering Analysis (HCA) of soil physicochemical properties in post-tin mining sites on Bangka Island is visualized through a dendrogram using standardized z-scores (mean=0, SD=1) (Figure 3), illustrating the soil characteristics at the three study sites. In the heatmap legend, blue denotes positive z-scores (above the overall mean), green ≈0, and yellow indicates negative z-scores (below the overall mean). The vertical dendrogram indicates that samples from Koba form a distinct cluster, reflecting the properties of newly mined soils. Belilik forms a relatively homogeneous group, though some outliers are present, whereas Nibung exhibits greater dispersion, indicating heterogeneous soil recovery due to inconsistent post-mining management.

The horizontal dendrogram highlights relationships between soil properties, with BD and SH clustering together, indicating their association with soil compaction. Clay, silt, and ADSM group within the moisture retention category, while CEC, TN, and EC are linked to nutrient retention and salinity potential. Furthermore, SOC, SOM, AP, and pH correlate with soil chemical quality in Belilik, whereas sand, IR, and AK are associated with the sandy soils of Koba, which exhibit high infiltration rates. A z-score-based heatmap reveals that Koba has negative values for fertility parameters, reflecting degraded soil quality. The Belilik site exhibits moderate to high z-scores for organic matter content and nutrient retention, indicating an improvement in these properties. In contrast, the Nibung site displays high z-scores for compaction alongside variable fertility parameters, suggesting that its recovery is hindered by suboptimal management practices.

HCA also reveals patterns of heavy metal accumulation across the three sites (Figure 4). Nibung (20 years) forms a distinct cluster with higher Cr and Cu concentrations due to limited reclamation efforts, as reflected by darker shades in the heatmap. In contrast, Belilik (7 years) and Koba (0 years) cluster more closely together, indicating lower metal concentrations. The clear separation of Nibung from the other sites underscores the long-term environmental impact of inadequate reclamation practices.

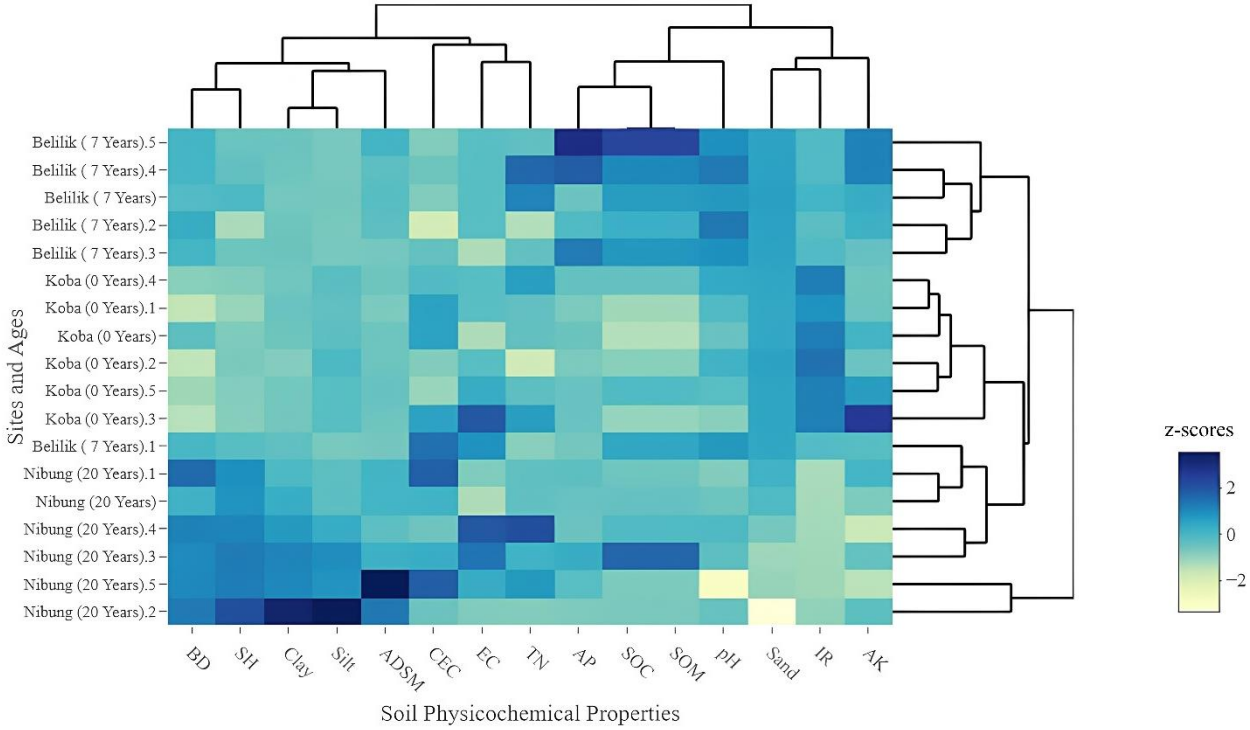

Figure 3. Hierarchical Clustering Analysis (HCA) of soil physicochemical properties in post-tin mining land on Bangka Island

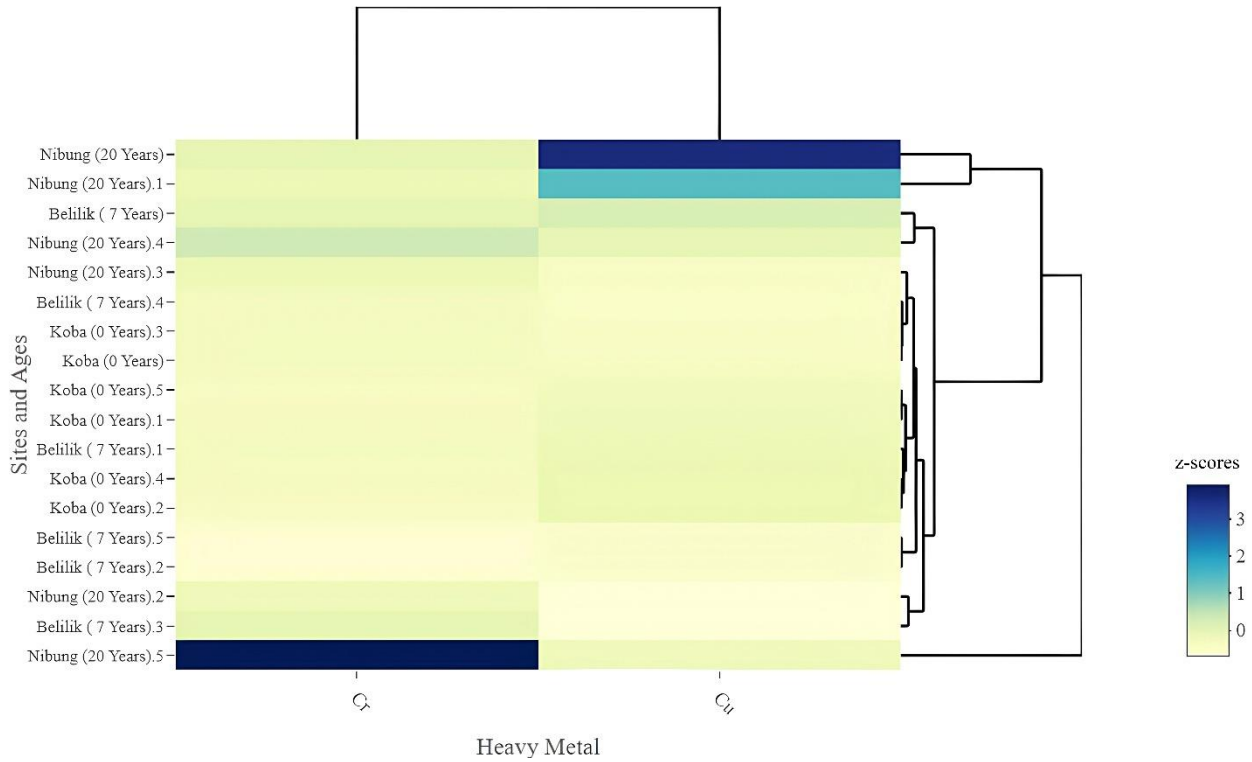

Figure 4. Hierarchical Clustering Analysis (HCA) of heavy metal (Cr and Cu) in post-tin mining land on Bangka Island

3.2.2 Principal Component Analysis (PCA) for key soil property differentiation

The Principal Component Analysis (PCA) biplot (Figure 5) illustrates differences in soil characteristics based on post-mining land age and management. The first two principal components, Dim1 and Dim2, account for 62.5% of the total variance, with contributions of 39.7% and 22.8%, respectively, indicating that site-specific factors strongly influence soil properties.

Dim1 is primarily influenced by Nibung, while Dim2 separates Belilik and Koba, with Belilik positioned in the positive quadrant and Koba in the negative. Koba (0 years) correlates with infiltration rate and sand content, reflecting its coarse texture and high infiltration capacity due to mining disturbances. Belilik (7 years), which underwent reclamation, exhibits higher soil organic carbon, soil organic matter, available phosphorus, and available kalium, indicating improvements in soil chemical quality. Although Nibung (20 years) is the oldest site, it is closely associated with BD, SH, clay, silt, ADSM, CEC, and TN, suggesting significant soil compaction despite having higher CEC and TN. The increase in CEC and TN in Nibung is likely due to the dominance of fine particles (Leinweber et al., 1993), while compaction over time may result from inadequate management, accelerating soil structural degradation, and reducing infiltration (Ngo-Cong et al., 2021). This distribution highlights the effectiveness of reclamation efforts in Belilik, whereas Nibung reflects the long-term negative impacts of poor management. Therefore, targeted rehabilitation is necessary for older post-mining land to restore soil structure and function optimally.

The PCA biplot of heavy metals (Figure 6) reveals that the first two principal components, PC1 (50.8%) and PC2 (49.2%), together explain 100% of the data variation. This indicates that the distribution of heavy metals in the post-mining sites can be fully described by these two components. The analysis considers only Cr and Cu, as Pb and Cd were not detected (Figure 3).

The biplot shows that Nibung (20 years) has a higher PC1 value, indicating a strong correlation with Cr and Cu. In contrast, Koba (0 years) and Belilik (7 years) are positioned near the centre, suggesting lower heavy metal concentrations compared to Nibung. These findings align with the HCA results (Figure 5), which previously highlighted a clear separation between Nibung and the other sites. The results indicate that without optimal management, heavy metals tend to accumulate over time, hindering long-term ecosystem recovery (Zhang et al., 2024).

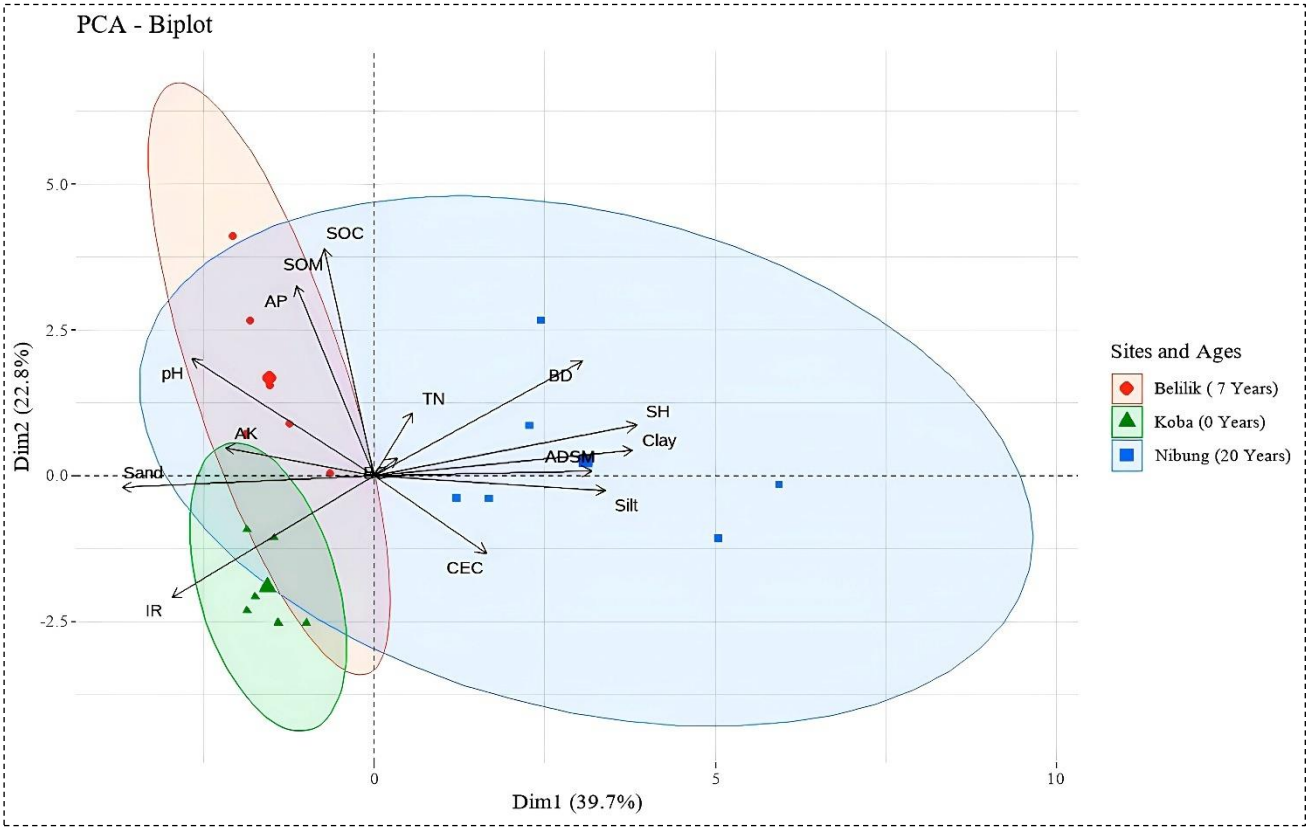

Figure 5. Biplot of Principal Component Analysis (PCA) of soil physicochemical properties in post-tin mining land on Bangka Island

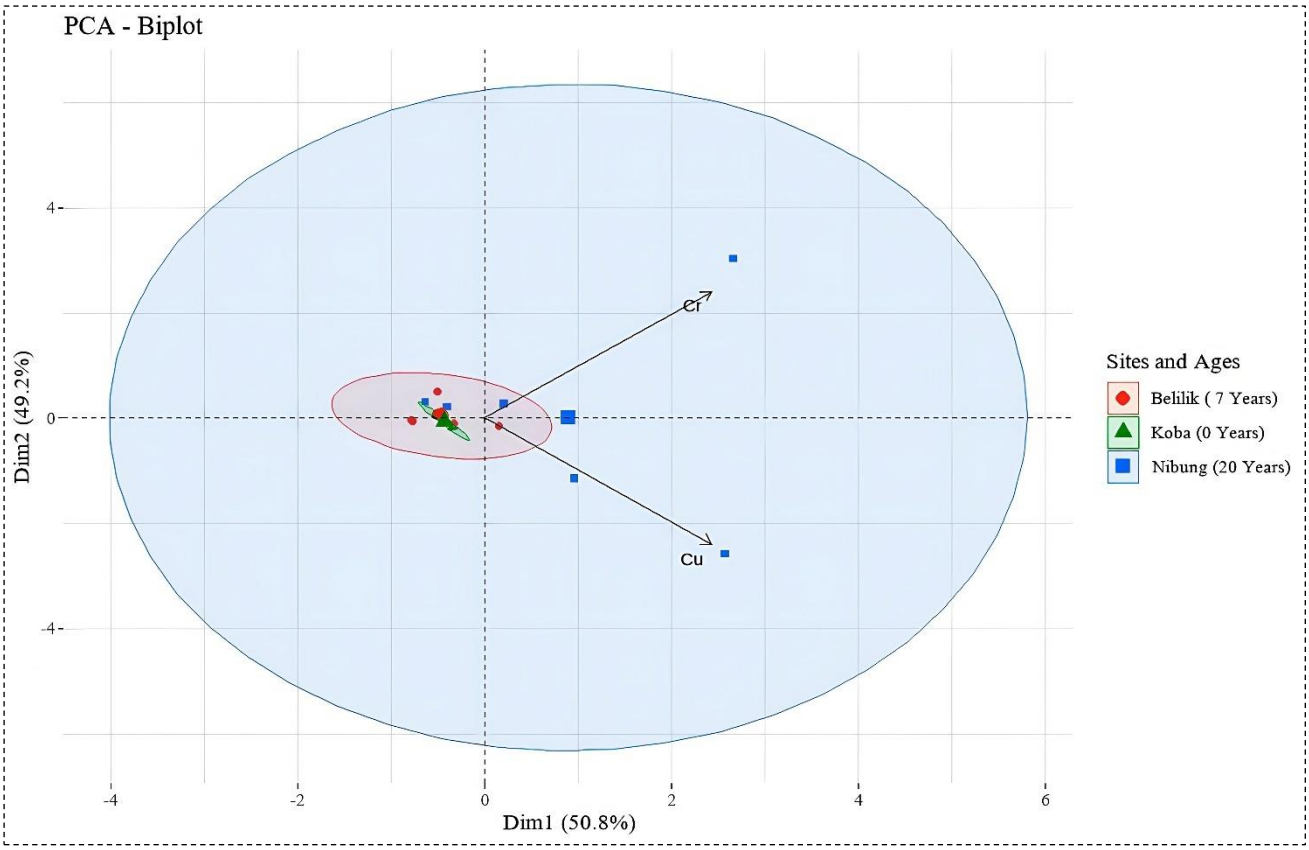

Figure 6. Biplot of Principal Component Analysis (PCA) of heavy metal (Cr and Cu) in post-tin mining land on Bangka Island

3.3 Modeling the influence of post-mining land age and management on soil physicochemical properties and heavy metal accumulation using partial least squares structural equation modeling (PLS-SEM)

The PLS-SEM analysis (Figure 7) indicates that soil physicochemical properties act as mediate in the relationship between land age, management practices, and heavy metal accumulation in post-tin mining sites on Bangka Island. Land age exerts a strong positive influence on soil physical properties (β=0.949), while management practices have a minor negative effect (β=-0.089). Together, these factors explain 84.9% of the variation in physical properties (R^2=0.849). As land age increases, bulk density (BD) (β=0.859) and soil hardness (SH) (β=0.958) rise, contributing to greater soil compaction and reduced root penetration. In contrast, infiltration rate (IR) declines (β=-0.844), elevating the risk of erosion. Textural shifts are also evident, with a decrease in sand content (β=-0.891) and increases in silt (β=0.79) and clay content (β=0.927), resulting in diminished soil aeration. The observed increase in air-dry soil moisture (ADSM) (β=0.738) indicates enhanced moisture retention, which is closely associated with clay accumulation. Overall, aging land tends to develop more compact soils due to organic matter buildup, clay migration, and mineral weathering, as described by Smart and Singer (2023) in their study on mined lands.

Regarding soil chemical properties, post-mining management has a positive influence (β=0.790), whereas land age has a negative effect (β=-0.471), with both factors together explaining 58.9% of the variation (R^2=0.589). Soil chemistry shows a strong positive correlation with SOC and SOM (β=0.861), as well as total nitrogen (TN) (β=0.788), available phosphorus (AP) (β=0.449), and available kalium (AK) (β=0.79). However, long-term recovery is constrained by nutrient leaching and weathering, which are common in post-tin mining sites (Macdonald et al., 2017). Cation exchange capacity exhibits a strong negative relationship (β= -0.624), particularly in Nibung, where high clay content but minimal management reduces nutrient retention efficiency.

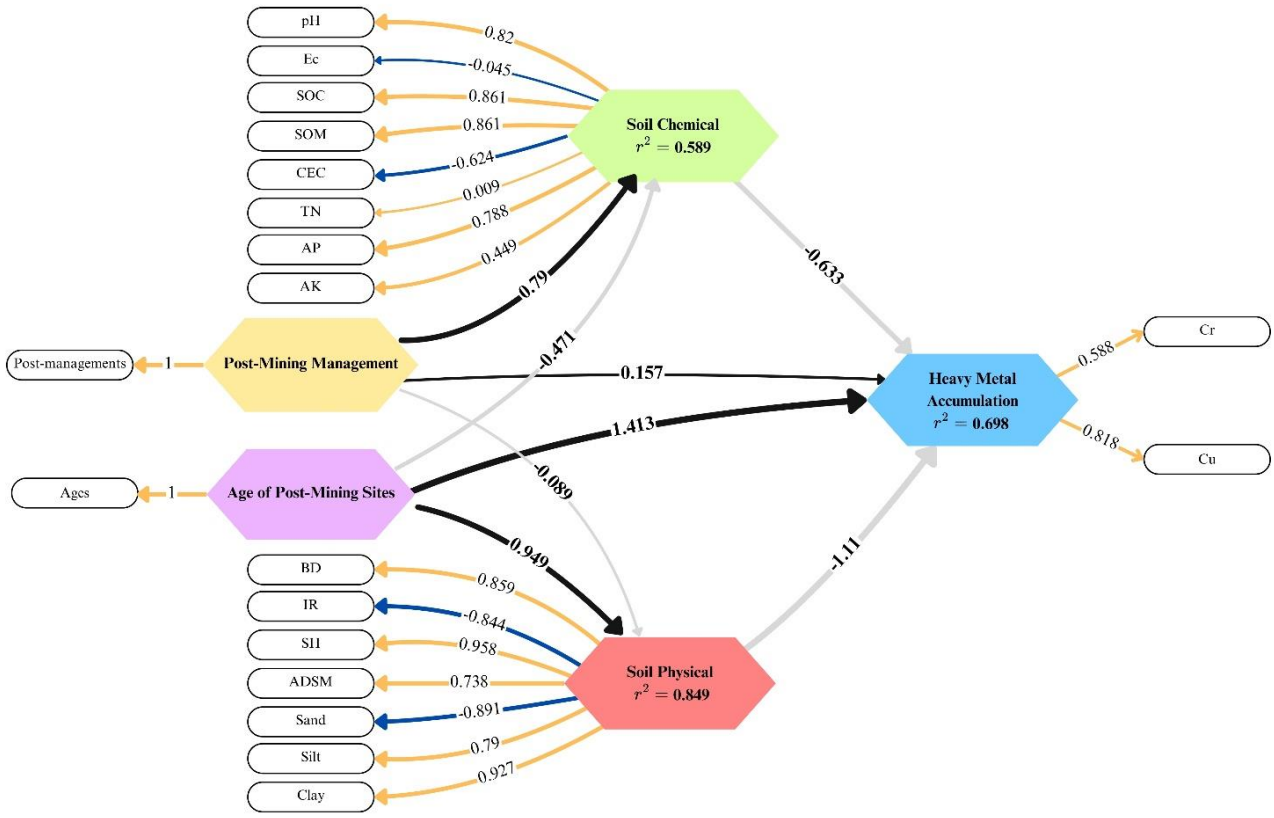

Figure 7. Partial Least Squares Structural Equation Modeling (PLS-SEM) illustrating the structural relationships between post-tin mining age, post-mining management, soil physicochemical properties, and heavy metal accumulation across several post-tin mining sites on Bangka Island

Heavy metal accumulation (R^2=0.698) is primarily driven by land age (β=1.413), with older sites exhibiting higher concentrations, aligning with findings by Zhu et al. (2024). In contrast, post-mining management has a comparatively lower impact (β=0.157). Soil physical (β=-1.110) and chemical properties (β=-0.633) contribute to reducing heavy metal bioavailability, highlighting the role of reclamation in mitigating accumulation impacts (Zhang et al., 2024). Chromium (Cr) (β=0.588) and Copper (Cu) (β=0.818) show significant accumulation, with Cu emerging as the most dominant element in this study.

4. DISCUSSION

4.1 Influence of post-tin mining age on soil physicochemical properties

As post-tin mining land ages, significant soil compaction occurs, as indicated by increased BD (1.39 → 1.60 g/cm³) and SH (25.88 → 45.38 kg/cm²) over 20 years (Table 3). This compaction reduces porosity, restricts root growth, and impedes vegetation recovery (Shah et al., 2017). Infiltration rate also declines sharply (135.75 → 52.49 cm/h), increasing the erosion risk (Ma et al., 2020). The elevated bulk density (BD) at the Nibung site (20 years post-mining) is primarily due to the accumulation of fine particles, such as clay (14.08%) and silt (5.84%), and reduced sand content (80.08%), as shown in Table 3. This shift in texture, resulting from the absence of reclamation, promotes macropore narrowing and aggregate densification. PLS-SEM analysis confirms a strong positive correlations between land age and clay (β=0.927) and silt (β=0.790) fractions. These changes enhance natural compaction and restrict infiltration, consistent with the observed decline in water movement at Nibung (Putra et al., 2024; Zhang et al., 2019; Huang et al., 2020).

The Principal Component Analysis (PCA) (Figure 6) further highlights a shift in soil texture towards finer particles, increasing compaction and reducing drainage, thus elevating the risk of waterlogging (Elkady et al., 2017). PLS-SEM (Figure 7) also shows that land age strongly influences physical properties (BD, SH, ADSM, Clay, and Silt), while its effect on chemical properties is negative. This is reflected in Table 4, where SOC, SOM, pH, and AP initially improve at year 7 (Belilik) but decline by year 20 (Nibung). Although CEC increases with clay content, it fails to enhance nutrient availability due to low organic matter (Rahayu et al., 2023b). Compaction further suppresses microbial activity and nutrient cycling (Longepierre et al., 2022), indicating that without active management, older post-tin mining soils continue to degrade.

These findings align with Putra et al. (2024), who reported increased compaction and reduced infiltration in aging post-tin mining soils in Belitung. However, unlike their study, which found slight increases in organic carbon, our results suggest that land age alone has limited influence on chemical recovery. This is consistent with Oktavia et al. (2014), who observed rising clay content and CEC in older tin mining lands in East Belitung, but not necessarily an improved fertility.

4.2 The role of post-tin mining management in restoring soil physicochemical properties

Post-tin mining land management plays a crucial role in improving soil chemical properties and accelerating ecosystem recovery. This study shows that active reclamation, as implemented in Belilik (7 years), significantly improves soil chemical quality compared to Nibung (20 years), which lacks consistent management, and Koba (0 years), which remains in an early post-mining state (Table 4). Reclamation through organic matter application and revegetation enhances soil carbon content, supporting nutrient retention and microbial activity (Beillouin et al., 2023). In contrast, Nibung suffers from nutrient and organic matter depletion due to minimal intervention, despite its older age, a pattern consistent with findings by Wang et al. (2021), who reported substantial nutrient loss in unmanaged post-mining soils.

Multivariate analyses reinforce these observations. HCA (Figure 3) groups Belilik with more fertile soils, while Nibung is associated with compact, nutrient-poor profiles, and Koba with sandy, highly permeable soils. PCA (Figure 5) further links Belilik to key chemical indicators (SOC, SOM, AP), whereas Nibung aligns with high bulk density and low infiltration. PLS-SEM (Figure 7) confirms that reclamation significantly improves soil chemical properties (β=0.790), with SOC and SOM being the most influential factors (β=0.861), although it has a limited effect on alleviating compaction (β=-0.089). These results align with Li et al. (2021), who found that organic matter-based reclamation enhances nutrient availability and microbial diversity. Similarly, Guan et al. (2020) reported that reclaimed grasslands exhibit higher phosphorus availability, a trend also observed in Belilik, where dense grass cover likely

contributed to elevated AP levels (Table 4). However, despite this improvement, AP remains low, reflecting the legacy of intensive tin mining, which involved methods that intensified the leaching of macro and micronutrients from the soil, an effect that persists on the landscape despite subsequent reclamation efforts (Wulandari et al., 2022).

Overall, these findings confirm that natural recovery based solely on land age is insufficient to restore soil chemical quality. Instead, active post-mining management, particularly through organic amendments and revegetation, is more effective in achieving sustainable soil improvement. This conclusion is supported by Nyenda et al. (2021), who found that changes in soil properties do not consistently correlate with land age, and by König et al. (2023), who emphasized that active reclamation is more effective than passive recovery, especially in severely degraded tailing zones.

4.3 Comparison of soil physicochemical properties in post-tin mining and non-mining lands

Soils in post-tin mining sites investigated in this study exhibit significant differences compared to non-mined soils, both in physical and chemical properties. Wulandari et al. (2022) reported that natural forest and agroforestry soils possess more stable textures, with sand contents of 61.97% and 67.67%, SOC levels of 2.25% and 2.35%, and CEC values of 11.18 and 10.34 meq/100 g, respectively. In contrast, the post-mining soils examined in this study are highly degraded, characterised by elevated sand content (80-97%), low SOC (0.24-0.45%), and CEC values ranging from only 2.5 to 2.79 meq/100 g. Rachman et al. (2019) also reported BD values of 1.23 and 1.27 g/cm³ for natural forest and agricultural land, respectively, substantially lower than those of post-tin mining soils, which ranged from 1.39 to 1.60 g/cm³. Although the Belilik site has undergone more optimal reclamation efforts compared to other locations we studied, these data indicate that post-tin mining soil remains inherently infertile and requires intensive and sustainable management to restore stable and productive soil conditions.

4.4 Heavy metal accumulation and environmental risks in post-tin mining land

Analysis of heavy metal distribution (Figure 3) shows that Cr and Cu were detected at all sites, with the highest concentrations in Nibung (20 years), likely due to its clay-rich, compacted soils and low infiltration, which limit metal mobility (Yan et al., 2017). In contrast, Pb and Cd were not detected, suggesting natural attenuation, consistent with previous findings on post-tin mining lands (Putra et al., 2024; Anda et al., 2022; Oorts et al., 2021). This may result in heavy metal concentrations declining naturally from leaching into former mining ponds (Mulligan and Javid, 2021), as observed by Saputra et al. (2023), who reported elevated Pb and Cd levels in pond sediments at Nibung. A similar process may have occurred in Koba and Belilik, given their comparable climatic conditions.

Lower Cr and Cu levels in Belilik (7 years) indicate that reclamation can effectively suppress heavy metal accumulation (Anda et al., 2022). PCA (Figure 7) and HCA (Figure 5) further show that Nibung forms a distinct cluster, reinforcing the role of land age in metal retention. Older soils with finer textures and higher bulk density tend to adsorb more metals while limiting leaching (Huang et al., 2020; Chileshe et al., 2020). Additionally, lower pH in Nibung enhances Cr retention (Zhang et al., 2023), while Cu is more closely associated with organic carbon fractions (Akbarpour et al., 2021). The absence of vegetation also limits phyto uptake and microbial degradation of metals (Sari et al., 2016).

PLS-SEM (Figure 7) confirms that land age is the dominant factor influencing heavy metal accumulation, while management plays a lesser role. Soil physicochemical properties contribute to metal stabilization, with Cu emerging as the most dominant element. These results align with Dusengemungu et al. (2022), who found that older, unmanaged post-mining sites tend to retain more heavy metals due to poor infiltration and low organic matter.

In summary, unmanaged older sites like Nibung are more prone to heavy metal retention, highlighting the need for targeted reclamation to stabilize contaminants. Although Cr and Cu levels remain within permissible limits (Table 5), Cr poses a potential long-term risk if left unaddressed (Jiang et al., 2023; Zulfiqar et al., 2023). Sampling in this study was conducted in August. Therefore, it is important to acknowledge that seasonal variations may influence the mobility of heavy metals such as Pb and Cd. Future studies involving repeated seasonal sampling are recommended to provide a more comprehensive understanding of Pb and Cd behavior in post-tin mining landscapes, particularly to verify the proposed leaching mechanisms.

Table 5. Permissible limits of heavy metals in soil

Elements	Cd (Cadmium)	Cr (Chromium)	Cu (Copper)	Pb (Lead)	Source
Normal limits of soil (mg/kg)	0.01-2.0	5-1,500	2-250	2-300	Alloway, (1995), BPSI, (2023)
Critical limit of soil (mg/kg)	3-8	75-100	60-125	100-400	

4.5 Phased reclamation strategy and sustainable management of post-tin mining land

Sustainable post-mining land use requires reclamation strategies tailored to site-specific conditions. The findings indicate that as land ages, it tends to undergo compaction and a decline in soil chemical quality, whereas post-tin mining management can mitigate these effects. Heavy metal accumulation is higher in older sites, necessitating efforts to reduce metal mobility through amelioration, revegetation, and microbial assistance (Agrawal et al., 2024).

All three study sites require remediation before being repurposed for agriculture, despite Pb and Cr concentrations remaining within permissible limits. To meet regulatory thresholds and ensure long-term soil productivity, heavy metal concentrations must be further reduced. Among the sites, Belilik shows the greatest potential for agricultural use due to its improved chemical properties following reclamation, although further enrichment with organic matter is still needed. In contrast, Nibung, characterised by severe compaction and inconsistent management, is more suitable for forestry or conservation purposes, though its current use as a tourism site can be maintained with continued ecological restoration. Koba, being recently mined and unmanaged, requires comprehensive rehabilitation before any productive use is possible.

Soil improvement across these sites can be effectively achieved through organic-based amendments such as compost and biochar. These materials enhance soil aeration, water retention, and nutrient availability, while also stabilizing heavy metals through adsorption and organo-metal complex formation (Tang et al., 2020). In parallel, revegetation plays a critical role in restoring soil structure and biological function. Deep-rooted species such as *Acacia mangium*, *Schima wallichii*, and *Albizia falcata* are effective in alleviating compaction, while shallow-rooted species like *Imperata cylindrica*, *Panicum maximum*, *Melastoma malabathricum*, and *Paspalum vaginatum* contribute to organic matter accumulation and soil aggregation (Bohrer et al., 2017; Cao et al., 2023; Rahayu et al., 2023a; Sari et al., 2023). Grassland revegetation, as demonstrated by Buta et al. (2019), has also been shown to enhance microbial activity, increase SOC, and reduce compaction, an approach that has proven effective in Belilik and could be replicated in Nibung and Koba.

To ensure long-term success, a phased reclamation strategy with measurable benchmarks is essential. In the initial 0-3 years, intensive interventions such as high-dose organic amendments (≥50 ton/ha), microbial inoculation, and pioneer vegetation should be applied to stabilize bulk density, reduce heavy metal concentrations, and raise SOC above 1%, a critical threshold in tropical soils (Lal, 2004). The 3-7 year phase should continue these efforts to achieve SOC>2% to enhance soil structure, water retention, and CEC (Patrick et al., 2013). Long-term management (10-20 years) should aim to increase and maintain SOC>2.5% and ensure heavy metals remain at safe levels (Haghighizadeh et al., 2024). This framework offers practical guidance for sustainable reclamation of post-tin mining landscapes.

5. CONCLUSION

This study demonstrates that the interaction between post-mining land age and management practices significantly influences soil physicochemical properties and heavy metal retention. As land age increases, soil compaction intensifies, with bulk density rising from 1.39±0.05 g/cm³ (0 years) to 1.60±0.05 g/cm³ (20 years) and infiltration rate declining from 135.75±9.13 cm/h to 25.26±4.79 cm/h, exacerbating soil structural degradation. A seven-year reclamation period has been proven to enhance soil chemical quality by increasing SOC, SOM, and AP, whereas older unmanaged land exhibits declines in soil quality. The accumulation of Cr (45.64-49.58 mg/kg) and Cu (1.76-4.55 mg/kg) is higher in 20-year-old land, with PLS-SEM analysis revealing that land age exerts a dominant influence on heavy metal accumulation (β=1.413), whereas post-mining management has a comparatively smaller impact (β=0.157). The deterioration of soil physical properties, including increased bulk density (β=0.859) and soil hardness (β=0.958), further exacerbates heavy metal retention. Overall, these findings highlight that while natural processes contribute to increased compaction and heavy metal accumulation, effective

reclamation interventions, such as organic matter amendments and revegetation, are crucial in improving soil quality and mitigating heavy metal contamination risks, underscoring the necessity of active management strategies to restore ecosystem function in post-tin mining lands.

ACKNOWLEDGEMENTS

This research was conducted with funding support from BIMA, provided by the Ministry of Education, Culture, Research and Technology of the Republic of Indonesia with Contract Letter Number: 086/E5/ PG.02.00.PL/2024 for the 2024 fiscal year. We would also like to thank the Central Bangka Regency Government and the Regional Development Planning and Research Agency of Kepulauan Bangka Belitung Province for granting permission to conduct regional research.

AUTHOR CONTRIBUTIONS

Farhan Erdaswin led the conceptual design, methodology, software development, formal analysis, investigation, data curation, draft writing, and visualization. Rahayu, Retno Rosariastuti, and Widyatmani Sih Dewi contributed to conceptualization, methodology, validation, supervision, manuscript review, and data curation. Aktavia Herawati assisted with validation and formal analysis, while Nurul Ichsan focused on investigation. Fatimah and Widyatmani provided resources, with additional visualisation support from Fatimah. All authors were involved in funding acquisition.

DECLARATION OF CONFLICT OF INTEREST

The authors declare no conflicts of interest.

REFERENCES

Agrawal K, Ruhil T, Gupta VK, Verma P. Microbial assisted multifaceted amelioration processes of heavy-metal remediation: A clean perspective toward sustainable and greener future. Critical Review in Biotechnology 2024;44(3):429-47.

Akbarpour F, Gitipour S, Baghdadi M, Mehrdadi N. Correlation between chemical fractionation of heavy metals and their toxicity in the contaminated soils. Environmental Earth Sciences 2021;80(21):1-12.

Alloway BJ. Heavy Metals in Soils. London: Chapman and Hall; 1995.

Anda M, Diah Purwantari N, Yulistiani D, Sajimin, Suryani E, Husnain, et al. Reclamation of post-tin mining areas using forages: A strategy based on soil mineralogy, chemical properties and particle size of the refused materials. Catena 2022;213:Article No. 106140.

Angon PB, Islam MS, KC S, Das A, Anjum N, Poudel A, et al. Sources, effects and present perspectives of heavy metals contamination: Soil, plants and human food chain. Heliyon 2024;10(7):1-15.

Indonesian soil and fertilizer instrument standards testing center (BPSI). Chemical Analysis of Soil, Plants, Water, and Fertilizers. 3rd ed. Bogor: Ministry of Agriculture of the Republic of Indonesia; 2023.

Beillouin D, Corbeels M, Demenois J, Berre D, Boyer A, Fallot A, et al. A global meta-analysis of soil organic carbon in the Anthropocene. Nature Communications 2023;14:Article No. 3700.

Blake GR, Hartge KH. Bulk density. In: Klute A, editor. Methods of Soil Analysis. Part 1. Physical and Mineralogical Methods. 2nd ed. Madison (WI): American Society of Agronomy and Soil Science Society of America; 1986. p. 363-75.

Bohrer SL, Limb RF, Daigh ALM, Volk JM. Belowground attributes on reclaimed surface mine lands over a 40-year chronosequence. Land Degradation and Development 2017;28(7):2290-7.

Briffa J, Sinagra E, Blundell R. Heavy metal pollution in the environment and their toxicological effects on humans. Heliyon 2020;6(9):e04691.

Buta M, Blaga G, Paulette L, Păcurar I, Roşca S, Borsai O, et al. Soil reclamation of abandoned mine lands by revegetation in Northwestern part of Transylvania: A 40-Year retrospective study. Sustainability (Switzerland) 2019;11(12):Article No. 3393.

Cao T, Zhang H, Chen T, Yang C, Wang J, Guo Z, et al. Research on the mechanism of plant root protection for soil slope stability. PLoS One 2023;18(11):e0293661.

Chileshe MN, Syampungani S, Festin ES, Tigabu M, Daneshvar A, Odén PC. Physico-chemical characteristics and heavy metal concentrations of copper mine wastes in Zambia: Implications for pollution risk and restoration. Journal of Forestry Research 2020;31(4):1283-93.

Duncan C, Good MK, Sluiter I, Cook S, Schultz NL. Soil reconstruction after mining fails to restore soil function in an Australian arid woodland. Restoration Ecology 2020;28(S1):35-43.

Dusengemungu L, Mubemba B, Gwanama C. Evaluation of heavy metal contamination in copper mine tailing soils of Kitwe and Mufulira, Zambia, for reclamation prospects. Scientific Reports 2022;12:Article No. 11283.

Elkady TY, Al-Mahbashi A, Dafalla M, Al-Shamrani M. Effect of compaction state on the soil water characteristic curves of sand-natural expansive clay mixtures. European Journal of Environmental and Civil Engineering 2017;21(3):289-302.

Gregory JH, Dukes MD, Miller GL, Jones PH. Analysis of double-ring infiltration techniques and development of a simple automatic water delivery system. Applied Turfgrass Science 2005;2(1):1-7.

Guan Y, Zhou W, Bai Z, Cao Y, Huang Y, Huang H. Soil nutrient variations among different land use types after reclamation in the Pingshuo opencast coal mine on the Loess Plateau, China. Catena 2020;188:Article No. 104427.

Haghighizadeh A, Rajabi O, Nezarat A, Hajyani Z, Haghmohammadi M, Hedayatikhah S, et al. Comprehensive analysis of heavy metal soil contamination in mining Environments: Impacts, monitoring techniques, and remediation strategies. Arabian Journal of Chemistry 2024;17(6):Article No. 105777.

Harahap RF. Post-tin mining land restoration on Bangka Island. Journal of Society 2016;6(1):61-9 (in Indonesian).

Haryadi D, Ibrahim, Darwance. Environmental Improvement Policy through the obligation of post-tin mining reclamation in the islands of Bangka Belitung. IOP Conference Series: Earth and Environmental Science 2023;1175:Article No. 012021.

Huang B, Yuan Z, Li D, Zheng M, Nie X, Liao Y. Effects of soil particle size on the adsorption, distribution, and migration behaviors of heavy metal(loid)s in soil: A review. Environmental Science: Processes and Impacts 2020;22:1596-615.

Irzon R, Syafri I, Hutabarat J, Sendjaja P, Permanadewi S. Heavy metals content and pollution in tin tailings from Singkep Island, Riau, Indonesia. Sains Malaysiana 2018;47(11):2609-16.

Jabro JD, Stevens WB, Iversen WM. Comparing two methods for measuring soil bulk density and moisture Content. Open Journal of Soil Science 2020;10(06):233-43.

Jain A, Taylor RW. Determination of cation exchange capacity of calcareous soils: Comparison of summation method and direct replacement method. Communications in Soil Science and Plant Analysis 2023;54(6):743-8.

Jiang S, Chen Y, Chen S, Hu Z. Removal and reclamation of trace metals from copper and gold mine tailing leachates using an alkali suspension method. Water (Switzerland) 2023;15:Article No. 1902.

Kivinen S, Vartiainen K, Kumpula T. People and post-mining environments: PPGIS mapping of landscape values, knowledge needs, and future perspectives in Northern Finland. Land 2018;7:Article No. 151.

König LA, Medina-Vega JA, Longo RM, Zuidema PA, Jakovac CC. Restoration success in former Amazonian mines is driven by soil amendment and forest proximity. Philosophical Transactions of the Royal Society B: Biological Sciences 2023;378:Article No. 20210086.

Lal R. Soil carbon sequestration impacts on global climate change and food security. Science 2004;304:1623-7.

Leinweber P, Reuter G, Brozio K. Cation exchange capacities of organo-mineral particle-size fractions in soils from long-term experiments. Journal of Soil Science 1993;44(1):111-9.

Li J, Yan X, Cao Z, Yang Z, Liang J, Ma T, et al. Identification of successional trajectory over 30 Years and evaluation of reclamation effect in coal waste dumps of surface coal mine. Journal of Cleaner Production 2020;269:Article No. 122161.

Li L, Li T, Meng H, Xie Y, Zhang J, Hong J. Effects of seven-year fertilization reclamation on bacterial community in a coal mining subsidence area in Shanxi, China. International Journal of Environmental Research and Public Health 2021;18:Article No. 12504.

Liu B, Tian K, Huang B, Zhang X, Bian Z, Mao Z, et al. Pollution characteristics and risk assessment of potential toxic elements in a tin-polymetallic mine area Southwest China: Environmental implications by multi-medium analysis. Bulletin of Environmental Contamination and Toxicology 2021;107(6):1032-42.

Longepierre M, Feola Conz R, Barthel M, Bru D, Philippot L, Six J, et al. Mixed effects of soil compaction on the nitrogen cycle under pea and wheat. Frontiers in Microbiology 2022;12:Article No. 822487.

Ma L, Li J, Liu J. Effects of antecedent soil water content on infiltration and erosion processes on loessial slopes under simulated rainfall. Hydrology Research 2020;51(5):882-93.

Macdonald SJ, Jordan GJ, Bailey TG, Davidson N. Early seedling establishment on aged Tasmanian tin mine tailings constrained by nutrient deficiency and soil structure, not toxicity. Soil Research 2017;55(7):692-703.

Madaras M, Koubová M. Potassium availability and soil extraction tests in agricultural soils with low exchangeable potassium content. Plant, Soil and Environment 2015;61(5):234-9.

Maftukhah R, Kral RM, Mentler A, Ngadisih N, Murtiningrum M, Keiblinger KM, et al. Post-tin-mining agricultural soil regeneration using local resources, reduces drought stress and increases crop production on Bangka Island, Indonesia. Agronomy 2023;13:Article No. 50.

Minasny B, McBratney AB, Wadoux AMJC, Akoeb EN, Sabrina T. Precocious 19th century soil carbon science. Geoderma Regional 2020;22:e00306.

Mulligan CN, Javid M. Application of natural and enhanced natural attenuation of heavy metals in soils and sediments. Japanese Geotechnical Society Special Publication 2021;9(11):504-12.

Nelson DW, Sommers LE. Total carbon, organic carbon, and organic matter. In: Methods of Soil Analysis: Part 2 Chemical and Microbiological Properties, 9.2.2. 2nd ed. American Society of Agronomy, Inc., Soil Science Society of America, Inc.; 1983. p. 539-79.

Ngo-Cong D, Antille DL, van Genuchten MTH, Nguyen HQ, Tekeste MZ, Baillie CP, et al. A modeling framework to quantify the effects of compaction on soil water retention and infiltration. Soil Science Society of America Journal 2021;85(6):1931-45.

Nyenda T, Gwenzi W, Jacobs SM. Changes in physicochemical properties on a chronosequence of gold mine tailings. Geoderma 2021;395:Article No. 115037.

Oktavia D, Setiadi Y, Hilwan I. Physical and chemical properties of soil in heath forest and post-tin mining land in East Belitung Regency. Journal of Tropical Silviculture 2014;5(3):149-54 (in Indonesian).

Olsen SR, Cole CV, Watanabe FS, Dean LA. Estimation of Available Phosphorus in Soils by Extraction with Sodium Bicarbonate. USDA Circular No. 939. Washington (DC): U.S. Department of Agriculture; 1954. p. 1-19.

Oorts K, Smolders E, Lanno R, Chowdhury MJ. Bioavailability and ecotoxicity of lead in soil: Implications for setting ecological soil quality standards. Environmental Toxicology and Chemistry 2021;40(7):1948-61.

Palihakkara PDBJ, Vitharana UWA. A time-efficient and accurate texture analysing method for tropical soils. Journal of Agriculture and Value Addition 2019;2(2):1-9.

Patrick M, Tenywa JS, Ebanyat P, Tenywa MM, Mubiru DN, Basamba TA, et al. Soil organic carbon thresholds and nitrogen management in tropical agroecosystems: Concepts and prospects. Journal of Sustainable Development 2013;6(12):31-43.

Provincial Government of the Bangka Belitung Islands. Regional Environmental Management Performance Information Document 2021. BOOK II. Pangkalpinang: Provincial Government of the Bangka Belitung Islands; 2022 (in Indonesian).

Putra HF, Bui LT, Mori Y. Microbial community shifts indicate recovery of soil physical properties in a post-tin-mining area on Belitung Island, Indonesia. Land Degradation and Development 2024;35(7):2395-408.

Rachman LM, Baskoro DPT, Bayu HH. The effect of tin mining on soil damage in pedindang sub-watershed, Central Bangka Regency. IOP Conference Series: Earth and Environmental Science 2019;399:Article No. 012026.

Rahayu R, Ariyanto DP, Usrotin AH, Hatami FR, Mo YG. Assessment of turf quality in *Paspalum vaginatum* Sw.

accessions of Sumatra, Java, and Bali (Indonesia) with clay and amended sand growing media. Biodiversitas 2023a;24(3):1650-8.

Rahayu, Supriyadi, Herdiansyah G, Herawati A, Erdaswin F. The influence of geological formations on soil characteristics and quality in the southeast region of Pacitan Regency, Indonesia. Soil Science Annual 2023b;74(3):1-13.

Rhee KC. Determination of total nitrogen. In: Current Protocols in Food Analytical Chemistry. Unit B1.2.1-B1.2.9. John Wiley and Sons, Inc.; 2001.

Saputra W, Azura SM, Sihombing IL, Nugraha A, Tua OS, Ega AD. Identification of heavy metal elements in Kaolin Lake. In: National Seminar on Researchers and Community Service. Pangkalpinang; 2023. p. 121-4 (in Indonesian).

Sari E, Giyanto G, Sudadi U. *Acacia auriculiformis* and *Eragrostis chariis*: Potential vegetations from tin-mined lands in Bangka Island as Pb and Sn phytoremediator. Journal of Soil and Environmental Science 2016;18(1):1-7.

Sari E, Nugroho AP, Retnaningrum E, Prijambada ID. Plant dispersal at Bangka post-tin mining revegetated land correlated with soil chemical physical properties and heavy metal distribution. Proceedings of the International Conference on Sustainable Environment, Agriculture and Tourism (ICOSEAT 2022) 2023;26:733-41.

Setyawan D, Hermawan A, Hanum H. Revegetation of tin post-mining sites in Bangka Island to enhance soil surface development. IOP Conference Series: Earth and Environmental Science 2019;393:Article No. 012093.

Shah AN, Tanveer M, Shahzad B, Yang G, Fahad S, Ali S, et al. Soil compaction effects on soil health and cropproductivity: An overview. Environmental Science and Pollution Research 2017;24(11):10056-67.

Smart KE, Singer DM. Surface coal mine soils: Evidence for chronosequence development. Soil Systems 2023;7:Article No. 59

Song U. Improvement of soil properties and plant responses by compost generated from biomass of phytoremediation plant. Environmental Engineering Research 2020;25(5):638-44.

Sukarman, Gani RA, Asmarhansyah. Tin mining process and its effects on soils in Bangka Belitung Islands Province, Indonesia. Sains Tanah - Journal of Soil Science and Agroclimatology 2020;17(2):180-9.

Sukarman N, Gani RA. Ex-mining land in Bangka and Belitung Islands, Indonesia and their suitability for agricultural commodities. Journal of Soil and Climate 2017;41:Article No. 101 (in Indonesian).

Tang J, Zhang L, Zhang J, Ren L, Zhou Y, Zheng Y, et al. Physicochemical features, metal availability and enzyme activity in heavy metal-polluted soil remediated by biochar and compost. Science of the Total Environment 2020;701:Article No. 134751.

Velásquez RMG, Barrantes JAG, Thomas E, Gamarra Miranda LA, Pillaca M, Tello Peramas LD, et al. Heavy metals in alluvial gold mine spoils in the Peruvian Amazon. Catena 2020;189:Article No. 104454.

Wang Z, Wang G, Wang C, Wang X, Li M, Ren T. Effect of environmental factors on soil nutrient loss under conditions of mining disturbance in a coalfield. Forests 2021;12:Article No. 1370

Wulandari D, Agus C, Rosita R, Mansur I, Fikri Maulana A. Impact of tin mining on soil physio-chemical properties in Bangka, Indonesia. Journal of Environmental Science and Technology 2022;14(2):114-21.

Yan X, Hu Y, Chang Y, Li Y, Liu M, Zhong J, et al. Effects of land reclamation on distribution of soil properties and heavy metal concentrations, and the associated environmental pollution assessment. Polish Journal of Environmental Studies 2017;26(4):1809-23.

Yang Y, Li C, Yang Z, Yu T, Jiang H, Han M, et al. Application of cadmium prediction models for rice and maize in the safe utilization of farmland associated with tin mining in Hezhou, Guangxi, China. Environmental Pollution 2021;285:Article No. 117202.

Zhang R, Zhao X, He Yanxia, He Yifeng, Ma L. Extraction methods optimization of available heavy metals and the health risk assessment of the suburb soil in China. Environmental Monitoring and Assessment 2023;195:Article No. 1221.

Zhang Y, Shen Z, Zhou W, Liu C, Li Y, Ding B, et al. Environmental problems of emerging toxic metals and treatment technology and methods. RSC Advances 2024;14(50):37299-310.

Zhang Z, Tang G, Zhu J. Study on compaction of reclaimed soil of nonmetallic mining area in northern foothills of Tianshan Mountains in Xinjiang, China. Advances in Materials Science and Engineering 2019;2019:Article No. 2834019.

Zhu D, Li Q, Yan B, Zhang Z, Li Y. Ecological risk assessment and spatial distribution of heavy metal in an abandoned mining area, a case study of liaoyang pyrite mining area in China: Implications for the environmental remediation of mine sites. Polish Journal of Environmental Studies 2024;33(2):1965-80.

Zulfiqar U, Haider FU, Ahmad M, Hussain S, Maqsood MF, Ishfaq M, et al. Chromium toxicity, speciation, and remediation strategies in soil-plant interface: A critical review. Frontiers in Plant Science 2023;13:Article No. 1081624.

Environment and Natural Resources Journal

Volume 23
Issue 6
2025

Levels of Microplastics in Aquatic Ecosystem Components of the Kedung Ombo Reservoir, Central Java: Analysis of Water, Tilapia (*Oreochromis mossambicus*), Sediment, Macroalgae, and Gastropods

Noor Maulidah[1], Muslim Muslim[1*], and Heny Suseno[2]

[1]*Aquatic Resources Management, Faculty of Fisheries and Marine Science, Diponegoro University, Semarang 50275, Central Java, Indonesia*
[2]*Research Center for Radioisotope, Radiopharmaceutical and Biodosimetry Technology Research Organization of Nuclear Energy, National Research and Innovation Agency (BRIN), South Tangerang 15314, Indonesia*

ARTICLE INFO

Received: 20 Mar 2025
Received in revised: 23 Jul 2025
Accepted: 27 Jul 2025
Published online: 8 Sep 2025
DOI: 10.32526/ennrj/23/20250071

Keywords:
Kedung Ombo Reservoir/ Microplastics/ *Oreochromis mossambicus*/ Food chain

*** Corresponding author:**
E-mail:
muslim@lecturer.undip.ac.id

ABSTRACT

The widespread use of plastics in daily activities poses a significant threat to aquatic environments and human health, primarily because plastics degrade into microplastics that easily accumulate in biota and may cause harm when ingested. The aim of this study was to identify the abundance and types of microplastics in water, gastropods, tilapia fish, macroalgae, and sediments. This study was conducted from September to December 2024 in the Kedung Ombo Reservoir. The abundance, shape, and size of microplastics were analyzed using an Olympus CX23 binocular microscope with a 4×/0.10 objective lens. Polymer type analysis of the microplastics was conducted using Fourier Transform Infrared (FTIR) spectroscopy. The abundance of microplastics found at each observation station, consisting of water, gastropods, tilapia fish, macroalgae, and sediment samples, was 122, 2,088, 2,700, 1,036, and 8,847 particles/kg, respectively. Microplastics were classified based on their size into small (<0.5 mm), medium (0.5-<1 mm), and large (1-5 mm), with percentages of 72%, 13%, and 15%, respectively. The shapes of the detected microplastics included fibers (39%), fragments (19%), films (17%), pellets (15%), and foams (11%). The microplastics detected were black (33%), red (15%), purple (6%), yellow (12%), blue (8%), green (6%), and clear (20%). The microplastics identified were polyethylene terephthalate (PET), polyethylene (PE), and polystyrene (PS). The abundance of microplastics has been detected in various compartments of the Kedung Ombo Reservoir. This needs to be monitored regularly, because microplastic accumulation on organisms can be harmful to health and the environment.

HIGHLIGHTS

This study aimed to identify the abundance and types of microplastics in water, tilapia, macroalgae, sediments, and gastropods in the Kedung Ombo reservoir, Central Java, Indonesia, which is the second largest reservoir in the region. To date, no publications have addressed the abundance of microplastics in this reservoir.

1. INTRODUCTION

Plastic waste smaller than 5 mm in aquatic ecosystem worldwide is a pressing concern, as it can harm both aquatic ecosystem and humans. This is because the extremely small size of microplastics allows them to easily enter aquatic ecosystems. This process can then be transferred to humans through the food chain (Kalčíková, 2023; Jimoh et al., 2023; Berlino et al., 2021). Microplastics in organisms can cause irritation of the gastrointestinal tract, inhibit growth, disrupt reproductive systems, and even lead to death (Ariyunita et al., 2022). Microplastic pollution has been observed in almost all aquatic environments, both lotic and lentic, including rivers (Xia et al., 2023), lakes (Ephsy and Raja, 2023), estuaries (Lee et al., 2022), and even deep oceans (Tsuchiya et al., 2023). Based on these studies, it is highly likely that Indonesia is also affected by microplastics, as it is one of the largest producers of plastic waste owing to its high population density (Ismanto et al., 2023b).

Citation: Maulidah N, Muslim M, Suseno H. Levels of microplastics in aquatic ecosystem components of the Kedung Ombo Reservoir, Central Java: Analysis of water, Tilapia (*Oreochromis mossambicus*), sediment, Macroalgae, and Gastropods. Environ. Nat. Resour. J. 2025;23(6):552-568. (https://doi.org/10.32526/ennrj/23/20250071)

Research on the abundance of microplastics in lentic waters is still limited, with some studies, such as those by Adji et al. (2022) and Rahmayanti et al. (2022), conducted in the Rawa Jombor Reservoir in Central Java. Although these studies have been useful, similar research has not yet been conducted in the Kedung Ombo Reservoir. This reservoir is the second largest in Central Java, after the Gajah Mungkur Reservoir, and has been developed to meet the needs of surrounding communities. It is already used for irrigation, tourism, fisheries, agriculture, and hydropower (Purnomo and Chika, 2022). High human activity in the reservoir area inevitably results in plastic waste, along with other forms of waste. Microplastics can be found throughout water bodies, including the water surface, water column, and sediments (Zhao et al., 2023). Water contaminated with microplastics can easily pollute aquatic animals, either through food intake or absorption via the skin and gills (Jimoh et al., 2023).

One of the most commonly farmed aquatic species is tilapia (*Oreochromis mossambicus*), which is easy to cultivate, resilient to changing conditions, and widely consumed. Both wild and farmed tilapia feed on algae, which are primary producers in aquatic ecosystems. The dominant type of macroalgae found in the Kedung Ombo Reservoir is *Filamentous algae*, which has a higher capacity to retain microplastics than non-filamentous macroalgae (Li et al., 2024; Primawati et al., 2025). This ability increases the risk of tilapia consuming microplastics, which accumulate in their bodies (Bao et al., 2023). This is supported by Pratomo et al. (2020), who reported that tilapia is an omnivorous fish and a voracious feeder.

In addition to water and biota, microplastics can accumulate in sediments. Microplastics that initially float on the water surface gradually settle, leading to an increase in their concentration over time (Ismanto et al., 2023a). Microplastics in sediment can impact benthic macroinvertebrates (Haque et al., 2023). One group of benthic macroinvertebrates are gastropods, with *Pila ampullacea* being the species found in the Kedung Ombo Reservoir. This group feeds on the leaves, organic matter, detritus, and algae found in the sediments (Supriatna et al., 2023). Given their habitat and food sources, gastropods are likely to be contaminated with microplastics.

Therefore, the aim of this study was to identify the abundance and types of microplastics in water, tilapia, macroalgae, sediments, and gastropods. This research is expected to provide additional information regarding microplastic pollution in the reservoir's aquatic environment, serving as a baseline data source for future studies and ongoing monitoring. Furthermore, it could provide essential information for governments or Non-Governmental Organizations (NGOs) to raise public awareness and encourage better plastic waste management practices, ultimately contributing to the creation of a safe and healthy aquaculture environment.

2. METHODOLOGY

2.1 Description of the study site

The research area was the Kedung Ombo Reservoir area, which includes three regencies: Grobogan Regency, Boyolali Regency, and Sragen Regency (Figure 1). This reservoir is located at the foot of the Kendeng Mountains, with a water source originating from Mount Merbabu, covering an area of 4,800 ha, and an average depth of 12.8 m. The water source of this reservoir comes from the Jerabung, Tuntang, Serang, Lusi, and Juwana River Basins (DAS). There are two sub-DAS flows: the Serang River with a flow to the northeast and the Uter River with a flow from south to north (Larasati et al., 2024). This reservoir was built after a survey, investigation, and feasibility study in 1969, was officially inaugurated on May 18, 1991, and has been in operation until now (Buldan et al., 2021). The construction of this reservoir contributes to improving community welfare, especially in economic and social fields. The utilization of this reservoir includes tourism, fisheries, irrigation, agriculture, and hydroelectric power (Nasution and Wulandari, 2021).

2.2 Sampling method

This study was conducted from September to December 2024, with sampling conducted in September and October. The timing was chosen based on the transitional season in Indonesia, which is considered to be more stable owing to the minimal influence of wind direction and speed on surface currents (Rifai et al., 2020). The study began with the determination of sampling locations for water and sediment using a purposive sampling method, in which sampling points were selected based on specific criteria that represent the study area. Four stations were chosen to represent the entire reservoir: Floating Net Cage (FNC) (station 1), tourist area (station 2), reservoir inlet (station 3), and reservoir outlet (station 4) (Figure 1).

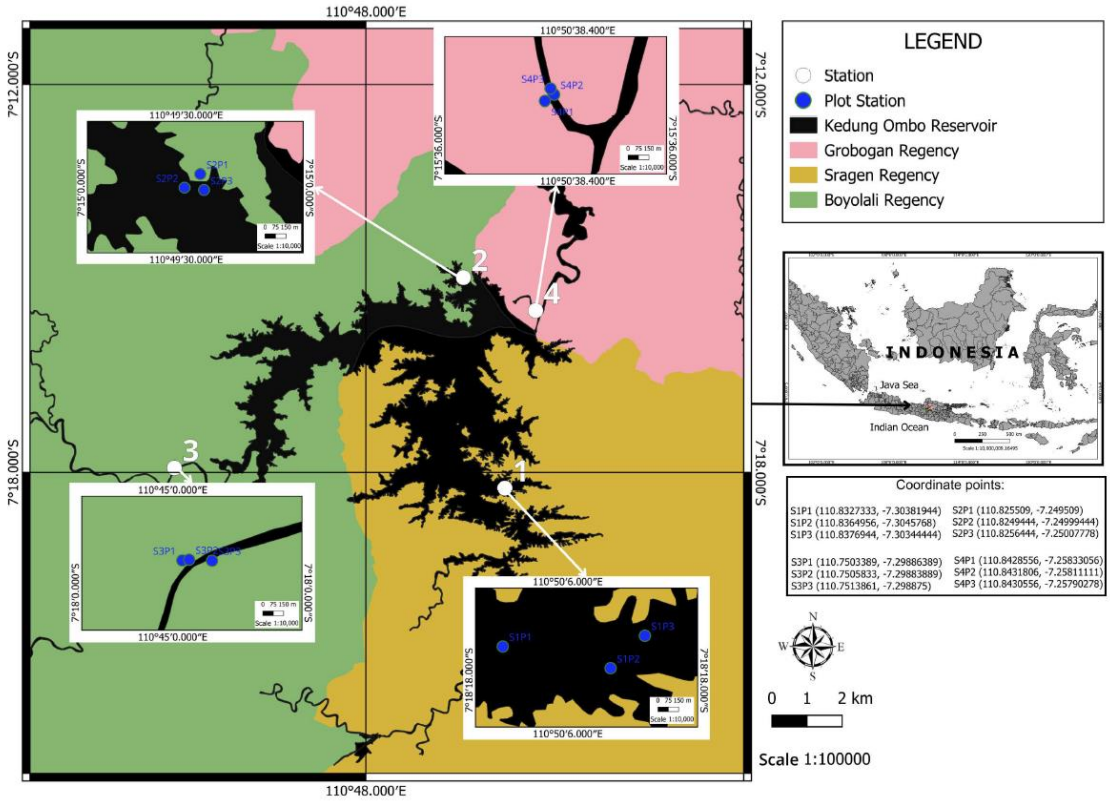

Figure 1. Location of the sampling stations in the Kedung Ombo Reservoir

The sampling method was also conducted using random sampling, which was applied to aquatic biota samples. Fish samples of consumable size were obtained from collectors and FNC (station 1), macroalgae samples were taken from FNC (station 1) and the tourist area (station 2), and gastropod samples were taken from the FNC (station 1) and the reservoir outlet (station 4).

The total samples analyzed included 24 water samples and 24 sediment samples collected from four (4) stations, with three (3) substations perstation. Additionally, eight (8) tilapia samples perstation were analyzed, with each fish sample divided into muscle and gastrointestinal tract samples. Four (4) gastropod and four (4) macroalgae samples were collected from each station.

2.3 Sample extraction method

2.3.1 Water

Upon arrival at the Laboratory of Fishery Resources and Environmental Management, FPIK, UNDIP-Semarang, 100 mL of a 30% H_2O_2 solution was added to each water sample, which was collected in 100 mL sample bottles to decompose organic matter. The bottles were then covered with aluminum foil (Haque et al., 2023; Wijayanti et al., 2023). The samples were incubated for 3 days in the dark before being filtered using Whatman No. 42 filter paper (pore size 2.5 µm) with the assistance of a vacuum pump (Anjeli et al., 2024).

2.3.2 Fish and gastropods

After weighing, the sample was extracted using a 10% KOH solution at a volume equivalent to two-thirds (2/3)of the sample's weight to dissolve organic particles surrounding the microplastics (Hassine et al., 2024). The sample was then incubated for 5 days at 40°C to ensure complete degradation, as indicated by a clear yellow solution and the presence of organic particle deposits in the beaker (Haque et al., 2023). After incubation, the samples were filtered through Whatman No. 42 filter paper using a vacuum pump.

2.3.3 Macroalgae

Upon arrival at the laboratory, sample extraction was performed using 1 mL of a 30% hydrogen peroxide (H_2O_2) solution to degrade organic matter, followed by storage at room temperature for five minutes. The sample was then maintained at 45°C until complete degradation (Taurozzi et al., 2024), after which microplastic filtration was performed using Whatman No. 42 filter paper with the assistance of a vacuum pump.

2.3.4 Sediment

Approximately 100 g of wet sediment sample was dried and sieved using a sieve shaker. All samples that passed through a 5 mm mesh sieve were weighed (3 g each) and mixed with a 30% hydrogen peroxide (H_2O_2) solution at a sample-to-solution ratio of 1:20 (1 g of sample to 20 mL of 30% H_2O_2 solution) (Haque et al., 2023; Anjeli et al., 2024). The samples were left to stand for six hours before adding an NaCl solution was added (prepared by dissolving 60 g of NaCl in 100 mL of distilled water and heating it on a hot plate/stirrer (PMC Data Plate Digital Model 739) at 25-40°C with a rotation speed of 300 rpm for 30 min). The sample was then centrifuged using a Gemmy Centrifuge (PLC-05 PLC 05) for two minutes at 1,000-4,500 rpm to obtain a supernatant containing microplastics, which was subsequently filtered using Whatman No. 42 filter paper with the aid of a vacuum pump. The remaining sediment sample underwent further density separation using a $ZnCl_2$ solution (density=1.70 g/mL), followed by centrifugation and microplastic filtration.

2.4 Observations on microplastic abundance

All microplastics filtered on Whatman filter paper were placed in Petri dishes and dried at 35°C for three hours until the filter paper was completely dry (Leitão et al., 2024). The dried samples were then examined under an Olympus CX23 binocular microscope using a 4×/0.10 objective lens to identify the shape, color, and abundance of microplastics.

2.5 Quality control

The samples obtained from the study location were transported using reusable containers that had been washed with distilled water (aquades) to minimize contamination. Upon arrival at the laboratory, the extraction procedure was performed using cotton lab coats and latex gloves (Haque et al., 2023). Furthermore, all the equipment used for sample extraction was made of non-plastic materials and also washed with aquades. To ensure the absence of microplastic contamination, a blank procedure was conducted using filter paper during the extraction process (Suparno et al., 2024). After completing the extraction and analysis procedures, the filter paper used in the blank procedure was analyzed using a microscope to ensure that no contamination occurred during the sample processing.

2.6 Calculation of microplastic abundance

The abundance of microplastics in water, aquatic biota, and sediment samples was calculated using the following formula (Anjeli et al., 2024).

$$\text{Microplastic abundance}\left(\frac{\text{particles}}{\text{Liter}}\right) = \frac{\text{a number of MPs particles}}{\text{filtered water volume}} \quad (1)$$

$$\text{Microplastic abundance}\left(\frac{\text{particles}}{\text{Kg}}\right) = \frac{\text{a number of MPs particles}}{\text{the wet weigh sample}} \quad (2)$$

$$\text{Microplastic abundance}\left(\frac{\text{particles}}{\text{Kg}}\right) = \frac{\text{a number of MPs particles}}{\text{the dry weigh sample}} \quad (3)$$

2.7 FTIR analysis

Fourier Transform Infrared (FTIR) analysis was conducted at the Research Center for Radioisotope Technology, Radiopharmaceuticals, and Biodosimetry (PRTRRB), National Research and Innovation Agency (BRIN), and Puspiptek-Serpong to identify the types of microplastics based on their polymer composition. Microplastic samples filtered on filter paper were placed in an FTIR spectrometer (Bruker Alpha II), which emits infrared light with a spectral range of 4,000-400 cm^{-1} and a spectral resolution of 2 cm^{-1}. The infrared rays emitted by FTIR are absorbed and re-emitted by the plastic polymer, generating an electromagnetic spectrum at specific wavelengths. Variations in these wavelengths correspond to differences in polymer types, facilitating the identification of microplastic compositions (Yona et al., 2021).

2.8 Data analysis

Microplastic data were analyzed for abundance using one-way analysis of variance (ANOVA) with the assistance of SPSS software (IBM SPSS Statistics 27). This analysis was used to determine whether there were significant differences in the average abundance of microplastics collected from each sampling station.

3. RESULTS AND DISCUSSION

3.1 Sample extraction method

3.1.1 Water

The microplastic abundance in the water samples taken from each observation station consecutively was 105±57 particles/L, 128±72 particles/L, 95±51 particles/L, and 158±51 particles/L (Figure 2). The average microplastic abundance across all stations was 122±28 particles/L, which is lower than that of Kaptai Lake, Bangladesh (131±67 particles/L) (Fardullah et al., 2025), but significantly

higher than that of Yahekou Reservoir, China (6.68 particles/L) (Shen et al., 2025). Based on these results, no significant difference was found between the stations ($p<0.303$), with the highest value observed at the reservoir outlet area (station 4), which was 158±51 particles/L. A similar finding was reported by Rahmayanti et al. (2022), who compared the microplastic abundance between the inlet and outlet areas of the Rawa Jombor Reservoir in Central Java. The microplastic abundance in water samples from the outlet area was higher than that from the inlet, as the reservoir outlet was the final point of the water flow, after passing through the inlet and the entire reservoir area. Reservoirs used for floating restaurants, fishing areas, and Floating Net Cages (FNC) can lead to an increase in microplastic waste concentration, which is eventually carried to the outlet during the release of reservoir water.

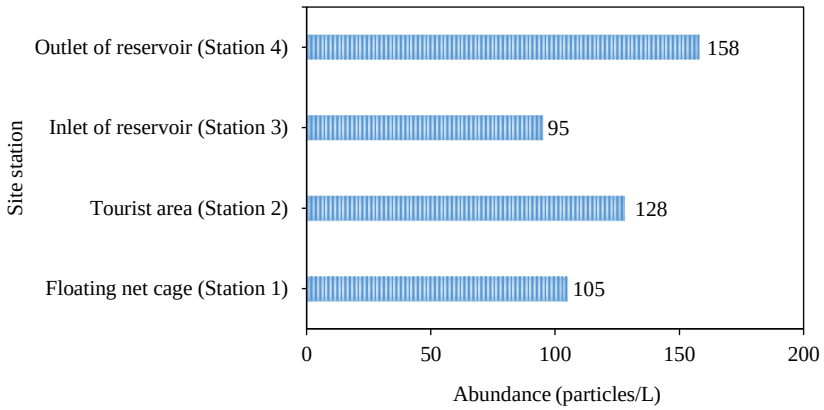

Figure 2. Average abundance of microplastics in water samples

3.1.2 Fish

The fish samples used in this study were of consumable size and suitable for human consumption. Wild fish tend to have smaller body lengths and weights than farmed fish from Floating Net Cages (FNC), as their food acquisition depends on natural foraging in aquatic environments. The average weight of the cultivated fish samples was approximately 189 g, while that of the wild fish was 105 g. The results of microplastic abundance detected in wild fish showed an average of 3,398±1,628 particles/kg, which was higher than that of cultivated fish samples, which had an average microplastic abundance of 2,003±393 particles/kg (Table 1). These results indicated a significant difference ($p<0.001$). Based on these findings, it can be concluded that the weight of fish does not correlate with the abundance of microplastics accumulated in their bodies. This aligns with the research of Haque et al. (2023), which rejects the initial assumption that larger fish require more energy, thus requiring more food and ultimately accumulating more microplastics. The weight and length of the fish did not influence their microplastic accumulation capacity. One factor that affects microplastic accumulation in fish is the method of food acquisition. Herbivores, planktivores, and omnivores are at a higher risk of microplastic exposure compared to fish with other feeding patterns (Adji et al., 2022).

Tilapia (*Oreochromis mossambicus*), an omnivorous fish known for its voracious appetite, tends to accumulate more microplastics in wild populations than farmed tilapia from FNC, because food in FNC systems is more controlled and limited. Microplastics that accumulate in fish bodies have the potential to enter the human food chain through consumption. Exposure to microplastics poses multidimensional health risks through various pathways, such as ingestion, inhalation, and skin contact. Although research on the long-term impacts of microplastics is ongoing, preliminary evidence suggests that the accumulation of these particles can affect the human digestive, hormonal, respiratory, and cardiovascular systems. Therefore, it is crucial to promote preventive efforts to reduce microplastic exposure to safeguard human health and environmental sustainability (Emenike et al., 2023).

A comparison of microplastic abundance in fish muscle and gastrointestinal tract (GIT) was also conducted to determine the potential intake of microplastics into the body of fish. The microplastic abundance in the GIT, measured at 2,428±1,283 particles/kg, was higher than that in the fish muscle, which was 272±123 particles/kg, showing a highly significant difference ($p<0.001$), as shown in Figure 3. A study by Adji et al. (2022) also indicated that the abundance of microplastics in the gastrointestinal

tract of fish was higher than that in the gills and muscles. Microplastics can enter the body of fish through the digestive system, where they are absorbed by the blood and transported throughout the body (Aryani et al., 2021).

Table 1. Average abundance of microplastics in tilapia fish samples

Fish sample	x̄ wet weight (g)	x̄ length (cm)	x̄ width (cm)	x̄ microplastic abundance (particles/kg)
Cultivated	189±45.5	18.5±7.0	6.0±2.1	2.003±393
Wild	105±27	17.1±1.5	5.2±0.6	3.398±1.628

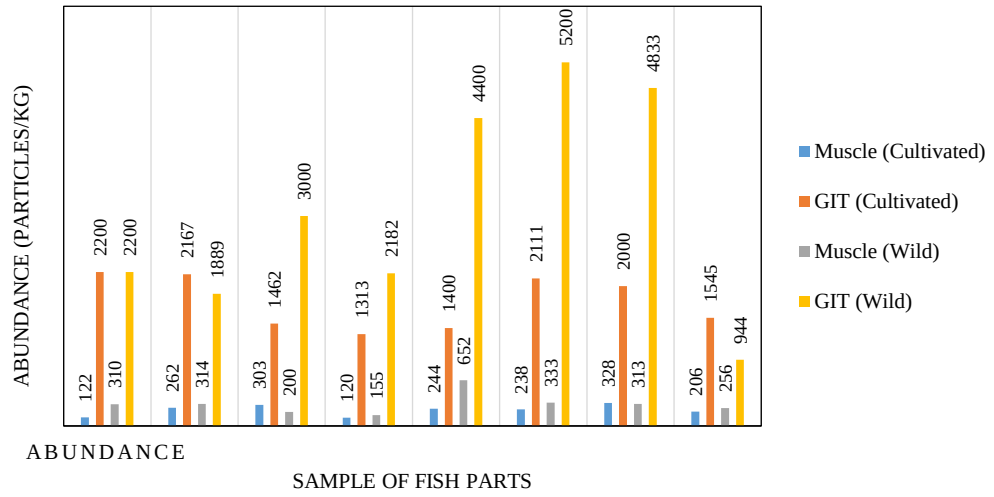

Figure 3. Average percentage of microplastic abundance in fish muscle and gastrointestinal tract samples

3.1.3 Macroalgae

The macroalgae found in the Kedung Ombo Reservoir are *Filamentous algae*. The microplastic abundance in the macroalgal samples was 964±237 particles/kg and 1,107±244 particles/kg, with the highest value observed at the tourist station (station 2), although no significant difference was found ($p<0.434$) (Figure 4). The wild-growing macroalgae in this reservoir serve as a food source for wild fish that are not farmed in cages. Most fish caught by fishermen (wild fish) feed on *Filamentous algae*, which represent the first trophic level in the food chain of this reservoir. *Filamentous algae* can capture microplastics because their branched surfaces. Microplastics not only adhere to them but can also become entangled, trapped, and caught in *Filamentous algae* (Li et al., 2024). This finding aligns with the results of this study, which indicate that fish that consume *Filamentous algae* contain higher levels of microplastics than fish that eat pellets.

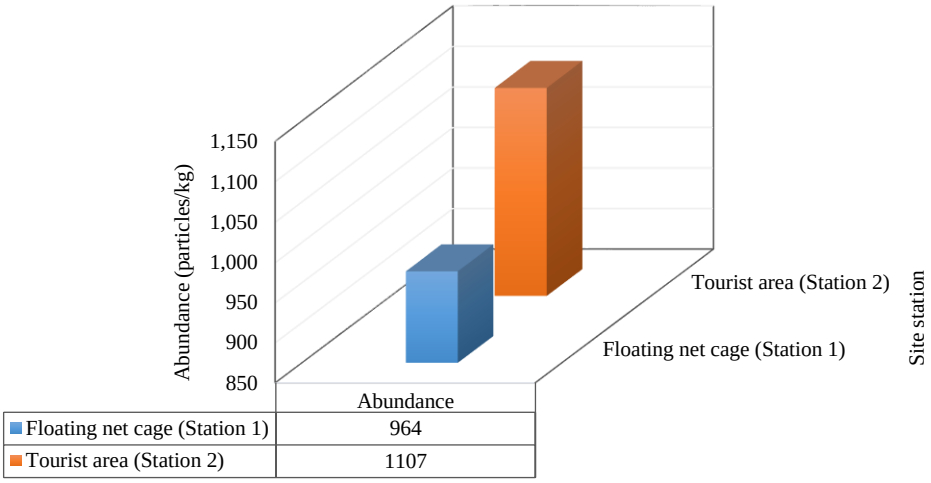

Figure 4. Average percentage of microplastic abundance in macroalgae samples

3.1.4 Sediment

The microplastic abundance in sediment samples taken from each observation station consecutively was 8,417±3,452 particles/kg, 11,111±2,711 particles/kg, 7,833±1,085 particles/kg, and 8,028±1,474 particles/kg. The average microplastic abundance across all stations was 8,847±1,529 particles/kg, which was higher than that of the Yahekou Reservoir, China (491 particles/kg) (Shen et al., 2025). These results indicate no significant difference between the stations ($p<0.140$), with the highest value recorded at the tourist station (station 2) at 11,111±2,711 particles/kg. This finding contrasts with the microplastic abundance in the water samples, where the highest value was found in samples taken from the reservoir outlet (Figure 2). One of the factors influencing microplastic abundance in sediment is current velocity (Rahmayanti et al., 2022). Stronger river-shaped currents at the reservoir outlet make it more difficult for microplastics to settle into the sediment. In contrast, the tourist area, which has calmer water, allows microplastics to settle more easily. The utilization of the tourist station (station 2) for fishing, floating restaurants, and Floating Net Cages (FNC) has led to higher microplastic abundance at this station compared to other stations. The microplastic abundance in sediment samples was much higher than that in other samples (Figures 9, 11), consistent with the findings of Ismanto et al. (2023b), which suggest that microplastics initially float on the water surface due to the current. Over time, microplastics begin to settle and accumulate in the sediment, making them a gradual repository for accumulated microplastics.

3.1.5 Gastropods

The gastropod samples obtained from the floating net cage area (station 1) and the reservoir outlet (station 4) consisted of Apple Snail (*Pila ampullacea*). The microplastic abundance in the gastropod samples was recorded as 2,456±867 particles/kg and 1,719±403 particles/kg, respectively. The highest value was observed in the sample obtained from the FNC (station 1), but no significant difference was observed ($p<0.174$) (Figure 6). Gastropods can be contaminated with microplastics both directly and indirectly, either from microplastics carried by water or from those settled in the sediment (Supriatna et al., 2023). This indicates that microplastic abundance in the sediment is directly proportional to microplastic accumulation in the bodies of gastropods. In line with this study, the microplastic abundance in the sediment at the FNC (station 1) was higher than that at the reservoir outlet (station 4) (Figure 5), which corresponds with the results of microplastic abundance in the gastropod samples living in these areas (Figure 6).

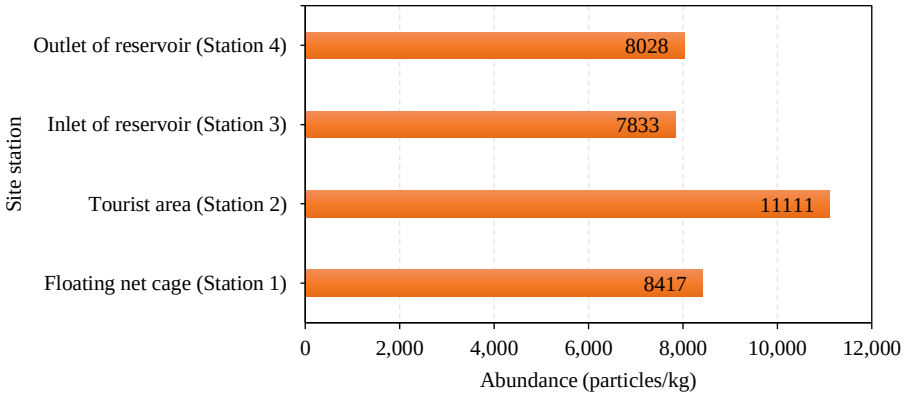

Figure 5. Average of microplastic abundance in sediment samples

3.2 Size of microplastic

The size of the microplastics in this study was divided into three categories: small (<0.5 mm), medium (0.5-<1 mm), and large (1-5 mm). The microplastic size percentages, in order, were 72%, 13%, and 15%, with small microplastics dominating (Figure 7). The percentages of microplastics in each sample, starting from the smallest size, were as follows: water (84%, 8%, and 8%), sediment (71%, 12%, and 16%), gastropods (74%, 12%, and 14%), macroalgae (79%, 16%, and 5%), and fish (77%, 9%, and 14%, respectively). These results are also in line with those of the study by Haque et al. (2023), conducted in the Buriganga River, Bangladesh. The percentage of microplastics smaller than 0.5 mm was dominant, which can be interpreted as an indication of long-term microplastic pollution in the water. This is due to the slow degradation of plastics under sunlight.

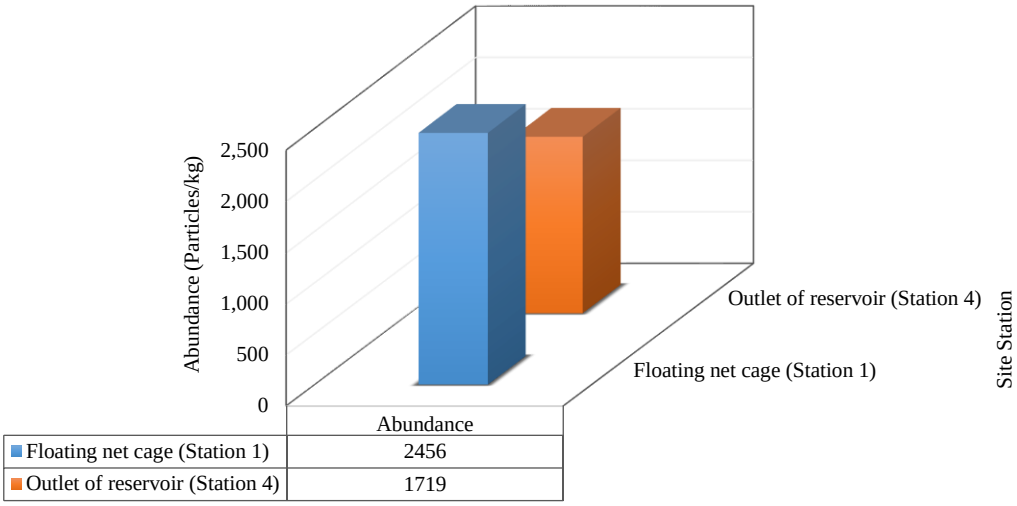

Figure 6. Average of microplastic abundance in gastropod samples

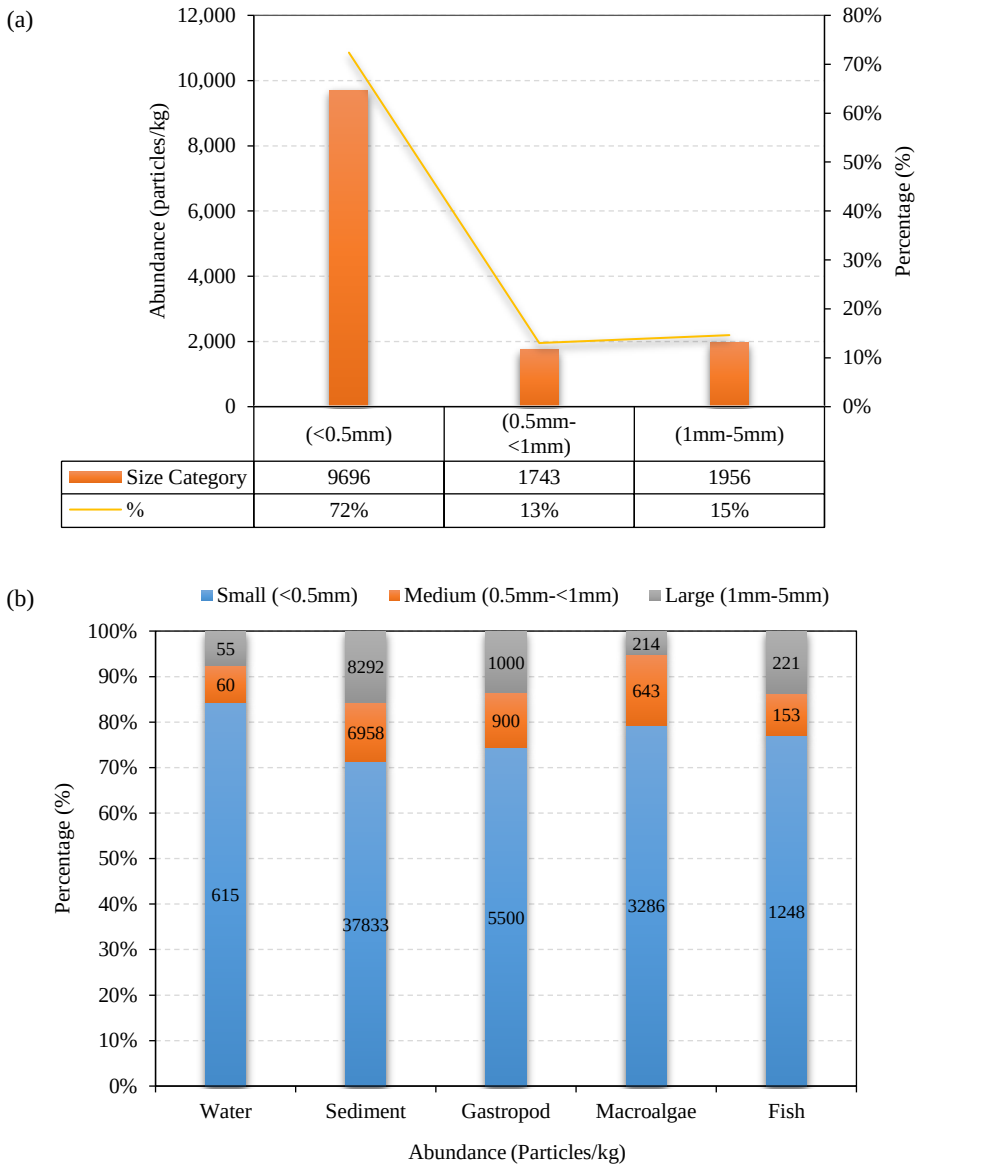

Figure 7. Microplastic abundance based on (a) size category and (b) sample category

3.3 Forms of microplastic

The forms of microplastics found in this study were divided into five categories: fiber, fragment, film, pellet, and foam (Figure 8), with the following percentage results: 39%, 19%, 17%, 15%, and 11%, respectively (Figure 9). The most common form of microplastics was fiber (39%). This is understandable, as the reservoir is also used for Floating Net Cages (FNC) and fishing activities that involve nets and other fishing gear. Plastic-based fishing gear is a source of microplastic pollution in the form of fibers (Ismanto et al., 2023b). The second-highest percentage, after fiber, was fragments (19%). Fragment microplastics originate from the degradation of larger plastics, such as beverage bottles and other single-use plastic packaging (Cordova et al., 2022; Cordova et al., 2019).

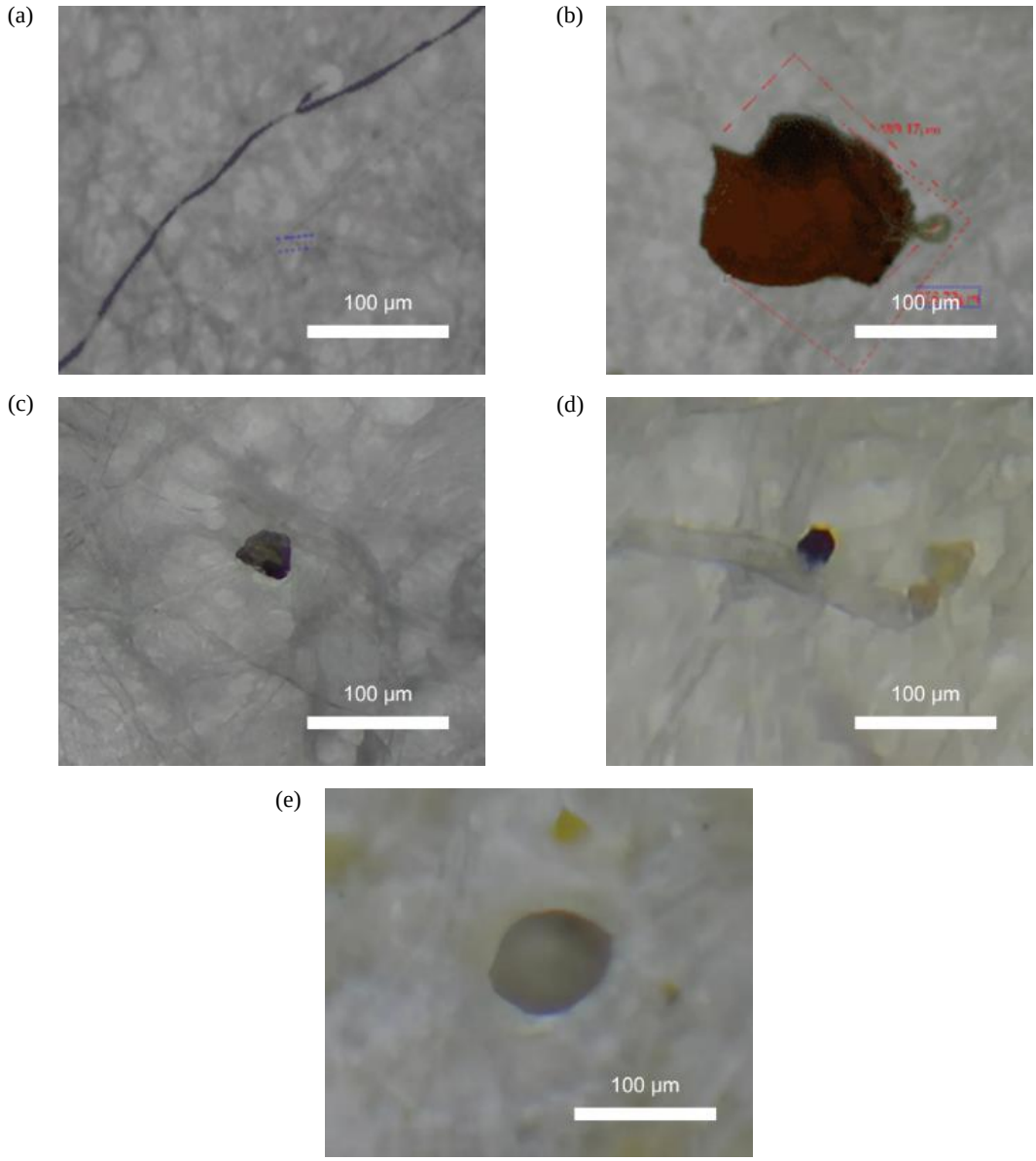

Figure 8. The form of microplastic (a) Fiber, (b) Fragment, (c) Film, (d) Pellet, and (e) Foam

3.4 Colors of microplastic

In addition to observing the size and shape of microplastics, a binocular microscope can be used to examine the color of microplastics. In this study, several colors of microplastics were found, including black, red, purple, yellow, blue, green, and clear (Figure 10), with percentages of 33%, 15%, 6%, 12%, 8%, 6%, and 20%, respectively (Figure 11). The majority of microplastics found were black. Black microplastics may indicate the amount of pollutants absorbed by them (Laksono et al., 2021). Dark colored microplastics, such as red, purple, yellow, blue, and

green, suggest that these microplastics have not undergone significant change or have retained the original color of their plastic source, while transparent microplastics indicate photochemical degradation due to ultraviolet (UV) light exposure (Anjeli et al., 2024). The presence of color in microplastics is believed to have little impact on their characteristics, as microplastics have subjective traits and cannot be used as a reference for visual identification. However, identifying color can be useful in the study of aquatic organisms, as some species consume microplastics present in aquatic environments (Frias and Nash, 2019).

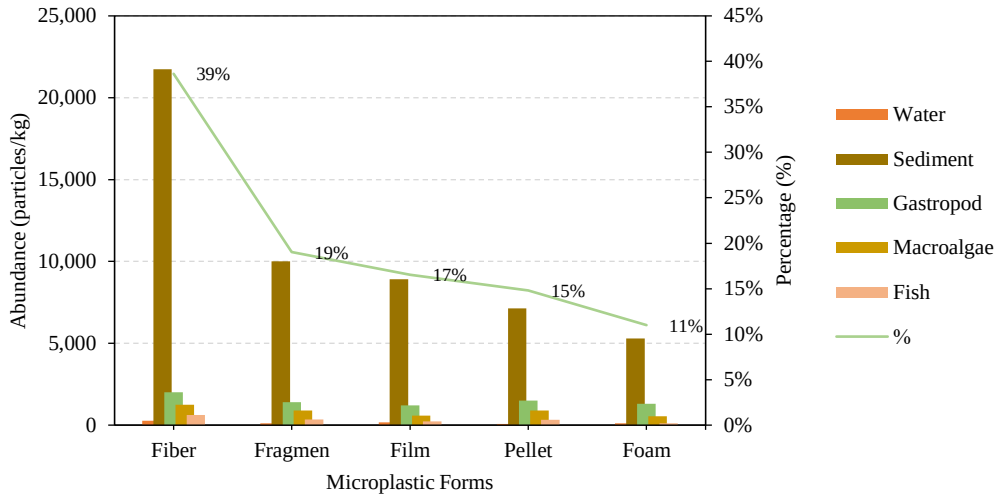

Figure 9. Percentage of microplastic quantity based on form

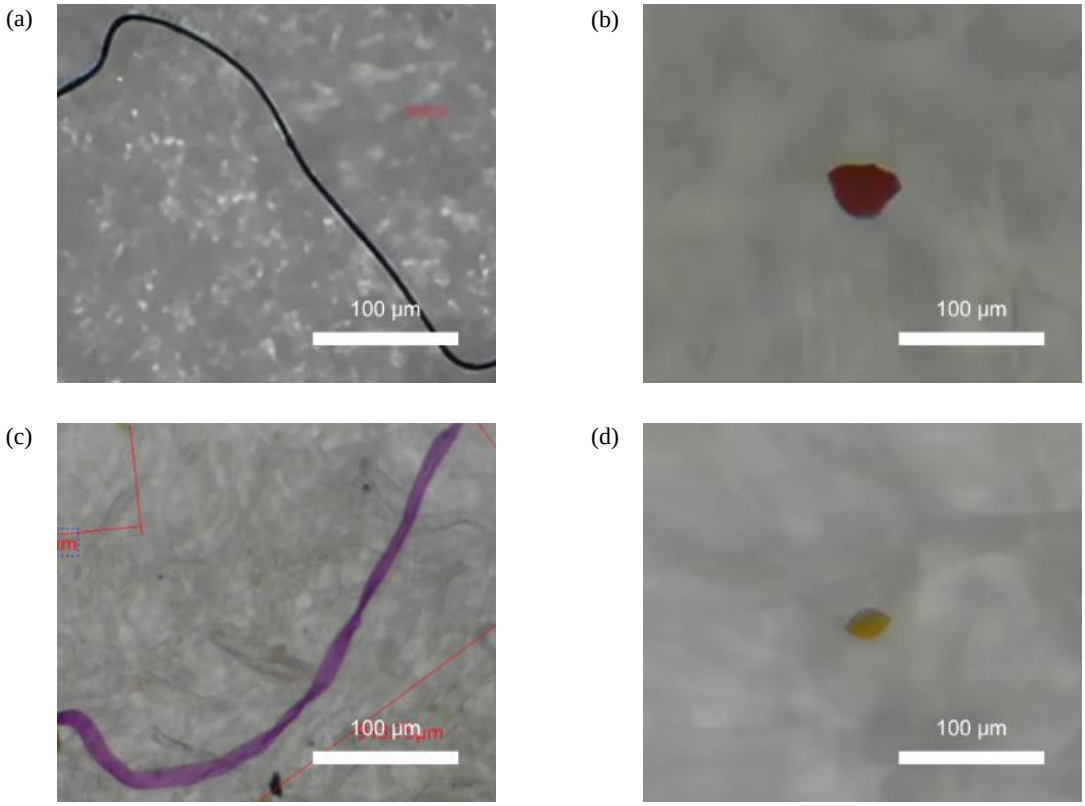

Figure 10. The color of microplastics (a) Black, (b) Red, (c) Purple, (d) Yellow, (e) Blue, (f) Green, and (g) Clear

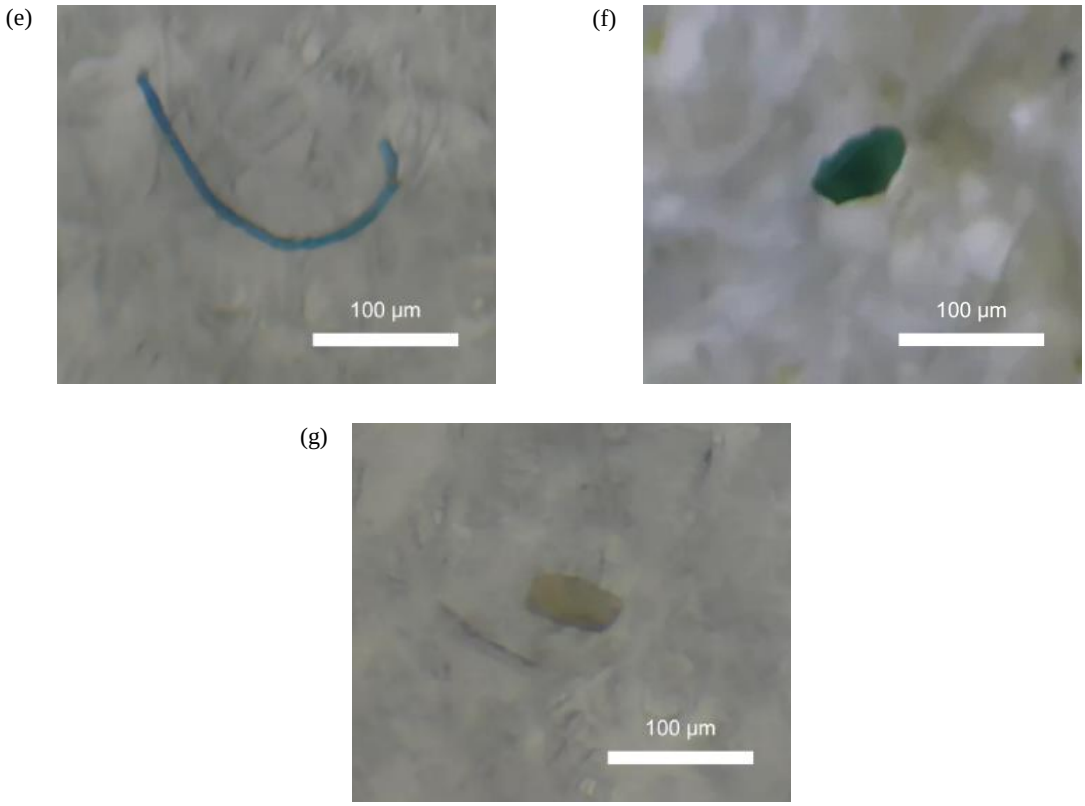

Figure 10. The color of microplastics (a) Black, (b) Red, (c) Purple, (d) Yellow, (e) Blue, (f) Green, and (g) Clear (cont.)

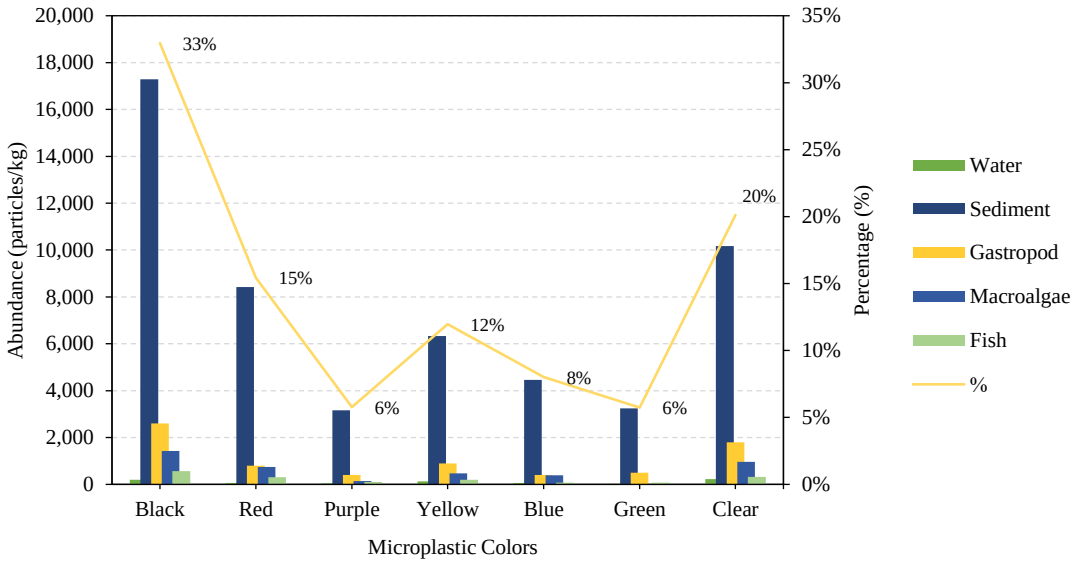

Figure 11. Percentage of microplastic quantity based on color

3.5 Types of microplastic

The microplastic types were determined using FTIR analysis, conducted at the Radioisotope Application Laboratory for Environmental Studies, Center for Radioisotope, Radiopharmaceutical, and Biodosimetry Technology Research, National Research and Innovation Agency (BRIN), Puspiptek-Serpong. The FTIR (Fourier Transform Infrared) analysis results (Figure 12) showed the presence of similar functional groups, namely hydroxyl/hydroxide groups, OH (3,331 cm^{-1}, 3,337 cm^{-1}, 3,338 cm^{-1}, and 3,283 cm^{-1}), C=C groups (1,625 cm^{-1}, 1,631 cm^{-1}, and 1,573 cm^{-1}), and C-O groups (1,029 cm^{-1}, 1,097 cm^{-1}, 1,029 cm^{-1}, and 1,054 cm^{-1}) (Figure 13). Based on these findings, the plastics identified are likely to be polyethylene terephthalate (PET/PETE), polyethylene (PE), and polystyrene (PS)

(Käppler et al., 2016; Veerasingam et al., 2021; Yona et al., 2021).

Research on the FTIR analysis of microplastics has been conducted in several aquatic environments in Indonesia, such as the study by Supriatna et al. (2023), which identified nine types of microplastic polymers in rivers in Surabaya, East Java Province. The polymers found in sediment were PVC, PET, Nylon, CA, PP, PE, PS, PA, and PMMA (Polymeric Methyl Methacrylate). The most common polymers found in the waters of Surabaya are PS, PP, and PE. A similar study was also conducted in one of the reservoirs located in Central Java Province, namely the Rawa Jombor Reservoir, by Adji et al. (2022) and Rahmayanti et al. (2022). In a study by Adji et al. (2022), the polymers identified in the water and sediment samples from the reservoir included Nitrile, Latex, HDPE, EVA, Nylon, LDPE, and PP. The polymers found in aquatic biota samples from the reservoir were PS, EVA, Nitrile, Latex, PET, PE, and PP. The aquatic biota species studied by Rahmayanti et al. (2022) included zooplankton, benthos, and fish.

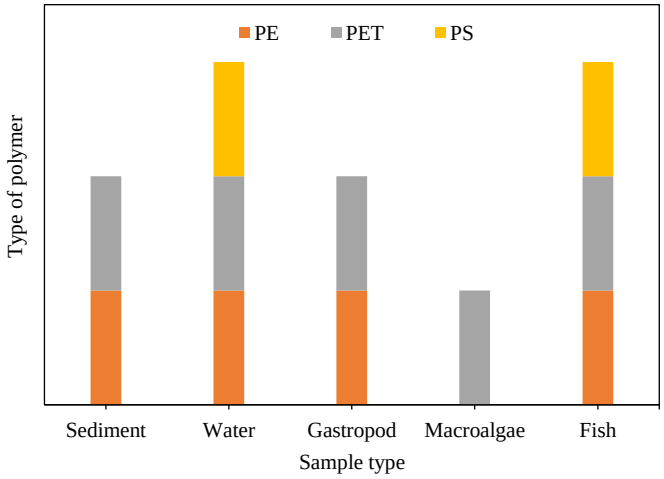

Figure 12. Types of plastic polymers detected from FTIR results

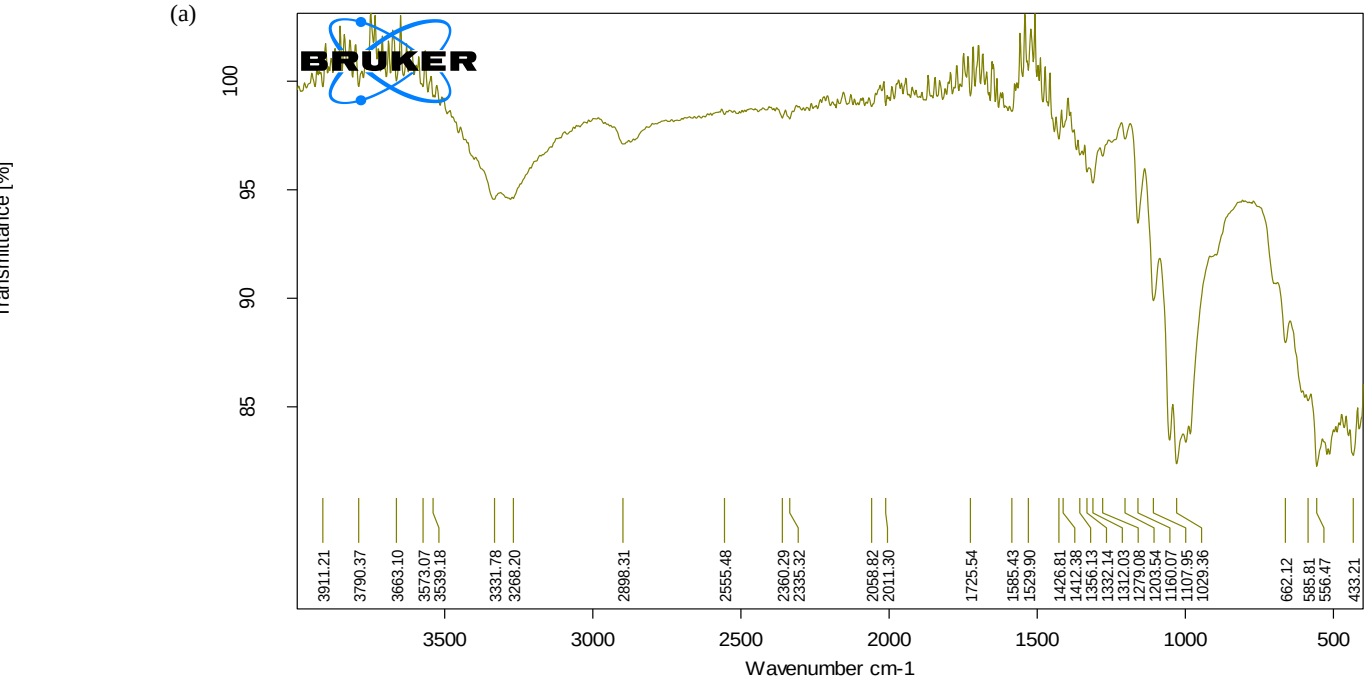

Figure 13. FTIR analysis results of microplastics in (a) water sample, (b) tilapia GIT sample, (c) tilapia muscle sample, (d) macroalgae sample, (e) sediment sample, and (f) gastropod sample

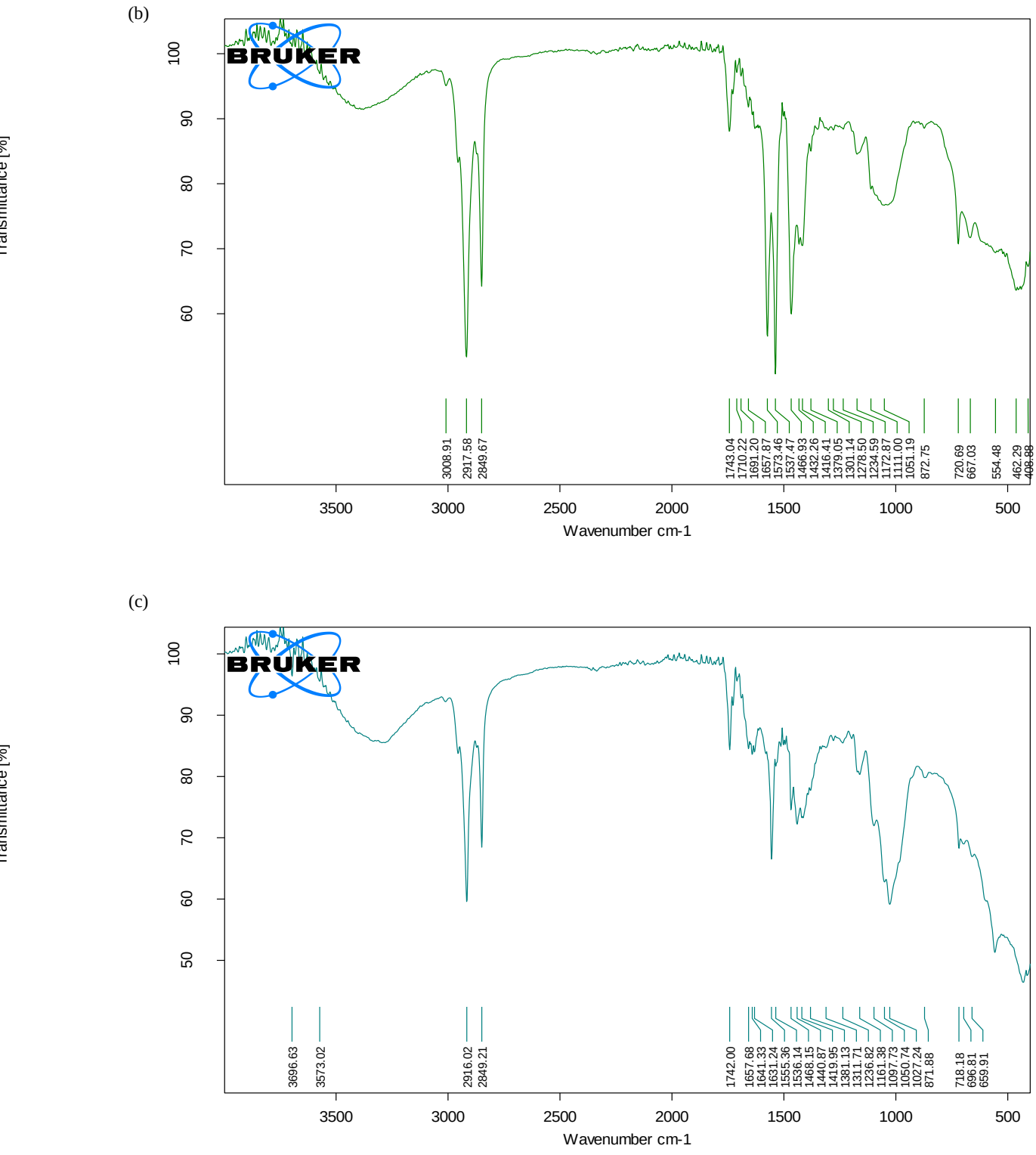

Figure 13. FTIR analysis results of microplastics in (a) water sample, (b) tilapia GIT sample, (c) tilapia muscle sample, (d) macroalgae sample, (e) sediment sample, and (f) gastropod sample (cont.)

(d)

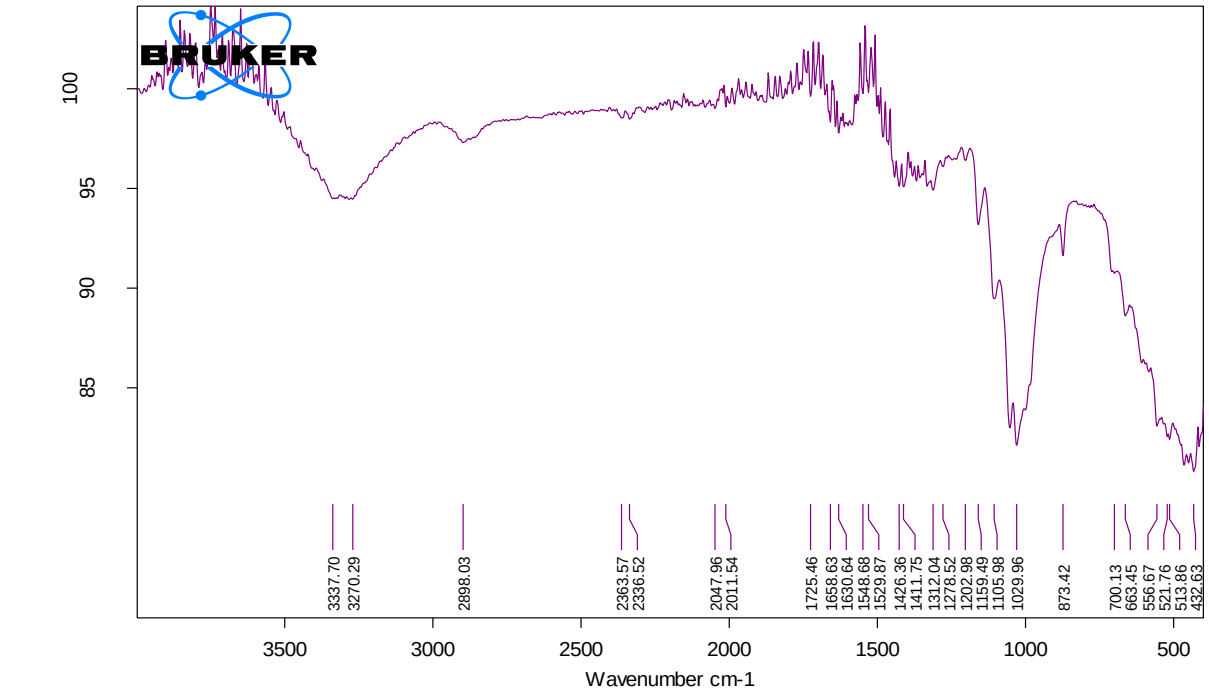

(e)

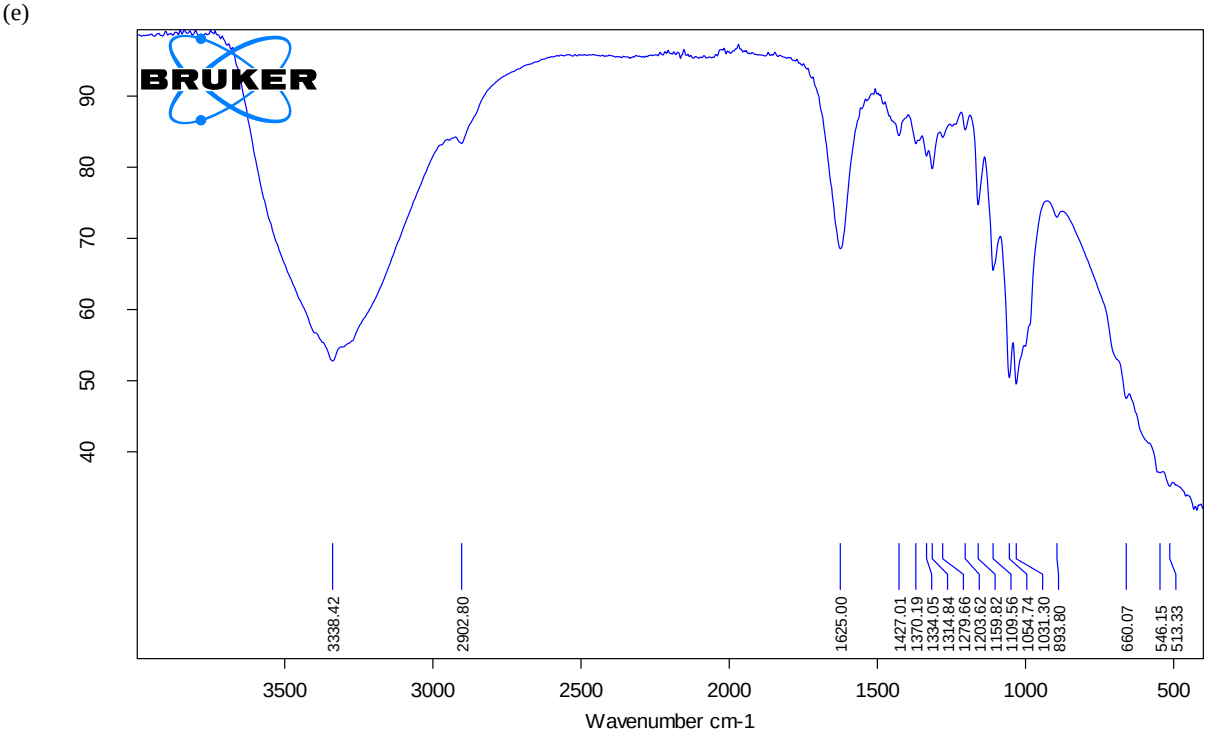

Figure 13. FTIR analysis results of microplastics in (a) water sample, (b) tilapia GIT sample, (c) tilapia muscle sample, (d) macroalgae sample, (e) sediment sample, and (f) gastropod sample (cont.)

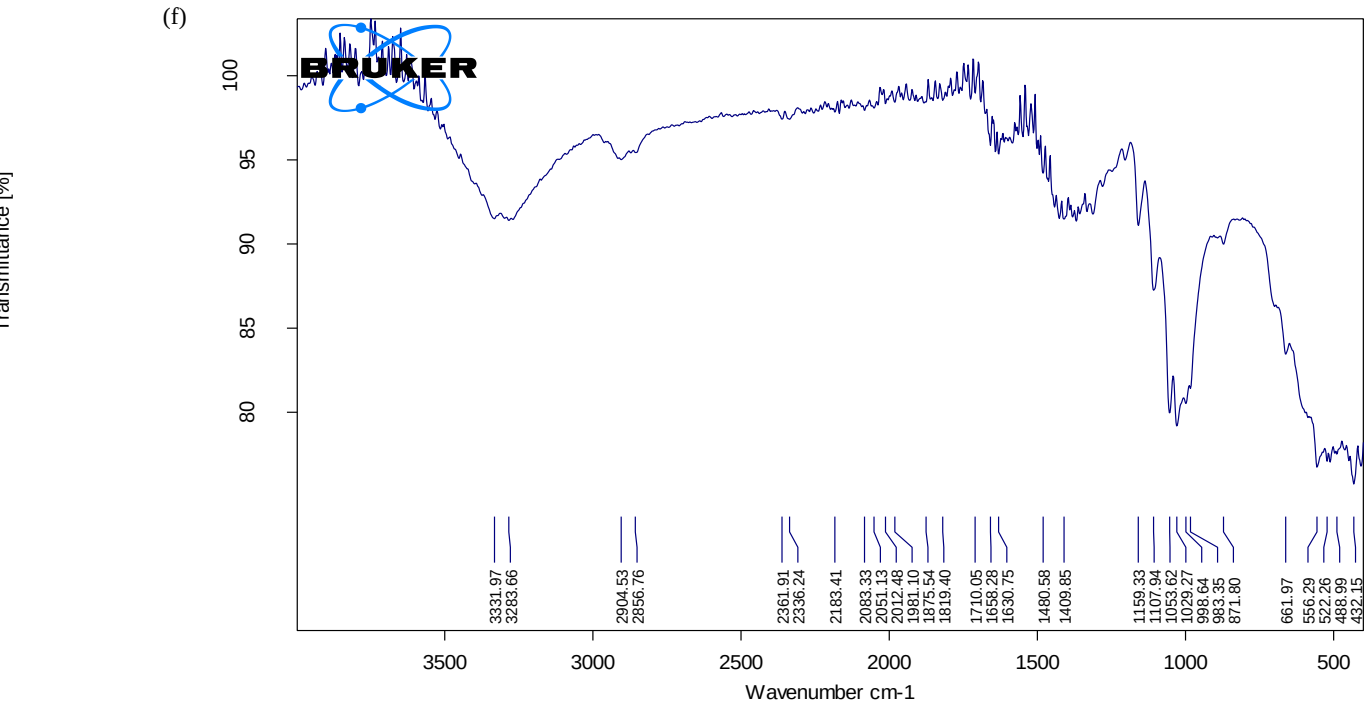

Figure 13. FTIR analysis results of microplastics in (a) water sample, (b) tilapia GIT sample, (c) tilapia muscle sample, (d) macroalgae sample, (e) sediment sample, and (f) gastropod sample (cont.)

4. CONCLUSION

It can be concluded that the microplastic abundance in water, gastropods, tilapia, macroalgae, and sediment samples was 122 particles/L, 2,088 particles/kg, 2,700 particles/kg, 1,036 particles/kg, and 8,847 particles/kg, respectively. The collected microplastics were classified into several sizes: small (<0.5 mm), medium (0.5-<1 mm), and large (1-5 mm), with percentages of 72%, 13%, and 15%, respectively. The forms of microplastics obtained included fibers (39%), fragments (19%), films (17%), pellets (15%), and foam (11%). The colors of microplastics found were black (33%), red (15%), purple (6%), yellow (12%), blue (8%), green (6%), and clear (20%). The detection of microplastics in various compartments of the ecosystem highlights the need for collective efforts to raise public awareness of plastic waste management, both through environmental education and policies to reduce plastic waste in the area. Further research is also required across various trophic levels of organisms and on an annual research timeline, as the Kedung Ombo Reservoir experiences different natural phenomena each season, such as upwelling.

ACKNOWLEDGEMENTS

We would like to express our deepest gratitude to all parties who supported the research activities and the preparation of this article. All authors listed have equal standing in the research process and writing of this article. We would also like to convey our appreciation to Diponegoro University and Badan Riset dan Inovasi Nasional (BRIN) for providing laboratory facilities, which greatly contributed to the smooth progress and continuation of this research.

AUTHOR CONTRIBUTIONS

Experimental Run and Data Collection, Noor Maulidah; Methodology, Validation, Supervision and Writing Original Draft Preparation, Noor Maulidah, Muslim Muslim; Formal Analysis; Data Curation, Visualization, Writing-Review and Editing, Noor Maulidah, Muslim Muslim, Heny Suseno.

DECLARATION OF CONFLICT OF INTEREST

The authors have no conflict of interest to declare.

REFERENCES

Adji BK, Octodhiyanto I, Rahmayanti R, Nugroho AP. Microplastic pollution in Rawa Jombor Reservoir, Klaten, Central Java, Indonesia: Accumulation in aquatic fauna, heavy metal interactions, and health risk assessment. Water, Air, and Soil Pollution 2022;233(4):1-23.

Anjeli UG, Sartimbul A, Sulistiyati TD, Yona D, Iranawati F, Seftiyawan FO, et al. Microplastics contamination in aquaculture-rich regions: A case study in Gresik, East Java, Indonesia. Science of the Total Environment 2024;927:1-13.

Ariyunita S, Subchan W, Alfath A, Nabilla NW, Nafar SA. Analysis of microplastic abundance in water and gastropods in

the Bedadung River Segment, Kaliwates District, Jember Regency. Jurnal Biosense 2022;5(2):47-51 (in Indonesian).

Aryani D, Khalifa MA, Herjayanto M, Solahudin EA, Rizki EM, Halwatiyah W, et al. Penetration of microplastics (polyethylene) to several organs of Nile Tilapia (*Oreochromis niloticus*). The 2nd International Conference on Agriculture and Rural Development; 2020 Nov 16; Serang City, Banten: Indonesia; 2021.

Bao R, Cheng Z, Peng L, Mehmood T, Gao L, Zhuo S, et al. Effects of biodegradable and conventional microplastics on the intestine, intestinal community composition, and metabolic levels in Tilapia (*Oreochromis mossambicus*). Aquatic Toxicology 2023;265:1-11.

Berlino M, Mangano MC, De Vittor C, Sarà G. Effects of microplastics on the functional traits of aquatic benthic organisms: A global-scale meta-analysis. Environmental Pollution 2021;285:1-10.

Buldan R, Suharyanto S, Najib N, Sadono KW. Seepage analysis on the safety of the Kedung Ombo Reservoir in Grobogan, Central Java. Journal of Hydraulic Engineering 2021;12(2):79-92 (in Indonesian).

Cordova MR, Nurhati IS, Shiomoto A, Hatanaka K, Saville R, Riani E. Spatiotemporal macrodebris and microplastic variations linked to domestic waste and textile industry in the supercritical Citarum River, Indonesia. Marine Pollution Bulletin 2022;175:1-11.

Cordova MR, Purwiyanto AIS, Suteja Y. Abundance and characteristics of microplastics in the northern coastal waters of Surabaya, Indonesia. Marine Pollution Bulletin 2019;142:183-8.

Emenike EC, Okorie CJ, Ojeyemi T, Egbemhenghe A, Iwuozor KO, Saliu OD, et al. From oceans to dinner plates: The impact of microplastics on human health. Heliyon 2023;9(10):1-19.

Ephsy D, Raja S. Characterization of microplastics and its pollution load index in freshwater Kumaraswamy Lake of Coimbatore, India. Environmental Toxicology and Pharmacology 2023;101:1-12.

Fardullah M, Islam MS, Akther K, Hossain MT, Robel FN. Spatial distribution, abundance, and risk assessment of microplastics in the surface water of Kaptai Lake: Southeast Asia's largest artificial reservoir. Journal of Hazardous Materials Advances 2025;18:Article No. 100640.

Frias JP, Nash R. Microplastics: Finding a consensus on the definition. Marine Pollution Bulletin 2019;138:145-7.

Haque MR, Ali MM, Ahmed W, Siddique MAB, Akbor MA, Islam MS, et al. Assessment of microplastics pollution in aquatic species (Fish, Crab, And Snail), water, and sediment from the Buriganga River, Bangladesh: An ecological risk appraisals. Science of the Total Environment 2023;857:1-15.

Hassine IB, Abidli S, Lahbib Y, El Menif NT. First characterization and spatial distribution of microplastics in *Sardina pilchardus* fish gathered along the northern Tunisian coast. Ecohydrology and Hydrobiology 2024;25:414-21.

Ismanto A, Hadibarata T, Kristanti RA, Sugianto DN, Widada S, Atmodjo W, et al. A novel report on the occurrence of microplastics in Pekalongan River Estuary, Java Island, Indonesia. Marine Pollution Bulletin 2023a;196:1-8.

Ismanto A, Hadibarata T, Sugianto DN, Zainuri M, Kristanti RA, Wisha UJ, et al. First evidence of microplastics in the water and sediment of Surakarta City River Basin, Indonesia. Marine Pollution Bulletin 2023b;196:1-7.

Jimoh JO, Rahmah S, Mazelan S, Jalilah M, Olasunkanmi JB, Lim LS, et al. Impact of face mask microplastics pollution on the aquatic environments and aquaculture organisms. Environmental Pollution 2023;317:1-10.

Kalčíková G. Beyond ingestion: Adhesion of microplastics to aquatic organisms. Aquatic Toxicology 2023;258:1-5.

Käppler A, Fischer D, Oberbeckmann S, Schernewski G, Labrenz M, Eichhorn KJ, et al. Analysis of environmental microplastics by vibrational microspectroscopy: FTIR, Raman, or both? Analytical and Bioanalytical Chemistry 2016;408:8377-91.

Laksono OB, Suprijanto J, Ridlo A. Microplastic content in sediment in Bandengan Waters, Kendal Regency. Journal of Marine Research 2021;10(2):158-64 (in Indonesian).

Larasati M, Rudiyanti S, Rahman A, Haeruddin H, Prakoso K. The relationship between phytoplankton community structure and nutrient concentration and turbidity in Kedung Ombo Reservoir. Indonesian Journal of Agricultural Sciences 2024;29(3):323-30 (in Indonesian).

Lee HC, Khan MM, Asmaa'Jaya N, Marshall DJ. Microplastic accumulation in oysters along a Bornean Coastline (Brunei, South China Sea): Insights into local sources and sinks. Marine Pollution Bulletin 2022;177:1-10.

Leitão IA, Van Schaik L, Iwasaki S, Ferreira AJD, Geissen V. Accumulation of airborne microplastics on leaves of different tree species in the urban environment. Science of the Total Environment 2024;948:Article No. 174907.

Li X, Liu W, Zhang J, Wang Z, Guo Z, Ali J, et al. Effective removal of microplastics by *Filamentous algae* and its magnetic biochar: Performance and mechanism. Chemosphere 2024;358:Article No. 142152.

Nasution I, Wulandari DA. Sedimentation dynamics of Kedungombo Reservoir, Grobogan Regency, Central Java Province. Cycle: Civil Engineering Journal 2021;7(2):106-18 (in Indonesian).

Pratomo GN, Nurcahyo H, Firdaus NR. Fermentation profile of tilapia fish (*Oreochromis mossambicus*) with the addition of NaCl. Al-Kauniyah: Biology Journal 2020;13(2):158-66 (in Indonesian).

Primawati L, Muslim M, Suseno H. Levels of microplastics in common carp (*Cyprinus carpio*), apple snails (*Pila ampullacea*), and macroalgae (*Filamentous Algae*) in the Kedung Ombo Reservoir, Central Java, Indonesia. Egyptian Journal of Aquatic Biology and Fisheries 2025;29(2):2625-49.

Purnomo E, Chika S. The potential of fish diversity in Kedung Ombo Reservoir as a sustainable food supply provider. Journal of Biogeneration 2022;7(1):99-107 (in Indonesian).

Rahmayanti R, Adji BK, Nugroho AP. Microplastic pollution in the inlet and outlet networks of Rawa Jombor Reservoir: Accumulation in aquatic fauna, interactions with heavy metals, and health risk assessment. Environmental and Natural Resources Journal 2022;20(2):192-208.

Rifai A, Rochaddi B, Fadika U, Marwoto J, Setiyono H. Study of the influence of monsoon winds on the distribution of sea surface temperatures (case study: Pangandaran Waters, West Java). Indonesian Journal of Oceanography 2020;2(1):98-104 (in Indonesian).

Shen M, Li Y, Qin L, Chen X, Ao T, Liang X, et al. Distribution and risk assessment of microplastics in a source water reservoir in Central China. Scientific Reports 2025; 15(1):Article No. 468.

Suparno S, Deswati D, Fitri WE, Pardi H, Putra A. Microplastics in the water of Batang Anai Estuary, Padang Pariaman Regency, Indonesia: Assessing effects on riverine plastic load in the marine environment. Environment and Natural Resources Journal 2024;22(1):55-64.

Supriatna I, Risjani Y, Kurniawan A, Yona D. Microplastics contaminant in *Telescopium telescopium* (gastropods), the keystone mangrove species and their habitat at brackish water pond, East Java, Indonesia. Emerging Contaminants 2023;9(4):Article No. 100245.

Taurozzi D, Gallitelli L, Cesarini G, Romano S, Orsini M, Scalici M. Passive biomonitoring of airborne microplastics using lichens: A comparison between urban, natural and protected environments. Environmental International 2024;187:1-10.

Tsuchiya M, Kitahashi T, Nakajima R, Oguri K, Kawamura K, Nakamura A, et al. Distribution of microplastics in bathyal-to-Hadal-depth sediments and transport processes along the deep-sea canyon and the Kuroshio extension in the northwest Pacific. Marine Pollution Bulletin 2023;199:1-12.

Veerasingam S, Ranjani M, Venkatachalapathy R, Bagaev A, Mukhanov V, Litvinyuk D, et al. Contributions of Fourier transform infrared spectroscopy in microplastic pollution research: A review. Critical Reviews in Environmental Science and Technology 2021;51:2681-743.

Wijayanti DP, Indrayanti E, Haryanti D. Coral Reef Ecosystems and Strategies for Facing Climate Change. Malang, Indonesia: Intimedia; 2023 (in Indonesian).

Xia F, Tan Q, Qin H, Wang D, Cai Y, Zhang J. Sequestration and export of microplastics in urban river sediments. Environment International 2023;181:1-12.

Yona D, Zahran MF, Fuad MAZ, Prananto YP, Harlyan LI. Microplastics in Water: Types, Sampling Methods, and Laboratory Analysis. Malang, Indonesia: UB Press; 2021 (in Indonesian).

Zhao W, Li J, Liu M, Wang R, Zhang B, Meng XZ, et al. Seasonal variations of microplastics in surface water and sediment in an inland river drinking water source in Southern China. Science of the Total Environment 2023;908:1-13.

Environment and Natural Resources Journal

Volume 23
Issue 6
2025

Soil Carbon Sequestration in Rice-Based Cropping Systems in Batac, Philippines

Arlene L. Gonzales[1*], Dionisio S. Bucao[2], Aprilyn D. Bumanglag[1], and Kenneth P. Tapac[1]

[1]College of Agriculture, Food and Sustainable Development, Mariano Marcos State University, City of Batac, Ilocos Norte, 2906 Philippines
[2]Research Directorate, Mariano Marcos State University, City of Batac, Ilocos Norte, 2906 Philippines

ARTICLE INFO

Received: 8 Feb 2025
Received in revised: 26 Jun 2025
Accepted: 31 Jul 2025
Published online: 3 Aug 2025
DOI: 10.32526/ennrj/23/20250035

Keywords:
Soil organic carbon/ Cropping pattern/ Climate change/ Mitigation

*** Corresponding author:**
E-mail: algonzales@mmsu.edu.ph

ABSTRACT

This study focused on the assessment of capacity of farm soils to sequester carbon under different rice-based cropping patterns. The results of this study may be valuable for the formulation of soil and crop management for climate change mitigation in the agriculture sector in Ilocos Norte, Philippines. This study was conducted in major cultivated areas in the City of Batac, characterized by intensified and diversified cropping patterns centered around rice cultivation. A quantitative research design was employed to determine the different cropping patterns and their influence on soil organic carbon (SOC). The dominant cropping patterns observed in Batac City was rice, followed by any of the following crops; corn, shallot, eggplant, rice, tomato, pepper, garlic and tobacco. These cropping patterns are assumed to have an influence in soil pH, organic matter (OM), % carbon, phosphorus (P), potassium (K), bulk density, soil texture, moisture content, and soil carbon stock (SOC). Results showed that soil organic matter content in various cropping patterns was proportional to the soil carbon stock in the soil. The analysis of variance between cropping patterns exhibited high variability in OM and SOC with an F-value >1. Rice-tobacco exhibited the highest carbon stock (1.80%), while rice-garlic (0.63%) and rice-corn (0.60%) had the lowest. Understanding the influence of crop biomass and management through this study can be beneficial in the design of informed decision-making strategies and advocacy on cropping pattern management, which can be disseminated to farmers to enhance the carbon sequestration potential of agricultural lands.

HIGHLIGHTS

This study highlights the potential of agricultural soils to contribute to climate change mitigation through integrated crop and soil management practices.

1. INTRODUCTION

Soil organic carbon (SOC) plays a critical role in maintaining the global carbon cycle and climate regulation. Soil organic matter (SOM) is a major carbon pool that maintains global atmospheric carbon balance. Its decomposition contributes not only to the emission of greenhouse gases (GHG) into the atmosphere but also to the release of minerals that serve as nutrients for plant growth (PohankovÃ¡, et al., 2024). Approximately 12% of soil carbon is held in cultivated soils covering around 35% of the terrestrial land area of the planet (Haddaway et al., 2017). Intensive cropping and organic matter (OM) mismanagement have depleted organic carbon from agricultural soils, leading to land degradation (Adekiya et al., 2023) and enhanced greenhouse emission.

Sustainable agricultural practices have been proposed as a nature-based solution to address climate change and simultaneously combat soil degradation and food security issues by enhancing SOC sequestration in

Citation: Gonzales AL, Bucao DS, Bumanglag AD, Tapac KP. Soil carbon sequestration in rice-based cropping systems in Batac, Philippines. Environ. Nat. Resour. J. 2025;23(6):569-580. (https://doi.org/10.32526/ennrj/23/20250035)

This paper was selected from the 5th Environment and Natural Resources International Conference (ENRIC 2024) which was held during 14-15 November 2024 in Thailand

soils. Sustainable practices such as conservation agriculture have been demonstrated to improve soil physical, chemical, and biological properties that are important in maintaining soil health and ecosystem resilience (Francaviglia et al., 2023). The critical threshold of soil organic carbon (SOC) in the root zone ranges from 1.5% to 2.0%, influenced by land use, soil management, and farming techniques. Over half of the total Carbon (C) pool at a 1-meter depth is concentrated between 0.3 and 1 meter (Lal, 2004). Enhancing soil quality necessitates augmenting SOC concentration by implementing best management practices, such as conservation agriculture, which fosters a positive carbon budget (Buyanovsky and Wagner, 1998).

Majority of the agricultural practices contribute to SOC depletion while others support accumulation. Farm practices like tillage, crop residue management, and land use changes play a significant influence in determining the SOC levels. In the Philippines, crop diversification is encouraged as part of the climate-resilient agriculture (CRA) initiative to increase productivity, enhance resilience, and remove/reduce greenhouse gases (GHGs) (Dikitanan et al., 2017). These community strategies can be strengthened to increase knowledge and awareness to create information for local mitigation and adaptation planning.

The flat regions of Ilocos Norte undergo heavy farming, whereas the hilly and elevated areas are less utilized. The province, including the City of Batac is characterized by rice-oriented farming practices. Rice is usually grown in the wet season (June-October), while a variety of crops are planted in the dry season, such as corn, tobacco, garlic, eggplant, pepper, tomato, and onion. With climate change increasing the severity of typhoons and other natural disasters such as drought in the province, it is essential to assess the SOC levels of the main rice-based cropping systems in Batac City to determine the carbon sequestration potential of the agricultural land in the local area. Although intensive cultivation is known to result in a 25 to 75% less SOC than their counterparts in undisturbed ecosystems, long term rice cropping systems can significantly increase SOC stock due to high crop biomass production and decomposition rates resulting from extended submergence (Valenzuela-Balcázar et al., 2022).

The significance of this study lies in its potential to enhance soil fertility, structure, and crop yields, fostering favorable conditions for cultivation and carbon sequestration. Carbon is vital for sustaining life on Earth, supporting biological activity, diversity, and ecosystem productivity. The abundance of organic matter and associated soil biological populations stemming from diversified crop rotations enhances soil health and vitality. It is, therefore, imperative to know the capacity of the soil to sequester carbon under different rice-based cropping patterns. Specifically, this study aimed to (1) identify the rice-based cropping patterns in the City of Batac; (2) determine the influence of the different crop management practices on SOC; (3) determine the influence of cropping pattern on the soil characteristics; and (4) determine the relationship between physical properties, organic matter, and soil organic carbon under the different rice cropping patterns.

2. METHODOLOGY

2.1 Study site

The City of Batac is situated in the central-southwestern region of Ilocos Norte. It covers a total land area of 16,101 hectares with terrain varying from gently flat to rolling and hilly, with some areas being very steep. The City of Batac experiences a warm climate with two distinct seasons: the wet season, spanning from the latter part of May to October, characterized by an annual average rainfall exceeding 2,000 mm, and the dry season from November to April. It has a total cultivated land area of 2,063.65 ha, and the agricultural production system is characterized by intensive and diversified cropping patterns centered around rice cultivation. Figure 1 illustrates the sampling sites representing eight different cropping patterns.

2.2 Research design

This study employed a quantitative, field-based research design to measure the variables and test the hypotheses on the relationship among different variables through correlation and regression analyses. Additionally, a qualitative approach was used to determine the cropping practices used by the farmers. A purposive sampling method was employed and considered the largest cultivated farm areas in three major barangays as the sampling sites for this purpose.

Secondary data were also collected from the City Agriculture Office for data collection on major crops planted, classification of the cropping patterns employed by farmers within the three major barangays with the largest cultivated areas in the City of Batac.

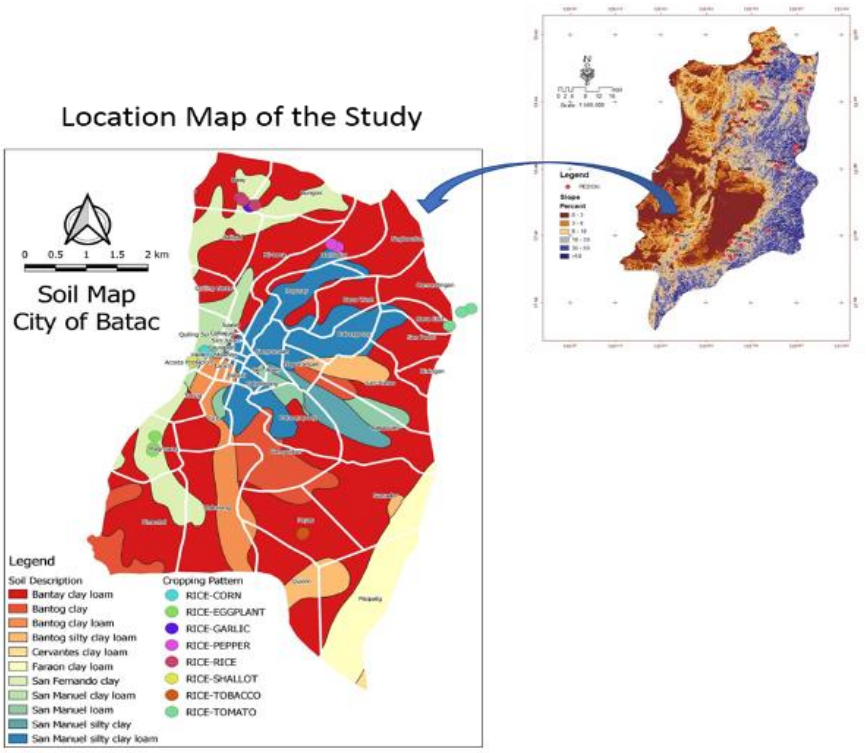

Figure 1. Study area of this study

2.3 Population and sample

This study considered 24 farmer respondents to obtain information needed to supplement the data obtained from the City Agriculture Office. A questionnaire designed to collect details on crop and farm management practices was used to obtain information from the farmers. For ethical purposes, the questionnaire survey was evaluated and approved first by the University Research Ethics Review Board (URERB) prior to the conduct of the survey.

The data on soil characteristics were obtained from 24 sampled farms (three farms for each cropping pattern) with distinct cropping patterns. Soils were collected from surface up to 30 cm in depth with three replicates per cropping type. Composite soil samples for each cropping pattern were employed for the soil analysis.

2.4 Research instrument

Information about the management practices implemented by the farmers was collected using a survey questionnaire.

2.5 Data gathering procedure

To accurately assess the physical and chemical attributes of the area, a composite sampling technique was utilized. A total of one kilogram of soil was collected from the composite samples per farm with distinct cropping pattern, securely packed in plastic containers, and kept in an icebox.

After collection, the soil samples were transported to the laboratory and subjected to air-drying. Following the drying process, the samples were ground and sifted through a soil sieve with a mesh size of 2 mm. The finely ground samples were then carefully stored in labeled plastic bags.

The following parameters were gathered with their corresponding procedures:

(1) Bulk density

Bulk density is an indicator of soil compaction. Bulk density is commonly determined using the core cylinder method (FAO, 2023). This method uses a core cylinder with a known volume. The core sampler was carefully inserted into the soil using a hammer to prevent compression. Subsequently, the samples were oven-dried at a temperature between 105°C and 110°C for one to three days, or until a constant dry weight was reached.

The bulk density was calculated by dividing the dry weight of soil by volume of the cylinder denoted in g/cm^3, as illustrated below:

$$\text{Bulk Density} = \frac{\text{Weight of ovendry soil (g)}}{\text{Volume of the sample}}$$

To calculate the volume, measurements of the core sampler's height and diameter were measured, and the volume was determined using the following formula:

$$V = \pi r^2 h$$

(2) Soil pH

Soil pH was determined using the soil-water slurry method. A 20 g soil sample was placed into a 100 mL beaker, and 20 mL of distilled water was added. The mixture was stirred at 20-minute interval over the course of an hour. Before the pH reading was obtained, the sample was thoroughly mixed.

(3) Soil organic matter content

The Walkley-Black Method (FAO, 2019) was selected due to the characteristics of the soil samples. The colorimetric method was employed since the soil samples exhibited a neutral to alkaline pH.

(4) Soil texture

Soil texture was determined by separating the different soil particle size fractions of sand, silt, and clay using the sieve method. Each separated particle was weighed, and the percentages were calculated.

(5) Soil potassium

The amount of potassium was determined using the standard Flame Photometry method. Available potassium in the soil was extracted and this solution was sprayed into the flame three times and the galvanometer readings were recorded. Distilled water was sprayed every after each sample to attain constant readings on galvanometer and readjusted to zero.

(6) Soil phosphorous

The analysis of soil phosphorus utilized the Modified Truog method, which involves the extraction of adsorbed phosphate from the soil using a specific solution. Within an acidic environment, soluble orthophosphates interact with molybdates, resulting in the formation of heteropoly molybdophosphoric acid. The intensity of color developed through this reaction is directly proportional to the amount of phosphates in the soil (Truog, 1930).

(7) X-ray fluorescence (XRF) analysis

X-ray fluorescence analysis is an analytical technique that uses the interaction of X-rays with a material to determine its elemental composition. Dried, ground soil samples were sieved to reduce particle size. A representative portion was placed in a sample cup and then irradiated with X-rays. The emitted X-rays were detected by the instrument and their energy frequencies are analyzed for the determination of the elemental composition. The standard procedure used by this study was based on the manufacturer's instructions for the benchtop XRF analyzer.

(8) X-ray diffraction (XRD) analysis

The XRD analysis was used to identify the mineral composition of the soil samples collected from the different farms. The samples were analyzed using an Olympus BTX (Laue method) with Cu kα metal target and 2 theta from 0 to 55 degrees. Phase identification was carried out using the match computer program and using the principle of the Hanawalt method.

(9) Determination of organic carbon per hectare

Determining soil bulk density readings is essential for computing the soil weight and quantifying soil organic carbon (SOC) stocks in tons per hectare. This computation used the formula outlined by the Agriculture and Food Division of the Department of Primary Industries and Regional Development in Australia (Hoyle and Murphy, 2018).

$$\text{Soil Weight per Ha} = 10{,}000 \frac{\text{m}^2}{\text{ha}} \times \text{soil depth} \times \text{bulk density}$$

$$\text{Soil Carbon Stock} \frac{\text{kg}}{\text{ha}} = \text{Soil carbon} \times \text{soil depth} \times \text{weight of soil per hectare}$$

2.6 Data analysis

The collected data were compiled and subjected to analysis of variance using STAR 2.0 v.1. Variations in means were assessed through the honestly significant difference (HSD) test at a significance level of 0.05 ($HSD_{0.05}$). Additionally, correlation and regression analyses were conducted using SPSS software to ascertain the connections and associations among the parameters.

3. RESULTS AND DISCUSSION

3.1 Major rice-based cropping patterns in the City of Batac

According to the City Agriculture Office of Batac City, approximately 2,053.65 ha are utilized for rice cultivation during wet season while various vegetables and other high-value crops are grown in the dry season. Table 1 shows the area planted with rice and other crops, along with the total of 5,193 farmers. The city adheres to 13 distinct cropping patterns, among which the predominant ones include rice-corn (1,497.45 ha), rice-tobacco (374.74 ha), rice-rice

(115.62 ha), rice-mungbean (53.91 ha), rice-garlic (41.10 ha), rice-eggplant (29.15 ha), and rice-shallot (14.68 ha). The rice-corn cropping pattern holds the largest area and engages the highest number of farmers, largely due to the support from the Department of Agriculture and the *cornick* industry. Conversely, the rice-tomato cropping pattern ranked last, as tomato is no longer a profitable crop to farmers because of the closure of the National Food Corporation known for tomato paste production.

Table 1. Cropping pattern and the number of farmers being engaged in 2020-2021.

Cropping pattern	Area (planted/ha)	Number of growers
Rice-Corn	1,497.45	3,637
Rice-Tobacco	274.74	593
Rice-Rice	115.62	316
Rice-Mungbean	53.91	288
Rice-Garlic	41.10	173
Rice-Eggplant	29.16	96
Rice-Shallot	14.68	62
Rice-Pepper	10.63	45
Rice-Squash	5.00	26
Rice-Stringbean	4.97	26
Rice-Ampalaya	3.63	23
Rice-Okra	1.24	5
Rice-Tomato	1.22	4
Total	2,053.65	5,193

Source: City Agriculture Office, City of Batac

3.2 Crop management practices

Table 2 assesses various crop management practices across different cropping patterns. The findings reveal that respondents follow the rice-rice, rice-pepper, and rice-eggplant cropping patterns integrated the use organic fertilizer. Conversely, rice-garlic and rice-tomato crops are treated with complete ammonium and sulfate fertilizer. At the same time, respondents engaged in rice-corn, rice-tobacco, and rice-shallot patterns do not apply fertilizer prior to planting. Nearly all participants apply urea, complete fertilizer, and sulfate fertilizers to their crops during the cropping period. With regards to pesticide use, all the respondents apply insecticides and fungicides to control insect pests and diseases. The application of fertilizer affects soil's ability to accumulate soil organic matter. On the other hand, continuous cropping and integrated use of organic and inorganic fertilizers increases soil C sequestration and crop yields (Brar et al., 2015) and several studies have proven that organic amendments improve soil fertility. In the study of Qui (2024), it was plausible that the stimulatory effect of the organic amendments on rice yield and above-ground dry biomass resulted at least partly from the increased availability of plant nutrients. Cropping pattern also influence soil properties. The impacts of cropping patterns are observed in the soil surface where crop residues are accumulated, and to the depth where tillage is exerted, as soil organic matter is highly dependent on the decomposition of crop residue (Gikonyo et al., 2022).

3.3 Soil physical characteristics under different cropping pattern

Soil physical properties are important in crop production due to their influence on root development, water accessibility, nutrient availability, and overall plant well-being. Furthermore, they affect nutrient cycling mechanisms within the soil, notably in the accumulation of organic matter. The physical attributes of soil also influence the availability, retention, and discharge of nutrients derived from organic matter. Soils the posses favorable structural characteristics contribute to effective nutrient cycling, ensuring that organic matter contributes to the nourishment essential for plant growth (Blanco-Canqui et al., 2009).

Table 2. Crop management practices of the different cropping patterns

Cropping pattern	Crop management practices				
	Code #	Rice-based	Fertilizer added before cropping	Fertilizer added during cropping	Pesticide used during cropping
Rice-Corn	1	√	None	Urea	Round up
	2		None	Urea	Round up
	3	√	None	Urea	Round up
Rice-Garlic	4	√	Complete, $NH_4^+$and SO_4	None	Insecticide and Boulder
	5	√	Complete, $NH_4^+$and SO_4	None	Insecticide and Boulder
	6	√	Complete, $NH_4^+$and SO_4	None	Insecticide and Boulder
Rice-Rice	7	√	Organic fertilizer	Urea and complete	Brodan and Magnum
	8	√	Organic fertilizer	Urea and complete	Brodan and Magnum
	9	√	Organic fertilizer	Urea and complete	Brodan and Magnum
Rice-Pepper	10	√	Organic fertilizer	Urea, sulfate and complete	Brodan
	11	√	Organic fertilizer	Urea, sulfate and complete	Brodan
	12	√	Organic fertilizer	Urea, sulfate and complete	Brodan
Rice-Tobacco	13	√	None	Urea	Brodan
	14	√	None	Urea	Brodan
	15	√	None	Urea	Brodan
Rice-Tomato	16	√	Complete	Urea	Lanid
	17	√	Complete	Urea	Lanid
	18	√	Complete	Urea	Lanid
Rice-Eggplant	19	√	Organic fertilizer	Complete	Magnum and Alika
	20	√	Organic fertilizer	Urea and complete	Gold
	21	√	Organic fertilizer	Urea and complete	Gold
Rice-Shallot	22	√	None	Urea and complete	Fungicide
	23	√	None	Urea and complete	Fungicide
	24	√	None	Urea and complete	Fungicide

Table 3 presents the soil physical properties of selected cropping patterns investigated in this study. Soil texture was determined based on the relative proportions of three distinct soil particles: sand, silt, and clay. The analysis of variance results indicated significant variations (p=0.01) among the observed soil physical properties. The highest percentage of clay content was found in the rice-rice cropping pattern at 46.20%, followed by rice-garlic at 38.67%. Other cropping patterns showed similar clay contents ranging from 3.37% to 6.03%.

On the other hand, the rice-eggplant cropping pattern exhibited the highest percentage of silt at 32.53%, followed closely by rice-corn, rice-rice, and rice-garlic patterns with 29.07%, 28.60%, and 27.07% respectively. These values were comparable to the rice-pepper pattern at 23.33%. The rice-pepper pattern was similar to rice-shallot and rice-tobacco patterns, with silt contents of 20.40% and 20.27%, respectively.

Furthermore, the highest percentage of sand was found in the rice-tobacco and rice-shallot patterns at 74.77% and 74.24%, respectively, closely followed by the rice-tomato pattern at 72.47%. Rice-garlic and rice-rice patterns had the least sand content, with 34.27% and 25.20% respectively.

Bulk density of soil is influenced by various factors, including clay content, land use, and management practices (Chaudhari et al., 2013). Similarly, sand content has a more significant effect on soil bulk density than other soil properties (Ahad et al., 2015). Similar trends were observed in the bulk density values derived from the soil with varying cropping patterns. In this study, cropping patterns with higher sand content exhibited greater soil bulk density. In the current study, the highest bulk density values were observed in cropping patterns rice-corn, rice-pepper, rice-tomato, rice-shallot, rice-eggplant, and rice-tobacco, all with comparable results. Conversely, the lowest bulk density values were found in the rice-garlic and rice-rice cropping patterns, characterized by clayey-textured soil, with 1.28 g/cm^{-3} and 1.30 g/cm^{-3}, respectively.

Table 3. The soil physical properties under the different cropping patterns

Cropping pattern	Soil physical properties				
	% Clay	% Silt	% Sand	Soil texture	Bulk density
	**	**	**	**	**
Rice-Corn	5.60^{c}	29.07^{ab}	65.33^{c}	Sandy loam	1.43^{a}
Rice-Garlic	38.67^{b}	27.07^{abc}	34.27^{d}	Clay loam	1.30^{bc}
Rice-Rice	46.20^{a}	28.60^{abc}	25.20^{e}	Clay	1.28^{c}
Rice-Pepper	6.03^{c}	25.57^{bcd}	68.40^{bc}	Sandy loam	1.41^{a}
Rice-Tobacco	4.97^{c}	20.27^{d}	74.77^{a}	Sandy loam	1.36^{ab}
Rice-Tomato	4.20^{c}	23.33^{cd}	72.47^{ab}	Sandy loam	1.41^{a}
Rice-Eggplant	3.37^{c}	32.53^{a}	64.10^{c}	Sandy loam	1.37^{ab}
Rice-Shallot	5.37^{c}	20.40^{d}	74.24^{a}	Sandy loam	1.41^{a}
CV (%)	14.23	7.59	3.00		2.14

**=Significant at 1% level; CV=coefficient of variation; Means with the same letter are significantly different at 1% level of significance using HSD Test.

3.4 Soil chemical properties under the different cropping patterns

The soil chemical properties significantly influence the accumulation of organic matter in the soil. Properties like pH, redox potential, and nutrient content directly impact the transformation of organic matter retained in the soil. Sufficient nutrient availability is essential for the decomposition of organic matter. Microorganisms engaged in the breakdown of organic substances require vital nutrients like nitrogen (N), phosphorus (P), and potassium (K) to fuel their metabolic processes. The activity and efficiency of microbial decomposition and the subsequent accumulation of organic matter are influenced by soil pH (Blanco-Canqui et al., 2009). Table 4 reveals the influence of chemical soil properties on the formation and accumulation of SOC. Among the cropping patterns, rice-shallot and rice-corn showed the highest and are significantly different (P) content in the soil. This higher P content is attributed to the crop management, where P application is more to enhance bulb production and robust crop growth. However, the potassium content of soils across the various cropping systems did not exhibit significant differences. Generally, N, P, K and macronutrients are needed by microorganisms in the soil to enhance the decomposition of organic matter and the formation of stable carbon compounds (Zhou et al., 2025).

The soil pH of the distinct cropping patterns also displayed significant variations. The results indicated that rice-corn, rice-garlic, rice-rice, and rice-pepper patterns were characterized by neutral pH, while the remaining cropping patterns featured slightly acidic soils. It is worth noting that soil pH affects microbial activity and the composition of microbial communities. Different microbial groups exhibit preferences for specific pH levels. Soil chemical attributes influencing pH levels can impact the abundance and activity of microorganisms in the decomposing organic matter. An optimal pH range, particularly a neutral pH, can stimulate microbial activity and enhance the breakdown of organic matter. Research has underscored that soil organic matter (SOM) associated with the sand-size fraction is more susceptible to decomposition, leading to higher turnover compared to the silt- or clay-size fractions (Angers and Mehuys, 1990). Crop sequencing is one important management practice in agriculture as it helps to improve soil's physical texture by rotating different crops whose roots reach various soil depths. Crop rotation helps improve aggregate stability and water-holding capacity, decrease bulk density, and reduce soil compaction (Qui et al., 2024).

A notable difference in the build-up of organic matter content among various cropping patterns was noted in this study. The rice-tobacco cropping pattern exhibited the highest organic matter content (3.11%), followed by rice-eggplant (2.46%). This can be attributed to the crops' characteristics, primarily their broad leaves leading to a greater biomass contribution to the soil. Conversely, the rice-corn and rice-garlic cropping patterns displayed the lowest organic matter content, measuring 1.04% and 1.07%, respectively.

The organic carbon estimation was conducted based on the assumption that soil organic matter comprises 58% carbon, which applies to certain soils or specific components of soil organic matter (Pribyl, 2010). The results demonstrate a direct proportionality between organic carbon (OC) and organic matter (OM). As a result, the rice-tobacco cropping pattern exhibited the highest OC content at 1.80%, followed by rice eggplant at 1.43%. Conversely, rice-corn

displayed the lowest OC content, accompanied by rice-garlic at 0.60% and 0.63%, respectively. The varying SOC in the soil under different crop patterns may be attributed to several factors such as crop and soil management. Crop rotation changes the amount and type of crop residues or root systems, which affects fixation, mineralization, and the total amount of soil organic carbon that a soil contains (Niu et al., 2024) while mineral and organic fertilization significantly enhance SOC quality and quantity in the soil (Zhange et al., 2024).

3.5 X-ray fluorescence (XRF) analysis

XRF analysis revealed the elemental composition of the soil samples under different cropping patterns. Figure 2 reveals that soil samples are Si-rich with significant amount of iron and aluminum with at least 60% light elements. Other inorganic ions such as magnesium, calcium, titanium and manganese were also detected. It can be noted that the soil samples for rice-onion cropping pattern have trace amounts of phosphorous.

Table 4. The soil chemical properties under the different cropping patterns

Cropping pattern	Soil chemical properties				
	% OM	% OC	P (ppm)	K (ppm)	pH
	**	**	**	ns	**
Rice-Corn	1.04^{e}	0.60^{e}	161.77^{b}	268.26	7.00^{a}
Rice-Garlic	1.07^{de}	0.63^{de}	61.50^{d}	210.79	7.00^{a}
Rice-Rice	1.33^{cde}	0.77^{cd}	54.16^{d}	223.47	7.00^{a}
Rice-Pepper	1.33^{cd}	0.77^{cd}	122.54^{c}	225.83	7.03^{a}
Rice-Tobacco	3.11^{a}	1.80^{a}	72.11^{d}	247.06	6.87^{a}
Rice-Tomato	1.57^{c}	0.91^{c}	46.56^{d}	257.62	6.80^{ab}
Rice-Eggplant	2.46^{b}	1.43^{b}	126.62^{bc}	222.95	6.57^{b}
Rice-Shallot	1.34^{cd}	0.78^{cd}	293.30^{a}	265.82	6.80^{ab}
CV (%)	5.96	5.90	11.11	8.68	1.25

**=Significant at 1% level; ns=not significant; CV=coefficient of variation; Means with the same letter are significantly different at 1% level of significance using HSD Test.

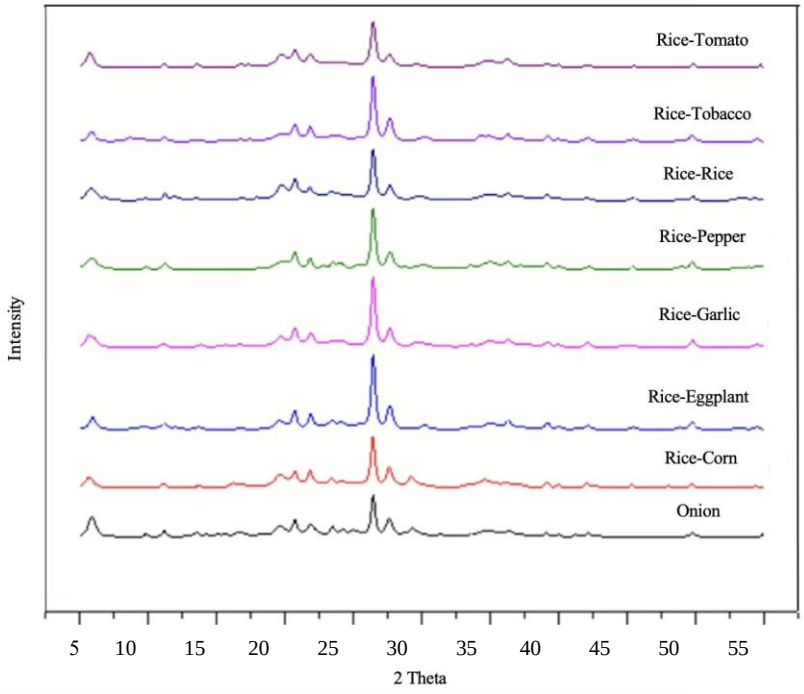

Figure 2. X-ray fluorescence analysis of soils under different cropping patterns in the City of Batac

The silicon-to-aluminum (Si/Al) ration was consistent across all samples, with an average of approximately 3.0 (Table 5). From an environmental standpoint, a high Si/Al ratio in soils or minerals significantly influences soil stability and water retention. Such soils often demonstrate greater structural stability and increased water-holding capacity, supporting plant growth and reducing erosion risk.

Similarly, the iron to aluminum (Fe/Al) ratio was consistent across all samples averaging at approximately 1.0. This consistency suggests the presence of substantial quantities of Fe-Al smectite minerals in the soil. Smectite minerals are known for their high cation exchange capacity (CEC), enabling them to retain and exchange essential nutrients such as calcium (Ca), magnesium (Mg), potassium (K), and sodium (Na). This property directly influences nutrient availability and overall soil fertility. Additionally, the expandable lattice structure of smectite-rich soils enhances water retention, which is particularly advantageous for plant growth in dry conditions. The presence of these minerals underscores the soil's capacity to support sustainable agricultural productivity.

Table 5. The chemical composition of soil based on the ratio of its components

Cropping pattern	Si/Al ratio (ppm)	Fe/Al ratio (ppm)
Rice-Shallot	3.45	1.14
Rice-Eggplant	3.21	1.22
Rice-Tomato	3.12	1.13
Rice-Tobacco	3.28	1.09
Rice-Sweet Pepper/Chili	3.13	1.07
Rice-Rice	2.95	1.0
Rice-Corn	3.27	1.09
Rice-Garlic	3.24	0.99

Minerals with higher Si/Al ratios may contribute to soil stability and water-holding capacity. Similarly, a consistent iron to aluminum ration of about 1.0 was observed in the samples. This ratio suggests the presence of significant amounts of Fe-Al smectite minerals in the soil. Smectite minerals are characterized by a high cation exchange capacity (CEC), facilitating the exchange of vatious positively charged ions (cations) such as calcium (Ca), magnessium (Mg), potassium (K), and sodium (Na). Thus, this affect nutrient availability in the soil. Smectite-rich soils have good water retention capabilities due to their expandable lattice structure, which can swell and hold water. This characteristic benefits plants by improving moisture retention during dry periods (Kumarti and Mohan, 2021).

3.6 Soil weight and soil carbon stock of the different cropping patterns

Soil weight was assessed at a depth of 30 cm, and the determination of carbon stock in the soil for each cropping pattern was based on bulk density. Findings indicated that soils characterized by higher bulk density tend to exhibit greater carbon weight, ranging from 4,090 kg C/ha (rice-tobacco) to 4,280 kg C/ha (rice-corn), as detailed in Table 6. These cropping patterns were associated with sandy loam and loamy sand soil textures, which contributed to their higher bulk density and carbon value stocks.

In contrast, soils with a clay composition demonstrated notably lower weight, registering at 3,830 kg C/ha (rice-rice) and 3,900 C/kg ha (rice-garlic). These findings indicate that carbon stock is significantly influenced by the presence of soil organic matter within various cropping patterns. The rice-tobacco pattern exhibited the highest carbon stock at 2,215.32 kg C/ha, which was statistically distinct from the rice-eggplant pattern (1,757.16 kg C/ha) and rice-tomato pattern (1,155.10 kg C/ha. These patterns also exhibited a higher soil bulk density (sandy loam) as compared to the others. Conversely, the lowest carbon stocks were observed in the rice-garlic (725.27 kg C/ha), rice-corn (776.33 kg C/ha), and rice-rice (883.19 kg C/ha) patterns.

3.7 Correlation analysis of the various factors affecting soil organic carbon

The correlation analysis shown in Table 7 shows that the clay content has a strong negative correlation with organic matter (OM) and sand content, while showing a positive correlation with carbon and silt content. Sand content has a strong negative correlation with clay, while it has a positive correlation with organic matter and silt content. Bulk density (BD) has a strong negative correlation with clay and silt content, suggesting that higher clay and silt content lead to lower bulk density. Phosphorus (P) has positive correlations with clay, sand, and silt content, indicating that it is associated with higher proportions of these components. pH has a strong negative correlation with clay, organic matter, and carbon content, suggesting that higher proportions of these components lead to lower soil pH. These

correlations provide insights into the relationships between different soil properties and can be useful in understanding soil composition and fertility.

Soil organic carbon (SOC) is a component of soil organic matter. Organic matter is primarily made of 58% carbon (Pribyl, 2010). Thus, the organic carbon in soil is directly proportional to the organic matter hence, rice-tobacco has the highest organic carbon at 1.80% followed by rice-eggplant at 1.43%. Accordingly, rice-corn obtain the lowest organic carbon followed by rice-garlic with 0.60% and 0.63%. The ability of the soil to store carbon is positively correlated with clay content since its larger surface area provides a protective environment against decomposition therefore increasing the capacity for carbon retention. Sand on the other hand, is inversely correlated soil carbon stock because sand has a lower capacity for carbon stabilization as compared to clay. Organic matter is the primarily source of carbon, thus, the higher the amount of OM, the higher the soil carbon stock.

Table 6. Soil weight and soil carbon stock of the different cropping patterns

Cropping pattern	Amount of carbon sequestered	
	WS (kg C/ha)	Carbon sequestered (kg C/ha)
	**	**
Rice-Corn	4,280[a]	776.33[e]
Rice-Garlic	3,900[bc]	725.27[e]
Rice-Rice	3,830[c]	883.19[de]
Rice-Pepper	4,220[a]	978.65[cd]
Rice-Tobacco	4,090[ab]	2,215.32[a]
Rice-Tomato	4,230[a]	1,155.10[c]
Rice-Eggplant	4,100[ab]	1,757.16[b]
Rice-Shallot	4,220[a]	980.40[cd]
CV (%)	2.14	5.36

Table 7. Correlation analysis

	CP	Clay	Silt	Sand	OM	C	WS	SC stock	P	K
Clay	-0.506*									
	0.012									
Silt	-0.343	0.234								
	1	0.27								
Sand	0.546**	-0.972**	-0.455*							
	0.006	<.001	0.025							
OM	0.453*	-0.384	-0.177	0.394						
	0.026	0.064	0.407	0.057						
BD	0.267	-0.837**	-0.245	0.825**	-0.023					
	0.207	<.001	0.249	<.001	0.916					
Carbon	0.453*	-0.384	-0.177	0.394	1.00**					
	0.026	0.064	0.407	0.057	0					
WS	0.267	-0.837**	-0.245	0.825**	-0.023	-0.023				
	0.207	<.001	0.249	<.001	0.916	0.916				
SC stock	0.475*	0.445*	-0.197	-0.455*	0.997**	0.997**	0.05			
	0.019	0.029	0.357	0.026	<.001	<.001	0.815			
P	0.410*	-0.419*	-0.201	0.433*	-0.2	-0.2	0.457*	-0.168		
	0.047	0.041	0.347	0.035	0.349	0.349	0.025	0.433		
K	0.165	-0.445*	-0.318	0.484*	-0.013	0.013	0.488*	0.023	0.433*	
	0.441	0.029	0.13	0.017	0.952	0.952	0.016	0.916	0.035	
pH	-0.706**	0.412*	-0.048	-0.366	-0.534**	-0.534**	-0.107	-0.543**	-0.193	-0.179
	<.001	0.046	0.825	0.079	0.007	0.007	0.619	0.006	0.367	0.402

4. CONCLUSION

Based on the comprehensive analysis of the study's findings, several noteworthy conclusions can be drawn, shedding light on the intricate relationships between soil properties, cropping patterns, and carbon sequestration.

The rice-corn cropping pattern was found to be the most dominant followed by rice-tobacco, in the City of Batac, with the latter obtained as a higher carbon stock mostly attributed to greater biomass (broad leaf) and management practice after crop harvesting. Additionally, the commonly practiced cropping management by farmers include the use and application of fertilizer and pesticides in the crops.

This study reveals that cropping patterns influence in the clay, silt, and sand particles of the soil. Generally, cropping patterns with higher proportions of clay tended to exhibit lower bulk density and soil weight while those dominated by sand showed higher bulk density and soil weight. Moreover, the phosphorus content of the soil varied significantly across cropping pattern while potassium did not differ significantly. The soil organic content was highest in the rice-tobacco cropping pattern, attributed to the biomass contribution of broadleaf crops, while other patterns displayed varying levels. These findings highlight the potential for strategic cropping choices to enhance carbon sequestration, thereby contributing to climate change mitigation efforts.

ACKNOWLEDGEMENTS

This paper was supported by Mariano Marcos State University through GAA-Funded Research Projects.

AUTHOR CONTRIBUTIONS

Conceptualization, Methodology, Validation, Supervision and Writing Original Draft Preparation, Formal Analysis, Data Curation, Visualization, Writing: Bucao and Gonzales Experimental run and Data Collection: Bucao, Gonzales, Bumanglag and Tapac; Review and Editing: Gonzales

DECLARATION OF CONFLICT OF INTEREST

The authors have no conflict of interest to declare.

REFERENCES

Adekiya A, Alori E, Ogunbode T, Sangoyomi T, Oriade O. Enhancing organic carbon content in tropical soils: Strategies for sustainable agriculture and climate change mitigation. The Open Agriculture Journal 2023;17:e18743315282476.

Ahad T, Kanth TA, Nabi S. Soil bulk density as related to texture, organic matter content and porosity in Kandi soils of District Kupwara (Kashmir Valley), India. Geography 2015; 4(1):198-200.

Angers D, Mehuys G. Barley and alfalfa cropping effects on carbohydrate contents of a clay soil and its size fractions. Soil Biology and Biochemistry 1990;22(3):285-8.

Brar B, Singh J, Singh G, Kaur G. Effects of long-term application of inorganic and organic fertilizers on soil organic carbon and physical properties in maize-wheat rotation. Agronomy 2015;5(2):220-38.

Blanco-Canqui H, Stone L, Schlegel A, Lyon D, Vigil M, Mikha M, et al. No-till induced increase in organic carbon reduces maximum bulk density of soils. Soil Science Society of America Journal 2009;73(6):1871-9.

Buyanovsky G, Wagner G. Carbon cycling in cultivate land and its global significance. Global Change Biology 2002;4(2):131-41.

Chaudhari PR, Ahire DV, Ahire VD, Chkravarty M, Maity S. Soil bulk density as related to soil texture, organic matter content and available total nutrients of coimbatore soil. International Journal of Scientific and Research 2013;3(2):1-8.

Dikitanan R, Grosjean G, Nowak A, Leyte J. Climate-Resilient Agriculture in Philippines. Climate-Smart Agriculture Country Profile for Asia series. Manila, Philippines: International Center for Tropical Agriculture (CIAT), Government of the Philippines; 2017. p. 1-24.

Francaviglia R, Almagro M, Vicente-Vicente L. Conservation agriculture and soil organic carbon: Principles, processes, practices and policy options. Soil Systems 2023;7(1):Article No. 17.

Food and Agriculture Organization of the United Nations (FAO). Standard Operating Procedure for Soil Bulk Density: Cylinder Method. Global Soil Laboratory Network, FAO; 2023.

Food and Agriculture Organization of the United Nations (FAO). Standard Operating Procedure for Soil Organic Carbon: Walkey-Black Method, Titration and Colorimetric Method. Global Soil Laboratory Network, FAO; 2019.

Gikonyo FN, Dong X, Mosongo PS, Guo K, Liu X. Long-term impacts of different cropping patterns on soil physico-chemical properties and enzyme activities in the low land plain of North China. Agronomy 2022;12(2):Article No. 471.

Haddaway NR, Hedlund K, Jackson LE, Katterer T, Lugato E, Thomsen IK, et al. How does tillage intensity affect soil organic carbon? A systematic review. Environmental Evidence 2017;6:Article No. 30.

Hoyle FC, Murphy. Soil Quality: Soil organic carbon Australia [Internet]. 2018 [cited 2025 June 12]. Available from: https://soilqualityknowledgebase.org.au/measuring-soil-organic-carbon/.

Kumarti N, Mohan C. Basics of clay minerals and their characteristics properties. In: Do Nascimento GMM, editor. Clay and Clay Minerals. IntechOpen; 2021.

Lal R. Soil carbon sequestration impact on global climate change and food security. Science 2004;304,1623-7.

Niu Z, An F, Suu Y, Li J, Liu T. Effects of cropping patterns on the distribution, carbon contents, and nitrogen contents of aeolian san soil aggregates in Northwest China. Scientific Reports 2024;14:Article No. 1498.

Pribyl DW. A critical review of the conventional SOC to SOM conversion factor. Geoderma 2010;156(3-4):75-83.

PohankovÃ¡ P, Hlavinka KC, Kersebaum C, Nendel A, RodrÃ-guez J, Balek M, et al. Expected effects of climate change on the soil organic matter content related to contrasting agricultural management practices based on a crop model

ensemble for locations in Czechia. European Journal of Agronomy 2024;156:Article No. 127165.

Qui NV, Khoa LV, Phuong NM, Vien DM, Dung TV, Linh TB, et al. Effects of rotating rice with upland crops and adding organic amendments, and of related soil quality on rice yield in the Vietnamese Mekong Delta. Agronomy 2024;14(6):Article No. 1185.

Truog E. Determination of readily available phosphorus in soil. Agronomy Journal 1930;(22)10:874-82.

Valenzuela-Balcázar IG, Visconti-Moreno EF, Faz Á, Acosta JA. Soil organic carbon dynamics in two rice cultivation systems compared to an agroforestry cultivation system. Agronomy 2022;12(1):Article No. 17.

Zhou D, Rui M, Lihua W, Jingru L, Yuanxiang T, Ji C, et al. Fertilization effects on soil organic matter chemistry. Soil and Tillage Research 2025;246:Article No. 106346.

Zhang C, Zhao Z, Li F, Zhang J. Effects of organic and inorganic fertilization on soil organic carbon and enzymatic activities. Agronomy 2022;12(12):Article No. 3125.

Environment and Natural Resources Journal

Volume 23
Issue 6
2025

Assessing Aquatic Plant Diversity and Management Potential in Wetlands in Northwestern and Southwestern Bangladesh

Md. Foysul Hossain[1,2*], Koushik Chakroborty[1], Gazlima Chowdhury[1], Sumiya Bhuyain[3], Abrar Hossain[3], Mst. Mosfeka Khatun Ritu[3], and Roksana Jahan[4]

[1]Department of Aquatic Environment and Resource Management, Sher-e-Bangla Agricultural University, Dhaka 1207, Bangladesh
[2]University of South Bohemia in Ceske Budejovice, Faculty of Fisheries and Protection of Waters, South Bohemian Research Center of Aquaculture and Biodiversity of Hydrocenoses, Institute of Aquaculture and Protection of Waters, České Budějovice 37005, Czech Republic
[3]Faculty of Fisheries and Marine Science, Sher-e-Bangla Agricultural University, Dhaka 1207, Bangladesh
[4]Department of Marine Fisheries and Oceanography, Sher-e-Bangla Agricultural University, Dhaka 1207, Bangladesh

ARTICLE INFO

Received: 16 Nov 2024
Received in revised: 29 Jul 2025
Accepted: 5 Aug 2025
Published online: 17 Sep 2025
DOI: 10.32526/ennrj/23/20240287

Keywords:
Gajner Beel/ Padma Beel/ Aquatic weed/ Control/ Upcycling

*** Corresponding author:**
E-mail: foysul.aerm@sau.edu.bd

ABSTRACT

Aquatic plants are essential organisms for assessing ecological health and for managing and conserving aquatic biodiversity. The present study investigated the diversity of aquatic flora, in addition to their applications and management, in northwestern (Gajner Beel) and southwestern (Padma Beel) Bangladesh. This research utilized a mixed-methods approach, incorporating observation of the study area for collecting samples, qualitative interviews, and quantitative surveys. A total of 38 aquatic plant species of 4 types belonging to 16 orders and 23 families were recorded from the two wetlands. Asterales was the predominant order in both wetlands, with Araceae and Asteraceae being the largest families. Almost half (44%) of the aquatic plants in both ecosystems bloomed during the rainy season. In Gajner Beel and Padma Beel, 41% and 48% of aquatic plants, respectively, rarely occurred, while 31% and 41% of aquatic weeds were frequent, respectively. Approximately a quarter of the plants have an unevaluated IUCN conservation status, with about 13% of plants in Gajner Beel and 15% in Padma Beel being exotic. Farmers only employ manual or mechanical techniques to control common aquatic weeds, without any preventive measures. About 74% of the aquatic plants in both regions are used for various purposes by local people, including traditional medicine, human food, animal feed, raw materials for handicrafts, and fertilizers. The study examined management approaches for the aquatic flora in both regions, emphasizing their potential utilization.

HIGHLIGHTS

This study recorded 38 aquatic plants (16 orders, 23 families) in two wetlands. Asterales was the dominant order; Araceae and Asteraceae were the richest families. 44% of species bloomed in the rainy season, while 13-15% were exotic. Management and control relied only on manual/mechanical methods. 74% of the species were used by locals for diverse applications.

1. INTRODUCTION

Wetlands are vital ecosystems that link people, life, and climate through mutual interactions (Maltby, 2009). They provide key environmental and ecological services (Schuyt, 2005), supported by their functionality. Aquatic and riparian vegetation are especially important for wetland structure, function, and service provision (Chambers et al., 2008). The symbiotic relationships between wetlands and aquatic flora yield substantial benefits for both the environment and human communities. Wetlands provide habitat for aquatic plants, which sustain ecosystem health by offering food, shelter, and breeding grounds for aquatic species (Kevin and Lancar, 2002). They also engage with a varied spectrum of other organisms, from microbes to vertebrates, by providing shelter and sustenance (Engelhardt and Ritchie, 2001; Wood et al., 2017). Furthermore, they facilitate the transport of nutrients into sediments and influence the hydrological,

Citation: Hossain MF, Chakroborty K, Chowdhury G, Bhuyain S, Hossain A, Ritu MMK, Jahan R. Assessing aquatic plant diversity and management potential in wetlands in Northwestern and Southwestern Bangladesh. Environ. Nat. Resour. J. 2025;23(6):581-594. (https://doi.org/10.32526/ennrj/23/20240287)

geomorphological, and physicochemical environments (Paul, 2022). In a different context, certain aquatic plants are classified as aquatic weeds, which are hazardous or unattractive species proliferating in aquatic environments where they are undesirable (Aloo et al., 2013). These aquatic weeds affect water bodies, leading to serious ecological and economic losses by affecting fisheries, impairing water quality and degrading floodplain farmland. Nonetheless, the extensive adaptability to diverse water levels and the inability to differentiate their natural habitat between aquatic and terrestrial contexts complicates the precise definition of an aquatic weed (Aloo et al., 2013). However, various major factors have compromised the diversity of aquatic plant populations, including the overexploitation of resources, water pollution, siltation, alterations in water flow such as abstraction, habitat destruction or degradation, and the invasion of alien species (Dudgeon et al., 2006; Schuyt, 2005; Sonal et al., 2010).

Gajner Beel (GB) and Padma Beel (PB) are two of the most significant wetlands found in the northwest and southwest regions of Bangladesh, respectively. These waterbodies are locally known as Beels, which are characterized by high biological diversity. Beels can be defined as a large surface water system that holds water from surface runoff through an internal drainage channel, usually starting with topographic lows produced by erosion (Banglapedia, 2012). The GB functions as a spawning and feeding ground for a number of fish species (Rahman et al., 2024). PB is popularly known as Bhutia Padma Beel, which is renowned for its fish and tourism attractions. This study selected these two ecosystems due to their geographical and topological distinctions.

The aquatic plants act as a useful bioindicator of ecological health owing to their high level of sensitivity to pollution (Lacoul and Freedman, 2006). They also serve as model organisms of the ecological cycle and play a significant role in alleviating eutrophication and carbon sequestration to mitigate climate change (Bao et al., 2022). To develop effective management plans, a proper listing of aquatic plants for a specific region is essential. These lists are also mandatory to prepare an environmental impact assessment and fulfill permit requirements (McKinley et al., 2017). In addition, management of aquatic weeds is one of the most important aspects of managing ponds (Giri, 2020). Thus, understanding aquatic plants and their roles in ecosystems helps effectively manage these, ensure the maximum yield, and maintain sustainability (Wilk-Woźniak et al., 2019). The application of modern control methods can effectively utilize aquatic weeds. However, research on aquatic plants focusing on their sustainable utilization is notably limited in Bangladesh. This study aimed to evaluate the species diversity in aquatic plants, compare compositional variations between two wetlands in Bangladesh, and suggest sustainable management strategies for aquatic plants.

2. METHODOLOGY

2.1 Study area

The study examined two wetlands in distinct agroecological zones of Bangladesh: Gajner Beel (northwestern region) at the Ganges floodplain confluence with silt loam to clay soils, and Padma Beel (southwestern region) with acidic, peat-underlain grey clays (Figure 1). The study area had three identified seasons: hot pre-monsoon/summer (March-May), wet monsoon (June-October), and cold, dry winter (November-February). Temperature in Pabna (8.4-34.3°C) and Khulna (12.0-34.8°C) peaked in April and was lowest in January. Monthly rainfall ranged from 8.1-335.6 mm in Pabna and 13.3-344.4 mm in Khulna, with July being the wettest month and January the driest (BMD, 2012). GB covers 5.54 ha with a mean depth of 135±36.34 cm and transparency of 102±21.52 cm, while PB spans 26.46 ha, with a mean depth of 172±34.65 cm and transparency of 78±13.65 cm.

2.2 Aquatic plant sampling and analysis

The survey was conducted from March 2022 to February 2023 across 24 sites (12 per wetland), each covering 5,000 m². Using a randomized design, the study applied a semi-quantitative method, assessing preselected locations via presence/absence appraoch to determine species frequency (Madsen and Wersal, 2017). Subjective evaluations of submerged plants were conducted by observers using plant rakes. The semiquantitative method was selected due to its lower effort and cost compared to other plant sampling methods and, its ability to regulate variability (Madsen and Wersal, 2017).

2.3 Identification of species and analysis

Visual inspection was used to identify aquatic weed samples, referencing studies by Journey et al. (1993), Pasha and Uddin (2013), Basar and Rahman (2023), and Kevin and Lancar (2002). The

Encyclopedia of Flora and Fauna of Bangladesh (Ahmed et al., 2008) was investigated, and recent nomenclature was cross-checked using Pasha and Uddin (2013). Origin and conservation status were assigned in accordance with the IUCN (2024) Red List categories.

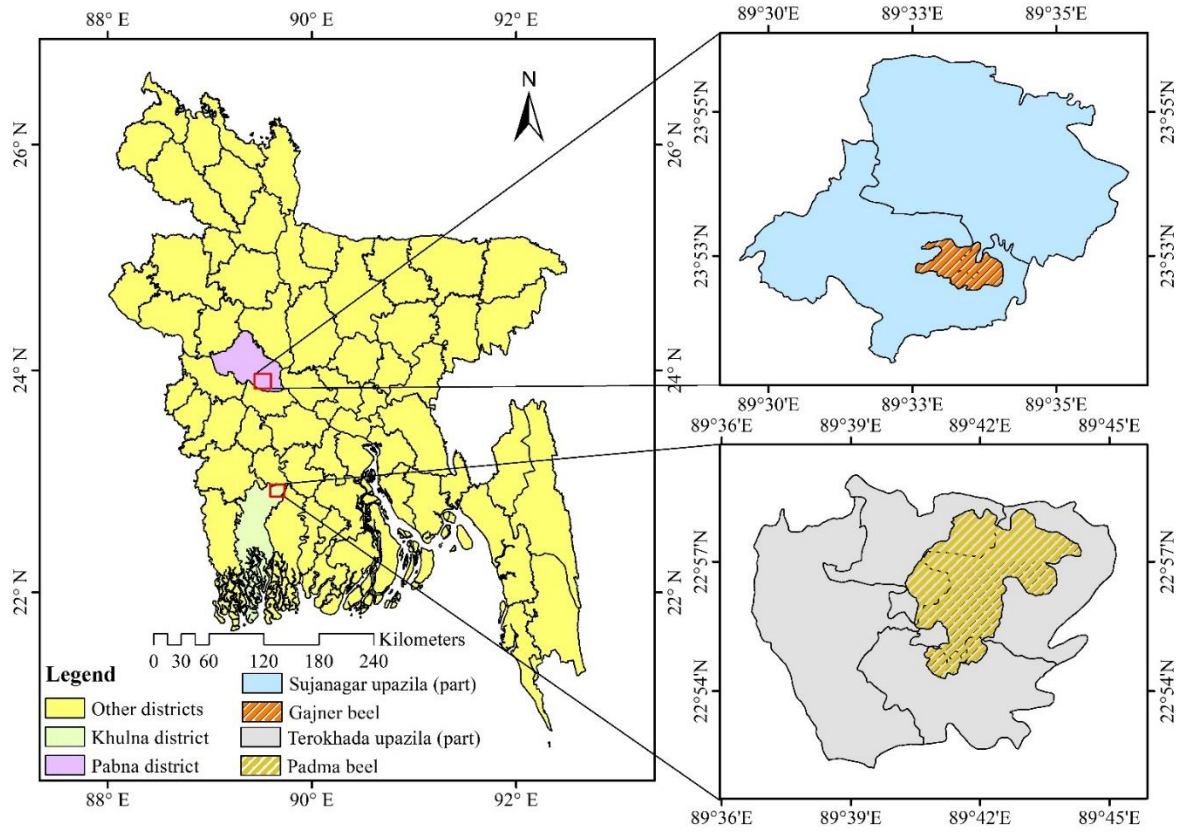

Figure 1. Map indicating the location of Gajner Beel and Padma Beel

The relative frequency of the aquatic plants was determined as follows:

$$F(\%) = [n/N] \times 100$$

Here; F(%)=frequency of aquatic plants; n=frequency of aquatic plants and N=total number of sites.

The frequency of occurrence was categorized as, Frequent=>50%; Moderate=25-50%; Rare=<25%. The Jaccard's similarity index (JSI) (Jaccard, 1912) and Sorensen's similarity index (SSI) (Sorensen, 1948) were determined as follows.

$$\text{Jaccard's similarity index (JSI): } S_j = \frac{a}{a+b+c}$$

$$\text{Sorensen's similarity index (SSI): } S_s = \frac{2a}{2a+b+c}$$

Here; a=number of common aquatic plants in GB and PB; c=number of aquatic plants in GB (site A); b=number of aquatic plants in PB (site B).

2.4 Data obtained from PRA tools

This study employed a mixed-methods approach, combining observation, interviews, and surveys. Data on aquatic macrophytes (local names, uses, seasonal availability, and management) were collected through interviews with 20 locals (15 men, 5 women) from diverse backgrounds (fishermen, farmers, ayurvedic practitioners, vegetable salesmen, and homemakers). A focus group discussion (FGD) with 10 people (experts and community leaders) was held in each region, along with 5 key informant interviews for data validation.

2.5 Statistical analysis

All qualitative and quantitative data were carefully collected and organized using MS Word and MS Excel 2019. Data were further analyzed using R and RStudio software. The map of the study area was generated using ArcGIS software (Version 10.8).

3. RESULTS

The study recorded 38 aquatic plant species (16 orders, 23 families) across both wetlands (GB and PB), with 21 species common between them (Table 1). Among the plants, Alismatales was documented as the most dominant order in both beels, followed by Poales (Figure 2), while Araceae and Asteraceae were the most abundant families (Figure 3).

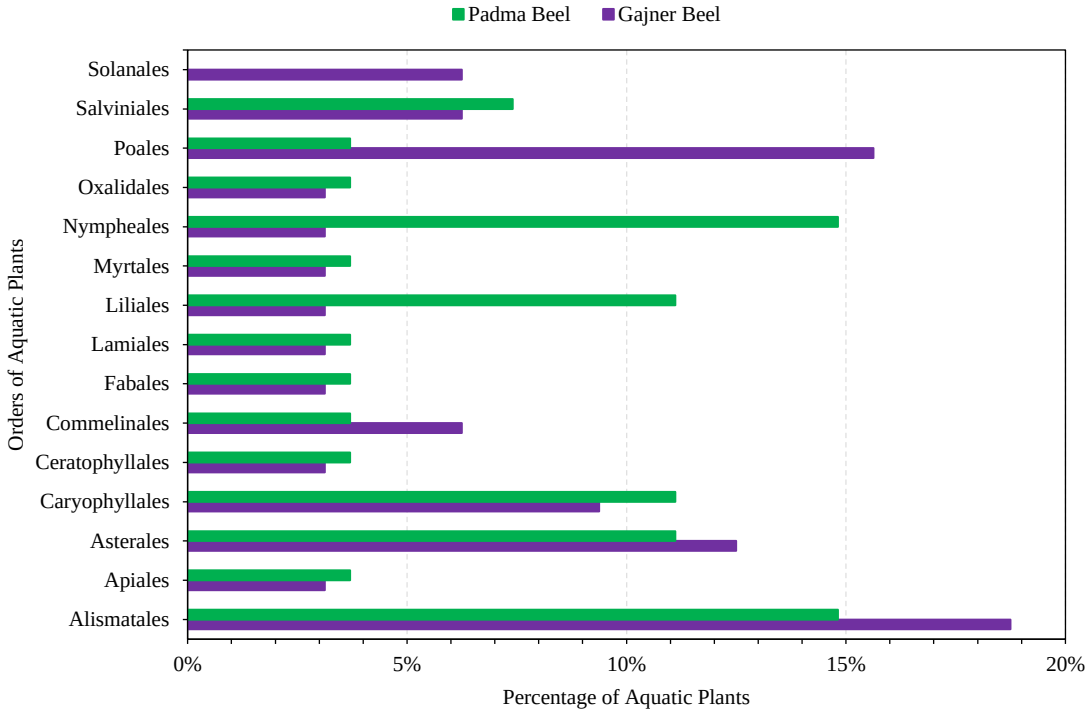

Figure 2. Orders of aquatic plants (%) recorded in northwestern (GB) and southwestern (PB) Bangladesh

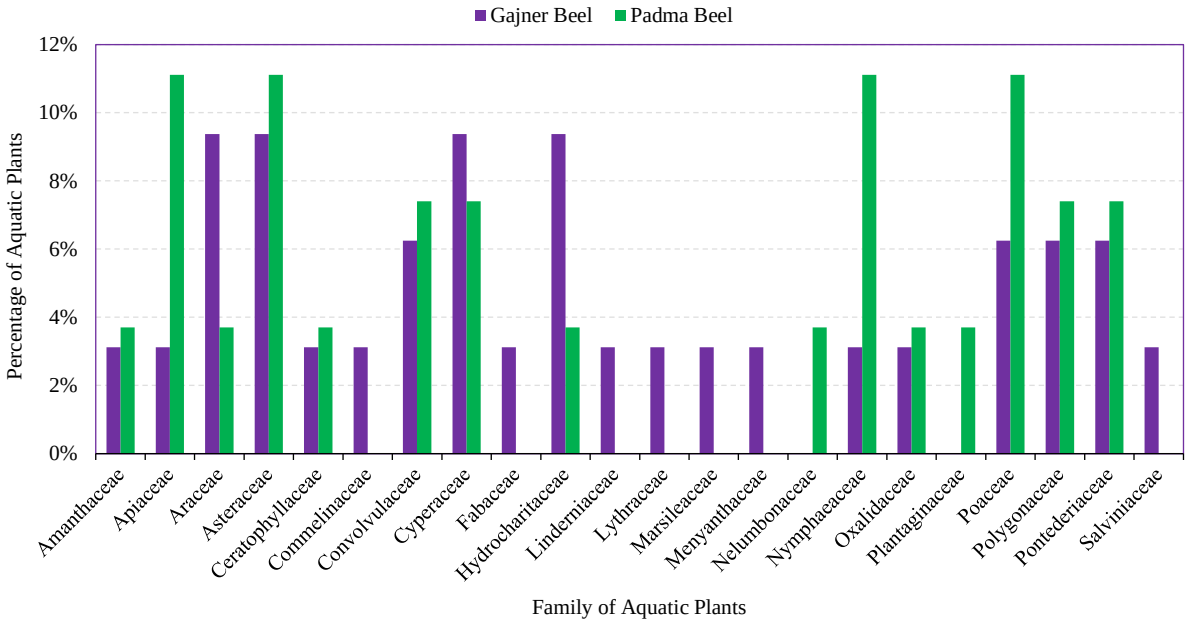

Figure 3. Families of aquatic plants (%) recorded in northwestern (GB) and southwestern (PB) Bangladesh

Table 1. List of aquatic macrophytes of northwestern and southwestern Bangladesh (GB and PB)

Aquatic weeds recorded both in GB and PB:										
Order	Family	Local name	Common name	Scientific name	Types	Frequency		Availability	Origin	Con. Stat.
						GB	PB			
Alismatales	Araceae	Topapana	Water lettuce	*Pistia stratiotes*	FF	F	F	AS	N	LC
		Kachu	Chinese Potato	*Colocasia esculenta*	EM	F	F	AS	N	LC
		Sonapana	Common duckweed	*Spirodela polyrhiza*	FF	R	R	AS	N	LC
	Hydrocharitaceae	Pata jhanji	Eel-grass	*Vallisneria spiralis*	SU	R	R	SS	N	LC
Asterales	Asteraceae	Helencha	Water cress	*Enhydra fluctuans*	EM	F	F	RS	N[(1)]	NE
		Kesuti	False daisy	*Eclipta prostrata*	EM	R	R	AS	N	LC
		Nak ful	Indian lilac	*Acmella paniculata*	EM	M	R	RS	N	LC
Commelinales	Pontederiaceae	Kachuripana	Water hyacinth	*Pontederia crassipes*	FF	F	F	AS	E[(2)]	NE
Caryophyllales	Amanthaceae	Malancha	Alligator weed	*Alternanthera philoxeroides*	EM	F	F	SS	E[(3)]	NE
	Polygonaceae			*Polygonum barbatum*	EM	M	R	SS	N	LC
		Redshank	Knotgrass							
		Bishkatali	Polygonum	*Polygonum glabrum*	EM	F	F	WS	N	LC
Ceratophyllales	Ceratophyllaceae	Kata jhanji/ Sheola	Con's tail	*Ceratophyllum demersum*	SU	M	R	RS	N	LC
Liliales	Pontederiaceae	Baranukha	Leaf pondweed	*Monochoria hastata*	FF	R	R	SS	N	LC
Nymphaeales	Nymphaeaceae	Shada shapla	Blue lotus	*Nymphaea nouchali*	RF	F	F	RS	N	LC
Oxalidales	Oxalidaceae	Amrool shak	Indian sord	*Oxalis corniculata*	EM	F	F	RS	U[(4)]	NE
Poales	Cyperaceae	Chechra	Bog bulrush	*Schoenoplectiella mucronata*	EM	M	M	RS	N	LC
		Mutha	Nut grass/Coco-grass	*Cyperus rotundus*	EM	M	M	WS	N	LC
	Poaceae	Dol	Asian	*Hygroryza aristata*	EM	R	R	RS	N[(5)]	NE
Solanales	Convolvulaceae	Kolmi	Water spinach	*Ipomoea aquatica*	EM	F	F	AS	N	LC
		Dhol kolmi	Bush morning glory	*Ipomoea fistulosa*	EM	M	M	RS	E[(6)]	NE
Salviniales	Salviniaceae	Kutipana	Mosquito fern	*Azolla pinnata*	FF	F	F	AS	N	LC

NB.: FF-Free floating, RF-Rooted floating, EM-Emergent, SU-Submerged, M-Moderate, R-Rare, F-Frequent, AS-All Season, RS-Rainy Season-SS-Summer Season, WS-Winter Season, E-Exotic, N=Native, U-Unknown, LC =Least concern, NE-Not Evaluated, VU-Vulnerable, Con. Stat.- Conservation Status, [1](Ali et al., 2013); [2](Cherwoo et al., 2024); [3](Sosa et al., 2008); [4](Groom et al., 2019); [5](Ahmed et al., 2008); [6](Acevedo-Rodríguez and Strong, 2012); [7](Acharya et al., 2009); [8](ITIS, 2011)

Table 1. List of aquatic macrophytes of northwestern and southwestern Bangladesh (GB and PB) (cont.)

Order	Family	Local name	Common name	Scientific name	Types	Frequency		Availability	Origin	Con. Stat.
						GB	PB			
Aquatic weeds recorded only in GB:										
Alismatales	Hydrocharitaceae	Najas	Brittle naiad	*Najas minor*	SU		R	RS	N	LC
		Hydrilla	Waterthyme	*Hydrilla verticillata*	SU		R	RS	N	LC
Apiales	Apiaceae	Thankuni	Gotu kola	*Centella asiatica*	EM		R	AS	N	LC
Asterales	Menyanthaceae	Chandmata	Crested floating heart	*Nymphoides cristata*	EM		R	RS	N	LC
Commelinales	Commelinaceae	Kanaidoga	Asiatic dayflower	*Commelina appendiculata*	EM		R	RS	N[(7)]	NE
Fabales	Fabaceae	Shola	Indian jointvetch	*Aeschynomene indica*	EM		M	RS	N	LC
Lamiales	Linderniaceae	Chhoto helencha	Spamow false pimpernel	*Lindernia antipoda*	EM		M	RS	N	LC
Myrtales	Lythraceae	Haincha	Yellow ammannia	*Ammannia pedicellata*	EM		R	WS	E	VU
Poales	Cyperaceae	Kesur	Giant bulrush	*Scripus grossus*	EM		R	WS	U	NE
	Poaceae	Arail	Swamp rice grass	*Leersia hexandra*	EM		R	AS	N	LC
Salviniales	Marsileaceae	Shusnishak	Pepperwort	*Marsilea quadrifolia*	EM		M	WS	N	LC
Aquatic weeds recorded only in PB:										
Apiales	Araliaceae	Poicha lily	Lawn Marshpennywort	*Hydrocotyle sibthorpioides*	EM	R		AS	N	LC
Lamiales	Plantaginaceae	Ambulla	Asian marsh weed	*Limnophila indica*	SU	R		RS	N	LC
Nymphaeales	Nymphaeaceae	Lalshapla	Red water lily	*Nymphaea rubra*	RF	R		RS	N	LC
		Golapi Shapla	pink water lily	*Nymphaea pubescens*	RF	R		RS	N	LC
Poales	Poaceae	Nolkhagra	Tall reed	*Phragmites karka*	EM	R		AS	N	LC
Proteales	Nelumbonaceae	Poddo	Pink lotus	*Nelumbo nucifera*	RF	F		RS	E[(8)]	NE

NB.: FF-Free floating, RF-Rooted floating, EM-Emergent, SU-Submerged, M-Moderate, R-Rare, F-Frequent, AS-All Season, RS-Rainy Season-SS-Summer Season, WS-Winter Season, E-Exotic, N=Native, U-Unknown, LC =Least concern, NE-Not Evaluated, VU-Vulnerable, Con. Stat.- Conservation Status, [1](Ali et al., 2013); [2](Cherwoo et al., 2024); [3](Sosa et al., 2008); [4](Groom et al., 2019); [5](Ahmed et al., 2008); [6](Acevedo-Rodríguez and Strong, 2012); [7](Acharya et al., 2009); [8](ITIS, 2011)

Based on habitats, four types of aquatic plants have been found, and their percentage distributions are presented in Figure 4.

Most of the species were emergent aquatic plants, comprising 69% and 56%, respectively. In the present study, most aquatic plants (44%) grew during the rainy season in both ecosystems, followed by year-round (all seasons), summer, and winter seasons (Figure 5).

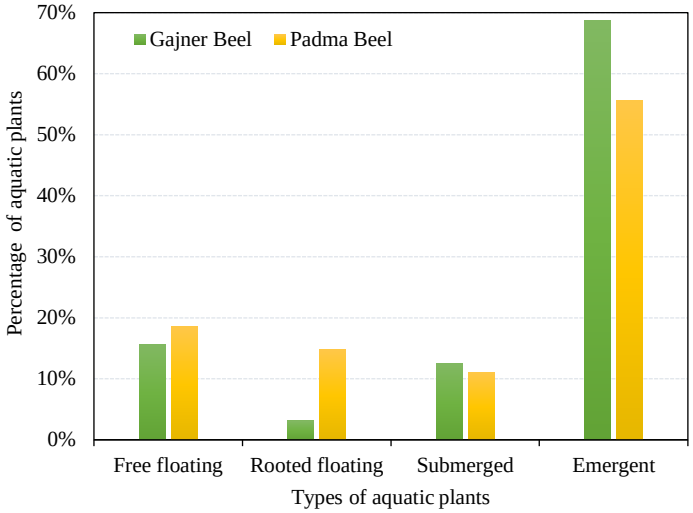

Figure 4. Types of aquatic plants (%) recorded in northwestern (GB) and southwestern (PB) Bangladesh

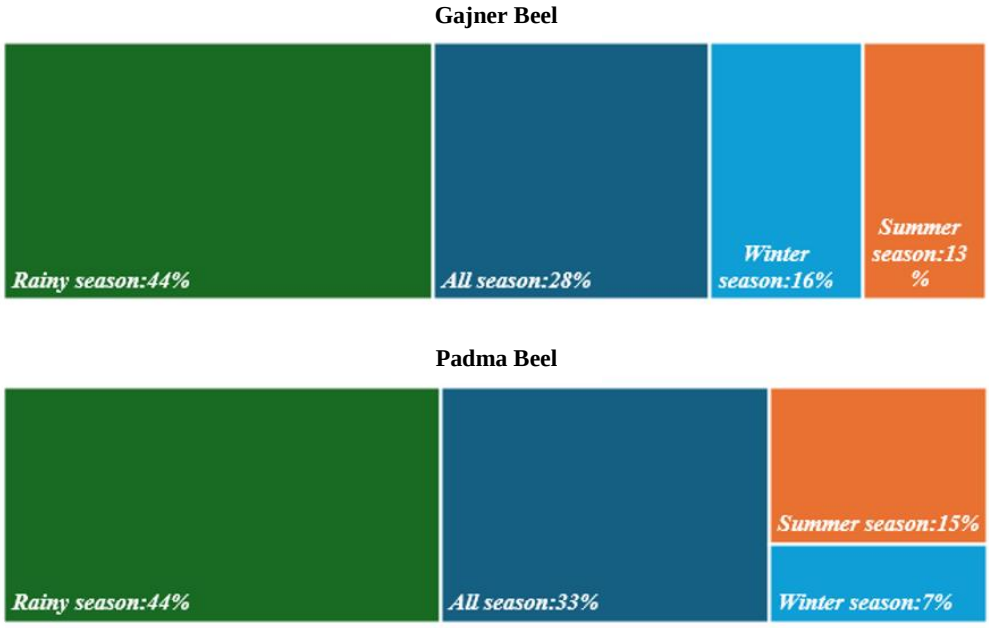

Figure 5. Seasonal availability of aquatic plants in northwestern (GB) and southwestern (PB) Bangladesh

In both ecosystems, most aquatic plants were rare, with 41% and 48% in GB and PB, respectively. 28% and 11% of aquatic macrophytes were classified as moderate, while 31% and 41% of aquatic weeds were frequently observed in GB and PB, respectively (Figure 6).

Figure 7 shows that native aquatic plants dominated (81%), followed by exotic species (13% in GB, 15% in PB). However, the origin of 6% and 4% of plants in GB and PB, respectively, was unknown. The conservation status, documented from the IUCN Red List, shows most aquatic plants represented as Least Concern (LC), accounting for 72% in GB and 74% in PB, respectively. In contrast, about a quarter of aquatic plants were classified as Not Evaluated (NE) in both wetlands. Only 3% of aquatic plants

recorded in GB were vulnerable (Figure 8). The Jaccard's similarity value between the two ecosystems was 0.5526, and Sorensen's similarity index (SSI) was 0.71186.

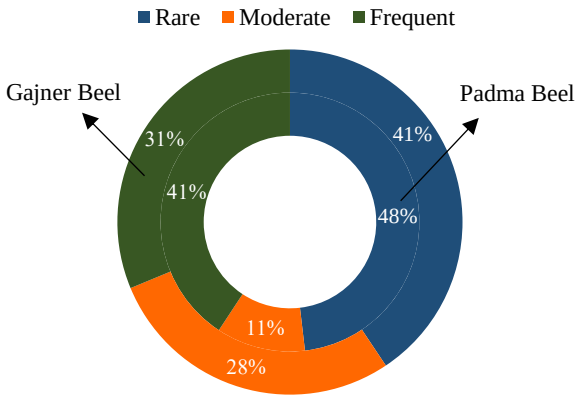

Figure 6. Frequency of occurrence of aquatic plants in northwestern (GB) and southwestern (PB) Bangladesh

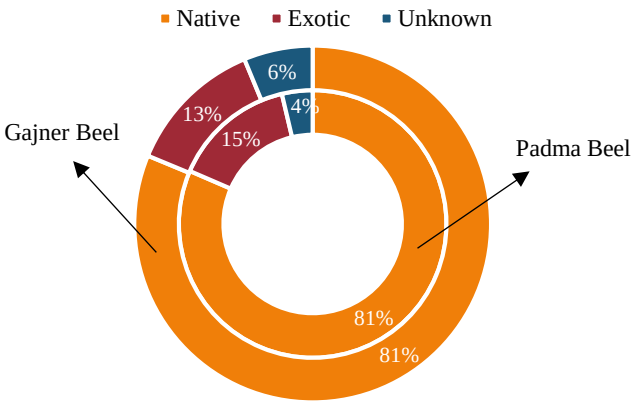

Figure 7. Origin of aquatic plants in northwestern (GB) and southwestern (PB) Bangladesh

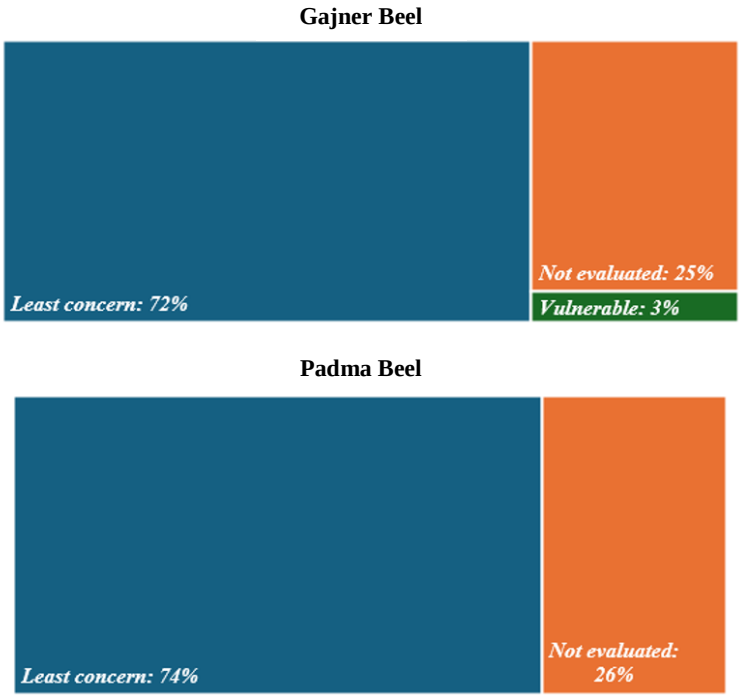

Figure 8. Conservation status of aquatic plants in northwestern (GB) and southwestern (PB) Bangladesh

No preventive measures were documented for the invasive aquatic plants in both regions. As a control measure for frequently available aquatic weeds, 94%, 3%, and 3% of the farmers followed manual/ mechanical, chemical and biological methods in GB. In contrast, only manual/mechanical (97%) and biological (3%) methods were used in PB. Eco-physiological approaches were not employed in any location. However, aquatic weeds found in both areas have several potential uses that have financial and environmental values (Figure 9). Figure 9 illustrates general methods of management of aquatic plants, prioritizing potential uses documented by the literature.

Twenty-eight aquatic plant species were documented as being used by communities, with similar utilization patterns observed across the study areas. Specifically, 21 species are used as traditional medicine (55%), while six are consumed as food (16%), four are provided as animal feed (11%), two are utilized as materials for handicrafts and fertilizers (5%), and five are used for other purposes (13%). In addition, 10 species (26%) in these regions remain untapped for any purpose (Table 2).

Table 2. Different uses of recorded aquatic plants in the northwestern (GB) and southwestern (PB) Bangladesh

Upcycling potential	Species number	Percentage (%)
Medicine	21	55
Human food	6	16
Fodder	4	11
Handcraft materials	2	5
Fertilizers	2	5
Others	5	13
No use	10	26

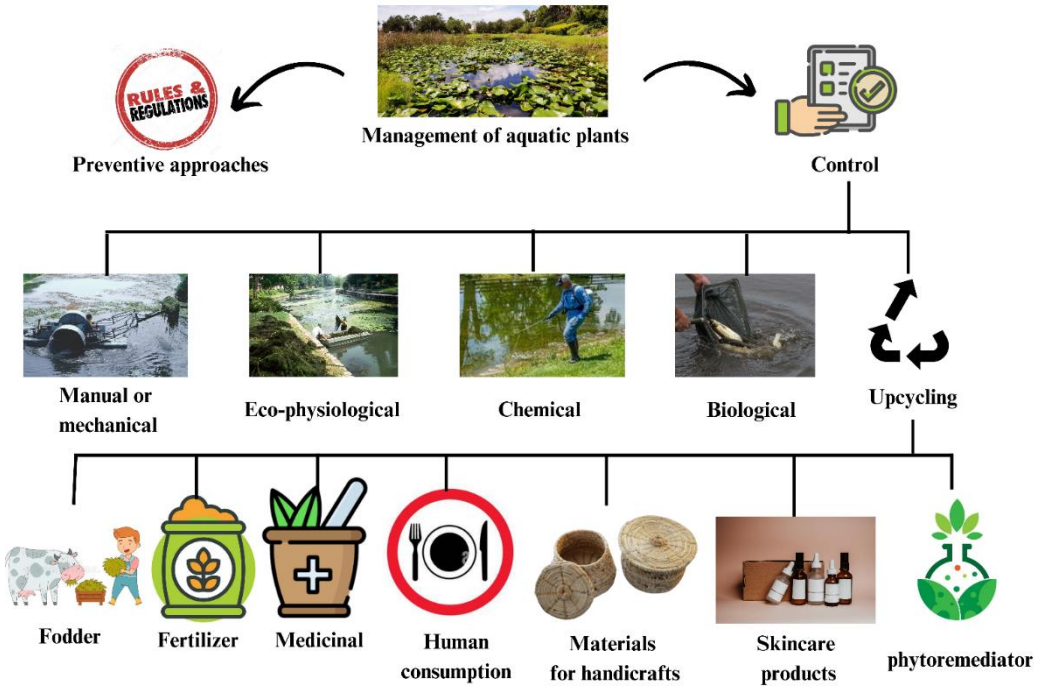

Figure 9. Schematic diagram of management of aquatic plants focusing on potential uses

Traditionally, 21 aquatic macrophyte species serve medicinal purposes for treating fever, jaundice, cough, wounds, snake bites, and food poisoning, administered raw, cooked, mashed, or liquefied. *Nymphaea nouchali* and *N. rubra* (Shapla) are consumed cooked or fried, while *A. philoxiroides* and *Centella asiatica* are prepared as vegetables. *Colocasia esculenta* is consumed fried/mashed, and *Nelumbo nucifera* seeds provide dietary protein. Several species (*Pistia stratiotes*, *Azolla pinnata*, *Spirodela polyrhiza*, *Hygroryza aristata*) serve as animal/fish feed, whereas *Pontederia crassipes* and *Schoenoplectiella mucronata* are crafted into mats, bags, boxes, and ropes. Agricultural applications include organic fertilizers (*P. stratiotes*, *Hydrilla verticillata*), floating beds (*A. pinnata*, *P. stratiotes*), and ornamental uses (*N. rubra*, *N. nucifera*).

4. DISCUSSION

This study documented 27 aquatic plant species in PB, fewer than the 32 recorded in GB. Other studies in Bangladesh, Rashid et al. (2014) documented 77 species (23 families) in the northwestern region, while Hossain et al. (2024) recorded 47 species (25 families) in the southeastern region, which supports the findings. However, Hasan et al. (2021) reported 23 species (15 families) in southwestern Bangladesh. There is not much data regarding the diversity and variation of aquatic plants in Bangladesh to compare. The observed variations are likely due to geographical differences, including soil composition, flood elevation, and hydrology (Rahaman et al., 2019; Wantzen and Junk, 2000).

Alismatales and Poales were the dominant orders in both wetlands, which is similar to the findings in southeastern Bangladesh (Hossain et al., 2024). Sultana et al. (2021) mentioned 50% emergent plant occurrence which is lower than our findings. The study highlighted the peak abundance during the rainy season. The observation is consistent with the result reported by Chowdhury and Ahmed (2012). Many plants were in the rare category, which is supported by the findings of Ame et al. (2022). Additionally, 72% of plants in GB and 74% in PB are classified as LC. A similar result has been recorded by Ashrafuzzaman et al. (2023), where 67.14% of plants were LC. In both ecosystems, about 25% plants are in the NE category, underscoring the necessity of studying the diversity and conservation status, focusing on the management of aquatic plants in Bangladesh. This study is the first of its kind and will form the baseline of future studies.

Effective invasive plant management requires either prevention, which demands comprehensive knowledge, or control, which often involves resource-intensive methods such as mechanical, chemical, or biological measures that lack scalability. Although eco-physiological approaches like habitat manipulation or allelopathy are promising (Gross, 2003; Inderjit and Duke, 2003), their implementation remains complex. As a result, current practices are predominantly manual. Upcycling could provide a sustainable alternative, generating both economic and ecological benefits. Upcycling aquatic plants means transforming undesired plant biomass into products like human food, fertilizer, therapeutics, cosmetics, handicraft materials, and phytoremediators, and thus contributes to renewable energy, sustainable agriculture, and water management (Ezzariai et al., 2021; Ansari et al., 2020; Mustafa and Hayder, 2021). Furthermore, the integration of these approaches into community-based management shifts invasive control towards proactive strategies, enhancing ecosystem health and local economic growth (Newaz and Rahman, 2019).

Among 38 aquatic plants studied, five are edible for humans with edible seeds, rhizomes, leaves, and petals. These are *Nymphaea nouchali*, *Nymphaea rubra*, *Colocasia esculenta*, *Alternanthera philoxeroides*, and *Nelumbo nucifera*, (Conard, 1905; Nahar et al., 2022; Jane et al., 1992; Temesgen and Retta, 2015). *Azolla pinnata*, *Colocasia esculenta*, *Hygroryza aristata*, *Pistia stratiotes*, and *Spirodela polyrhiza* demonstrate suitability as cost-effective feed alternatives for livestock and aquaculture, maintaining production efficiency (Babu et al., 2022; Mathur et al., 2013; Sudaryono, 2006; Fasakin et al., 1999; Ravindran et al., 1996).

The study recorded a total of 24 aquatic plant species that possess significant therapeutic potential. For example, *Pistia stratiotes* and *Enhydra fluctuans* exhibit diuretic and antimicrobial activities, respectively (Ali et al., 2013; Gupta and Prakash, 2014). Anti-cancer, antioxidant, antibacterial, and skin nourishing properties are evident in aquatic plants like *Eclipta prostrata* (Feng et al., 2019; Zhu, 2016), *Spirodela polyrhiza* (Lee et al., 2016), and *Marsilea quadrifolia* (Ripa et al., 2009). Several species displayed anti-diabetic (*Nymphaea rubra*, *Nymphaea pulescens*, *Nelumbo nucifera*) and anti-inflammatory (*Colocasia esculenta*, *Lindernia antipoda*) effects (Angadi et al., 2013; Ishrat et al., 2024; Phulera et al., 2014; Kaur et al., 2019; Sahare et al., 2023; Prajapati et al., 2011). Furthermore, hepatoprotection by *Centella asiatica* (Roy et al., 2013), antiparasitic action by *Cyperus rotundus* and *Polygonum glabrum* (Peerzada et al., 2015; Muddathir et al., 1987), and neuroprotection by *Ipomoea fistulosa* (Phulera et al., 2014) were evident. *Hydrocotyle sibthorpioides* exhibits anti-hepatitis-B activities (Huang et al., 2013).

Aquatic plants demonstrate other applications across multiple sectors. *Pontederia crassipes* offers sustainable alternatives for plastic-reducing handicrafts (Sierra-Carmona et al., 2022), while *Nymphaea rubra* and *Centella asiatica* hold cosmetic potential (Kamma et al., 2019; Hoque et al., 2023). Several species, including *Azolla pinnata*, *Hydrilla verticillata*, *Spirodela polyrhiza*, *Marsilea quadrifolia*, *Phragmites karka*, and *Ceratophyllum demersum*, effectively remove heavy metals (Jangwattana and Iwai, 2010; Ahmed et al., 2018;

Rahman et al., 2007; Rai, 2021; Singh et al., 2022; Qadri et al., 2022), with *Vallisneria spiralis* and *Leersia hexandra* aiding broader environmental remediation (Chen et al., 2022; Han et al., 2020). Beyond these uses, *Azolla pinnata* functions as a bioinsecticide (Ravi et al., 2020), *Hydrilla verticillata* enhances biogas production (Jain and Kalamdhad, 2018), *Colocasia esculenta* provides plastic alternatives (Briones et al., 2020), and *Scirpus grossus* mitigates noise pollution (Suhaeri et al., 2024).

Local communities of both Beels play a vital role in utilizing and managing aquatic plants, similar to global practices where wetlands provide essential resources for livelihood (FAO, 2019; Campos-Silva and Peres, 2016, Khan et al., 2022). The multiple uses of these plants, covering food security, traditional medicine and income generation, pave the way for achieving sustainability (Prasad et al., 2008; Wiart, 2017; World Bank, 2016) but are hindered by a lack of awareness, market access, and management (Gettys et al., 2014; King et al., 2021). Addressing the challenges, aligning with conservation strategies and collaboration among stakeholders will be key to ensuring sustainability in both ecological and economic aspects in the long run (FAO, 2019; King et al., 2021).

The study perfectly aligns with international conservation frameworks and strongly supports the Ramsar Convention (1971) and the Sustainable Development Goals (SDGs) 6, 13, 14, and 15 (UN, 2015), thus escalating the integrity of the ecosystem and sustainable use of the resources in changing climates. However, the lack of preventative measures against invasive species highlights the critical need for the enhancement of control mechanisms in Bangladesh, which will also support the aims of the Global Invasive Species Programme (GISP) (Meyerson et al., 2022). These findings promote eco-physiological approaches, upcycling invasive biomass, and community-based management for long-term wetland sustainability and resource management.

5. CONCLUSION

Despite their label as “aquatic weeds,” it is essential to recognize the significance of native and beneficial aquatic flora. Although Bangladesh is rich in aquatic plants, regional data on these species remains limited. The diversity, origin, and conservation status of aquatic plants in northwest and southwest Bangladesh have been stated in this study. The study emphasized upcycling aquatic plants over eradication. Shifts in these plant communities indicate ecological changes and pollution impacts, making accurate species identification key for management. Despite moderate biodiversity, invasive species remain a major threat due to weak prevention. Future strategies should combine invasive species control with upcycling to boost ecosystem resilience and human benefits. Effective conservation depends on community involvement, policies aligned with global standards, and focused research on wetland and aquatic plant management.

ACKNOWLEDGEMENTS

The authors would like to acknowledge local people for their assistance during data collection.

AUTHOR CONTRIBUTIONS

Conceptualization and Methodology, Md. Foysul Hossain; Formal Analysis, Md. Foysul Hossain, Koushik Chakroborty; Data Curation, Md. Foysul Hossain, Sumiya Bhuyain, Abrar Hossain, Mst. Mosfeka Khatun Ritu; Writing-Original Draft Preparation, Md. Foysul Hossain, Koushik Chakroborty, Gazlima Chowdhury, Writing-Review and Editing, Md. Foysul Hossain, Koushik Chakroborty, Gazlima Chowdhury, Roksana Jahan.

DECLARATION OF CONFLICT OF INTEREST

The authors declare no conflict of interest.

REFERENCES

Acevedo-Rodríguez P, Strong MT. Catalogue of Seed Plants of the West Indies. Washington, D.C.: Smithsonian Institution; 2012.

Acharya J, Banerjee D, Mukherjee A. A contribution to the study of *Commelinaceae* R.Br. in Darjeeling - Sikkim Himalayas. Pleione 2009;3(1):18-27.

Ahmed ZF, Ameer QAA, Abbas RF. Release cumulative power between (*Ceratophyllum demersum* L) and) *Hydrilla verticillata* (plant to Phytoremediation lead in the polluted water aquatic ecosystem. Journal of the College of Basic Education 2018;24(101):79-91.

Ahmed ZU, Hassan MA, Begum ZNT, Khondker M, Kabir SMH, Ahmad M, et al. Encyclopedia of Flora and Fauna of Bangladesh, Volume 6: Angiosperms: Dicotyledons Acanthaceae-Asteraceae. Dhaka: Asiatic Society of Bangladesh; 2008. p. 1-408.

Ali R, Billah M, Hassan M, Dewan SMR. *Enhydra fluctuans* Lour: A review. Research Journal of Pharmacy and Technology 2013;6(9):927-9.

Aloo P, Ojwang W, Omondi R, Njiru JM, Oyugi D. A review of the impacts of invasive aquatic weeds on the biodiversity of some tropical water bodies with special reference to Lake Victoria (Kenya). Biodiversity Journal 2013;4(4):471-82.

Ame MA, Khatun L, Khatun S, Sumona SA, Rahman AM. Investigation of aquatic vascular flora at Sadullapur Upazila of Gaibandha District, Bangladesh. GSC Biological and Pharmaceutical Sciences 2022;21(1):175-87.

Angadi KK, Kandru A, Rahaman A. Antihyperglycaemic, antihyperlipidaemic and antioxidant assays (in vivo) of *Nymphaea pubescens* leaf extract. International Journal of Pharma and Bio Science 2013;4(2):624-30.

Ansari AA, Naeem M, Gill SS, AlZuaibr FM. Phytoremediation of contaminated waters: An eco-friendly technology based on aquatic macrophytes application. The Egyptian Journal of Aquatic Research 2020;46(4):371-6.

Ashrafuzzaman M, Jone MJH, Ashraf SB. Aquatic plants of Bangladesh agricultural University botanical Garden: Species diversity and potential uses. Indian Journal of Ecology 2023;50(3):555-65.

Babu AS, Krishna CR, Kumari NN. Estimation of fodder quality and digestibility parameters of *Pistia stratiotes* plant meal. Journal of Krishi Vigyan 2022;10(2):137-40.

Banglapedia. The Asiatic Society of Bangladesh [Internet]. 2012 [cited 2024 Sep 14]. Available from: https://en.banglapedia.org/index.php/Beel.

Bao Q, Liu Z, Zhao M, Hu Y, Li D, Han C, et al. Role of carbon and nutrient exports from different land uses in the aquatic carbon sequestration and eutrophication process. Science of the Total Environment 2022;813:Article No. 151917.

Basar MH, Rahman AHMM. Aquatic vascular flora at Sadar Upazila of Chapai Nawabganj District, Bangladesh. Discovery 2023;59:e17d1019.

Bangladesh Meteorological Department (BMD). Temperature data [Internet]. 2012 [cited 2024 Sep 14]. Available from: https://live6.bmd.gov.bd/p/Temperature-Data.

Briones MF, Jazmin PF, Pajarillaga BE, Juvinal JG, Leon AA, Rustia JM, et al. Biodegradable film from wild taro *Colocasia esculenta* (L.) Schott starch. Agricultural Engineering International: CIGR Journal 2020;22(1):152-5.

Campos-Silva JV, Peres CA. Community-based management induces rapid recovery of a high-value tropical freshwater fishery. Scientific Reports 2016;6(1):Article No. 34745.

Chambers PA, Lacoul P, Murphy KJ, Thomaz SM. Global diversity of aquatic macrophytes in freshwater. Hydrobiologia 2008;595(1):9-26.

Chen M, Zhang X, Jiang P, Liu J, You S, Lv Y. Advances in heavy metals detoxification, tolerance, accumulation mechanisms, and properties enhancement of *Leersia hexandra* Swartz. Journal of Plant Interactions 2022;17(1):766-78.

Cherwoo L, Berwal B, Kumar S, Datta A, Prabhu GN, Oo HN, et al. Water hyacinth biomass valorization: fostering biodiversity and sustainable development in the bioeconomy. In: Biodiversity and Bioeconomy: Status Quo, Challenges, and Opportunities. Elsevier Inc; 2024. p. 445-74.

Chowdhury AH, Ahmed R. Water, sediment and macrophyte quality of some shrimp culture ponds and freshwater ecosystems of Koyra. Bangladesh Journal of Botany 2012;41(1):35-41.

Conard HS. The Waterlilies: A Monograph of the Genus *Nymphaea.* Washington, DC: Carnegie Institution of Washington; 1905. p. 243-63.

Dudgeon D, Arthington AH, Gessner MO, Kawabata ZI, Knowler DJ, Lévêque C, et al. Freshwater biodiversity: Importance, threats, status and conservation challenges. Biological Reviews 2006;81(2):163-82.

Engelhardt KA, Ritchie ME. Effects of macrophyte species richness on wetland ecosystem functioning and services. Nature 2001;411(6838):687-9.

Ezzariai A, Hafidi M, Ben Bakrim W, Kibret M, Karouach F, Sobeh M, et al. Identifying advanced biotechnologies to generate biofertilizers and biofuels from the world's worst aquatic weed. Frontiers in Bioengineering and Biotechnology 2021;9:Article No. 769366.

Fasakin EA, Balogun AM, Fasuru BE. Use of duckweed, *Spirodela polyrrhiza* L. Schleiden, as a protein feedstuff in practical diets for tilapia, *Oreochromis niloticus* L. Aquaculture Research 1999; 30(5):313-8.

Feng L, Zhai YY, Xu J, Yao WF, Cao YD, Cheng FF, et al. A review on traditional uses, phytochemistry and pharmacology of *Eclipta prostrata* (L.) L. Journal of Ethnopharmacology 2019;245:Article No.112109.

Food and Agricultural Organization of the United Nations (FAO). The State of the World's Biodiversity for Food and Agriculture. Rome, Italy: FAO Commission on Genetic Resources for Food and Agriculture Assessments; 2019.

Gettys LA, Haller WT, Petty DG. Biology and Control of Aquatic Plants: A Best Management Practices Handbook. 4th ed. Marietta, GA, USA: Aquatic Ecosystem Restoration Foundation; 2014. p. 214.

Giri A. Various types of aquatic weeds in a village fish pond and their control. International Journal of Environmental Sciences and Natural Resources 2020;25(3):142-6.

Groom QJ, Van der Straeten J, Hoste I. The origin of *Oxalis corniculata* L. Peer J 2019;7:e6384.

Gross EM. Allelopathy of aquatic autotrophs. Critical Reviews in Plant Sciences 2003;22(3-4):313-39.

Gupta C, Prakash D. Phytonutrients as therapeutic agents. Journal of Complementary and Integrative Medicine 2014;11(3):151-69.

Han F, Zhang Y, Liu Z, Wang C, Luo J, Liu B, et al. Effects of maifanite on growth, physiological and phytochemical process of submerged macrophytes *Vallisneria spiralis.* Ecotoxicology and Environmental Safety 2020;189:Article No. 109941.

Hasan MM, Islam MT, Laskar MA, Sultana T. Distribution and diversity of aquatic macrophytes and the assessment of physico-chemical parameters of Dakatia Beel in Khulna district, Bangladesh. Asian Journal of Medical and Biological Research 2021;7(2):118-25.

Hoque M, Rafi IK, Hossain MS. *Centella asiatica*: A mini review of its medicinal properties and different uses. World Journal of Advanced Research and Reviews 2023;19(2):1185-91.

Hossain MF, Chowdhury G, Nabil TA, Hossain A, Bhuyain S, Mithi MMF, et al. Diversity, abundance, and seasonal variation of aquatic macrophytes in Southeastern Bangladesh. Asian Journal of Fisheries and Aquatic Research 2024;26:55-66.

Huang Q, Zhang S, Huang R, Wei L, Chen Y, Lv S, et al. Isolation and identification of an anti-hepatitis B virus compound from *Hydrocotyle sibthorpioides* Lam. Journal of Ethno-Pharmacology 2013;150(2):568-75.

Inderjit, Duke SO. Ecophysiological aspects of allelopathy. Planta 2003;217:529-39.

Ishrat N, Gupta A, Khan MF, Shahab U, Khan MS, Ahmad N, et al. Phytoconstituents of *Nymphaea rubra* flowers and their anti-diabetic metabolic targets. Fitoterapia 2024;176:Article No. 106014.

Integrated Taxonomic Information System (ITIS). Integrated Taxonomic Information system [Internet]. 2011 [cited 2024 Sep 14]. Available from: https://www.itis.gov/.

International Union for Conservation of Nature (IUCN). The IUCN Red List of Threatened Species [Internet]. 2024 [cited 2024 Sep 14]. Available from: https://www.iucnredlist.org.

Jaccard P. The distribution of the flora in the alpine zone. New Phytologist 1912;11(2):37-50.

Jain MS, Kalamdhad AS. A review on management of *Hydrilla verticillata* and its utilization as potential nitrogen-rich biomass for compost or biogas production. Bioresource Technology Reports 2018;1:69-78.

Jane J, Shen L, Chen J, Lim S, Kasemsuwan T, Nip W. Physical and chemical studies of taro starches and flours. Cereal Chemistry 1992;69(5):528-35.

Jangwattana R, IWAI CB. Using *Azolla pinnata* for wastewater treatment from poultry farm. International Journal of Engineering Research and Development 2010;1(2): Article No. 23.

Journey WK, Skillicorn P, Spira W. Duckweed Aquaculture: A New Aquatic Farming System for Developing Countries. Washington DC: The World Bank; 1993.

Kamma M, Lin WC, Lau SC, Chansakaow S, Leelapornpisid P. Anti-aging cosmeceutical product containing of *Nymphaea rubra* Roxb. ex Andrews Extract. Chiang Mai Journal of Science 2019;46:1143-60.

Kaur P, Kaur L, Kaur N, Singh A, Kaur J, Kaur H, et al. A brief review on pharmaceutical uses of *Nelumbo nucifera*. Journal of Pharmacognosy and Phytochemistry 2019;8(3):3966-72.

Kevin MK, Lancar ML. Aquatic Weeds and Their Management. India: International Commission on Irrigation and Drainage; 2002. p. 15-64.

Khan MHI, Ahsan SMM, Fatema MK, Iqbal SMS, Molla MHR, Gabr MH, et al. Institutionalizing the community-based management approach for natural wetlands toward the exploring policy gaps. Egyptian Journal of Aquatic Biology and Fisheries 2022;26(6):439-65.

King SL, Laubhan MK, Tashjian P, Vradenburg J, Fredrickson L. Wetland conservation: Challenges related to water law and farm policy. Wetlands 2021;41(5):Article No. 54.

Lacoul P, Freedman B. Environmental influences on aquatic plants in freshwater ecosystems. Environmental Reviews 2006; 14(2):89-136.

Lee HJ, Kim MH, Choi YY, Kim EH, Hong J, Kim K, et al. Improvement of atopic dermatitis with topical application of *Spirodela polyrhiza*. Journal of Ethnopharmacology 2016; 180:12-7.

Madsen JD, Wersal RM. A review of aquatic plant monitoring and assessment methods. Journal of Aquatic Plant Management 2017;55(1):1-2.

Maltby E. The Changing wetland paradigm. In: Maltby E, Barker T, editors. The Wetlands Handbook. John Wiley and Sons, Inc.; 2009.

Mathur GN, Sharma R, Choudhary PC. Use of Azolla (*Azolla pinnata*) as cattle feed supplement. Journal of Krishi Vigyan 2013;2(1):73-5.

McKinley DC, Miller-Rushing AJ, Ballard HL, Bonney R, Brown H, Cook-Patton SC, et al. Citizen science can improve conservation science, natural resource management, and environmental protection. Biological Conservation 2017;208:15-28.

Meyerson LA, Pauchard A, Brundu G, Carlton JT, Hierro JL, Kueffer C, et al. Moving toward global strategies for managing invasive alien species. In: Global Plant Invasions. Cham: Springer International Publishing; 2022. p. 331-60.

Muddathir AK, Balansard G, Timon-David P, Babadjamian A, Yagoub AK, Julien MJ. Anthelmintic properties of *Polygonum glabrum*. Journal of Pharmacy and Pharmacology 1987; 39(4):296-300.

Mustafa HM, Hayder G. Recent studies on applications of aquatic weed plants in phytoremediation of wastewater: A review article. Ain Shams Engineering Journal 2021;12(1):355-65.

Nahar L, Nath S, Sarker SD. "Malancha" [*Alternanthera philoxeroides* (Mart.) Griseb.]: A potential therapeutic option against viral diseases. Biomolecules 2022;12(4): Article No. 582.

Newaz MW, Rahman S. Wetland resource governance in Bangladesh: An analysis of community-based co-management approach. Environmental Development 2019;32:Article No. 100446.

Pasha MK, Uddin SB. Dictionary of Plant Names of Bangladesh (Vascular Plants). Chittagong, Dhaka, Bangladesh: Janokalyan Prokashani; 2013. p. 1-434.

Paul P. Aquatic plant diversity of ponds in Thrissur District, Kerala, India. Indian Journal of Ecology 2022;49(1):174-7.

Peerzada AM, Ali HH, Naeem M, Latif M, Bukhari AH, Tanveer A. *Cyperus rotundus* L.: Traditional uses, phytochemistry, and pharmacological activities. Journal of Ethnopharmacology 2015;174:540-60.

Phulera S, Gurung N, Arora KM, Kumar G, Karthik L, Rao KV. Evaluation of phytochemical composition, antioxidant and cytotoxic activity of *Ipomoea fistulosa* leaves (*Convolvulaceae*). Research Journal of Pharmacy and Technology 2014;7(4):454-9.

Prajapati R, Kalariya M, Umbarkar R, Parmar S, Sheth N. *Colocasia esculenta*: A potent indigenous plant. International Journal of Nutrition, Pharmacology, Neurological Diseases 2011;1(2):90-6.

Prasad KN, Shivamurthy GR, Aradhya SM. *Ipomoea aquatica*, an underutilized green leafy vegetable: A review. International Journal of Botany 2008;4(1):123-9.

Qadri H, Uqab B, Javeed O, Dar GH, Bhat RA. *Ceratophyllum demersum*: An accretion biotool for heavy metal remediation. Science of the Total Environment 2022;806:Article No.150548.

Rahaman MA, Rahman MM, Hossain MS. Climate-resilient agricultural practices in different agro-ecological zones of Bangladesh. In: Filho WL, editor. Handbook of Climate Change Resilience. Cham: Springer; 2019. p. 1-27.

Rahman MA, Hasegawa H, Ueda K, Maki T, Okumura C, Rahman MM. Arsenic accumulation in duckweed (*Spirodela polyrhiza* L.): A good option for phytoremediation. Chemosphere 2007;69(3):493-9.

Rahman MA, Sultana MA, Islam MA, Hossain MY. Stock assessment of barred spiny eel, *Macrognathus pancalus* (Hamilton, 1822) in a wetland ecosystem, northwestern Bangladesh: A fundamental approach to ensure sustainability and conservation. Heliyon 2024;10(5):e26492.

Rai PK. Heavy metals and arsenic phytoremediation potential of invasive alien wetland plants *Phragmites karka* and *Arundo donax*: Water-Energy-Food (WEF) Nexus linked sustainability implications. Bioresource Technology Reports 2021;15:Article No. 100741.

Ramsar Convention. The Ramsar Convention on Wetlands. Iran: Ramsar; 1971.

Rashid MA, Naz S, Zaman M, Hasan M, Sarkar MAQ. Hydrobiological studies of the Chalan Beel Wetland in

Bangladesh. Plant Environment Development 2014;3(1): 35-41.

Ravi R, Rajendran D, Oh WD, Mat Rasat MS, Hamzah Z, Ishak IH, et al. The potential use of *Azolla pinnata* as an alternative bio-insecticide. Scientific Reports 2020;10(1):Article No. 19245.

Ravindran V, Sivakanesan R, Cyril HW. Nutritive value of raw and processed colocasia (*Colocasia esculenta)* corn meal for poultry. Animal Feed Science and Technology 1996; 57(4):335-45.

Ripa FA, Nahar L, Haque M, Islam MM. Antibacterial, cytotoxic and antioxidant activity of crude extract of *Marsilea quadrifolia*. European Journal of Scientific Research 2009;33(1):123-9.

Roy DC, Barman SK, Shaik MM. Current updates on *Centella asiatica*: Phytochemistry, pharmacology and traditional uses. Medicinal Plant Research 2013;3(4):20-36.

Sahare AY, Chavhan BK, Dhoke PS, Agrawal TR. Phytochemical investigation and evaluation of antioxidant, and anti-inflamatory activity of aerial parts of *Lindernia antipoda*. Rasayan Journal of Chemistry 2023;16(1):284-9.

Schuyt KD. Economic consequences of wetland degradation for local populations in Africa. Ecological Economics 2005;53(2):177-90.

Sierra-Carmona CG, Hernández-Orduña MG, Murrieta-Galindo R. Alternative uses of water Hyacinth (*Pontederia crassipes*) from a sustainable perspective: A systematic literature review. Sustainability 2022;14(7):Article No. 3931.

Singh S, Karwadiya J, Srivastava S, Patra PK, Venugopalan VP. Potential of indigenous plant species for phytoremediation of arsenic contaminated water and soil. Ecological Engineering 2022;175:Article No. 106476.

Sonal D, Jagruti R, Geeta P. Avifaunal diversity and water quality analysis of an inland wetland. Journal of Wetlands Ecology 2010;4:1-32.

Sorensen T. A method of establishing groups of equal amplitude in plant sociology based on similarity of species content and its application to analyses of the vegetation on Danish commons. Biologiske Skrifter 1948;5:1-34.

Sosa A, Greizerstein E, Cardo MV, Telesnick MC, Julien MH. The evolutionary history of an invasive species: Alligator weed, *Alternanthera philoxeroides*. In: Julien MH, Sforza R, Bon MC, Evans HC, Hatcher PE, Hinz HL, et al, editors. Proceedings of the XII International Symposium on Biological Control of Weeds: CAB International United Kingdom; 2008. p. 443-50.

Sudaryono A. Use of Azolla *(Azolla pinnata*) meal as a substitute for defatted soybean meal in diets of juvenile black tiger shrimp (*Penaeus monodon*). Journal of Coastal Development 2006;9(3):145-54.

Suhaeri S, Fulazzaky MA, Husaini H, Dirhamsyah M, Hasanuddin I. Application of *Scirpus grossus* fiber as a sound absorber. Heliyon 2024;10(7):e28961.

Sultana T, Islam MT, Hasan MM, Laskar MA. Survey on aquatic macrophytes and physico-chemical quality of water from Satla Beel of Barishal District, Bangladesh. International Journal of Fisheries and Aquatic Studies 2021;9(5):1-5.

Temesgen M, Retta N. Nutritional potential, health and food security benefits of taro *Colocasia esculenta* (L.): A review. Food Science and Quality Management 2015;36(0):23-30.

United Nations (UN). Transforming our world: the 2030 agenda for sustainable development [Internet]. 2015 [cited 2024 Sep 15]. Available from: https://sdgs.un.org/2030agenda.

Wantzen KM, Junk WJ. The importance of stream-wetland-systems for biodiversity: A tropical perspective. In: Gopal B, Junk WJ, DJA, editors. Biodiversity in Wetlands: Assessment, Function and Conservation; Volume 1. Leiden: Backhuys Publishers; 2000. p. 11-34.

Wiart C. Medicinal Plants in Asia for Metabolic Syndrome: Natural Products and Molecular Basis. 1st ed. Boca Raton, FL: CRC Press; 2017. p. 520.

Wilk-Woźniak E, Walusiak E, Burchardt L, Cerbin S, Chmura D, Gąbka M, et al. Effects of the environs of waterbodies on aquatic plants in oxbow lakes (habitat 3150). Ecological Indicators 2019;98:736-42.

Wood KA, O'Hare MT, McDonald C, Searle KR, Daunt F, Stillman RA. Herbivore regulation of plant abundance in aquatic ecosystems. Biological Reviews 2017;92(2):1128-41.

World Bank. Seaweed Aquaculture for Food Security, Income Generation and Environmental Health. Washington, DC: World Bank; 2016.

Zhu F. Chemical composition, health effects, and uses of water caltrop. Trends in Food Science and Technology 2016;49: 136-45.

Environment and Natural Resources Journal

Volume 23
Issue 6
2025

Selective Adsorption of Cationic Dyes by Hydrochar Derived from *Spirogyra* sp. Algae via Temperature-Varying Hydrothermal Carbonization

Muhammad Badaruddin[1], Laila Hanum[3], Elda Melwita[2,5], Sahrul Wibiyan[2,4], Yulizah Hanifah[6], and Aldes Lesbani[2,4*]

[1]*Environmental Science, Postgraduate Program, Universitas Sriwijaya, Palembang, 30139, South Sumatera, Indonesia*
[2]*Materials Science, Graduate School, Universitas Sriwijaya, Palembang, 30139, South Sumatera, Indonesia*
[3]*Biology Department, Faculty of Mathematics and Natural Sciences, Universitas Sriwijaya, Indralaya, 30662, South Sumatera, Indonesia*
[4]*Research Center of Inorganic Materials and Coordination Complexes, Universitas Sriwijaya, Palembang, 30139, South Sumatera, Indonesia*
[5]*Department of Chemical Engineering, Faculty of Engineering, Universitas Sriwijaya, Ogan Ilir, South Sumatera, 30862, Indonesia*
[6]*National Research and Innovation Agency (BRIN), PUSPIPTEK, Tangerang Selatan, 15311, Indonesia*

ARTICLE INFO

Received: 30 May 2025
Received in revised: 30 Jul 2025
Accepted: 6 Aug 2025
Published online: 16 Sep 2025
DOI: 10.32526/ennrj/23/20250138

Keywords:
Hydrothermal carbonization/ *Spirogyra* sp./ Hydrochar/ Cationic dye selectivity/ Regeneration

*** Corresponding author:**
E-mail:
aldeslesbani@pps.unsri.ac.id

GRAPHICAL ABSTRACT

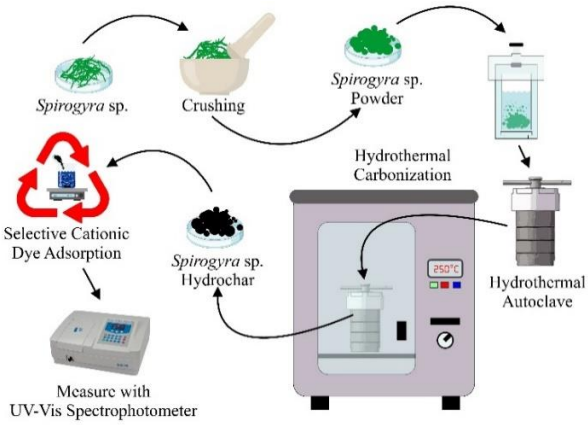

ABSTRACT

This study synthesized hydrochar adsorbents at varying temperatures 150°C (HC150) and 250°C (HC250), using the hydrothermal carbonization (HTC) method from *Spirogyra* sp. (SPG) and characterized them using XRD, FTIR, SEM, and BET analyze. XRD results confirmed a dominant $CaCO_3$ phase (JCPDS 01-086-2334) in all samples, with new peaks and shifts in HC150 and HC250 indicating structural changes from hydrochar formation. FTIR spectra revealed functional groups such as O-H, C=O, C-O, and C-N-S in SPG, with notable reductions in O-H and phenolic signals in HC150 and HC250, suggesting chemical transformations. SEM analysis revealed that SPG exhibits a smooth, sheet-like morphology, while HC150 formed uniform particles and HC250 developed a rough, porous surface, indicating increased carbonization, surface heterogeneity, and enhanced adsorption potential. BET analysis showed a marked increase in surface area and a transition from macroporous to mesoporous structures in HC150 and HC250, enhancing their adsorption capabilities. Adsorbents exhibited selective adsorption toward methylene blue (MB). Surface charge analysis revealed similar pHpzc values slightly below neutral, promoting favorable electrostatic interactions with cationic MB. Adsorption followed pseudo second order (PSO) kinetics compared to pseudo first order (PFO), indicating chemisorption, while isotherm modeling highlighted HC250 strong fit to the Freundlich model. Thermodynamic assessments confirmed HC250 superior performance, exhibiting more negative ΔG, lower ΔH, and higher ΔS values, signifying spontaneous, energy-efficient, and affinity-driven adsorption. Regeneration tests further underscored HC250 stability, with removal efficiency maintaining above 50% after four cycles (90.14% to 53.55%). In comparison, HC150 showed good reusability (80.56% to 51.88%), while SPG declined significantly (56.23% to 50.20%) after two cycles.

HIGHLIGHTS

Hydrochars derived from *Spirogyra* sp. (SPG) were successfully synthesized via hydrothermal carbonization at 150°C (HC150) and 250°C (HC250), and characterized using XRD, FTIR, SEM, and BET. All adsorbents exhibited selective methylene blue (MB) adsorption, with HC250 showing the highest removal efficiency (69.02%) and maximum adsorption capacity (89.29 mg/g). Moreover, HC250 maintained over 50% efficiency after four regeneration cycles, confirming its stability and reusability.

Citation: Badaruddin M, Hanum L, Melwita E, Wibiyan S, Hanifah Y, Lesbani A. Selective adsorption of cationic dyes by hydrochar derived from *Spirogyra* sp. algae via temperature-varying hydrothermal carbonization. Environ. Nat. Resour. J. 2025;23(6):595-611. (https://doi.org/10.32526/ennrj/23/20250138)

1. INTRODUCTION

Water is essential for all living things and life forms; however, its availability is increasingly threatened by limited supply and ever-growing demand (Hamad et al., 2024). Industrial effluents containing synthetic dyes are a considerable environmental challenge (Singh et al., 2024). Synthetic dyes are widely used in various industries, such as chemical, textiles, papermaking, food, printing, plastics, and cosmetics, replacing natural dyes due to their wide availability (Laggoun et al., 2025; Mon et al., 2023; Shi et al., 2022). The waste generated has the potential to pollute the environment (Cui et al., 2025; Ullah et al., 2022). Wastes containing toxic dyes can enter the food chain, increase the risk of health problems in living organisms, are both toxic and carcinogenic, and can form toxic compounds that harm aquatic flora and fauna, negatively impacting human health, such as the risk of mutagenesis, allergies, and cancer (Doondani et al., 2024; Ahmad et al., 2025; Sornaly et al., 2024). Its complex chemical structure makes it highly physically, chemically, thermally, and optically stable, making it difficult to degrade by chemicals, microbial enzymes, oxidizing agents, or heating, causing difficulties in textile industry wastewater treatment (Kumar et al., 2021). Coagulation (Ren et al., 2022), filtration (Norrahma et al., 2023), phytoremediation (Wibowo et al., 2023), electrochemical degradation (Ganash et al., 2024), photodegradation (Kala et al., 2024), and adsorption (Wang et al., 2024) are some methods for reducing the pollution caused by the dye. Adsorption is frequently employed because it is thought to have benefits such as high effectiveness, ease of use, low cost, and environmental safety (Lesbani et al., 2024; Umesh et al., 2024).

Activated carbon was employed as a dye adsorbent in earlier research. However, because it uses bases or acids to activate the adsorption active sites, which may affect the environment, activated carbon has a less environmentally friendly process (Neme et al., 2022). Accordingly, recent research has focused on cost-effective and eco-friendly biomass adsorbent technologies including hydrothermal carbonization (HTC) (Badaruddin et al., 2025). One of the best thermochemical methods for treating biomass with a high moisture content is hydrothermal carbonization. In order to transform the biomass into a solid that is rich in carbon namely hydrochar, the method involves thermally breaking down natural feedstock biomass in an aqueous medium at mild conditions to induce dehydration and decarboxylation processes (Spagnuolo et al., 2023).

Hydrochar is an effective and economical adsorbent for dyes due to its highgly porous structure. In addition, hydrochar is porous, eco-friendly, affordable, and rich in functional groups (González-Fernández et al., 2024; Le et al., 2025; Normah et al., 2022). Previous studies using rambutan peel (Normah et al., 2021), longan fruit (Palapa et al., 2023), and algae (Arora et al., 2024) have identified potential sources of raw materials that can be be converted into hydrochar, which is a more valuable product used in various applications such as dye adsorbent. Algae are effective adsorbents for dyestuffs because the hydrochar produced has a high adsorption capacity without the need for additional activation and its hydrothermal process synthesis is environmentally friendly. The nitrogen groups in the hydrochar also strengthen the bond with the adsorbate, making it an efficient and sustainable solution for dye wastewater treatment (Spagnuolo et al., 2023). According to previous research by (Badaruddin et al., 2025), hydrochar algae *Spirogyra* sp. has a greater adsorption capacity than its raw form which amounts to 34.96 mg/g to 99.01 mg/g when used to adsorbed malachite green dye. Research by (Wijaya et al., 2025), using *Spirogyra* sp. algae which used the anionic dye remazol red as an adsorbate showed the maximum capacity of NiCr-LDH composited with *Spirogyra* sp. algae increased from 11.976 mg/g to 47.170 mg/g.

Spirogyra sp. is a green algae with high potential as a cationic dye adsorbent. These algae were chosen due to their abundant availability, low cost, and high carbohydrate content as a carbon source. Algae *Spirogyra* sp. has been a topic of several studies due to its variety of applications. *Spirogyra* sp. cell wall is composed of several layers that contain various polysaccharides, including cellulose, pectin, and algaenan. Pectin, particularly low-methylated homogalacturonan, lends flexibility, whereas cellulose gives structure. Durability is increased by algaenan, a heteropolymer that is extremely resistant to acids and bases. The outer layers also contain xyloglucans and arabinogalactans. In combination, these elements support the ductility and resilience of the *Spirogyra* sp. cell wall (Permann et al., 2022). Research has demonstrated that *Spirogyra* sp. algae may be used as bioindicators for the presence of heavy metal contamination (Chand and Vanavana, 2022). *Spirogyra* sp. is effective in adsorbing Cu, Cd, and Pb,

and grows optimally at 20-25°C (Vetrivel et al., 2017). *Spirogyra* sp. contains a carbohydrate content of 55.7±2.4% (range 42.8-62.0%), making it an excellent raw material for hydrochar synthesis (Tipnee et al., 2015). With this ability, the algae has the potential not only as a heavy metal biosorbent, but also as a cationic dye adsorbent in industrial wastewater treatment.

Based on these data, this study used *Spirogyra* sp. algae carbonized into hydrochar by hydrothermal method for selective adsorption of cationic dyes (rhodamine b, malachite green, methylene blue). It is expected to increase the adsorption capacity and structure stability that be used repeatedly and become an environmentally friendly adsorbent.

2. METHODOLOGY

2.1 Chemical and instrumental

Chemicals with analytical reagent purity levels were used in this study as solvents, such as distilled water (H_2O), chemicals such as sodium hydroxide (NaOH, ≥98%, Merck), and hydrochloric acid (HCl, 37% w/w, Sigma-Aldrich). Analytical grade rhodamine b (RB, ≥98%), malachite green (MG, ≥98%), and methylene blue (MB, ≥98%) used in the cationic dye adsorption selectivity tests were purchased from Sigma-Aldrich. The area of Lebung Jangkar Village, Pemulutan Subdistrict, Ogan Ilir Regency, South Sumatra Province, with geographical coordinates of -3.113052°N and 104.786218°E, was the sampling location of algae *Spirogyra* sp.

Analytical tools and common laboratory equipment were used in the experiments. A 100 mL stainless steel hydrothermal autoclave was used for adsorbents synthesis. The *Spirogyra* sp. samples were subjected to a preliminary morphological investigation under a microscope. XRD (Rigaku MiniFlex600) was used to study the crystal structure using Cu-Kα radiation at 2θ = 5° - 80°. FTIR (Shimadzu Prestige-21) was used to identify functional groups in the 4,000-400 cm^{-1} range. SEM (Hitachi SU-3500 & JEOL JSM-IT200, No. BMN) was used to analyze surface morphology and particle size distribution. Using the N_2 adsorption-desorption isotherm at 77 K, BET analysis (Quantachrome NovaWin) was used to calculate the specific surface area, pore size, and volume. A UV-Vis spectrophotometer (EMC-18PC-UV) was used to measure the adsorption efficiency towards the dyes at each dye's distinctive wavelength.

2.2 *Spirogyra* sp. algae pretreatment

After being carefully washed with distilled water, *Spirogyra* sp. algae were examined under a microscope and crushed into small components. The component were crushed and filtered through a 100 mesh sieve after being dried thoroughly in an oven set to 105°C. Following that, XRD, FT-IR, SEM and BET studies were used to analyze the obtained adsorbents (Wibiyan et al., 2024b).

2.3 *Spirogyra* sp. algae carbonization through hydrothermal method

50 mL of distilled water and 2.5 g of *Spirogyra* sp. algae were combined and set in a 100 mL stainless steel hydrothermal autoclave. Following that, the autoclave was heated for 10 h at different temperatures 150°C and 250°C, in the oven. After the heating procedure, the equipment was cooled to room temperature, the adsorbents were washed with distilled water, and dried in an oven at 100°C for 12 h. After being crushed with a mortar and filtered through a 100 mesh sieve, the adsorbents were analyzed with XRD, FT-IR, SEM and BET (Badaruddin et al., 2025; Wibiyan et al., 2023).

2.4 Analysis of the pH of the zero charge point (pHpzc) on the adsorbent

The pHpzc was determined by adding 0.02 g of each adsorbent with 20 mL of 0.1 M NaCl solution that was modified at different pH values from 2 to 11, the pHpzc was determined. A 0.1 M NaOH and HCl solution was used to alter the pH. The mixture was stirred for 24 h, then separated. A pH meter was used to determine the filtrate's final pH, and graphs were used to examine the correlation between the initial and final pH values.

2.5 Selectivity of cationic dye

Rhodamine b, malachite green, and methylene blue cationic dye solutions were made by mixing 10 mL of each dye in a beaker, with concentration values determined at 15 mg/L. during that, the dye mixture was mixed with 0.03 g of adsorbent and allowed to stir for 60 minutes. To measure wavelengths, a UV-visible spectrophotometer was employed. On the selection of cationic dyes. An adsorption efficiency (%) investigation was carried out using Equation 1 to select the selective cationic dyes.

$$\text{Adsorption efficiency (\%)} = \frac{C_0 - C_e}{C_0} \times 100 \quad (1)$$

Where; C_0 represents the initial and C_e represents the remaining concentrations of the dyes mixture in the solution after t minutes of adsorption (mg/L) (Jefri et al., 2025; Wibiyan et al., 2024c).

2.6 Adsorption method

The process of adsorption was carried out by determining variations in pH from 2 to 11, contact time from 0 to 300 min, dye concentration from 30, 40, 50, and 60 mg/L, and temperature from 30, 40, 50, and 60°C was used to optimize the adsorption process. Using a 20 mL methylene blue solution 30 mg/L in variations in pH and 50 mg/L in contact time, the initial concentration was determined using UV-Vis. Before determining the final concentration, 0.02 g of adsorbent was added and stirred for 2 h. HCl and NaOH were used to adjust the pH during the pH variations. Absorbance was measured for time variation at each interval. Utilizing 0.02 g of adsorbent and the ideal contact duration, the effects of temperature and concentration were assessed in a similar manner. To evaluate the adsorption capacity, a mass balance equation was used as shown in Equation 2.

$$q\ (mg/g) = (C_0 - C_e)\frac{V}{m} \quad (2)$$

The dye adsorbed q (mg/g) was calculated from the difference between the initial concentration C_0 (mg/L) and the equilibrium concentration Ce (mg/L), multiplied by the solution volume V (L), and divided by the mass of the adsorbent m (g).

The adsorption kinetics were analyzed using both the pseudo first order and pseudo second order models. The pseudo first order and pseudo second order models are, expressed in Equation 3 and 4.

$$\ln\left(q_e - q_t\right) = \ln q_e - k_1 t \quad (3)$$

$$\frac{t}{q_t} = \frac{1}{k_2 q_e^2} + \frac{t}{q_e} \quad (4)$$

In this equation, q_t (mg/g) is the amount of dye adsorbed at time t (minutes), q_e (mg/g) is the amount adsorbed at equilibrium, and k_1 (1/min) is the rate constant of the first order model and k_2 (g/mg·min) is the rate constant of the pseudo second order model.

Thermodynamic parameters were evaluated to determine the spontaneity and energy changes involved in the adsorption process. The equilibrium constant (KC) was calculated as the ratio of the concentration of adsorbate on the solid phase (CA) to that in the liquid phase (CE), as shown in Equation 5. The Gibbs free energy change ΔG (kJ/mol) was calculated using Equation 6, which incorporates the equilibrium constant (KC), the gas constant R (8.314 J/mol·K), and the temperature T (K). To further determine the enthalpy ΔH (kJ/mol) and entropy changes ΔS (J/mol·K), the van't Hoff equation was applied as shown in Equation 7, where the natural logarithm of KC is plotted against the reciprocal of temperature (1/T).

$$K_C = \frac{C_A}{C_E} \quad (5)$$

$$\Delta G = -RT \ln K_C \quad (6)$$

$$\ln K_C = -\frac{\Delta H}{RT} + \frac{\Delta S}{R} \quad (7)$$

To understand the adsorption equilibrium, both the Langmuir and Freundlich isotherm models were applied. The Langmuir and Freundlich models are described in Equation 8 and 9.

$$\frac{C_e}{q_e} = \frac{1}{K_L q_m} + \frac{C_e}{q_m} \quad (8)$$

$$\ln q_e = \ln K_F + \frac{1}{n}\ln C_e \quad (9)$$

In this model, C_e is the equilibrium concentration, q_e is the amount adsorbed at equilibrium, KL (L/mg) is the Langmuir constant, q_m (mg/g) is the maximum adsorption capacity, KF ((mg/g)(L/mg)$^{(1/n)}$) is the Freundlich constant, and n is the adsorption intensity factor.

2.7 Adsorbent due to regeneration cycles

A beaker was filled with a 20 mL solution of methylene blue dye at a concentration of 50 mg/L, and the pH was adjusted to optimal levels. Subsequently, 0.02 g of adsorbent was added. A magnetic stirrer was used to stir the mixture for 120 min. After that, the adsorbent was separated from the adsorbate. The filtrate, which included the adsorbate, was analyzed for absorbance with a UV-Vis spectrophotometer. The adsorbent was subsequently washed with distilled water and desorbed the assistance of an ultrasonic device. After drying, the adsorbent was prepared and disposed for reuse in the continuing adsorption cycle, using the same method as during the initial adsorption.

3. RESULTS AND DISCUSSION

3.1 Adsorbents characterizat

3.1.1 X-ray diffraction (XRD) characterization analysis

Based on XRD analysis in Figure 1(a), the diffraction patterns of sharp peaks were found and identified in the diffraction patterns of SPG, HC150, and HC250, confirming a good crystalline structure. All of the peaks correspond to JCPDS card 01-086-2334, indicating that calcium carbonate ($CaCO_3$) is the primary phase in all adsorbents. While adsorbents HC150 and HC250 show slight peak shift from 22.99° to 23.28° and the appearance of a new peak at 25.46°, adsorbent SPG shows the main characteristic peaks at 2θ angles of 22.99°, 26.13°, 28.86°, 36.23°, 42.74°, 47.33°, 56.19°, 60.92°, and 65.42. This shows that the hydrochar synthesis procedure generated an insignificant shift in peak site, indicating structural modification or the formation of secondary components, but did not affect the primary crystal structure (Djezzar et al., 2024).

3.1.2 Fourier Transform Infrared (FTIR) spectroscopy characterization analysis

Spirogyra sp. contains polysaccharides such as cellulose, alginic acid, and sulfate, which have ion exchange capabilities and can interact with cationic dye ions through certain functional groups. According to Figure 1(b), *Spirogyra* sp. algae have C-O and C-N-S groups, hydroxyl (O-H), carboxyl (C-H), amine (N-H), and carbonyl (C=O). About 3,400 cm^{-1} (O-H), 2,932 cm^{-1} (C-H), 1,640 cm^{-1} (C=O and COOH), 1,535 cm^{-1} (C-H), 1,020 cm^{-1} (C-O), and 528 cm^{-1} (C-N-S) were identified as the positions of absorption bands (Susanti et al., 2023). Peaks 3,400 cm^{-1}, 2,932 cm^{-1}, 1,640 cm^{-1}, 1,020 cm^{-1}, and 528 cm^{-1} reduced in HC150 and HC250, indicating a decrease in hydroxyl functional groups originating from water content or phenolic N-H groups. This suggests that the process of hydrochar synthesis was successful (Tsarpali et al., 2022).

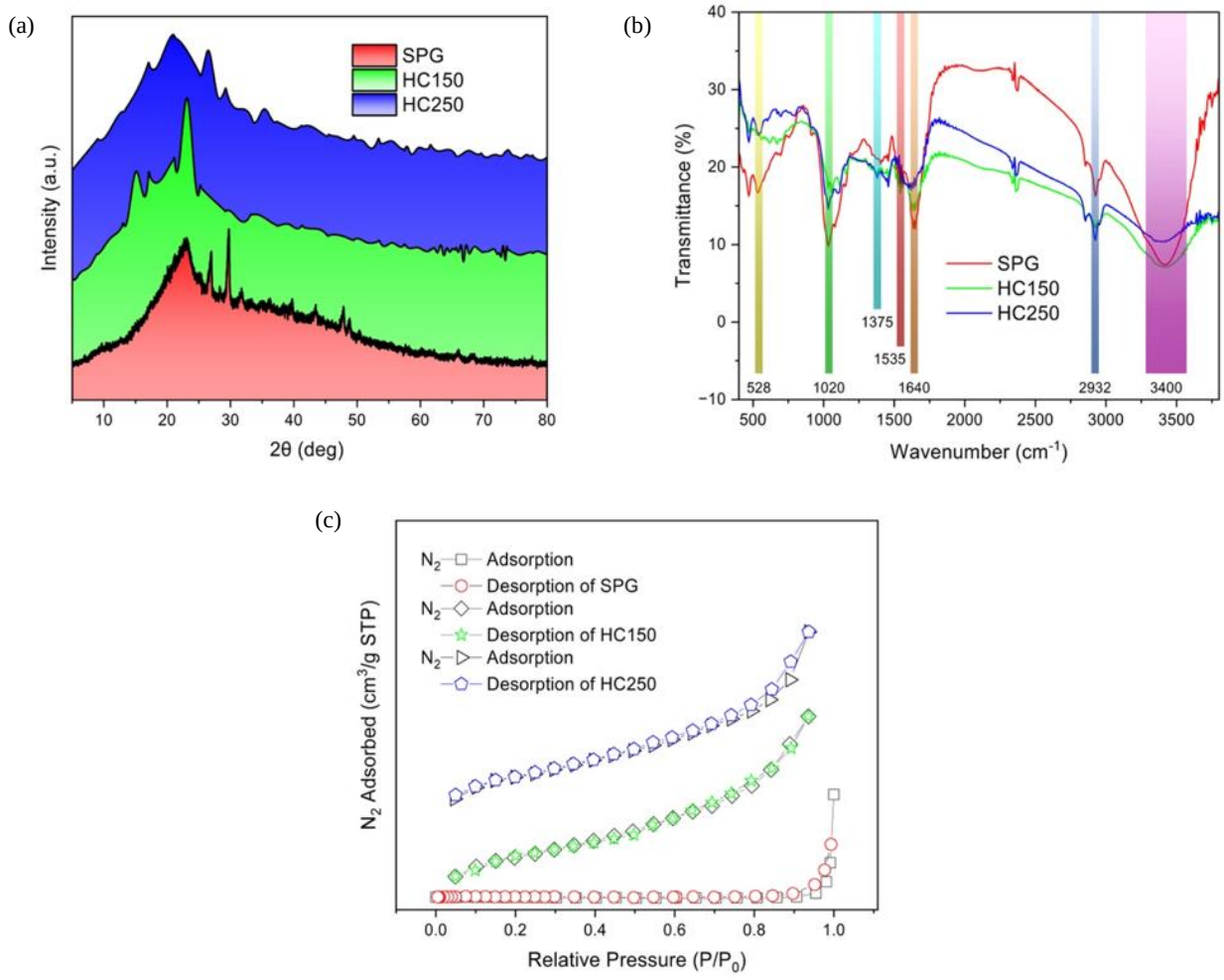

Figure 1. The characterization result of XRD (a), FTIR (b), and BET (c) of SPG, HC150 and HC250

3.1.3 Brunauer-Emmett-Teller (BET) surface area and porosity characterization analysis

The shrinking pore size signifies internal restructuring towards a more stable mesoporous configuration suitable for small molecule diffusion. In the context of cationic dye adsorption, this change is particularly beneficial as the larger surface area provides more active sites, while the meso pore size allows diffusion and sorption of methylene blue dye molecules. In addition, adsorbents usually contain surface oxygen groups (such as carboxyl or hydroxyl) that are able to electrostatically interact with cations (Luo et al., 2023).

BET analysis showed at Table 1 and Figure 1(c) that the surface characteristics and pore structure of *Spirogyra* sp. algae underwent significant changes after undergoing the HTC process at HC150 and HC250. Adsorbent SPG has a very low surface area of 0.2 m^2/g, with a very large average pore size of 87.635 nm and a high pore volume of 2.697 cm^3/g, indicating a large porous structure that is inefficient for small molecule sorption. After HTC treatment, the surface area increased sharply to 5.4 m^2/g in HC150 and 5.5 m^2/g in HC250, with the pore size narrowing to the mesoporous range of about 4.4-4.8 nm and the pore volume decreasing drastically to 0.014-0.015 cm^3/g (Gibson et al., 2019; Li et al., 2024). This increase in surface area resulted from the partial decomposition of biomass and removal of volatile compounds during the HTC process, which opened up the pore structure and formed a more active amorphous carbon surface (Yihunu et al., 2019).

Table 1. Surface area (BET), pore size, and average pore volume of SPG, HC150, and HC250

Adsorbents	Surface area BET (m^2/g)	Pore size average (nm)	Pore volume average (cm^3/g)
SPG	0.2	87.635	2.697
HC150	5.4	4.883	0.014
HC250	5.5	4.438	0.015

3.1.4 Scanning Electron Microscopy (SEM) characterization analysis

The surface morphology characterization of SPG, HC150, and HC250 is shown in Figure 2. SEM reveals that SPG has a smooth, sheet-like structure. This relatively flat surface reflects the natural condition of the biomass before being converted into hydrochar. The absence of large pores or structural irregularities indicates that the surface area of SPG is still limited (Siri-anusornsak et al., 2024). After heat treatment, the morphology of HC150 begins to show significant changes with the formation of relatively uniform, separated particles, indicating the initial decomposition process and the formation of a carbon structure. At higher temperatures, the morphology of HC250 changes drastically into a very rough and irregular surface, with numerous cavities and porous structures spread across the surface. This reflects a higher degree of carbonization and adsorbent decomposition, resulting in increased surface porosity and heterogeneity (Badaruddin et al., 2025).

The particle size distribution analysis of HC150 and HC250 from SEM images, as shown in Figures 2(d) and 2(e), reveals significant differences. HC150 particles exhibit a more uniform distribution with an average size of approximately 4.54 µm and a low standard deviation, reflecting a stable and homogeneous structure. In contrast, although HC250 has an average particle size of 4.13 µm, the particle sizes vary more widely, ranging from 0.669 µm to 14.366 µm, with a higher standard deviation and a median lower than the average, indicating particle fragmentation and agglomeration. HC250 has a broader particle size distribution, suggesting the possible formation of more complex porous structures and a larger surface area. The fragmentation and agglomeration processes occurring at higher temperatures are believed to generate more active sites and pores that contribute to the enhanced adsorption capacity. Meanwhile, HC150, with its more uniform size distribution, indicates a more stable structure but with a relatively lower active surface area compared to HC250. Thus, the increase in heating temperature has a positive effect on the adsorption capability of HC250 by promoting the formation of a more reactive and porous morphology (Li et al., 2023).

3.2 Selective adsorption study of cationic dyes using synthesized adsorbents

Adsorbents SPG, HC150 and HC250 were tested on the selectivity of cationic dyes referring to the ability of the adsorbent to selectively separate

certain dyes from the mixture (Wibiyan et al., 2024a). The cationic dyes mixture in Figure 3 has overlapping wavelengths, which requires spectral deconvolution to figure out the UV-Vis absorption bands. The maximum λ detection accuracy is increased, and overlapping components are successfully identified by using Gaussian fitting (Tones et al., 2020).

Based on the deconvolution curve in Figure 3 and the adsorption efficiency data at Table 2, it can be concluded that all adsorbents used including SPG, HC150, and HC250, have a selective tendency towards MB compared to other cationic dyes. This is indicated by the highest adsorption efficiency of MB adsorption by all adsorbents 39.13% for SPG, 69.29% for HC150, and reached 78.53% for HC250.

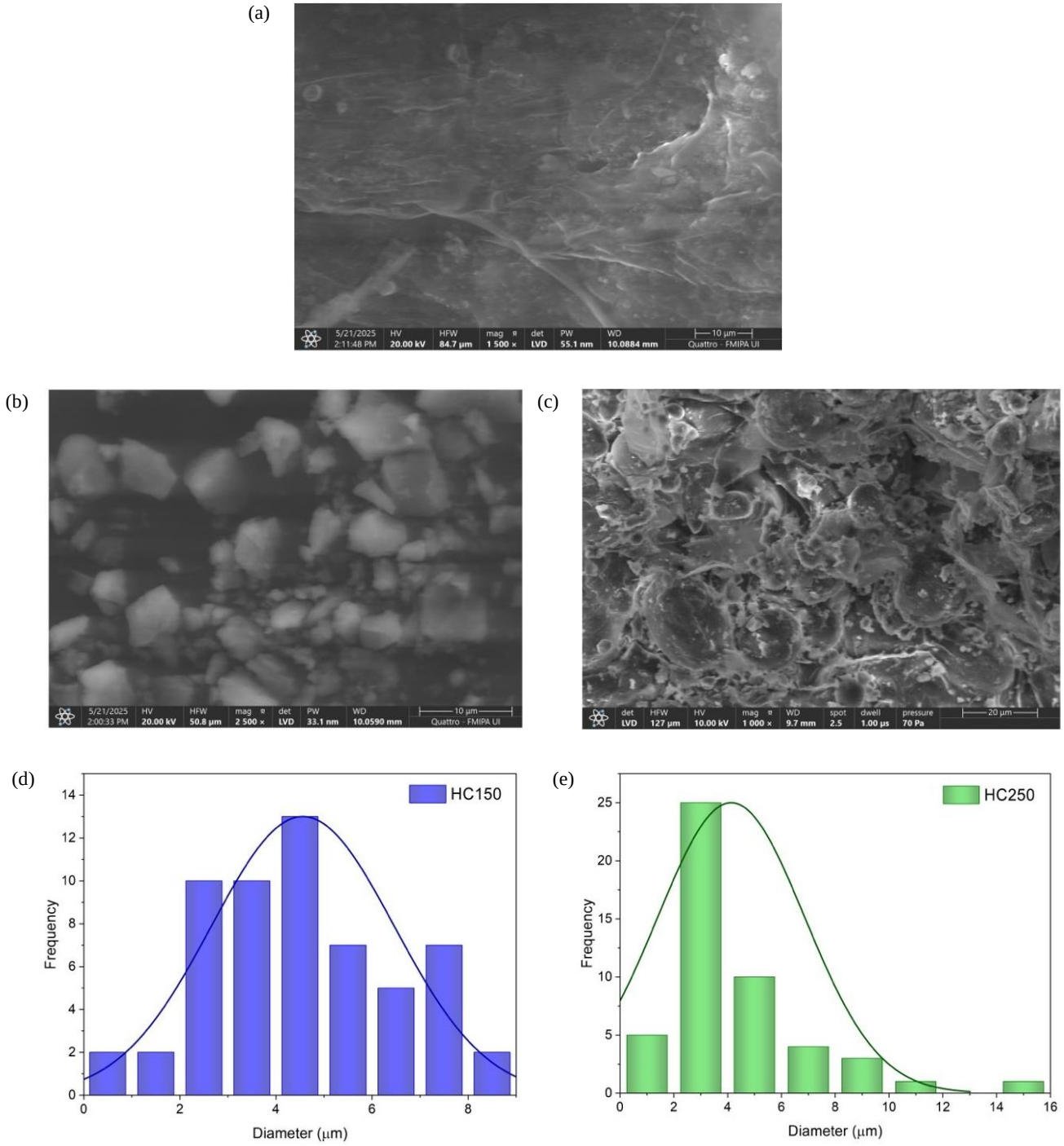

Figure 2. SEM images of SPG (a), HC150 (b), and HC250 (c), with particle distribution graphs of HC150 (d) and HC250 (e)

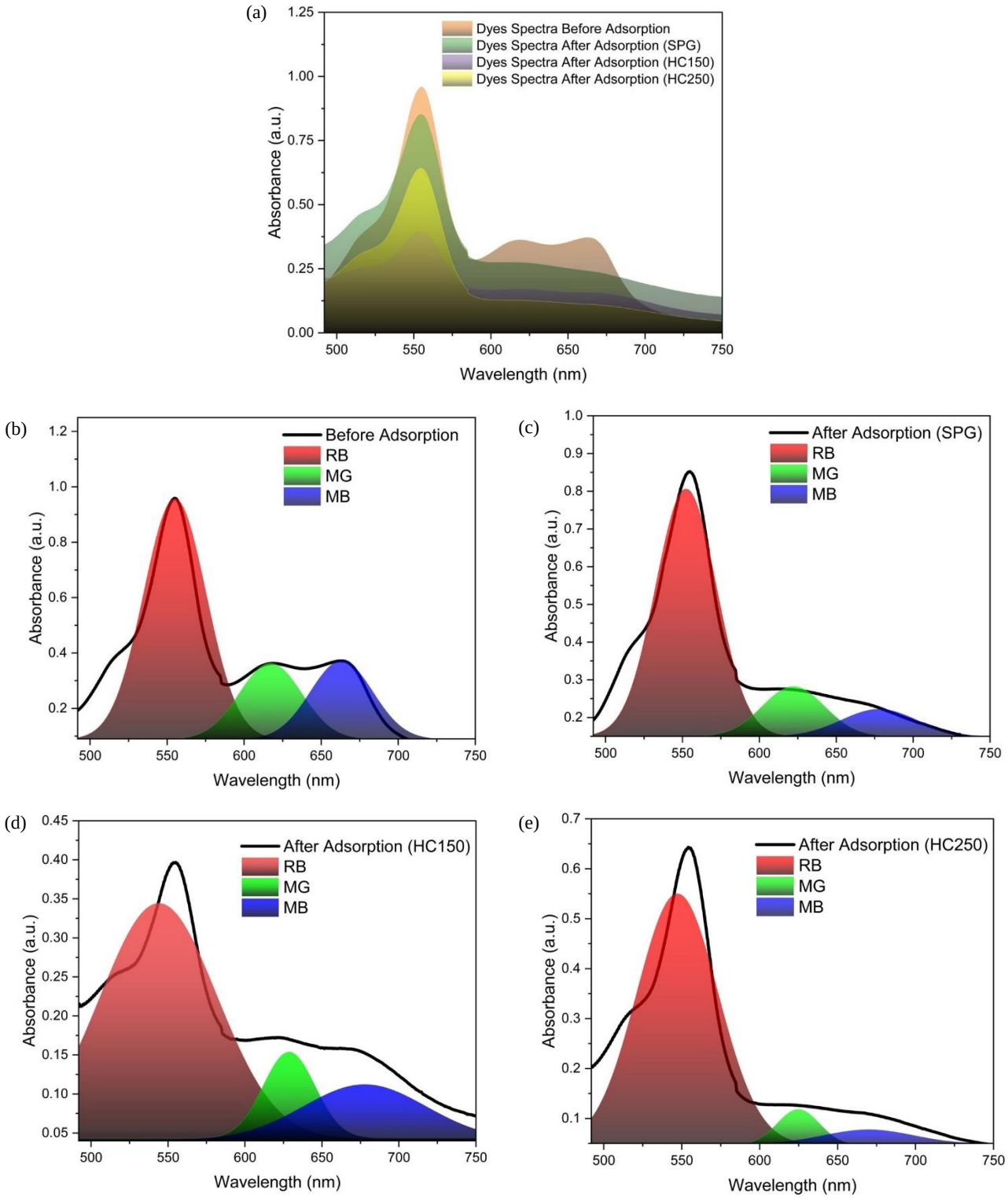

Figure 3. Combined spectra of cationic dye before and after adsorption (a); deconvolution curve of the initial spectrum before adsorption (b); after adsorption by Spirogyra sp. (SPG) (c); after adsorption by HC150 (d); and after adsorption by HC250 (e)

Table 2. The adsorption efficiency of cationic dyes Selectivity by SPG, HC150 and HC250

Dyes	Adsorption efficiency (%)		
	SPG	HC150	HC250
RB	16.35±1.03	64.17±1.18	42.81±1.03
MG	22.40±1.16	57.92±1.16	67.21±0.77
MB	39.13±1.15	69.29±0.77	78.53±0.38

This trend indicates that the structure and chemical properties of MB, such as molecular size, charge, and affinity to active groups on the adsorbent surface, are more compatible with all adsorbents. MB has a planar structure with amine and aromatic groups that allow for stronger π-π interactions and electrostatic bonds with the adsorbent surface, especially if the surface has negatively charged groups or pores of suitable size. In addition, HTC modification of HC150 and HC250 seems to improve the physicochemical properties of the adsorbents, such as surface area and pore regularity, which ultimately contributes to the improved selectivity towards MB (Khan et al., 2022; Wu et al., 2024).

3.3 Adsorption study on pH parameters

The pH of the adsorbents point zero charge is indicated by the pHpzc. The pHpzc values of adsorbents SPG, HC150, and HC250, as shown in Figure 4(a), are 6.60, 6.36, and 6.47, respectively. These values are below the optimum pH value at 7, as shown in Figure 4(b), which explains the way the negatively charged hydroxyl functional groups on the adsorbents surface interact with the MB positive sites. This electrostatic attraction facilitates the adsorption of MB molecules onto the adsorbents surface. Additionally, the relatively close pHpzc values suggest similar surface charge characteristics among the samples, indicating that surface modification only slightly alters their overall charge behavior under near-neutral pH conditions (Wierzbicka et al., 2022).

3.4 Adsorption study on kinetics parameters

Based on the Figure 5 and Table 3, analysis of MB adsorption kinetics with an optimum time of 120 minutes shows that the PSO model fits better than the PFO model for adsorbents SPG, HC150, and HC250.

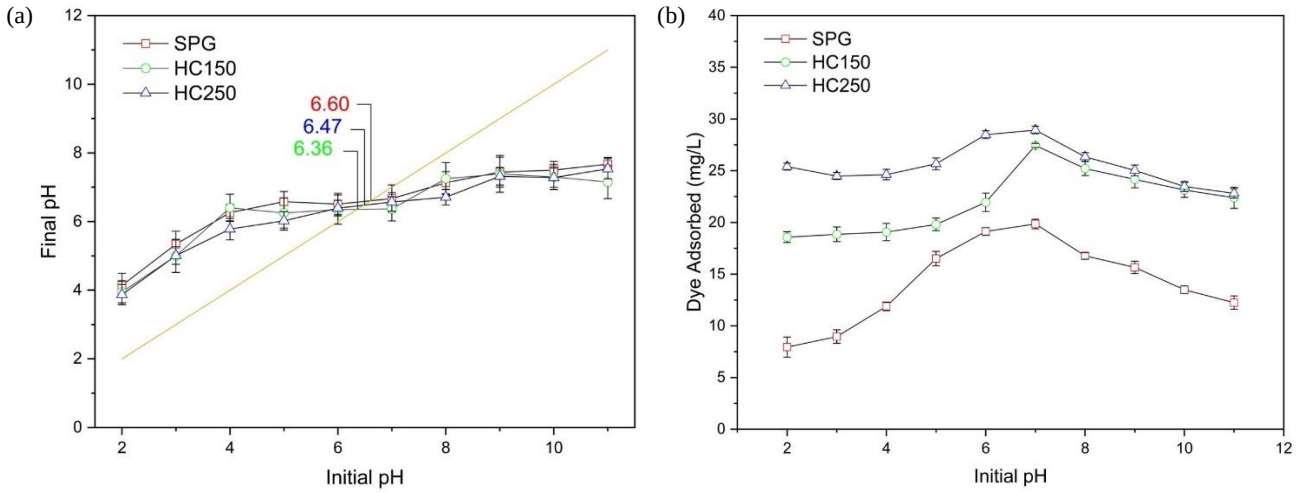

Figure 4. The pHpzc of adsorbents (a), and adsorption variations with pH (b) of SPG, HC150, and HC250

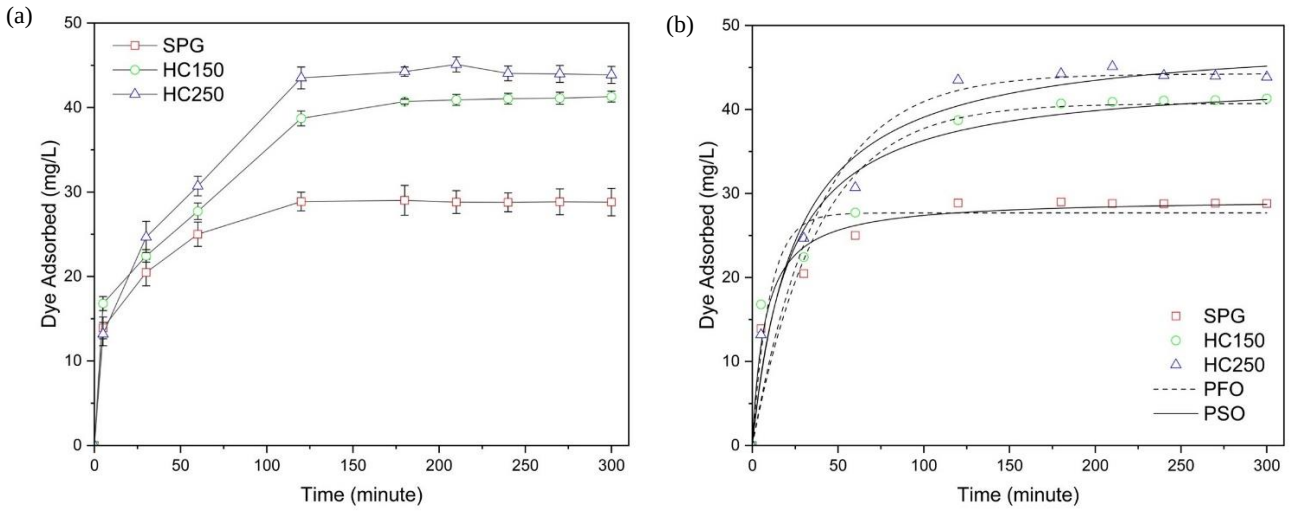

Figure 5. Adsorption vs. contact time (a), and kinetic curves of PFO and PSO Models for SPG, HC150, and HC250 (b)

This is indicated by the very high coefficient of determination (R^2) values in model (≥0.993), compared to the lower PFO between 0.851-0.937. In addition, the Qe_{calc} of the PSO model is closer to the Qe_{exp} value, such as in adsorbents SPG, HC150 and HC250 with Qe_{exp} 28.87, 38.72 and 43.51 mg/g and Qe_{calc} 29.59, 43.48, and 46.73 mg/g, respectively. These results indicate that the adsorption mechanism of MB follows PSO kinetic model, which involves a chemisorption process (Palapa et al., 2025). The increase in adsorption capacity on HC150 and HC250 also suggests that thermal treatment improved the adsorbent performance (Krishna Murthy et al., 2020; Lu et al., 2021).

Table 3. The kinetic parameters of the PFO and PSO models of SPG, HC150, and HC250

Adsorbent	Qe exp (mg/g)	PFO			PSO		
		Qe calc (mg/g)	k_1 (min^{-1})	R^2	Qe calc (mg/g)	k_2 (g/mg)/min	R^2
SPG	28.87	22.24	0.03	0.937	29.59	0.005	0.999
HC150	38.72	30.13	0.02	0.851	43.48	0.001	0.993
HC250	43.51	37.18	0.02	0.937	46.73	0.001	0.993

3.5 Adsorption study on isotherm and thermodynamics parameters

Adsorption isotherms are essential for explaining adsorbent-adsorbate interactions and designing industrial processes, as they reflect adsorbent performance at equilibrium (Eltaweil et al., 2020). They depend on the adsorbent, adsorbate, and solution properties such as temperature, pH, and ionic strength (Mohadi et al., 2023a; Mohadi et al., 2023b; Priatna et al., 2023). According to the Langmuir model Qe_{max} values that shown at Table 4, HC250 had the highest adsorption capacity when compared to HC150 and SPG. At 60°C, the HC250 Qe_{max} decreased to 89.29 mg/g from 125 mg/g at 30°C. At 50°C, HC150 Qe_{max} reached a maximum of 94.34 mg/g, at higher temperatures, it slightly declined. With a capacity of 62.89 mg/g at 30°C and 53.76 mg/g at 60°C, Adsorbent SPG had the lowest capacity. As the temperature increased, the overall decrease in Qe_{max} suggests an exothermic adsorption process (Al-Ghouti and Da'ana, 2020; Ayawei et al., 2017). The R^2 values were higher for the Freundlich isotherm model, indicating a better fit than Langmuir for all adsorbents. All n values of the Freundlich model were above 1, suggesting that the adsorption was favorable and physical in nature. A higher adsorption capacity on heterogeneous surfaces was shown by increased kF values with temperature. A stronger affinity of the adsorbate for the adsorbent surface is indicated by the increasing trend of the kL parameter of the Langmuir model with temperature, particularly in adsorbents SPG and HC250.

Table 4. The Freundlich and Langmuir adsorption isotherms of SPG, HC150, and HC250

Adsorbent	T (°C)	Langmuir			Freundlich		
		Qe_{max}	kL	R^2	n	kF	R^2
SPG	30	62.89	0.037	0.896	1.687	4.528	0.951
	40	60.98	0.044	0.933	1.772	5.212	0.967
	50	56.50	0.057	0.902	1.960	6.464	0.931
	60	53.76	0.077	0.891	2.251	8.478	0.925
HC150	30	77.52	0.138	0.922	1.949	13.72	0.944
	40	89.29	0.119	0.973	1.747	13.08	0.984
	50	94.34	0.111	0.957	1.684	12.78	0.984
	60	85.47	0.134	0.838	1.788	13.75	0.925
HC250	30	125	0.107	0.898	1.493	14.65	0.989
	40	119	0.119	0.840	1.538	15.39	0.975
	50	92.59	0.190	0.837	1.785	18.03	0.945
	60	89.29	0.206	0.807	1.820	18.43	0.923

Table 5 shows the adsorption thermodynamic parameter of SPG, HC150, and HC250. Among the three, HC250 demonstrated thermodynamic superiority in the adsorption process. The most negative ΔG values across the entire temperature range (30-60°C) indicated that the adsorption on HC250 was the most spontaneous, reflecting the strongest adsorbate-adsorbent affinity among the samples. Although the ΔH value of HC250 (3.11 kJ/mol) is lower than HC150 (6.40 kJ/mol) and SPG (7.47 kJ/mol), this indicates that HC250 requires less energy from the environment for adsorption to take place, making it more energy efficient. In addition, the higher ΔS value of HC250 than SPG indicates that adsorption still causes increased disorder at the solid-liquid interface, which favors an effective adsorption mechanism. In summary, the combination of spontaneity (most negative ΔG), energy efficiency (lowest ΔH), and increased interfacial disorder (higher ΔS) establishes HC250 as the most thermodynamically advantageous adsorbent in this system (Krishna Murthy et al., 2020).

Table 5. Adsorption thermodynamic parameter of SPG, HC150 and HC250

Adsorbent	Concentration (mg/L)	ΔH (kJ/mol)	ΔS (kJ/mol)	ΔG (kJ/mol)			
				30°C	40°C	50°C	60°C
SPG	60	7.47	0.026	-0.277	-0.532	-0.788	-1.044
HC150	60	6.40	0.033	-3.629	-3.960	-4.291	-4.622
HC250	60	3.11	0.027	-5.183	-5.456	-5.730	-6.004

3.6 Regeneration cycles study

The regeneration data shown in Figure 6 indicate that adsorbents SPG, HC150, and HC250 experienced a decrease in adsorption efficiency as the cycles of use increased. In the first cycle, the adsorption efficiency of each adsorbent was 56.23% for SPG, 80.56% for HC150, and 90.14% for HC250. Adsorbent SPG was only able to maintain an efficiency above 50% until the second cycle (50.20%), while HC150 and HC250 showed better performance, with efficiencies above 50% until the fourth cycle, which were 51.88% (HC150) and 53.55% (HC250), respectively. This indicates that HC150 and HC250 have higher regeneration stability than SPG. HC250 consistently showed the highest adsorption efficiency in each cycle, indicating that the synthesis of hydrochar with HTC of a certain temperature variations has different characteristics in the adsorbent and more effective in maintaining adsorption capacity after multiple reuses. The main advantage of HC150 and HC250 over SPG lies in their ability to effectively maintain high adsorption efficiency over more reuse cycles.

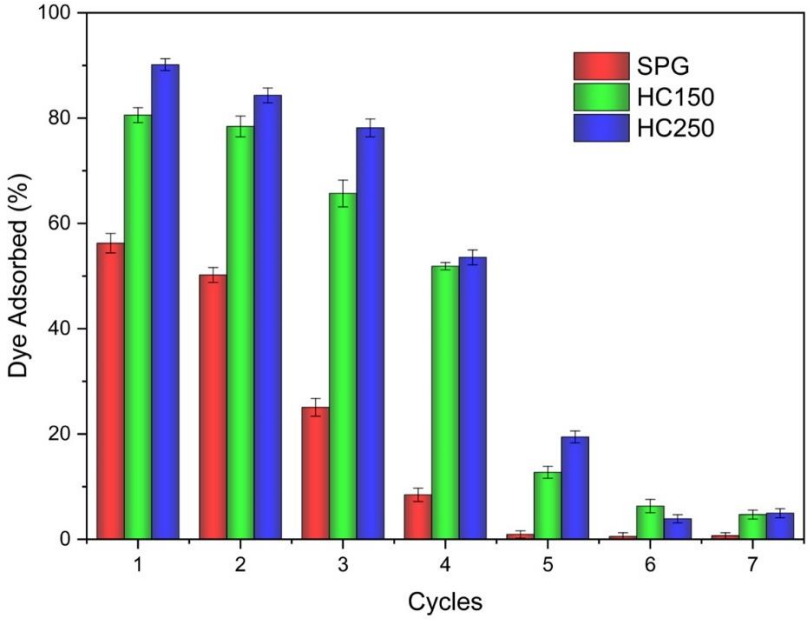

Figure 6. Regeneration cycles of SPG, HC150 and HC250

3.7 Adsorption mechanism study

The comparison of the FTIR spectra before and after MB adsorption of SPG, HC150 and HC250 shown in Figure 7, reveals significant changes in the surface functional groups of SPG, as well as HC150 and HC250, indicating the active involvement of these groups in the adsorption process. The observed decrease in intensity around 3,412 cm^{-1} across all materials suggests the participation of hydroxyl and amine groups through hydrogen bonding or electrostatic interactions with the positively charged MB molecules. Furthermore, shifts and intensity changes at 1,645 and 1,531 cm^{-1}, corresponding to carbonyl and phenolic groups, particularly in SPG and HC150, further support the occurrence of specific interactions between polar functional groups of the adsorbents and MB.

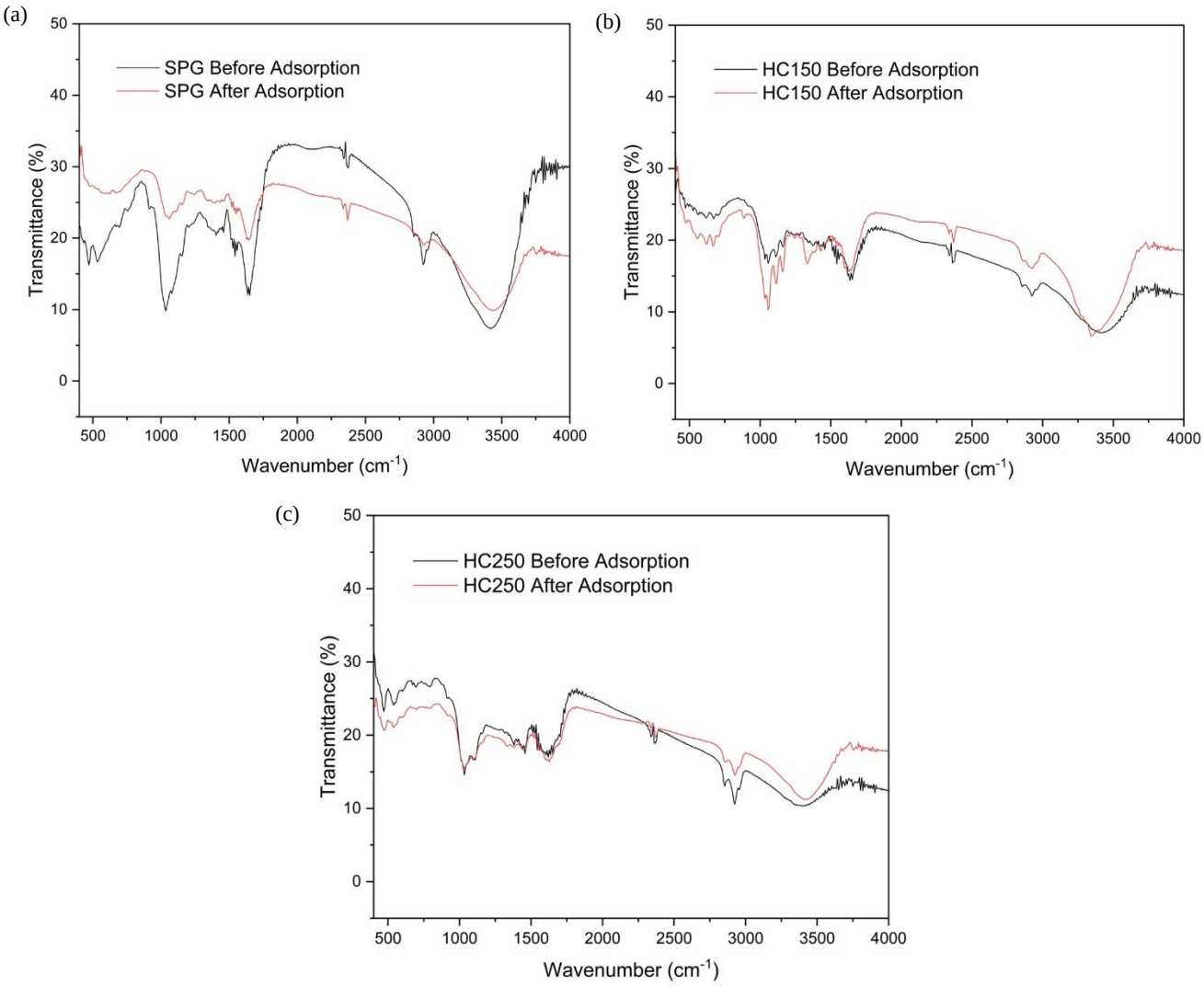

Figure 7. Comparative FTIR spectra of SPG (a), HC150 (b), and HC250 (c) before and after MB adsorption

Additionally, changes in the spectral region between 1,000-500 cm^{-1}, especially involving C-O, C-N, and C-N-S vibrations, indicate possible direct interactions between MB functional groups and the adsorbent surface. Notably, HC250 exhibited fewer spectral changes compared to SPG and HC150, suggesting that its adsorption mechanism is more dominated by π-π stacking interactions between aromatic domains of the hydrochar and the aromatic rings of MB. Overall, the adsorption of MB onto these materials involves a combination of electrostatic interactions, hydrogen bonding, and π-π stacking, with the degree of carbonization influencing the dominant adsorption mechanism. The possible adsorption mechanism is illustrated in Figure 8.

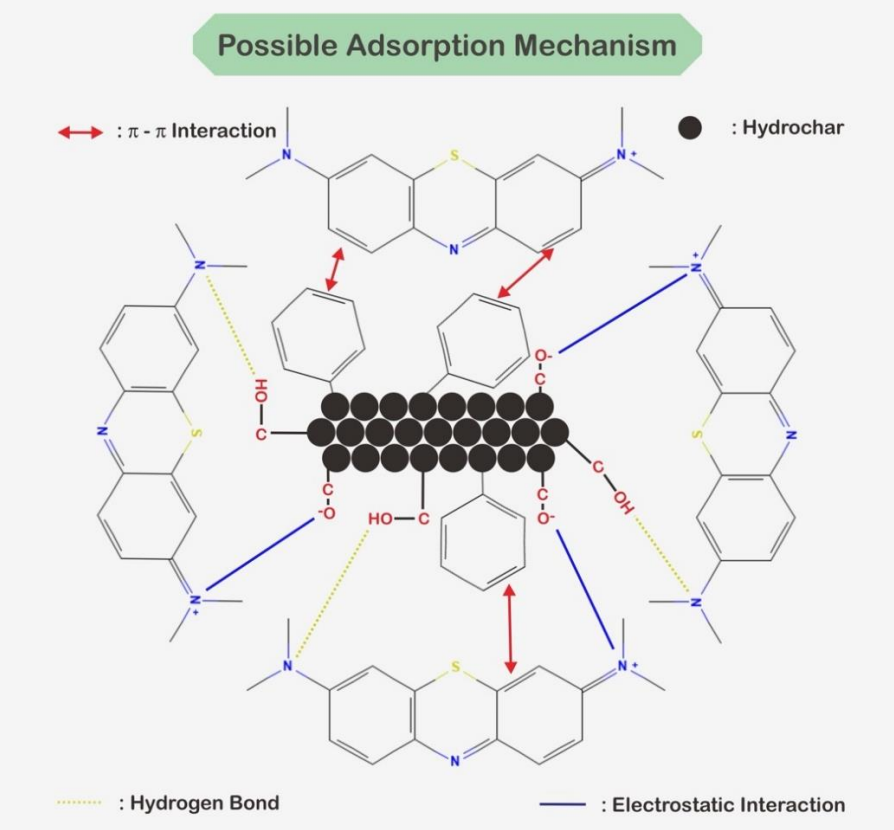

Figure 8. Illustration of the possible adsorption mechanism of MB onto SPG, HC150, and HC250 via electrostatic interaction, hydrogen bonding, and π-π stacking

3.8 Comparison of adsorption capacity of various biomass-based adsorbents for MB adsorption

Table 6 presents a comparison of the adsorption capacities of various biomass-derived adsorbents for MB, synthesized using either pyrolysis or hydrothermal methods. In general, adsorbents produced via the hydrothermal method exhibit higher adsorption capacities compared to those obtained through pyrolysis. For example, biochar derived from *Melia azedarach* fruit and *Chenopodium formosanum*, prepared via pyrolysis, showed adsorption capacities of 25.77 mg/g and 41.16 mg/g, respectively (Karadeniz and Güzel, 2023; Morgan et al., 2025). In contrast, corn straw biochar demonstrated a relatively low capacity of 6.25 mg/g (Zhao et al., 2023). On the other hand, hydrochars synthesized from sunflower stalks and *Shorea* spp. through hydrothermal carbonization achieved higher capacities, reaching 49.37 mg/g and 37.80 mg/g, respectively (Elhassan et al., 2025; Saini et al., 2025). In this study, the hydrochars HC150 and HC250 exhibited even greater adsorption capacities of 85.47 mg/g and 89.29 mg/g, respectively. These results highlight the positive effect of elevated hydrothermal temperatures on the development of surface properties favorable for adsorption. Thus, HC150 and HC250 demonstrate superior performance as adsorbents for MB removal and outperform several other bio-based adsorbents reported in the literature.

Table 6. Comparison of adsorption capacities of various biomass-based adsorbents for MB adsorption

Adsorbents	Methods	Adsorption capacity (mg/g)	References
Biochar from *Melia azedarach* fruit	Pyrolysis	25.77	Karadeniz and Güzel (2023)
Biochar from *Chenopodium formosanum*	Pyrolisis	41.161	Morgan et al. (2025)
Biochar from corn straw	Pyrolisis	6.25	Zhao et al. (2023)
Hydrochar from sunflower stalks (biomass)	Hydrothermal	49.37	Saini et al. (2025)
Hydrochar from *Shorea* spp.	Hydrothermal	37.80	Elhassan et al. (2025)
HC150	Hydrothermal	85.47	This study
HC250	Hydrothermal	89.29	This study

4. CONCLUSION

The successful synthesis of adsorbents SPG, HC150, and HC250 is confirmed through XRD, FTIR, SEM, and BET analyze. XRD analysis confirmed the presence of a dominant $CaCO_3$ crystalline phase (JCPDS 01-086-2334) in all adsorbents, with new peaks and slight shifts in HC150 and HC250 indicating structural changes due to hydrochar synthesis. FTIR spectra showed the presence of O-H, C=O, C-O, and C-N-S groups in SPG, with reduced O-H and phenolic peaks in HC150 and HC250, confirming chemical changes.

SEM analysis confirmed that increasing the carbonization temperature significantly alters the surface morphology and particle distribution of the adsorbents. The raw sample SPG exhibited a smooth, sheet-like surface, while HC150 showed the formation of uniform particles. In contrast, HC250 developed a rough, porous, and heterogeneous structure with broader particle size distribution, indicating advanced carbonization and enhanced potential for adsorption applications.

BET analysis revealed a significant increase in surface area and a shift from macroporous to mesoporous structure in HC150 and HC250, improving their adsorption potential. Adsorbents showed selective adsorption toward MB, with HC250 having the highest removal 69.02%. The study demonstrates that adsorbents possess similar surface charge characteristics, with pHpzc values slightly below neutral, facilitating electrostatic attraction with cationic MB.

Adsorption kinetics follow the PSO model, indicating a chemisorption mechanism with high reliability. Among the adsorbents, HC250 exhibits the best performance, showing the highest adsorption capacity and strong alignment with the Freundlich isotherm model. Thermodynamic evaluations further highlight HC250 superior spontaneity, energy efficiency, and adsorbate affinity, as evidenced by its more negative ΔG, lower ΔH, and higher ΔS values.

Regeneration tests show that HC250 maintains the highest adsorption efficiency across cycles, starting at 90.14% and remaining above 50% through the fourth cycle (53.55%). HC150 also performs well, from 80.56% to 51.88%, while SPG drops from 56.23% to 50.20% by the second cycle. These results confirm that HC250 has the best regeneration stability and reusability among the tested adsorbents.

ACKNOWLEDGEMENTS

We gratefully acknowledge the support provided by the Research Center of Inorganic Materials and Coordination Complexes, Universitas Sriwijaya, in facilitating this research.

AUTHOR CONTRIBUTIONS

Conceptualization: M.B., A.L., L.H., E.M. Data curation: M.B., S.W. Formal Analysis: M.B., S.W., Y,H. Funding acquisition: M.B., A.L. Investigation: M.B., A.L., S.W., Y.H. Methodology: M.B., A.L., L.H., E.M., S.W. Project administration: M.B., A.L., L.H., E.M., S.W. Resources: M.B., S.W. Software: M.B., S.W. Supervision: A.L., L.H., E.M. Validation: A.L., L.H., E.M. Visualization: M.B., S.W. Writing-original draft: M.B., S.W. Writing-review and editing: M.B., A.L., L.H., E.M., S.W.

DECLARATION OF CONFLICT OF INTEREST

The authors declare no conflict of interest.

REFERENCES

Ahmad N, Kameda T, Rahman MT, Rahman F, Lesbani A. Preparation of a new hybrid MgAlLDH@Magnetite activated charcoal by hydrothermal method for stability and adsorption mechanism of congo red. Results in Surfaces and Interfaces 2025;18:Article No. 100440.

Al-Ghouti MA, Da'ana DA. Guidelines for the use and interpretation of adsorption isotherm models: A review. Journal of Hazardous Materials 2020;393:Article No. 122383.

Arora N, Tripathi S, Bhatnagar P, Gururani P, Philippidis GP, Kumar V, et al. Algal-based biochar and hydrochar: A holistic and sustainable approach to wastewater treatment. Chemical Engineering Journal 2024;496:Article No. 53953.

Ayawei N, Ebelegi AN, Wankasi D. Modelling and interpretation of adsorption isotherms. Journal of Chemistry 2017;1:Article No. 3039817.

Badaruddin M, Hanum L, Melwita E, Wibiyan S, Lesbani A. Hydrothermal carbonization of *Spirogyra* sp. algae for adsorption and regeneration of malachite green dye. Chimica Techno Acta 2025;12(1):Article No. 12113

Chand V, Vanavana I. Evaluation of *Spirogyra* Sp. as a bioindicator of heavymetal pollution in a tropical aquatic environment. Pollution Research 2022;41(2):445-50.

Cui C, Qiao W, Li D, Wang L-J. Dual cross-linked magnetic gelatin/carboxymethyl cellulose cryogels for enhanced Congo red adsorption: Experimental studies and machine learning modelling. Journal of Colloid and Interface Science 2025;678:619-35.

Djezzar Z, Aidi A, Rehali H, Ziad S, Othmane T. Characterization of activated carbon produced from the green algae *Spirogyra* used as a cost-effective adsorbent for enhanced removal of copper(ii): Application in industrial wastewater treatment. RSC Advances 2024;14(8):5276-89.

Doondani P, Panda D, Gomase V, Peta KR, Jugade R. Novel chitosan-ZnO nanocomposites derived from Nymphaeaceae fronds for highly efficient removal of Reactive Blue 19, Reactive Orange 16, and Congo Red dyes. Environmental Research 2024;247:Article No. 118228.

Elhassan M, Kooh MRR, Chou Chau YF, Abdullah R. Hydrochar from *Shorea* spp.: A dual-purpose approach for sustainable biofuel and efficient methylene blue adsorbent. Biomass Conversion and Biorefinery 2025;15(4):5779-93.

Eltaweil AS, Ali Mohamed H, Abd El-Monaem EM, El-Subruiti GM. Mesoporous magnetic biochar composite for enhanced adsorption of malachite green dye: Characterization, adsorption kinetics, thermodynamics and isotherms. Advanced Powder Technology 2020;31(3):1253-63.

Ganash A, Othman S, Al-Moubaraki A, Ganash E. An electrodeposition of Cu-MOF on platinum electrode for efficient electrochemical degradation of tartrazine dye with parameter control and degradation mechanisms: Experimental and theoretical findings. Applied Surface Science Advances 2024;19:Article No. 100577.

Gibson N, Kuchenbecker P, Rasmussen K, Hodoroaba VD, Rauscher H. Chapter 4.1 - Volume-specific surface area by gas adsorption analysis with the BET method. In: Characterization of Nanoparticles: Measurement Processes for Nanoparticles. Elsevier; 2019. p. 265-94.

González-Fernández LA, Medellín-Castillo NA, Navarro-Frómeta AE, Castillo-Ramos V, Sánchez-Polo M, Carrasco-Marín F. Optimization of hydrochar synthesis conditions for enhanced Cd(II) and Pb(II) adsorption in mono and multimetallic systems. Environmental Research 2024;261:Article No. 119651.

Hamad N, Galhoum AA, Saad A, Wageh S. Efficient adsorption of cationic and anionic dyes using hydrochar nanoparticles prepared from orange peel. Journal of Molecular Liquids 2024;409:Article No. 125349.

Jefri J, Fithri NA, Ramadhan N. Enhanced selectivity of Ni/Al LDH for cationic dye adsorption via Gambier Leaf Extract Modification. Indonesian Journal of Material Research 2025;3(1):1-7.

Kala K, Vasumathi V, Sivalingam S, Kapali BSC. Optimization of organic dyes photodegradation and investigation of the anticancer performance by copper oxide/graphene oxide nanocomposite. Surfaces and Interfaces 2024;50:Article No. 104482.

Karadeniz F, Güzel F. Adsorptive performance of *Melia azedarach* fruit-derived biochar in removing methylene blue, diclofenac, and copper(II) from aqueous solution. Biomass Conversion and Biorefinery 2023;13(3):2429-47.

Khan I, Saeed K, Zekker I, Zhang B, Hendi AH, Ahmad A, et al. Review on methylene blue: Its properties, uses, toxicity and photodegradation. Water (Switzerland) 2022;14(2):Article No. 242.

Krishna Murthy TP, Gowrishankar BS, Krishna RH, Chandraprabha MN, Mathew BB. Magnetic modification of coffee husk hydrochar for adsorptive removal of methylene blue: Isotherms, kinetics and thermodynamic studies. Environmental Chemistry and Ecotoxicology 2020;2:205-12.

Kumar A, Singh R, Upadhyay SK, Sanjay Kumar S, Charaya MU. Biosorption: The removal of toxic dyes from industrial effluent using phytobiomass: A review. Plant Archives 2021;21(Supplement 1): 1320-5.

Laggoun Z, Khalfaoui A, Derbal K, Ghomrani AF, Benalia A, Pizzi A. Experimental study of selective batch bio-adsorption for the removal of dyes in industrial textile effluents. Journal of Renewable Materials 2025;13(1):127-46.

Le TTU, Ngo TG, Hoang NA, Nguyen VH, Nguyen VD, Hoang LP, et al. Adsorption characteristics of single and binary mixture of methylene blue and rhodamine B of novel hydrochar derived from lemongrass essential oil distillation residue. Journal of Molecular Liquids 2025;425:Article No. 127205.

Lesbani A, Ahmad N, Mohadi R, Royani I, Wibiyan S, Amri, et al. Selective adsorption of cationic dyes by layered double hydroxide with assist algae (*Spirulina platensis*) to enrich functional groups. JCIS Open 2024;15:Article No. 100118.

Li C, Zhong F, Liang X, Xu W, Yuan Q, Niu W, et al. Microwave-assisted hydrothermal conversion of crop straw: Enhancing the properties of liquid product and hydrochar by varying temperature and medium. Energy Conversion and Management 2023;290:Article No. 117192.

Li W, Tao E, Hao X, Li N, Li Y, Yang S. MMT and ZrO_2 jointly regulate the pore size of graphene oxide-based composite aerogel materials to improve the selective removal ability of Cu(II). Separation and Purification Technology 2024; 331:Article No. 125506.

Lu YC, Kooh MRR, Lim LBL, Priyantha N. Effective and simple NaOH-modification method to remove methyl violet dye via *Ipomoea aquatica* Roots. Adsorption Science and Technology 2021;2021:Article No. 5932222.

Luo M, Wang L, Li H, Bu Y, Zhao Y, Cai J. Hierarchical porous biochar from kelp: Insight into self-template effect and highly efficient removal of methylene blue from water. Bioresource Technology 2023;372:Article No. 128676.

Mohadi R, Ahmad N, Wibiyan S, Zahara ZA, Fitri ES, Mardiyanto, et al. Synthesis of Zn/Al-ZnO composite using Zn/Al-layered double hydroxide for oxidative desulfurization of 4-methyldibenzothiophene. Science and Technology Indonesia 2023a;8(4):701-9.

Mohadi R, Palapa NR, Wibiyan S, Mardiyanto, Rohmatullaili, Fitri ES, et al. Catalytic oxidative desulfurization of 4-methyldibenzothiophene by Ni/Al modified titanium dioxide and zinc oxide. Science and Technology Indonesia 2023b;8(3):414-21.

Mon PP, Cho PP, Chandana L, Srikanth VVSS, Madras G, Ch S. Biowaste-derived Ni/NiO decorated-2D biochar for adsorption of methyl orange. Journal of Environmental Management 2023;344:Article No. 118418.

Morgan HM, Jiang TJ, Tsai WT, Yen TB. Initial physiochemical characterization of Djulis (*Chenopodium formosanum*) spent mushroom substrate biochar and its application for methylene blue dye adsorption, isotherm, kinetics, and parameters. Biomass Conversion and Biorefinery 2025;15:19947-61.

Neme I, Gonfa G, Masi C. Activated carbon from biomass precursors using phosphoric acid: A review. Heliyon 2022;8(12):e11940.

Normah N, Juleanti N, Palapa NR, Taher T, Siregar PMSBN, Wijaya A, et al. Hydrothermal carbonization of rambutan peel (*Nephelium lappaceum* L.) as a green and low-cost adsorbent for Fe(II) removal from aqueous solutions. Chemistry and Ecology 2022;38(3):284-300.

Normah N, Juleanti N, Siregar PMSBN, Wijaya A, Palapa NR, Taher T, et al. Size selectivity of anionic and cationic dyes using LDH modified adsorbent with low-cost rambutan peel to hydrochar. Bulletin of Chemical Reaction Engineering and Catalysis 2021;16(4):869-80.

Norrahma SSA, Hamid NHA, Hairom NHH, Jasmani L, Sidik DAB. Industrial textile wastewater treatment using *Neolamarckia cadamba* NFC filter paper via cross-flow

filtration system. Journal of Water Process Engineering 2023;55:Article No. 104188.

Palapa NR, Putra MBK, Musifa E, Yuliasari N, Adawiyah R. Preparation and application of biochar from *Areca catechu* L. peel for malachite green and reactive blue dyes removal. Indonesian Journal of Environmental Management and Sustainability 2025;9(1):28-35.

Palapa NR, Wijaya A, Ahmad N, Amri A, Mohadi R, Lesbani A. Activated hydrochar prepared from Longan Fruit (*Dimocarpus longan* Lour.) peel via hydrothermal carbonization-NaOH activation for cationic dyes removal. Science and Technology Indonesia 2023;8(3):461-70.

Permann C, Gierlinger N, Holzinger A. Zygospores of the green alga *Spirogyra*: New insights from structural and chemical imaging. Frontiers in Plant Science 2022;13:Article No. 1080111.

Priatna SJ, Hakim YM, Wibyan S, Sailah S, Mohadi R. Interlayer modification of west java natural bentonite as hazardous dye rhodamine B adsorption. Science and Technology Indonesia 2023;8(2):160-9.

Ren Y, Liu S, Tan Y, Liu Y, Yuan T, Shen Z, et al. Application of QSAR for investigation on coagulation mechanisms of textile wastewater. Ecotoxicology and Environmental Safety 2022;244:Article No. 114035.

Saini R, Pandey M, Mishra RK, Kumar P. Adsorption potential of hydrochar derived from hydrothermal carbonization of waste biomass towards the removal of methylene blue dye from wastewater. Biomass Conversion and Biorefinery 2025;15(6):9229-49.

Shi Y, Chang Q, Zhang T, Song G, Sun Y, Ding G. A review on selective dye adsorption by different mechanisms. Journal of Environmental Chemical Engineering 2022;10(6)Article No. 108639.

Singh S, Verma N, Umar A, Kansal SK. ZnCdS nanoparticles decorated three-dimensional MoO_3 polygonal structure: A novel photocatalyst for enhanced solar light-driven degradation of methyl orange dye. Journal of Alloys and Compounds 2024;997:Article No. 174714.

Siri-anusornsak W, Kolawole O, Soiklom S, Petchpoung K, Keawkim K, Chuaysrinule C, et al. Innovative use of *Spirogyra* sp. biomass for the sustainable adsorption of Aflatoxin B1 and Ochratoxin A in aqueous solutions. Molecules 2024;29(21):Article No. 5038.

Sornaly HH, Ahmed S, Titin KF, Islam MN, Parvin A, Islam MA, et al. The utility of bioremediation approach over physicochemical methods to detoxify dyes discharges from textile effluents: A comprehensive review study. Sustainable Chemistry and Pharmacy 2024;39:Article No. 101538.

Spagnuolo D, Iannazzo D, Len T, Balu AM, Morabito M, Genovese G, et al. Hydrochar from *Sargassum muticum*: A sustainable approach for high-capacity removal of Rhodamine B dye. RSC Sustainability 2023;1(6):1404-15.

Susanti E, Ristanti Widoretno M, Oktaviyani D, Sumi Lestari F, Muit N, Kurniawan R, et al. Sorption kinetics of heavy metals from aqueous solution using *Spirogyra* sp.: A microcosm study. LIMNOTEK Perairan Darat Tropis di Indonesia. 2023;29(1):Article No. 1190.

Tipnee S, Unpaprom Y, Ramaraj R, Tipnee S, Ramaraj R, Unpaprom Y. Nutritional evaluation of edible freshwater green macroalga *Spirogyra varians*. Emerging Topics in Life Sciences 2015;1(2):1-7.

Tones ARM, Eyng E, Zeferino CL, Ferreira S de O, Alves AA de A, Fagundes-Klen MR, et al. Spectral deconvolution associated to the Gaussian fit as a tool for the optimization of photovoltaic electrocoagulation applied in the treatment of textile dyes. Science of the Total Environment 2020;713:Article No. 136301.

Tsarpali M, Kuhn JN, Philippidis GP. Hydrothermal carbonization of residual algal biomass for production of hydrochar as a biobased metal adsorbent. Sustainability (Switzerland) 2022;14(1):Article No. 455.

Ullah F, Ji G, Irfan M, Gao Y, Shafiq F, Sun Y, et al. Adsorption performance and mechanism of cationic and anionic dyes by KOH activated biochar derived from medical waste pyrolysis. Environmental Pollution 2022;314:Article No. 120271.

Umesh AS, Puttaiahgowda YM, Thottathil S. Enhanced adsorption: Reviewing the potential of reinforcing polymers and hydrogels with nanomaterials for methylene blue dye removal. Surfaces and Interfaces 2024;51:Article No. 104670.

Vetrivel SA, Diptanghu M, Ebhin MR, Sydavalli S, Gaurav N, Tiger KP. Green algae of the genus *Spirogyra*: A potential absorbent for heavy metal from coal mine water. Remediation 2017;27(3):81-90.

Wang H, Chen C, Dai K, Xiang H, Kou J, Guo H, et al. Selective adsorption of anionic dyes by a macropore magnetic lignin-chitosan adsorbent. International Journal of Biological Macromolecules 2024;269(2):Article No. 131955.

Wibiyan S, Royani I, Ahmad N, Lesbani A. Assessing the efficiency, selectivity, and reusability of ZnAl-layered double hydroxide and *Eucheuma cottonii* composite in removing anionic dyes from wastewater. Inorganic Chemistry Communications 2024a;170:Article No. 113347.

Wibiyan S, Royani I, Lesbani A. Selective adsorption of cationic and anionic dyes using Ni/Al layered double hydroxide modified with *Eucheuma cottonii*. Indonesian Journal of Material Research 2024b;2(1):1-6.

Wibiyan S, Royani I, Lesbani A. Synthesis and performance of ZnAl@ layered double hydroxide composites with *Eucheuma cottonii* for adsorption and regeneration of Congo red dye. Indonesian Journal of Environmental Management and Sustainability 2024c;8(3):126-34.

Wibiyan S, Wijaya A, Siregar PMSBN. Adsorption of phenol using cellulose and hydrochar: Kinetic, isotherm, and regeneration studies. Indonesian Journal of Material Research 2023;1(2):61-7.

Wibowo YG, Syahnur MT, Al-Azizah PS, Arantha Gintha D, Lululangi BRG, Sudibyo. Phytoremediation of high concentration of ionic dyes using aquatic plant (Lemna minor): A potential eco-friendly solution for wastewater treatment. Environmental Nanotechnology, Monitoring and Management 2023;20:Article No. 100849.

Wierzbicka E, Kuśmierek K, Świątkowski A, Legocka I. Efficient rhodamine B dye removal from water by acid- and organo-modified halloysites. Minerals 2022;12(3):Article No. 350.

Wijaya A, Ahmad N, Hanum L, Melwita E, Lesbani A. *Spirogyra* sp. macro-algae-supported NiCr-LDH adsorbent for enhanced remazol red dye removal. Results in Surfaces and Interfaces 2025;18:Article No. 100427.

Wu J, Wang T, Li S, Tang W, Yu S, Zhao Z, et al. A green method to improve adsorption capacity of hydrochar by ball-milling: Enhanced norfloxacin adsorption performance and mechanistic insight. Carbon Research 2024;3(1):Article No. 60.

Yihunu EW, Minale M, Abebe S, Limin M. Preparation, characterization and cost analysis of activated biochar and hydrochar derived from agricultural waste: A comparative study. SN Applied Sciences 2019;1(8):Article No. 873.

Zhao Y, Qi K, Pan J. Efficient corn straw and poplar leaf biochar-based adsorbents for the eradication of methylene blue from aqueous solutions. Desalination and Water Treatment 2023;303:236-44.

INSTRUCTION FOR AUTHORS

Publication and Peer-reviewing processes of Environment and Natural Resources Journal

Environment and Natural Resources Journal is a peer reviewed and open access journal that is published in six issues per year. Manuscripts should be submitted online at https://ph02.tci-thaijo.org/index.php/ennrj/about/submissions by registering and logging into this website. Submitted manuscripts should not have been published previously, nor be under consideration for publication elsewhere (except conference proceedings papers). A guide for authors and relevant information for the submission of manuscripts are provided in this section and also online at: https://ph02.tci-thaijo.org/index.php/ennrj/author. All manuscripts are refereed through a **single-blind peer-review** process.

Submitted manuscripts are reviewed by outside experts or editorial board members of **Environment and Natural Resources Journal**. This journal uses double-blind review, which means that both the reviewer and author identities are concealed from the reviewers, and vice versa, throughout the review process. Steps in the process are as follows:

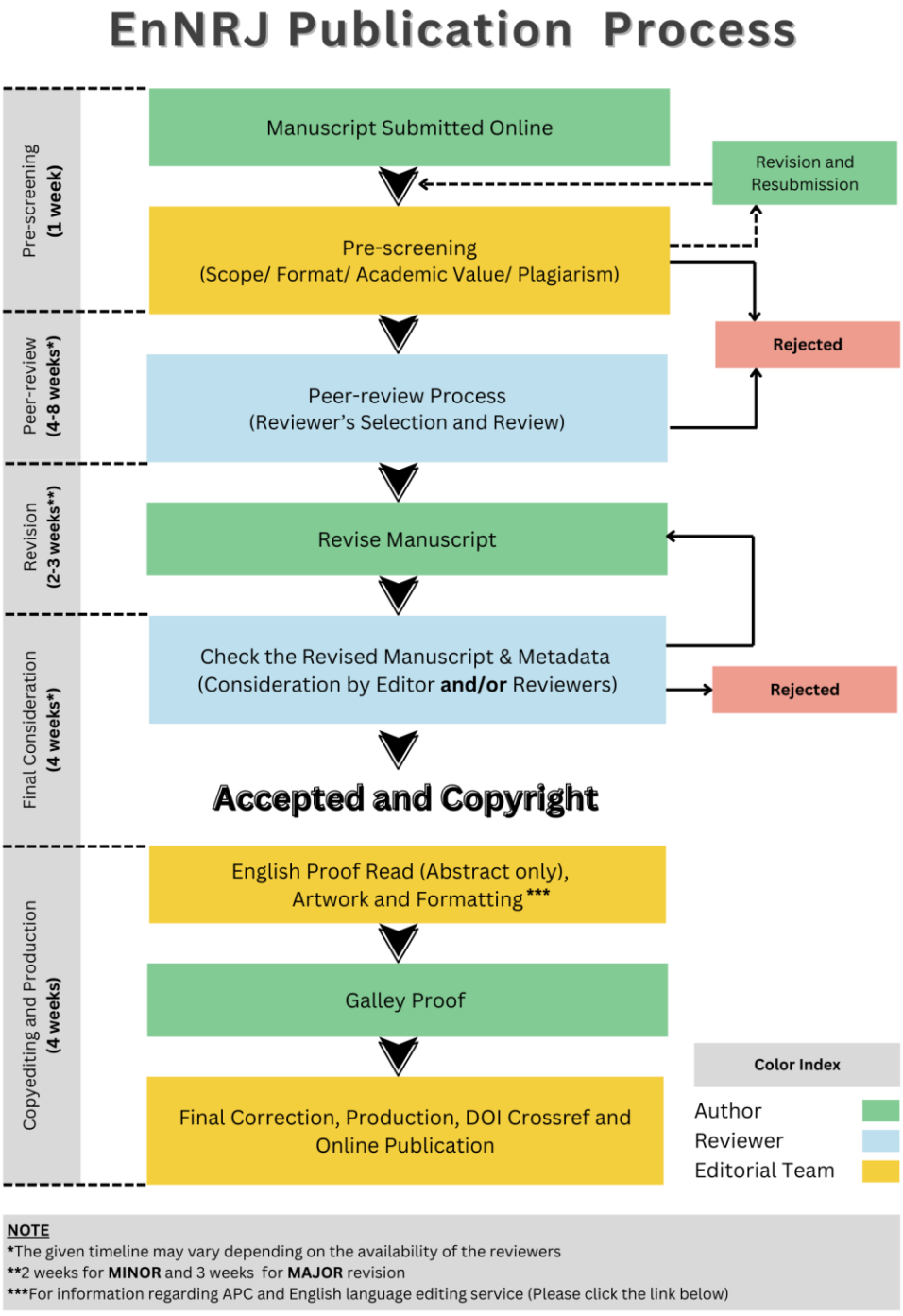

The Environment and Natural Resources Journal (EnNRJ) considers and accepts two types of articles for publication as follows:

- *Original Research Article*: This is the most common type of article. It showcases new, innovative or unique findings surrounding a focused research question. Manuscripts should not exceed 4,000 words (excluding references) - see more details in the Preparation of Manuscript section below.
- *Review Article (by invitation)*: This type of article focuses on the in-depth critical review of a special aspect of an environmental-related research question, issue, or topic. It provides a synthesis and critical evaluation of the state of the knowledge of the subject. Manuscripts should not exceed 6,000 words (excluding references).

Submission of Manuscript

The items that the author needs to upload for the submission are as follows:

Manuscript: The manuscript must be submitted as a Microsoft Word file (.doc or .docx). Refer to the **Preparation of Manuscript** section below for detailed formatting instructions.

Cover Letter: The letter should address the Editor and include the following: a statement declaring that the author's paper has not been previously published and is not currently under consideration by another journal.

- a brief description of the research the author reports in the paper, including why the findings are important and why the journal readers should be interested
- contact information of the author and any co-authors
- a confirmation that the author has no competing interests to disclose

Graphical Abstract (Optional): The author is encouraged to submit a graphical abstract with the manuscript. The graphical abstract depicts the research and findings with visuals. It attracts more potential readers as it lets them understand the overall picture of the article within a few glances. Note that the graphical abstract must be original and unpublished artwork. It should be a high-quality illustration or diagram in any of the following formats: TIFF, PDF, JPEG, or PNG. The minimum required size is 750 × 750 pixels (height × width). The size should be of high quality (600 dpi or larger) in order to reproduce well.

Reviewers Suggestion (mandatory): Please provide the names of three potential reviewers, with information about their affiliations as well as their email addresses. The recommended reviewers should not have any conflict of interest with the authors. Each reviewer must represent a different affiliation and not have the same nationality as the author. Please note that the editorial board retains the sole right to decide whether or not the recommended reviewers will be selected.

Declaration of Competing Interest: The author must include a declaration of competing interest form during submission. If there is no conflict of interest, please state, "The authors declare no conflict of interest." Otherwise, authors should declare all interests to avoid inappropriate influence or bias in their published work. Examples of potential conflicts of interest in research projects include but are not limited to financial interests (such as employment, consultancies, grants, and other funding) and non-financial interests (such as personal or professional relationships, affiliations, and personal beliefs).

CrediT (Contributor Roles Taxonomy) Author Statement or Author Contributions: For research articles with several authors, we require corresponding authors to provide co-author contributions to the manuscript using the relevant CRediT roles. CRediT is a taxonomy that shows the contributions of the author and co-author(s), reduces possible authorship disputes, and facilitates collaboration among research team members. The CRediT taxonomy includes 14 different roles describing each contributor's specific contribution to the scholarly output.

The roles are: Conceptualization; Data curation; Formal analysis; Funding acquisition; Investigation; Methodology; Project administration; Resources; Software; Supervision; Validation; Visualization; Roles/Writing – original draft; and Writing – review & editing.

Note that authors may have contributed through multiple roles, and those who contributed to the research work but do not qualify for authorship should be listed in the acknowledgments.

An example of a CRediT author statement is given below:
"Conceptualization, X.X. and Y.Y.; Methodology, X.X.; Software, X.X.; Validation, X.X., Y.Y. and Z.Z.; Formal Analysis, X.X.; Investigation, X.X.; Resources, X.X.; Data Curation, X.X.; Writing – Original Draft Preparation, X.X.; Writing – Review & Editing, X.X.; Visualization, X.X.; Supervision, X.X.; Project Administration, X.X.; Funding Acquisition, Y.Y."

Artwork for the Journal Cover: The author may provide and propose a piece of artwork (with a description) for the journal issue cover. This is an excellent opportunity for the author to promote their article, if accepted, on the cover of a published issue. Alternatively, the editorial team may invite the author to submit a piece of artwork for the cover after their manuscript has been accepted for publication. The final cover artwork selection will be made by the editorial team.

Final Author Checks: In addition to the basic requirements, the author should review this checklist before submitting their manuscript. Following it ensures the manuscript is complete and in accordance with all standards.

Preparation of Manuscript

Format and Style

The manuscript should be prepared strictly as per the guidelines given below. Any manuscript with an incorrect format will be returned, and the corresponding author may have to resubmit a new manuscript with the correct format.

Overall Format

The manuscript must be submitted as a Microsoft Word file (.doc or .docx). The formatting should be as follows:

- File format - .doc or .docx
- Page size - A4
- Page orientation - portrait (some landscape pages are accepted if necessary)
- Page margin - 2.54 cm (left and the right margin) and 1.9 cm (bottom and the top margin)
- Page number (bottom of the page)
- Line number
- Line spacing - 1.5
- Font - 12 point, Times New Roman (unless stated otherwise)

Unit - The use of abbreviation must follow the International System of Units (SI Unit) format.

- The unit separator is a virgule (/) and not a negative coefficient: 10 mg/L not 10 mgL^{-1}
- Liter always has a capital letter: mg/L

Equations

- Insert equations using the dedicated tool in Microsoft Word. Do not use pictures or text boxes.
- Equations that are referenced in the text should be identified by parenthetical numbers, such as (1), and should be referred to in the manuscript as “Equation 1”.

Inclusive Language: The language used in the manuscript acknowledges diversity, promotes equal opportunity, respects all people, and is sensitive to all aspects of differences. The manuscript content should not make assumptions about the beliefs or commitments of any individual. It should not imply superiority regarding age, race, ethnicity, culture, gender, sexual orientation, disability, or health conditions. Moreover, the manuscript must be free from bias, stereotypes, slang, and derogatory terms.

Reference Style: Vancouver style should be used for the reference list and in-text citations throughout the manuscript. Please follow the format of the sample references and citations, as shown in the Body Text Sections portion below.

Front Page

Title: The title of the manuscript should be concise and not longer than necessary. The title should be bold, 12-point size, and Times New Roman. The first letter of major words should be capitalized (as in standard title case).

Author(s) Name: The first and last names of all authors must be given, in bold, Times New Roman, and 12-point font.

Affiliation of All Author(s): Affiliation(s) must be in italics, Times New Roman, and 11-point font. Specify the Department/School/Faculty, University, City/Province/or State, and Country of each affiliation. Do not include positions or fellowships, or postal zip codes.
Each affiliation should be indicated with superscript Arabic numerals. The Arabic numeral(s) should appear immediately after the author’s name, and represent the respective affiliation(s).

Corresponding Author: One author should be responsible for correspondence, and their name must be identified in the author list using an asterisk (*).

- All correspondence with the journal, including article submission and status updates, must be handled by the corresponding author.

- The online submission and all associated processes should be operated by the corresponding author.

*Corresponding author: followed by the corresponding author's email address.

Example:

Papitchaya Chookaew[1], Apiradee Sukmilin[2], and Chalor Jarusutthirak[1*]
[1]Department of Environmental Technology and Management, Faculty of Environment, Kasetsart University, Bangkok, Thailand
[2]Environmental Science and Technology Program, Faculty of Science and Technology, Phranakhon Rajabhat University, Bangkok, Thailand
**Corresponding author: abcxx@xx.ac.th*

Abstract Page

Abstract: The abstract should include the significant findings paired with relevant data. A good abstract is presented in one paragraph and is limited to 250 words. Do not include a table, figure, or references.
Keywords - Up to six keywords are allowed, and they should adequately index the subject matter.

Highlights: Please include 3-5 concise sentences describing innovative methods and the findings of the study. Each sentence should contain at most 85 characters (not words).

Body Text Sections
The main body text of the manuscript normally includes the following sections: 1. Introduction 2. Methodology 3. Results and Discussion 4. Conclusions 5. Acknowledgments 6. Author Contributions 7. Declaration of Competing Interests 8. References

Introduction should include the aims of the study. It should be as concise as possible, with no subheadings. The significance of the problem and the essential background should also be given.

Methodology is sufficiently detailed so that the experiments can be reproduced. The techniques and methods adopted should be supported with standard references.
There should be no more than three levels of headings in the **Methodology and Results and Discussion** sections. Main headings are in bold letters, second-level headings are in bold and italic letters, and third-level headings are in normal letters.

Here is an example:

2. Methodology
2.1 Sub-heading
2.1.1 Sub-sub-heading

Results presents the key findings in figures and tables with descriptive explanations in the text.

Tables
- Tables - look best if all the cells are not bordered; place horizontal borders only under the legend, the column headings, and the bottom.

Figures
- Figures - should be submitted in color. The author must ensure that the figures are clear and understandable. Regardless of the application used to create them, when electronic artworks are finalized, please 'save as' or convert the images to TIFF or JPG and send them separately to EnNRJ. Images require a resolution of at least 600 dpi (dots per inch) for publication. The labels of the figures and tables must be Times New Roman, and their size should be adjusted to fit the figures without borderlines.
- Graph - The font style in all graphs must be Times New Roman, 9-10 size, and black color. Please avoid bold formatting, and set the border width of the graphs to 0.75 pt.

- Graph from MS Excel: Please attach an editable graph from MS Excel within your manuscript. Then please also submit the full MS Excel file used to prepare the graph as a separate document. This helps us customize our layout for aesthetic beauty.
- Graph from another program: Feel free to use whichever program best suits your needs. But as noted above, when your artwork is finalized, please convert the image to TIFF or JPG and send them separately Again, images should be at least 600 dpi. Do not directly cut and paste.

***All figures and tables should be embedded in the text, and also mentioned in the text.**

Discussion shows the interpretation of findings with supporting theory and comparisons to other studies. The Results and Discussion sections can be either separated, or combined. If combined, the section should be named Results and Discussion. **Conclusions** should include a summary of the key findings and take-home messages. This should not be too long, or repetitive but this section is absolutely necessary so that the argument of the manuscript is not uncertain or left unfinished.

Acknowledgments should include the names of those who contributed substantially to the work, but do not fulfill the requirements for authorship. It should also include any sponsor or funding agency that supported the work.

Author Contributions: For research articles with several authors, we require corresponding author contributions listed using the relevant CRediT roles. This should be done by the author responsible for correspondence.

Declaration of Competing Interest: The author must include a declaration of competing interest form during submission. If there is no conflict of interest, please state, "The authors declare no conflict of interest." Otherwise, authors should declare all interests to avoid inappropriate influence or bias in their published work.

References should be cited in the text by the surname of the author(s) and the year. This journal uses the author-date method of citation. The author's last name and date of publication are inserted in the text in the appropriate place. If there are more than two authors, “et al.” must be added after the first author’s name. Examples: (Frits, 1976; Pandey and Shukla, 2003; Kungsuwas et al., 1996). If the author’s name is part of the sentence, only the date is placed in parentheses: “Frits (1976) argued that . . .”

Please ensure that every reference cited in the text is also in the reference list (and vice versa).

In the list at the end of the manuscript, complete references must be arranged alphabetically by the surnames of the first author in each citation. Examples are given below.

Book

Tyree MT, Zimmermann MH. Xylem Structure and the Ascent of Sap. Heidelberg, Germany: Springer; 2002.

Chapter in a book

Kungsuwan A, Ittipong B, Chandrkrachang S. Preservative effect of chitosan on fish products. In: Steven WF, Rao MS, Chandrkachang S, editors. Chitin and Chitosan: Environmental and Friendly and Versatile Biomaterials. Bangkok: Asian Institute of Technology; 1996. p. 193-9.

Journal article

Muenmee S, Chiemchaisri W, Chiemchaisri C. Microbial consortium involving biological methane oxidation in relation to the biodegradation of waste plastics in a solid waste disposal open dump site. International Biodeterioration and Biodegradation 2015;102(3):172-81.

Journal article with Article Number

Sah D. Concentration, source apportionment and human health risk assessment of elements in $PM_{2.5}$ at Agra, India. Urban Climate 2023;49:Article No. 101477.

Non-English articles

Suebsuk P, Pongnumkul A, Leartsudkanung D, Sareewiwatthana P. Predicting factors of lung function among motorcycle taxi drivers in the Bangkok metropolitan area. Journal of Public Health 2014;44(1):79-92 (in Thai).

Article in press

Dhiman V, Kumar A. Biomass and carbon stock estimation through remote sensing and field methods of subtropical Himalayan Forest under threat due to developmental activities. Environment and Natural Resources Journal 2024. DOI: 10.32526/ennrj/22/20240018.

Published in conference proceedings

Wiwattanakantang P, To-im J. Tourist satisfaction on sustainable tourism development, Amphawa floating market Samut Songkhram, Thailand. Proceedings of the 1st Environment and Natural Resources International Conference; 2014 Nov 6-7; The Sukosol hotel, Bangkok: Thailand; 2014.

Ph.D./Master thesis

Shrestha MK. Relative Ungulate Abundance in a Fragmented Landscape: Implications for Tiger Conservation [dissertation]. Saint Paul, University of Minnesota; 2004.

Website

Orzel C. Wind and temperature: why doesn't windy equal hot? [Internet]. 2010 [cited 2016 Jun 20]. Available from: http://scienceblogs.com/principles/2010/08/17/wind-and-temperature-why-doesn/.

Report organization

Intergovernmental Panel on Climate Change (IPCC). IPCC Guidelines for National Greenhouse Gas Inventories: Volume 1-5. Hayama, Japan: Institute for Global Environmental Strategies; 2006.

Royal Gazette

Royal Gazette. Promotion of Marine and Coastal Resources Management Act 2059. Volume 132, Part 21, Dated 26 Mar B.E. 2558. Bangkok, Thailand: Office of the Council of State; 2015a. (in Thai).

Remark

** Please be note that manuscripts should usually contain at least 15 references and some of them must be up-to-date research articles.*

** Please strictly check all references cited in text, they should be added in the list of references. Our Journal does not publish papers with incomplete citations.*

Changes to Authorship

This policy of journal concerns the addition, removal, or rearrangement of author names in the authorship of accepted manuscripts:

Before the accepted manuscript

For all submissions, that request of authorship change during review process should be made to the form below and sent to the Editorial Office of EnNRJ. Approval of the change during revision is at the discretion of the Editor-in-Chief. The form that the corresponding author must fill out includes: (a) the reason for the change in author list and (b) written confirmation from all authors who have been added, removed, or reordered need to confirm that they agree to the change by signing the form. Requests form submitted must be consented by corresponding author only.

After the accepted manuscript

The journal does not accept the change request in all of the addition, removal, or rearrangement of author names in the authorship. Only in exceptional circumstances will the Editor consider the addition, deletion or rearrangement of authors after the manuscript has been accepted.

Copyright transfer

The copyright to the published article is transferred to Environment and Natural Resources Journal (EnNRJ) which is organized by Faculty of Environment and Resource Studies, Mahidol University. The accepted article cannot be published until the Journal Editorial Officer has received the appropriate signed copyright transfer.

Online First Articles

The article will be published online after receipt of the corrected proofs. This is the official first publication citable with the Digital Object Identifier (DOI). After release of the printed version, the paper can also be cited by issue and page numbers. DOI may be used to cite and link to electronic documents. The DOI consists of a unique alpha-numeric character string which is assigned to a document by the publisher upon the initial electronic publication. The assigned DOI never changes.

Mahidol University

Wisdom of the Land

Faculty of Environment and Resource Studies, Mahidol University, Thailand
999 Phutthamonthon Sai 4 Rd, Salaya, Phutthamonthon District, Nakhon Pathom 73170
E-mail: ennrjournal@gmail.com